ACADEMIC STUDIES IN
ENGINEERING - II

Editor :

Assist. Prof. Dr. Abdurrahman GÜNDAY

Academic Studies in Engineering - II

Editor

Assist. Prof. Dr. Abdurrahman GÜNDAY

TABLE OF CONTENTS

Chapter 1

ARTIFICIAL INTELLIGENCE ON SOIL-STRUCTURE INTERACTION:

Artificial Neural Networks and Support Vector Machines

Ahmet Emin KURTOĞLU[1]

1 Doç. Dr., İstanbul Rumeli Üniversitesi, aemin.kurtoglu@rumeli.edu.tr

Artificial intelligence (AI) has the potential to revolutionize every aspect of our life. The goal is to create intelligent systems that can learn and make logical interpretations [1]. AI has been the focus of research for more than half a century and it has applications in almost every discipline be it psychology, economy, mobility, engineering and so on.

Machine learning and deep learning, the subfields of AI, are concerned with computer programs that learn from previous data and extract meaningful functions and/or patterns. Among these algorithms, artificial neural networks (ANN) and support vector machines (SVM) will be the focus of current study.

Support vector machines (SVM) approach was originally developed by Boser et al. (1992) and is defined as an artificial intelligence learning method developed to solve classification problems [2]. Researchers began using SVM to solve regression problems and named it support vector regression (SVR). In addition to its solid numerical basis in statistics and learning theory, SVMs are most up to date approach in text analysis, face recognition, image processing, and bioinformatics [3].

Artificial neural networks (ANN) approach is one of the artificial intelligence techniques developed by imitating the working structure of human brain. Thanks to high learning ability of ANN, highly complex problems can be resolved in minutes. Artificial Neural Networks, which work only with numerical information, have the features such as storing information, learning using examples and producing information about unseen examples, classification and shape completion [1]. Both SVM and ANN approaches have been used in creating predictive models and solving classification problems in various fields of civil engineering [4-10]

Engineering analysis includes the application of scientific analytic rules and actions to expose the properties and state of the system, device or mechanism under study. The aim of any engineering analysis is to guess the behavior of an engineering system under defined circumstances. In other words: given the input to the system what is the output from the system? The engineering system under analysis might be, for example, a simple elastic beam, a complicated nonlinear three-dimensional structure, mechanic equipment or a hydraulic network. Engineering analysis is the action of taking given "input" data and defining the physical situation at hand. But an appropriate set of handlings, converting that input into a different sort of data, the "output," which provides the response to some questions of concern.

In this study, SVM and ANN approaches are implemented to create AI models that predict the results of FEM analysis concerning soil-structure interaction reported in [11].

Soil-Structure Interaction

Most civil engineering structures are designed for earthquake effects assuming that the structure base is fixed to the ground (control point). The ground motion at the control point, termed as control motion, is typically calculated empirically based on variables such as the seismic hazard at the site, the design life of the structure, and local site conditions, but not accounting for the presence of the structure. For a structure founded on rock, the ground motion is almost the same throughout the supporting medium, and its presence does not affect the characteristics (frequency content, amplitude and duration). Since the rock does not deform due to the forces imposed by the foundation above, the fixed base assumption is reasonable. For soft soil sites, the presence of a relatively rigid foundation changes the ground motion in the neighborhood of the structure, forces from the structure deform the soil, fixed base assumption is invalid and therefore, the responses of the soil and the structure are coupled. This coupled response is termed Soil Structure Interaction (SSI) and its effects are described below.

SSI effects can be best explained by comparing the behavior of a structure built on the rock to the response of the same structure on soft soil, subjected to the same control ground motion. Consider the soil-structure system shown in Figure 1 with point A as the control point. Both structures are identical and only vertically propagating SH waves are considered for simplicity [12]. Assuming that the two structures are equidistant from the earthquake source, the incident seismic waves in the rock below the structures are assumed to be identical. For the structure on founded rock, the motion of the foundation is the same as control ground motion, and its response is determined by subjecting its base to the control motion. Although inertial forces developed in the structure due to this base excitation generate overturning moment at the foundation and base shear that are transferred to the rock, no additional displacements occur at the foundation because the rock is very stiff: the fixed base assumption.
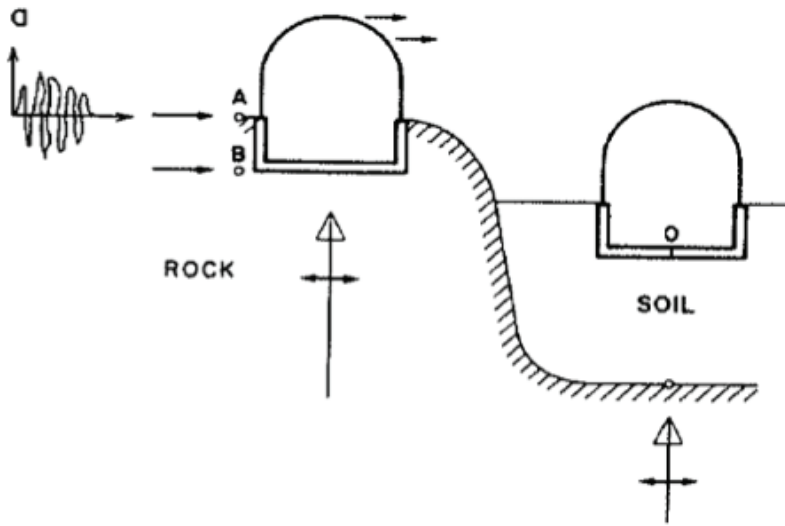
Figure 1. Seismic response of a structure on rock and soil [12-13]

For a soft soil site, the ground motion at Point O could be considerably different from the control motion at Point A. This difference can be attributed to the following effects: Firstly, in the free-field response (response of the soil profile when no structure is present), the ground motion is modified as the waves travel vertically to points D and E (see Figure 1.2b). Secondly, when a rigid foundation is constructed in the soil, the ground motion is scattered due to reflections from the foundation resulting in deviation of ground motion in the vicinity of the structure from the free-field motion. As a result, the foundation experiences geometrically averaged translational and rocking components, as opposed to the structure on rock which experiences the control ground motion (Figure 2c). This aspect of SSI is termed kinematic interaction. Thirdly, when the components of ground motion at the foundation are input to the superstructure, lateral inertial forces are created that vary along the height of the structure. These inertial forces generate a base shear force and overturning moment at the foundation, which deforms the soil and further changes the ground motion (see Figure 2d). This aspect of SSI is termed inertial interaction.

| (a) | (b) | (c) | (d) |
| Outcropping rock | Free-field response | Kinematic interaction | Inertial interaction |
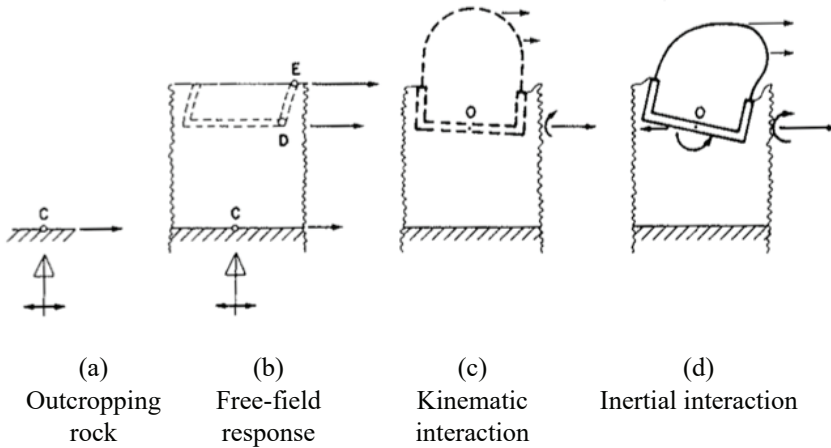
Figure 2. *Behavior of soil-structure system on a soft soil site [12-13]*

SSI can modify the response of a structure significantly, with the percentage change being dependent on a number of factors. The flexibility of the soil column above the rock usually increases the translational component. Kinematic and inertial interactions introduce a rocking component to the base excitation. Each frequency of the ground motion is modified differently and the resultant motion can vary significantly from the control motion. These interaction effects usually act as a low-pass (high-period) filter, removing much of the higher frequency content from the control motion. The extent of these modifications depends upon the intensity of excitation at the rock (control motion), the frequency content of the control motion, natural frequency of the soil column and the natural frequency of the structure. Aside from the modification of the ground motion, the dynamic properties of the soil-structure system can be quite different from those of the fixed base structure. Additional flexibility at the base increases natural time period of the structure, with the percentage increase being dependent upon the relative stiffness of the soil and structure. This added flexibility often decreases the spectral accelerations and the design seismic lateral forces on a structure. Propagation of the earthquake waves away from the structure will result in radiation damping to the soil-structure system. Rocking of the foundation causes hysteretic action in the soil which further increases the damping ratio of the system. In addition to modifying the inertial lateral forces, SSI generally increases the absolute lateral displacements in a structure. This may be significant in tall structures since rocking can substantially increase the lateral displacement at the top of such structures.

Soil-structure interaction effects increase when the structure is very stiff relative to the soil. For flexible structures on stiff soil, these effects are generally negligible. For stiff structures on softer soil SSI effects can be substantial and should be accounted for.

The presence of soil below the foundation of a structure modifies the response of the structure by increasing the effective first mode period of the structure (time-period lengthening) adding damping to the system by the hysteretic response of the soil and radiation of energy away from the building, and alteration of ground motion due to kinematic and inertial effects. Approximate analytical solutions for the calculation of these effects have been developed and implemented in building codes, with levels of simplicity being consistent with those of the design procedure for buildings.

Methodology

For the analysis of steel or reinforced concrete structures and soil bodies, the software packages are effective and completely integrated modules which allow users to create, customize, analyze and design the structural models within the same interface. Additionally, users can examine the stress conditions, make suitable modifications, and re-examine the outcomes without the need to re-run the analysis. Detailed design information brings up with a single click on an element. Members can be grouped together for design purposes. Both tabulated and graphic formats can be readily printed as output results [14].

PLAXIS [15] is a 2D finite element package program suitable for the modeling of soil systems and earth structures. Additionally, soil-structure interaction problems can also be solved by integrated soil-structure interface model. PLAXIS represents PLAne strain and AXISymmetric analysis. PLAXIS contain various soil types, complicated geometry and different material types, boundary conditions and loadings. Multiple soil models available, including the linear elastic models and Mohr-Coulomb. In this study, Mohr-Coulomb soil model is preferred for modeling. Elastic beam elements, spring elements or extension elements can be integrated for modeling the structural elements on which the loads, displacements, boundary conditions and fixities can be applied. A gradual staged process can be defined according to the construction sequence projected in the field. Outputs such as stresses and displacements can be obtained at any node and point anywhere within the model.

Initially, model is generated to simulate the concrete multi-storey building. The geometrical parameters, concrete properties, soil parameters shown in the Table and the first 10 seconds of real time accelerogram of Imperial Valley - El Centro Earthquake are used as input. (Figure 3) Then, static analysis, seismic analysis and phi/c reduction analysis (factor of safety analysis) are performed, respectively.

Table 1 summarizes the variables used for creating FEM models. Six input variables each having three values were used to create a total of 729 cases ($3^6 = 729$).
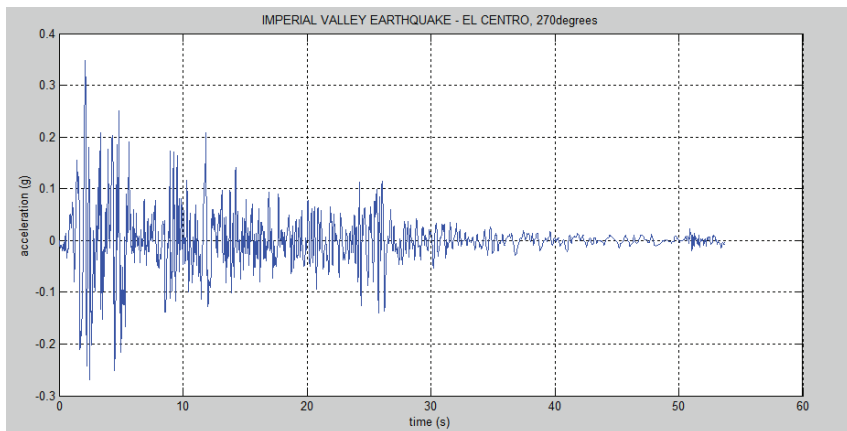
Figure 3. *Real time accelerogram of Imperial Valley - El Centro earthquake*

Table 1 Input parameters used for case studies

Parameter	Soil Parameters			Concrete and Geometry Parameters		
	Cohesion	Friction Angle	Unit Soil Weight	Weight	Foundation Depth	Height of Building
Unit	kPa	degree	kN/m³	kN/m/m	m	m
Values	5	16	14	7.5	1	9
	15	24	18	10	2	12
	25	32	22	12.5	3	15

Figure 4 represents the generated mesh of the present model used in this analysis [11]
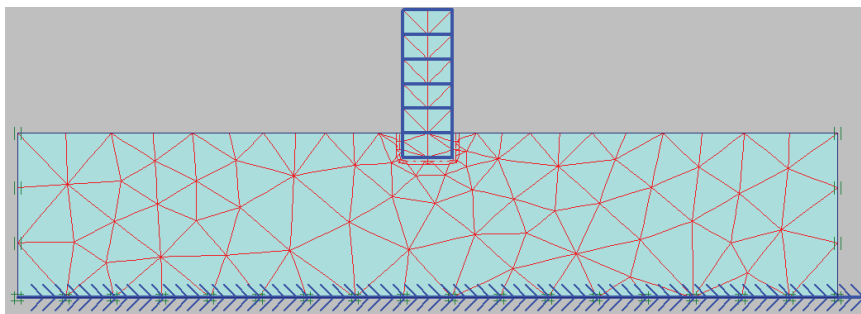
Figure 4. *Model mesh*

Calculation of safety factor was carried on by using reduction of strength parameters of soil (Phi-c reduction). In this method, the strength parameters c and $\tan \varphi$ are reduced until the failure of the structure.

The total multiplier ΣM_{sf} is used to describe the strength parameters of soil at specified phase in the analysis [16].

$$\Sigma M_{sf} = \frac{\tan\varphi_{input}}{\tan\varphi_{reduced}} = \frac{c_{input}}{c_{reduced}}$$

The strength parameters are successively reduced until the failure occurs. The factor of safety, at this point, is given by,

$$FS = \frac{\text{available strength}}{\text{strength at failure}} = \Sigma M_{sf} \text{ at failure}$$

Factor of safety was calculated for 729 cases (6 variables having 3 values each). SVR and ANN were applied to predict the results obtained from FEM analysis.

Support vector regression (SVR) models were created using two model types (i.e., Epsilon SVR and Nu-SVR) and two kernel functions (i.e., radial basis function and polynomial). FEM database having six input variables (cohesion, friction angle, unit soil weight, structure weight, foundation depth and height of building) and one output (factor of safety) was used for training and testing the models. Models are labeled in accordance with model type and kernel function, e.g., NR indicating the model with Nu-SVR model type and Radial basis function, EP with epsilon-SVR and Polynomial function etc.

On the other hand, a back-propagation based artificial neural network (ANN) was established using the same database. Testing and training sets are selected from the database randomly. Optimal ANN structure is was found to be 7-11-1 (7 inputs including bias, 11 hidden layers).

Results and Discussion

As reported in [11], safety factor of the structure is highly influenced by soil parameters as illustrated in Figure 5. It is clear from the main effect plots that soil parameters (cohesion, friction angle, unit soil weight) are directly proportional to the factor of safety of the structure. In other words, the increase in cohesion, friction angle and unit soil weight parameters cause safety factor to be greater as expected. Remarkable negative slopes indicate the inversely proportional relationships between concrete weight (and height of building) and the safety factor of structure.

Main Effects Plot for Factor of Safety
Data Means
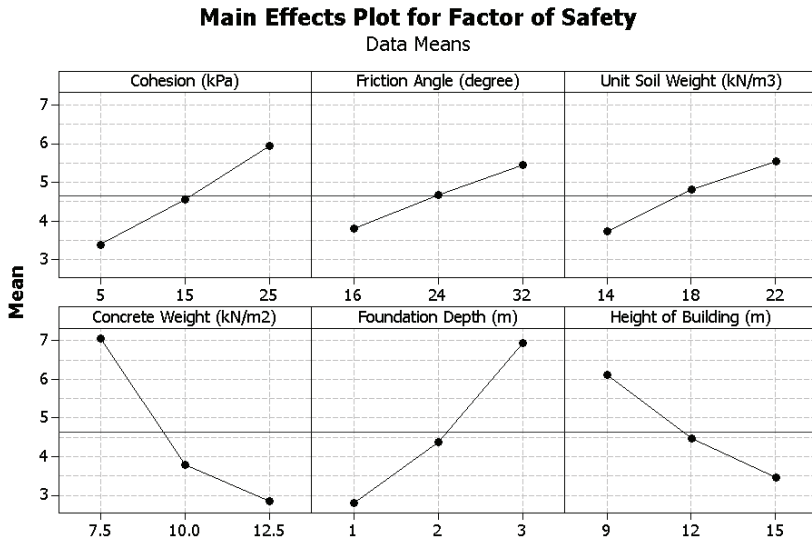
Figure 5. *Main effect plot for factor of safety [18]*

(e)
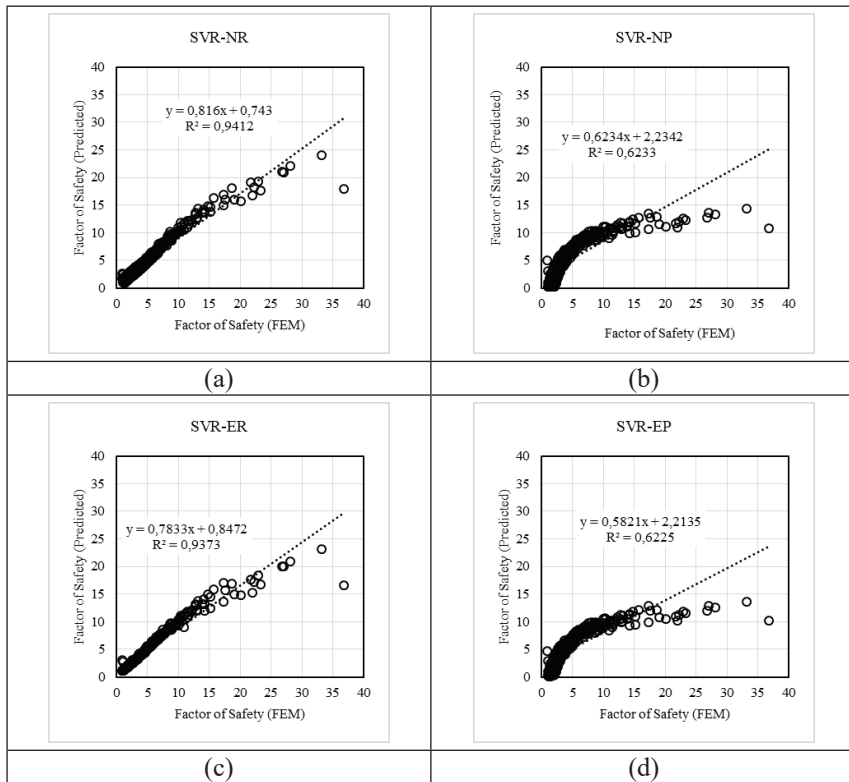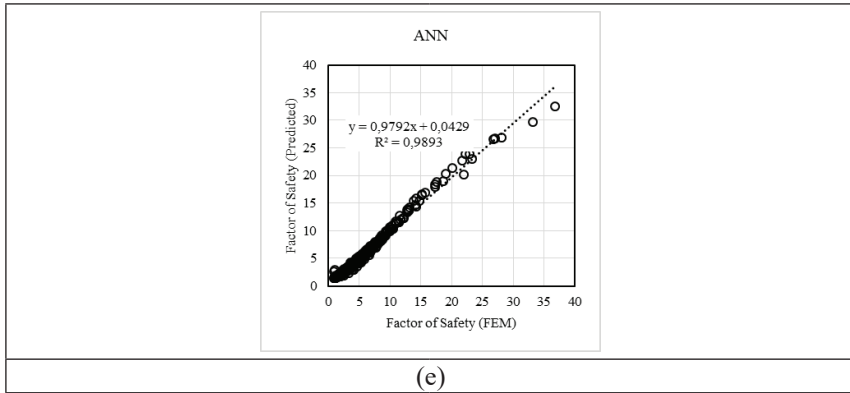
Figure 6. *Prediction performances of models*

Figure 6 illustrates the comparison of model predictions (y-axis) and FEM results (x-axis). Among the SVR models, those with radial basis function (Figure 6a and 6c) yielded superior prediction performance as compared to those of polynomial functions. As per the kernel functions, SVR models based on Nu-SVR kernel function appear to result in slightly more accurate predictions. This is also confirmed by the comparison of root mean squared error (RMSE) values shown in Figure 7. ANN model, on the other hand, appears to have highly accurate results and given best predictions with high coefficient of determination ($R^2 = \%98.93$) and lowest RMSE values.
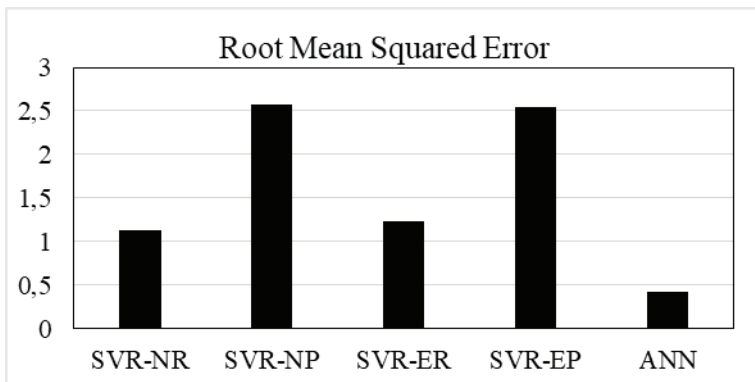
Figure 7. *Statistical evaluation of models*

Conclusion

The significance of soil effects on seismic behavior of structures was not well-known by researchers until recently. Recent studies on interaction effects between soil and structure foundations indicated that soil does not behave like a fixed base rather it has a substantial effect on the behavior of structure. In this study, the importance of this effect has been investigated by employing the finite element method based software PLAXIS.

It is observable from the main effect plots that soil parameters (cohesion, friction angle, unit soil weight) have directly proportional relation with safety of the structure. It is also found that the effect of cohesion on the factor of safety is much larger compared to the effect of friction angle and unit soil weight.

Artificial intelligence concepts such as Support Vector Machines (SVM) and Artificial Neural Networks (ANN) allow users to create simple yet robust and accurate models to interpret the behavior of structures under any given condition. For the example of soil-structure interaction, ANN approach was found to be superior in terms of prediction accuracy.

References

[1] Russell, S., & Norvig, P. (2002). Artificial intelligence: a modern approach.

[2] Boser, B. E., Guyon, I. M., & Vapnik, V. N. (1992, July). A training algorithm for optimal margin classifiers. In *Proceedings of the fifth annual workshop on Computational learning theory* (pp. 144-152).

[3] Wang, L. (Ed.). (2005). *Support vector machines: theory and applications* (Vol. 177). Springer Science & Business Media.

[4] Cevik, A., Kurtoğlu, A. E., Bilgehan, M., Gülşan, M. E., & Albegmprli, H. M. (2015). Support vector machines in structural engineering: a review. *Journal of Civil Engineering and Management*, *21*(3), 261-281.

[5] Bakbak, D., & Kurtoğlu, A. E. (2019). Shear Resistance of Reinforced Aerated Concrete Slabs: Prediction via Artificial Neural Networks. *Journal of Sustainable Construction Materials and Technologies*, *4*(2), 344-350.

[6] Kurtoglu, A. E. (2018). Patch load resistance of longitudinally stiffened webs: Modeling via support vector machines. *Steel and Composite Structures*, *29*(3), 309-318.

[7] Çevik, A. (2006). *A new approach for elastoplastic analysis of structures: neural networks* (Doctoral dissertation, Thesis). Gaziantep: Mechanical Engineering Department, University of Gaziantep).

[8] Kurtoglu, A. E. Predicting the Shear Strength of Fiber Reinforced Concrete Corbels Via Support Vector Machines. *Cumhuriyet Science Journal*, *39*(2), 496-514.

[9] Sonebi, M., Grünewald, S., Cevik, A., & Walraven, J. (2016). Neural network technique: modelling fresh properties of self-compacting concrete. *Computers and Concrete*, *18*(4), 903-920.

[10] Sonebi, M., Cevik, A., Grünewald, S., & Walraven, J. (2016). Modelling the fresh properties of self-compacting concrete using support vector

machine approach. *Construction and Building materials*, *106*, 55-64.

[11] Kurtoglu, A. E. (2013). *Effect of Soil Characteristics on Dynamic Behavior of Structures*

(Master dissertation, Thesis). Gaziantep: Civil Engineering Department, University of Gaziantep).

[12] Wolf, J. P. (1985). Soil-structure interaction. *Prentice Hall Inc., Englewood Cliffs, New Jersey ISBN 0 l3*, *221565*(9), 01.

[13] Veletsos, A. S., & Wei, Y. T. (1971). Lateral and rocking vibration of footings. *Journal of Soil Mechanics & Foundations Div*.

[14] Berkeley, C. S. I. (2000). SAP2000 Concrete Design Manual. *Compute & Structures, Inc*, 17-41.

[15] Brinkgreve, R. B. J., Swolfs, W. M., Engin, E., Waterman, D., Chesaru, A., Bonnier, P. G., & Galavi, V. (2010). PLAXIS 2D 2010. *User manual, Plaxis bv*.

[16] Arslan, H. (2005). Finite element study of soil structure interface problem. *EJGE, paper-0533*.

Chapter 2

CODE GENERATOR MODEL FOCUSED ON RELATIONAL DATA MODEL AND USER MOVEMENT

Çağla EDİZ[1]

1 Dr., Sakarya University, Department of Management Information Systems,cediz@sakarya.edu.tr

1. INTRODUCTION

The relational database system, suggested by F. Codd, has formed a common structure for recording and processing of data (Codd, 1970; Codd, 1986). In Codd's suggestion, data is stored in two-dimensional relations with rows and columns within certain rules. As a result of this standardization, SQL has been developed for using as a standard language in data management. Database Management Systems (DBMS) record, secure and report data in a systematic way by using SQL. However, DBMS are not often used by the end user. End users use interfaces instead of DBMS, because they provide security, ease of use, visualization and fast entries. On the other hand, these interfaces have to provide data entries by obeying DBMS rules in the database they use. Features, relationships and rules which are already defined in databases are redeclared in interfaces during preparation of these programs. This situation brings a huge workload to the software developers and also negatively affects the maintenance and volume of the interface programs.

This chapter describes how to prepare data entry interfaces for relational databases automatically with Model Oriented Engineering (MDE) approach. Although relational database is used frequently for data management in software projects, the lack of model software working with these databases in real-time is the main reason of this study. Some libraries automatically display the database table entered on the screen with the entry of the table name. These libraries read and display data in their databases, but do not provide real-time interaction in data management. On the other hand, even in professional ERPs, software programmers do a lot of work to design interfaces of database management. They add tables and fields manually in order to manage data in ERP programs. They also redeclare relationships between table fields in their own programs. For these reasons, software developers who prepare various projects using relational databases spend long time to prepare their program. Even when working in DBMS such as MSSQL, users have some difficulties. For instance, when entering a record in a field defined as foreign key, the user must know the previous rules and behave according to them. To reduce all these problems, code generator model was proposed in this study. Code generator model decreases preparation time of these projects and sustain easy usability. Thus, by using only name of the table and DBMS, it is provided to prepare record interface automatically. So users automatically display default values, select data of foreign field data from associated field. In addition they can add or update data without clicking any buton by using this model.

In the second part of this chapter, development of MDE is mentioned and the prepared model is drawn by MDE approach. In the third part, concepts and constraints of the relational data model are examined. In the

fourth part, user movements and metadata of database are analyzed and according to these variation, the flowchart of the model is drawn. In the last part, a case study related with employee timekeeping are evaluated according to the usability of the prepared model.

2. MODEL DRIVEN ENGINEERING

In the 1990s, agile management system, making employees more valuable than process management, gained popularity in the preparation of software projects. On the other hand, although the customers are satisfied with the fast solutions; agile systems do not develop systematic approaches. Thus, they do not provide an input for later projects (Gencer and Kayacan, 2017). Therefore, more systematic approaches that take into account processes are more effective in the long run. That is, although preparations of processes are seen as waste of time at first glance, they save a lot of time on software, maintenance and renewal costs especially for big projects.

Object oriented programming approach, which is prepared with a systematic principle, arises from the need to prevent complexity of software. With object-oriented programming, necessary data and codes are considered as packets, thus code duplications and confusions in software are reduced (Cakiroglu, 2007). Object-oriented programming techniques enable abstractions in programs, and developers create more leaner and more understandable structures. On the other hand, with the development of technology, data have increased and software developers have been forced to manage much more complex systems. This was due to not only increased code and data volume, but also requirements such as performance and security provisioning, update technology, changing platforms. These experiences caused a paradigm change, so studies based on model representing images of a system and its elements have been preferred instead of object-bases systems (Bezivin et al, 2004).

In model-based architecture, developers intensively benefit from UML tools (Rumpe, 2017). With MDE, software developers can work more effectively by focusing on the model that they want to develop, rather than dealing with complex and huge volumes codes. In addition, with MDE approach, researchers can make improvements and evaluations on their database and softwares and they can receive visual data (Ruiz et al, 2017; Rasool and Arshad, 2017; Muzammul, 2018). MDE plays a key role, especially in reducing repeat operations and errors (Paige et al, 2016). In this way, more understandable, accurate and cheap software can be developed; maintenance and updating operations becomes easier (Selic, 2003). Similarly, since automatic code generators generate codes from a higher level of abstraction, it allows developers to focus on higher-level design problems rather than codes (Gurunule and Nashipudimath, 2015).
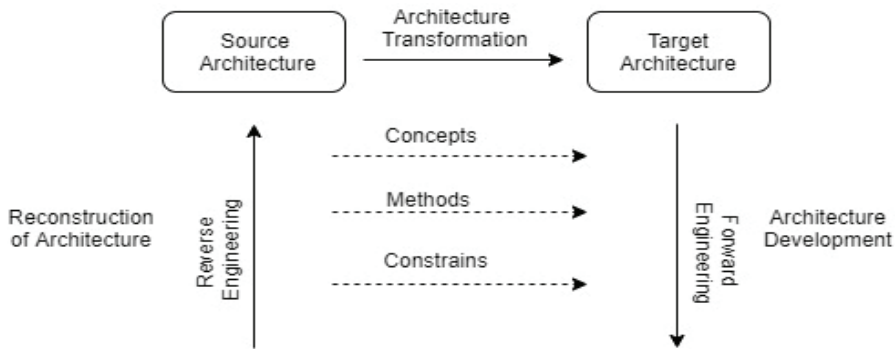
Figure 1. Model Driven Engineering with Horseshoe Model Source ([14-15])

The horseshoe model [Kazman et al, 1998; Candel et al, 2019; Yu et al, 2005] can be considered in three stages according to the architectural stages. In the first stage, it changes from platform-specific model level to platform-independent model. At this stage, concepts and basic architectural structure are reached by using codes and func tions in the current application. In the next stage, a higher level, which is expressed in a declarative manner and independent of the algorithms, is reached. This stage is also the stage where diagrams such as status diagram and activity diagram are created. At this stage, the necessary analysis and the changes are made and the targeted high level is obtained. In the third stage, a platform independent model is obtained which contains the classes that will form the infrastructure of the target system. Afterwards, target platform dependent model is created with the platform language (Candel et al, 2019; Maldonado et al, 2014). During the restructuring process, the transformations can be done manually by the software developers or automatically through the programs (Candel et al, 2019).

Reconstraction architecture is generally used for transformation purposes in MDE. After transformation, it reaches its purpose and isn't used anymore generally. Hovever, in this study, MSSQL database, which is the primary architecture, is used dynamically. In other words, codes in Visual Studio are formed by considering database's concepts, constraints, properties, relationships and data structure according to user movements. This formation is continuous. So the transformation of the model is not unilateral. The platforms shape each other interactively.
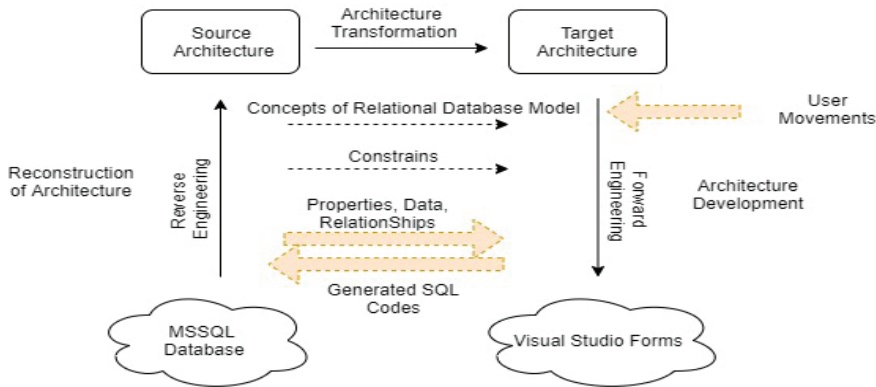
Figure 2. *Code Generator Model Focused on Relational Data Model and User Form*

3. RELATIONAL DATA MODEL

In the relational data model, data is formed of data groups and each data group is located in one row of the table. Each row has the same number of columns and the data added to each column has the same column property (Turker and Gertz, 2001). Each row of data in the tables also called as the record of the table.

Integrity of records in the database can be achieved at different levels. Basically, constraints, rules, triggers and stored procedures ensure data integrity in databases. While the codes in the constraint level cause the lowest workload, the codes written in the stored procedure level cause the most workload. Within workload increment, software requires higher disk space and speed reduces. Therefore, achieving integrity with constraints is the most suitable way. The constraints can be examined in five groups as primary key, single field, type or value control, foreign key, and default (Kemal, 2016). General rules of constraints are as follows;

•Repetitive records cannot be added in the fields with primary or unique key constraint. That is, each value in these fields must be different from others.

•Default value indicates the value assigned to this field and comes automatically when a new record is created.

•A foreign key field associates with a primary key field in a different table. Data entered in foreign key field take its value from associated primary key field's data.

• The data recorded in any field must ensure its type constrain requirement. For example, a string value cannot be entered in a field defined as date type.

A relational database changes its state by insert, delete or update transactions. While these transactions occur, data integrity constraints must be ensured. In addition, for the secondary key fields, there are some options in transactions. The most used option in adding/updating transactions is "dependent insertion " rule. According to this rule, the record to be added or updated in the secondary key field must exist in the associated primary field (Nizam, 2016). On the other hand, the most preferred rule for delete transaction is that, a record which will be deleted from the primary key field must not have in any foreign key fields.

The relational data model is universally accepted and used to record data for many businesses. These records are stored using relational DBMS generally and SQL language is used to manage these systems. However, SQL is usually a language known by IT employees. Therefore, user interfaces are prepared for employees in businesses. During preparation of these programs, tables, relationships and constraints are defined again in the interface program. Instead of defining these, using algorithms depending on user movements and database relations explained in this study will be advantageous to reduce project preparation times.

4. ALGORITHMS OF PROGRAM

4.1 Evaluation of User Movements

The most common operations performed by data operators are adding, deleting and updating records to the tables they call. These operations are done in user interfaces mostly. Because user interfaces provide system security, authorizations and providing convenient access. On the other hand, doing these operations manually in the DBMS are easy. Table is opened to add a new record and data group is written on bottom line of the table. If you move to a different line after this operation, the data, written in the previous line, is added. Also, if you change the value of a cell in a row except the last one, you can update this data. With the proposed algorithms in this study, adding and updating operations can be done in a similar way using the interface programs.
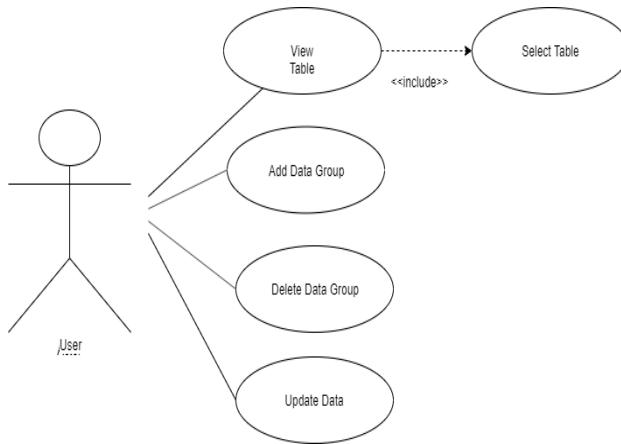
Figure 3. *User Case Diagram for Database Transactions*

The following evaluations are made by the program in user movements.

- Which one (system or user) is writing to the interface table?
- Is the first record added to the table?
- Is a new data group added?
- Which data is selected from the secondary field values?

```
1 başvuru
Sub Delete()
    Dim tip As String
    tip = tipler(0) + "00000000000"
    If tip.Substring(0, 4) = "nchar" Or tip.Substring(0, 4) = "ntext" Or tip.Substring(0, 8) = "nvarchar" +
        "" Or tip.Substring(0, 4) = "text" Or tip.Substring(0, 4) = "char" Or tip.Substring(0, 4) = "time" +
        "" Or tip.Substring(0, 7) = "varchar" Or tip.Substring(0, 4) = "date" Then
        sql = "Delete " + TabloAdi + " where " + Me.Columns(0).Name.ToString() + " = '" & Me.CurrentRow.Cells(0).Value & "'"
    Else
        sql = "Delete " + TabloAdi + " where " + Me.Columns(0).Name.ToString() + " = " & Me.CurrentRow.Cells(0).Value & ""
    End If
    da.InsertCommand = New SqlCommand(sql, con)
    Form1.TextBox1.Text = sql
    Try
        da.InsertCommand.ExecuteNonQuery()
        Me.DataSource = Me.Yenilen().Tables(0)
    Catch
        MsgBox("Primary field records added to different tables cannot be deleted")
    End Try

End Sub
```

Figure 4. *The Screenshot of the Program Delete Method written in C#*

4.2 Database Metadata Evaluation

In addition to user movements' analysis, the metadata of the fields are also analysed by the "Transaction Table" class. This analysis depends on user movements also, but the queries work in the database instead of interface program in this case. The main queries here are:

- Is the changing data in a secondary key field ?
- If the changing data in a secondary key field, what is the table name with the primary key associated with that field?

- What is the primary key type of the updated or deleted record?

- Are there default values in new record?

In addition a check query was added like that.

- Does the value changing on interface table belong to an existing record?

4.3. Dataview Class Events Used

Some events of the Dataview class were used in the realization of the above queries. These events are:

- CellDoubleClick: If this event takes place in the "TransactionTable" class, it queries whether the field clicked in the table image is the secondary key field. If the queried field is the secondary key field, the table image opens containing the primary key field to which this field is associated. Thus, the user can select records from this field. If the event is in the "ReferenceTable" class, the primary key value in the double-clicked record is assigned to the table cell (DataGridView object) in the "TransactionTable" class that calls it.

- UserAddedRow: This event runs if the user moves to the new line for the new record entry. This information is transmitted to the next processes with the prepared codes. Also, if any field is assigned a default value, this value is added to the field in the new row.

- RowEnter: Before this event, if the "User AddedRow" event is run or if this event is run after the first record is entered in the table view, the prepared codes add the record to the database.

- CellValueChanged: When this event is used, it is evaluated whether the user performs an update or an adding, and then the operation is performed accordingly.

4.4. Flow Chart of The Program

In this study, user movements and database metadata are analyzed and two classes are created to manage transaction processes. These classes are derived from the "DataGridView" class, which are already in Visual Studio and present data in database visually.

The first of these classes is the "TransactionTable" class. This class brings selected table's data into interface program as a table view and allows the user to transact database data in real time. To do this, "TransactionTable" class stores data and properties of the table in temporary memory. These properties such as field numbers, field names, default values of fields are used by the algorithm in generating codes. In addition, this

class evaluates user movements. When the user clicks the bottom row of the table view, software understands that a new record will be added to the database in this class. It evaluates next movements according to this information.

On the other hand, if the user clicks on a cell that is not in the last row of the table view and change its value, software update this cell's value also in the database.

The first query of each clicked cell is that, whether the field of the clicked cell is defined as a secondary field. This query works in the database and investigates whether this field has a referenced primary key field. If there is a primary key field for this field, an object of "ReferenceTable" class, derived from the "DataGridView" class, is added to the existing user interface. The user selects input data by using the adding object. This object removes after selection.

After the decision of adding or updating, code generation activates. The following data are considered during generation of codes:

•   If a new data group is to be added to the table, the count of fields of this table,

•   If data to be updated, the first field name and the changing data field name ,

•   The primary key type of the table to be transacted.

The study assumes that the user behaves in a certain order when adding records to the table. That is, if a new record is to be added, user completes to write to the last line first and then moves another line. On the other hand, if the user moves to another line without completing adding data group, the algorithm gives null values to the absent cells and adds the record to the database in this way.
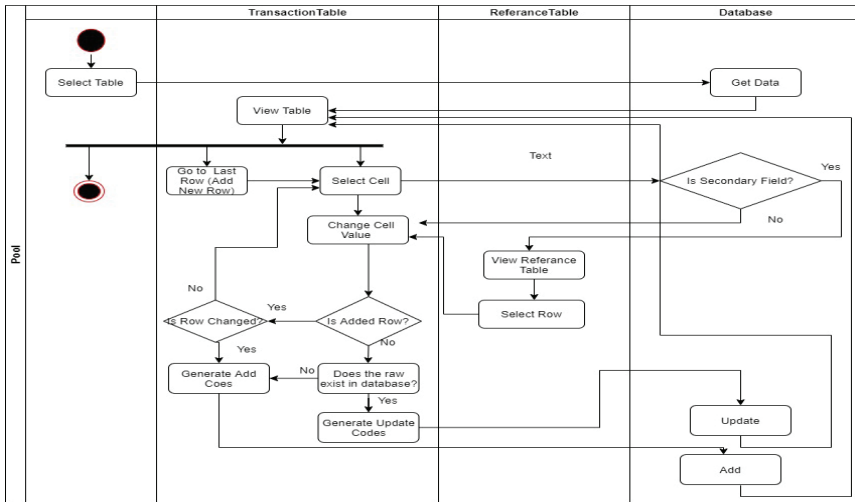
Figure 4. *Flow Chart of Prepared Model Software*

4.5. Case Study

An employee tracking program is prepared for a food business using proposed model. A program has been prepared to manage and track the working hours of the employees. In this program, prepared model is used and an analysis is performed. The tables using for input activities created during the preparation of this project can be classified into two main groups:

1. Tables which are managed by using model software: Tables in this group represent the highest number of tables in the project. In preparing these tables, the first columns are defined as primary keys in accordance with the working constraint of the model.

2. Tables which are managed not by using model software: These can be grouped like that:

•   Tables with auto-records: These tables get records from devices such as RFID or another table-view.

•   Tables used for report or approval: These tables are derived from data from different tables and manual record entries are made for only a few fields.

Apart from these, some demands such as entering the employee permissions by selecting the days from the calendar are wanted. The model is not used for these cases.

5. LIMITATIONS OF THE STUDY

There are two limitations for tables when data transaction will be done via proposed model software. First one is that, the first column of the table must be defined as the primary key. Actually, this case is the most common preference in the preparation of relational database projects and so the proposed model was prepared according to this rule. The second one is that, any field in the table should not be defined as automatically incremented. Because, if there is an autoincrement field, this field must be ignored in adding queries. So, extra algorithms are needed to use automatically incremented fields.
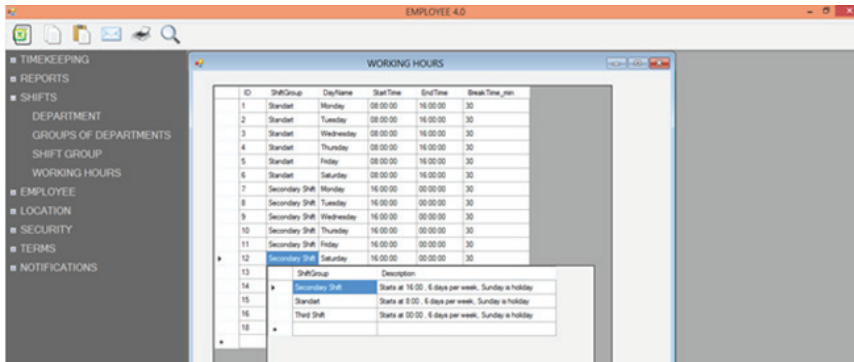
Figure 5. *A screenshot from the prepared monitoring progr*

CONCLUSION & SUGGESTIONS

In traditionally prepared software using relational database, almost a separate user interface is created for each table. For each interface form, the programmer defines the fields to be seen on the screen. Also programmer redefines the relationships of the fields in the interface program. Besides, add, delete and update queries must be written for each interface. These preparations create a huge workload for developers. At the same time, these codes, which are prepared separately, negatively affect the disk usage volume of the program. One of the other disadvantage of the programs prepared with traditional methods is that the software prepared with traditional methods cannot adapt to the changings in databases. For this reason, software prepared by traditional methods must be revised after every change in the database.

Because of these disadvantages of traditional programs, the proposed program in the study, focusing on the relational data model and user movements. Using model-based code generation algorithms, interface developers do not spend time for preparing interface design of each table, so they

can deal with jobs that having higher added value for the customer. Also, although if there are changes in database such as table name, field name, number of fields, field type, relationships etc. , the user use proposed interface program without changing anything. In addition, algorithms prepared in this study provide ease of use for the users. By using this model, users can record database by acting as if they were filling an excel sheet without clicking save and update buttons. Finally, the user can enter the values of fields assigned as secondary key fields by using the auto shown table.

In addition to these advantages, there are some parts of the program that can be developed. For example, some tables in ERP projects, data, such as user name, record insertion date, record revision date, are stored without being displayed in the user interface. This information is displayed by the authorized users when necessary. In this study, all fields in the table are displayed and users are allowed to changed these fields. Perhaps in future, the scope of this model can be extended not to show these fields with added algoritms. Also, no feedback about control limit values of the fields is given to user in this study. If the user encounters an error during recording, the system reports that the record wasn't done, but it does not provide any feedback on why the recording could not be done. Future additions to the existing algorithm can eliminate the limits required for the application and increase feedback to the user.

REFERENCES

Bezivin J, Hammoudi S, Lopes D and Jouault F., (2004), "Applying MDA approach for web service platform", In *Proceedings. Eighth IEEE International Enterprise Distributed Object Computing Conference, EDOC 2004,* pp. 58-70, IEEE, September.

Cakiroglu U., (2007), "Web tabanli egitim icerigi gelistirmede nesneye dayali programlama kullanimi", *XII. Elektrik, Elektronik, Bilgisayar ve Biyomedikal Muhendisligi Ulusal Kongresi ve Fuari, Eskisehir*

Candel CJ F, Molina JG, Ruiz FJB, Barcelo JRH, Ruiz DS and Viera BJC (2019), "Developing a model-driven reengineering approach for migrating PL/SQL triggers to Java: A practical experience", *Journal of Systems and Software,* 151:38-64.

Codd EF. (1986), "An evaluation scheme for database management systems that are claimed to be relational", *In: 1986 IEEE Second International Conference on Data Engineering.* IEEE, pp. 720-729

Codd EF. (1970), "Relational model of data for large shared data banks", *Commun. ACM*, 13(6):377–387, June

Gencer C and Kayacan A. (2017), "Yazilim Proje Yonetimi: Selale Modeli ve Cevik Yontemlerin Karsilastirilmasi", *Bilisim Teknolojileri Dergisi*, 10(3), 335-352

Gurunule D. and Nashipudimath M. (2015), "A Review: Analysis Of Aspect Orientation And Model Driven Engineering For Code Generation", *Procedia Computer Science*, *45*, 852-861

Kazman R, Woods SS and Carrière SJ. (1998), "Requirements For İntegrating Software Architecture And Reengineering Models: CORUM II", In: 5th Working Conference on Reverse Engineering, WCRE '98, Honolulu, Hawai, USA, October 12–14, 1998, pp. 154–163

Kemal O. (2016), *Veri Tabani Programlama*, Anadolu University, Part IV, Editors: Sinan A, Ozturk GO.

Maldonado CA, (2014), "Gomez-Lopez MT, Quintero AMR and Ramos I. An architecture to infer business rules from event condition action rules implemented in the persistence layer", *Uncovering Essential Software Artifacts through Business Process Archeology*, IGI Global, 201-221.

Muzammul M. (2018), "Model Driven Re-engineering with the Fields of Re- structuring: Software Quality Assurance Theory", *International Journal of Scientific and Research Publications*, 8(6), June

Nizam A. ,(2016), *Veritabani Teorisi ve Uygulamalari,* Papatya Yayinlari, Ocak.

Paige RF, Matragkas N and Rose LM. (2016), "Evolving models in model-driven engineering: State-of-the-art and future challenges", *Journal of Systems and Software*, *111*, 272-280.

Rasool G and Arshad Z. (2017), "A lightweight approach for detection of code smells", *Arabian Journal for Science and Engineering*, *42*(2), 483-506.

Rumpe B. (2017), *Agile Modeling with UML: Code Generation, Testing, Refactoring*. Springer.

Ruiz FJB, Molina JG and García OD.(2017), "On The Application Of Model-Driven Engineering In Data Reengineering", *Information Systems*, *72*, 136-160.

Turker C. and Gertz M. (2001), Semantic Integrity Support In SQL: 1999 And Commercial (Object-) Relational Database Management Systems, *The VLDB Journal—The International Journal on Very Large Data Bases*, *10*(4), 241-269.

Selic B. (2003), The Pragmatics Of Model-Driven Development. *IEEE Software*, *20*(5), 19-25

Yu Y, Wang Y, Mylopoulos J, Liaskos S, Lapouchnian A and Prado Leite do JCS. (2005), "Reverse Engineering Goal Models From Legacy Code", *13th IEEE International Conference on Requirements Engineering (RE'05)*.

Chapter 3

EMBEDDED SYSTEM FOR AUTOMATIC LICENSE PLATE RECOGNITION

Ercan BULUŞ[1]

---

1 Associate Professor Doctor, Tekirdağ Namık Kemal University, Çorlu Engineering Faculty,ercanbulus@nku.edu.tr

1   INTRODUCTION

Digital image processing is the rapidly growing field of computer science. There are various applications in order to achieve different processes like face recognition, product control, optical character recognition etc. One of its major applications is license plate recognition in intelligent transportation system (ITS) area. Number plate (or license plate) recognition is one of the interesting and challenging approaches in digital image processing field. Accurately locating the car number plate is a challenging objective. Different shapes and sizes of plate also create hurdles in this process. Recognition process comes after the localization of the plate. Different countries use different colors and coding styles for identification of vehicles.

There are many systems for identification of license plates of vehicles today. However, these systems are often expensive and these are working with a link to a computer. Also, generally it is not possible to teach new information to these systems. In this study, it was aimed to develop a low-budget, stand-alone embedded system without connecting another computer.

In Turkey, the coding style which is shown in Fig.1 is used.

XX YYY ZZZZ		
XX = City Code (2 number)		
YYY = Series Code (max. 3 alphabetical value)		
ZZZZ = Series Number (max. 4 number)		

Fig 1. Example of License Plate Recognition Phases

Civilian vehicle number plates are written in black fonts with white backgrounds while non-civilian vehicles use number plates written in white font and black background. In this paper, we have focused on ALPR in civilian vehicles as detailed in next chapters.

This manuscript is organized as follows. Section II involves the literature survey for the system. Used hardware is described in section III. Section IV includes a detailed explanation of the software developed. Section V describes the test results. Discussions are given in section VI and Conclusions are given in section VII.

In this paper, we proposed a system that works on a minicomputer as an embedded system. First, the system finds the location of the license plate. Conversion image to ASCII to find out the characters, which the license plate is composed of, is done afterwards. The technique we have used to get ASCII codes of characters is template matching. Briefly, template matching is comparison of an image pattern through a database to find resemblance to any of the records.

2   RELATED WORKS

Intelligent Transport Systems (ITS) becomes a more popular subject with each passing day. ITS is generally used to ensure safety, security, vehicle tracing, producing smart vehicles and etc. Automatic license plate recognition (ALPR) process is one the major components of ITS.

Recently there are many studies on only detecting the LP location of a vehicle for a specific reason. Lijuan Qin and Ting Wang designed an anti-collision warning system based on monocular vision sensor in 2016. They detected the LP location and the distance between vehicles [1]. Min Wang et al. used a component-based model that uses masking, Gaussian Filtering and Sobel operator in order to find the location of LP such as other components like front lights, logo etc. [2]. Şafak Öztürk et al. aimed to gain the color information of a vehicle by finding the locations of the components. LP is one of those components that they used [3]. Another car make and model recognition study belongs to Noppakun Boonsim and Simant Prakoonwit [4]. Their paper proposes a method, which can be used under limited lighting conditions at night. Ran Yang et al. introduced a novel method that is based on Sparse Auto – Encoder to detect the location of LP [5]. In [6] Fourier-Mellin transform (FMT) and Vandewalle algorithm are used to validate the LP's location. Another work for LP localization is the work of Paunwala and Patnaik [7] which they used Gradient Analysis and prolonged Haar Wavelet Transform. In the work of Zhang Meng LP localization is done by using Probabilistic Principal Component Analysis (PPCA) [8]. The work of Shapiro et al. introduced Adaptive License Plate Image Extraction [9].

Many researchers have studied on recognizing the LPs after detecting the locations. They have used several methods and algorithms in order to achieve this goal. Most commonly preferred approach in LPR process is using Support Vector Machines (SVM). Cheng–Yu Wen et al. used SVMs combined with Neural Network (NN) for LPR [10]. Hussein Samma et al. had a Fuzzy Support Vector Machine approach on their paper to achieve LPR process [11]. Tiange Li and Song Yu made a parallel LPR work in [12] by using SVMs. Nguyen Thai-Nghe and Nguyen Chi-Ngon used Haar-like features combined with SVM in their work in order to achieve ALPR process [13].

Also another most frequent approach is using Neural Networks (NN) in LPR process. Shaimaa Ahmed El-said used Discrete Time Cellular Neural Network approach in [14] with a 85% success rate. In [15] Liu Pan et al. aimed to recognize the license plate on low quality videos by using Convolutional Neural Network (CNN). Besides this, Deep CNN approacs is used in the work of Vishal Jain et al. [16]. Also in [17] Neural Network

approach has been used in LPR. The work of Sangita Kumari is another example of using Artificial Neural Networks in LPR system [18].

Different approaches in LPR like RGB Color Extraction [19], Tesseract OCR [20], Computer Vision Algorithms [21] and sharpness based methods for character segmentation [22] etc. have been used. Researchers also intended to recognize the LPs in different lightning conditions or blurred/low quality images [23, 24, 25].

In this paper, an automated system, which uses a smart template matching approach on different versions of Raspberry Pi, has been introduced. In recent studies, template-matching technique has been used in wide range [26]. In addition, there are also studies in the literature where hardware solutions are the forefront. Using PLCs for triggering the image capturing [27], FPGA programming for LPR process [28, 29] and using industrial computers dealing with bad outdoor conditions [30] are examples of this. The difference of these solutions from our work is in installation costs. Also using microcomputers like Raspberry Pi in LPR has been studied in recent years [31, 32].

3   USED HARDWARE AND SOFTWARE

This work was aimed at developing a low-budget, stand-alone embedded system without the need for a primary computer. The embedded system was chosen for the raspberry pi 2 because it was cheap and used by very few people. During the study, Raspi 3, which is the new version of Raspi 2, was moved to the market so experiments were carried to it and the results were examined.

Subsequently, algorithms were developed to introduce new plate characters from outside to this system. The work was primarily carried out with vehicles standing or moving at very low speeds. As a result of the study, it was observed that the system was an intelligent system and other country plate formats could easily be converted to text. The fact that the plate is converted to text is the reason why it takes less space in memory and can be transferred quickly when it is necessary to transfer information via WI-FI.

Program runs on both Raspberry Pi 2 and Raspberry Pi 3 and results obtained in ASCII format. After ASCII results have been searched on raspi database, the query returns an "access permitted" or an "access denied" flag. The proposed system is shown in Fig. 2

Fig 2. **Proposed System Scheme**

In this study, we used embedded systems, which are Raspberry Pi 2 (raspi 2) and Raspberry Pi 3 (raspi 3). In Table 1 the hardware structures of raspi 2 and raspi 3 are compared. The results show us: *a)* The frequency of processor of raspi 3 is more than the one of raspi 2. *b)* raspi 3 has got on-board Wi-Fi connectivity. The raspi 3 has 802.11 b/g/n 2.4 GHz Wireless LAN and Bluetooth Classic & Low Energy (BLE) connectors. You can get connected much quicker without the need for any external device. *c)* Raspi 3 needs 2.5 A power supply. With more processor speed and on-board connectivity, it needs more power

In both Raspberries, we used an operating system that is Linux pi01 4.4.26-v7. Both Raspberries have a 16 GB microsd card. On this operating system, we wrote ALPR program in Python 2.7.9 and used a library that contains the version 2.4.9.1 of opencv2.

Table 1 **Raspberry 2 vs Raspberry 3**

	Raspberry pi 2	**Raspberry pi 3**
CPU	900MHz Quad-Core ARM Cortex-A7, Broadcom bcm2836 chipset	1.2GHz Quad-Core ARM Cortex-A53, Broadcom BCM2387 chipset.
No. Of Cores	4	4
GPU	VideoCore IV	VideoCore IV
RAM	1GB LPDDR2 SDRAM (same RAM)	
Wifi	-	802.11 b/g/n Wireless LAN
Bluetooth	-	Bluetooth 4.1
USB	4 x USB2.0 port	4 x USB2.0 port
power source	Micro USB power source, DC 5V 1500mA (1.5A)	Micro USB power source, DC 5V 2500mA (2.5A)
Video Output	Full HDMI port	Full HDMI port
10/100 Ethernet RJ45	Yes	Yes

GPIO	40 GPIO pins	40 GPIO pins
Analog Video Out	Combined 3.5mm audio jack and composite video	Combined 3.5mm audio jack and composite video
Camera interface	Yes	Yes
Display interface	Yes	Yes
SD/MMC	Micro SD card slot	Micro SD card slot
Dimensions	86mm x 56mm x 20mm	85 x 56 x 17mm

In addition, we used picam and webcam to get images. It can be seen from Table 2 that two cameras have almost same features. In our study 960×720 resolution was enough for ALPR process.

We also used microSD card and RAMDrive as recording medium (Table 3). We compared their performances in stability and speed. As expected, using RAM as a recording medium accelerated the duration of the calculations. This method is called using the ram drive.

4   THE PROPOSED SOFTWARE

The technique used to compare the portions of images against one another is Template Matching (Fig 3). The template matching is suitable to use if the standard deviation of the template image in comparison to the source image is negligible. The source image is passed through the matching process, which is carried out pixel by pixel. The template image is moved to all available positions in the source image, which results in numerical index value. This value shows how well the template resembles the image in that position. The template is of size 24 x 42 as depicted in Fig 3. Since the template is fixed, it leads to inaccurate recognition. As seen in pseudo code (Algorithm 1), this method involves the following six stage steps.

- Pre-processing image
- Detection of license plate
- Segmentation of character is done from detected number plate
- Recognition of segmented character
- Access control application
- Template teaching

4.1   Pre-processing Image

We used three stages to increase the performance of the system while preprocessing of the input image (Fig 4a, 5a, 6a).

4.1.1　Converting RGB Image to Gray Scale.　Gray scale conversion technique is used to convert the color image captured by the digital camera to the gray scale image (Fig 4b, 5b, 6b). The function used for gray scale conversion is cv2.cvtColor().

4.1.2　Gausian Blur Filtering.　Gaussian blur is the type of the low-pass filter. It is used for the edge detection. The counterpart of the Gaussian filtering method in the OpenCV library is the Cv2.GaussianBlur() command (Fig 4c, 5c, 6c).

4.1.3　Adaptive Thresholding.　Usually the threshold value is used to convert the image into binary format. But it may not be good in all the conditions where image has different lighting conditions in different areas. In that case, we go for adaptive thresholding. In this situation, the algorithm calculates the threshold for small regions of the image. So we get different thresholds for different regions of the same image and it gives us better results for images with varying illumination (Fig 4d, 5d, 6d). The function which has been used is cv2.adaptive Threshold().

Table 2 **Picam and WebCam Specifications**
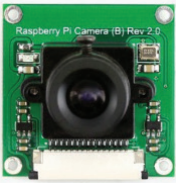
PiCam	WebCam
•　　　　Raspberry Pi Camera (B) Rev 2.0, supports all revisions of the Pi •　　　　5 megapixel OV5647 sensor in an adjustable-focus module •　　　　2592 x 1944 still picture resolution •　　　　720p and 1080p HD video at 30fps •　　　　CCD size: 1/4inch •　　　　Aperture (F): 2.0 •　　　　Focal Length: 6MM (adjustable) •　　　　Diagonal: 75.7 degree •　　　　Sensor best resolution: 1080p •　　　　Dimension: 32mm × 32mm •　　　　amazon.com price: $30	•　　　　Logitech C920 HD Webcam •　　　　Full HD 1080p video calling (up to 1920 x 1080 pixels) with the latest version of Skype for Windows •　　　　720p HD video calling (up to 1280 x 720 pixels) with supported clients •　　　　Full HD video recording (up to 1920 x 1080 pixels) •　　　　H.264 video compression •　　　　Built-in dual stereo mics with automatic noise reduction •　　　　Automatic low-light correction •　　　　Carl Zeiss® optical •　　　　amazon.com price: $65

Table 3 **MicroSD Card and LPDDR2 SDRAM Specifications**

Micro SD CARD	RAM
• SDC4/16GB – 16GB* microSDHC (Class 4) • Capacities: 16GB • microSDHC Card Dimensions 11mm x 15mm x 1mm • Class 4 Speed Rating 4MB/s minimum data transfer rate • Operating Temperature -25°C to 85°C • Storage Temperature -40°C to 85°C	• 1GB LPDDR2 SDRAM • 167 MHz, 200 MHz, 400 MHz, 533 MHz,
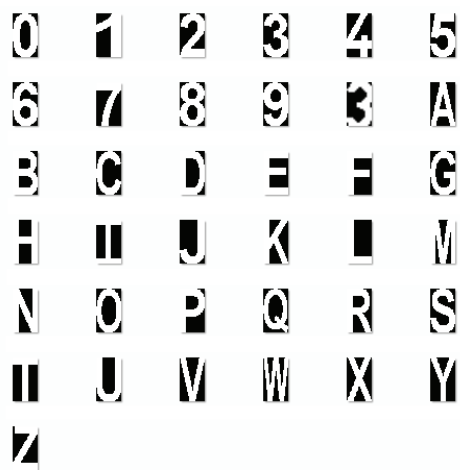
Fig 3 **Templates Used for Matching**
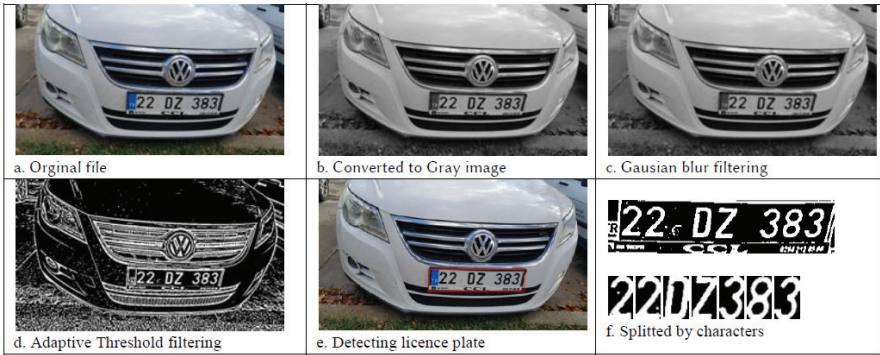
Fig 4 **Examples of License Plate Recognition Phases**

ALGORITHM 1: LPR Process

1. Start

2. Open Webcam

3. If webcam is not activated then

4.   go to step 2

5. Else

6.   take a color photo

7.   convert RGB image to Gray Scale

8.   apply Gaussian and Threshold Filtering

9.   find contours and rectangle

10.   If (contours and rectangle bounding borders) OR (predetermined boundaries) are not found then

11.   go to step 6

12.   End if

13.   cut and save filtered LPP (License Plate Photo)

14.   open saved filtered LPP

15.   find contours and rectangle

16.   If (contours and rectangle bounding borders) OR (predetermined boundaries) are not found then

17.   go to step 6

18.   End if

19.   cut sample character image (SCI) from LPP

20.   resize SCI to 24x42 pixel

21.   write SCI name with X-axis number

22.   if last contours and rectangle

23.   go to step 26

24.   End if

25.   go to step 19

26.   locate first sample

27.   If it is not last sample then

28.   read sample

29.   Else

30.   go to 43

31.   End if

32.   locate first template

33.   If it is not last template then

34.   read template
35.   Else
36.   go to 27
37.   End if
38.   if rmsdiff_2011(sample, template)>125
39.   // Calculate the root-mean-square difference between two images
40.   add template ASCII code to output text
41.   End if
42.   go to step 36
43.display output text
44.End if
33.End if
34.End if
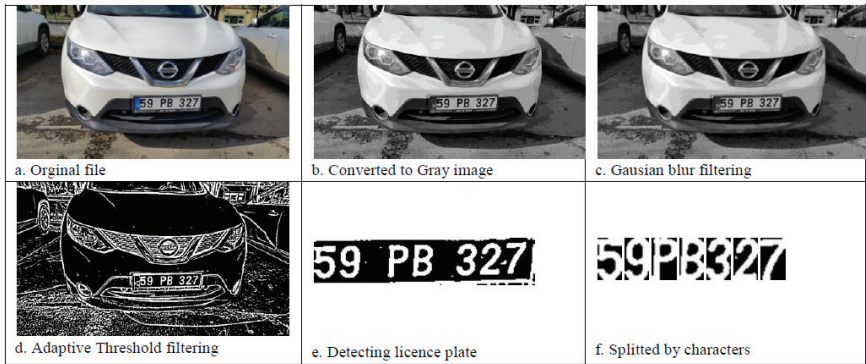
Fig 5 **Examples of License Plate Recognition Phases**
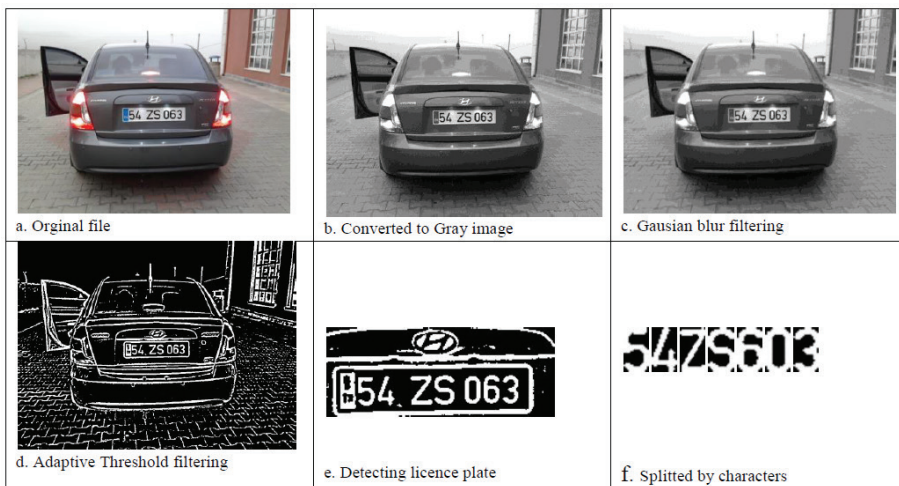
Fig 6 **Example of License Plate Recognition Phases**

4.2   Detection of License Plate

The detection of LP is the most challenging task as the license plate is incorporated in a small region of the whole image and can resist anywhere in the image.

Firstly, if image has different lighting conditions, we use adaptive thresholding. In adaptive threshold technique, the threshold value at each pixel location depends on the neighboring pixel intensities.

Secondly, we try to find contours. Contours can be explained simply as a curve joining all the continuous points (along the boundary), having same color or intensity. The contours are a useful tool for shape analysis and object detection and recognition.

Finally, we calculate and return the minimal up-right bounding rectangle for the specified point set. Then we select and cut the rectangle in appropriate size. This is a license plate (Fig 4e, 5e, 6e).

4.3   Segmentation of Character is Done from Detected Number Plate

We are starting to look for characters on the license plate that we have found in previous stage. For this process we are try to find contours again, select and cut the appropriate size rectangle. We save these rectangles as separate pictures (Fig 4f, 5f, 6f).

4.4   Recognition of Segmented Character

The technique used to compare the portions of images against one another is Template Matching. The template matching is suitable to be used if the standard deviation of the template image in comparison to the source image is negligible. The source image is passed through the matching process, which is carried out pixel by pixel. The template is of size 42×24 as depicted in Fig 3.
To get a measure of how similar two images are, you can calculate the root-mean-square (RMS) value of the difference between the images. If the images are identical, this value is zero. The used function uses the difference function and then calculates the RMS value from the histogram of the resulting image.
Finally, the most appropriate template is selected and the corresponding ASCII code is obtained.

4.5   Access Control Application

The resulting ASCII text is searched in previously defined database.

If the searched text is found in the database, the door is opened. If it is not found, the door is not opened and a new picture-taking process is started.

4.6 Template Teaching

This system is designed to be smart and flexible. When a vehicle with different characters on its LP has been met, it is photographed to be recognized. Then the system divides to the plate characters with the help of the developed software. The ASCII code of the characters is found through the templates of the LP image and characters are saved in order to construct data set for next LPs. Thus, the vehicle plate will be easily recognizable on their arrival.

Fig 7 illustrates some incorrect character samples, which have been taken during the experiments. Incorrect characters that are regularly repeated can be taken to the black list and assumed to be ignored. Likewise, characters that are correct but in different formats can be added to the template list to avoid errors. In Fig 7, examples from the characters in the different forms, which have been taken, are given. Character "4" is seemed to be a good example for showing different formats in Fig 7.

Fig 7 **Learned Different Characters**

5 EXPERIMENTAL RESULTS

In the study, the time from photo taking to conversion to the ASCII code was measured in terms of msec that is called "conversion time". There is zero error in obtaining ASCII code in program results. We collect the experiments in 8 main topics (Table 4).

Table 4 **List of Experiments**

Exp. num.	Embedded system	Auxiliary memory	Picture taking numbers	Picture taking environment	Corresponding figure
1	Raspi 2	Micro SD Card	1000 times	PiCam	Fig 9a. Blue line
2	Raspi 2	Micro SD Card	1000 times	WebCam	Fig 9a. Red line
3	Raspi 2	RAM Drive	1000 times	PiCam	Fig 9b. Blue line
4	Raspi 2	RAM Drive	1000 times	WebCam	Fig 9b. Red line
5	Raspi 3	Micro SD Card	1000 times	PiCam	Fig 10a. Blue line
6	Raspi 3	Micro SD Card	1000 times	WebCam	Fig 10a. Red line
7	Raspi 3	RAM Drive	1000 times	PiCam	Fig 10b. Blue line
8	Raspi 3	RAM Drive	1000 times	WebCam	Fig 10b. Red line

A linear equation was established to select more stable one as the result of the experiment. A common form of a linear equation with two variables x and y is;

$$y = mx + b \tag{1}$$

where m and b designate constants (parameters). The origin of the name "linear" comes from the fact that the set of solutions of such an equation forms a straight line in the plane. In this particular equation, the constant m determines the slope or gradient of that line and the constant term b determines the point at which the line crosses the y-axis, otherwise known as the y-intercept.

It is preferred that the slope we want for our experiments is parallel to the horizontal axis as much as possible. Therefore, the slope m must come close to zero.

6   DISCUSSIONS

We tried to find the configuration we could get from 2 embedded systems and 2 cameras. We have planned 8 different experiments that repeat 1000 times for this.

For Raspi 2, we wrote the images from the webcam and picam to the microSD card and measured the duration (Fig 8a). Then we plotted a linear slope to make a decision. Since $m_{pi\,\mu sd} = 0.0093$ is smaller than

$m_{Web\ \mu sd} = 0.1422$ (Table 5), as it is seen here, we have obtained the result that Picam has given more favorable results.

Table 5 **Linear Equations Obtained from the Plotted Graph**

Exp. num.	Linear Equation		The slope	
1	y = 0,0093x + 2068	(2)	$m_{pi\_\mu sd}$=0,0093	(3)
2	y = -0,1422x + 2059,1	(4)	$m_{Web\_\mu sd}$=0,1422	(5)
3	y = -0,0088x + 2073,3	(6)	m_{pi_RAM}=0,0088	(7)
4	y = -0,0378x + 2103,3	(8)	m_{Web_RAM}=0,0378	(9)
5	y = -0,0587x + 1512,8	(10)	$m_{pi\_\mu sd}$=0,0587	(11)
6	y = -0,412x + 1484,3	(12)	$m_{Web\_\mu sd}$=0,412	(13)
7	y = 0,0003x + 1447	(14)	m_{pi_RAM}=0,0003	(15)
8	y = -0,0252x + 1464,9	(16)	m_{Web_RAM}=0,0252	(17)

a. Raspi 2 with microsd, PiCam vs WebCam

b. Raspi2 with RAM, PiCam vs WebCam
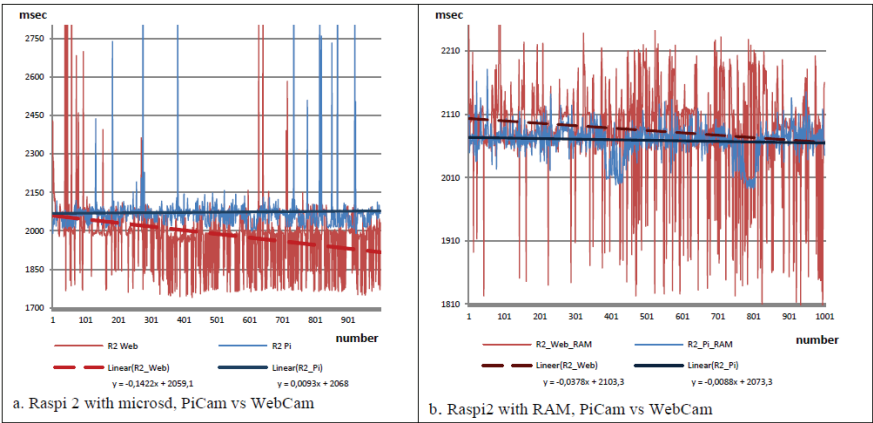
Fig 8 **Raspi 2 PiCam vs WebCam**

Same way for Raspi 2, we wrote the images from the webcam and Pi-Cam to the RAMdrive and measured the duration (Fig 8b). We then plotted a linear slope to make a decision. Since $m_{pi\ RAM} = 0.0088$ is smaller than $m_{Web\ RAM} = 0.0378$, as it is seen here, we have obtained the result that Picam has given more favorable results.

However, $m_{pi\ RAM} = 0.0088$ and $mean = 2068.8$ msec (Fig 9a) are smaller than others, this means that for Raspi 2 we can achieve the result of PiCam's faster and more stable operation in RAMDrive.

a. Raspi 2, fastest, slowest, geometric mean

b. Raspi 3, fastest, slowest, geometric mean
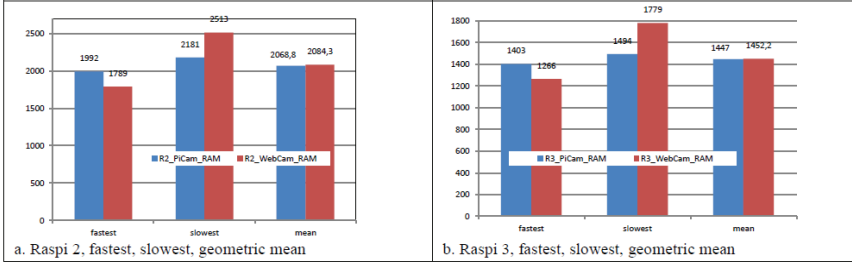
Fig 9 **Raspi 2&3, Fastest, Slowest, Geometric Means**

For Raspi 3, we wrote the images from the webcam and PiCam to the microSD card and measured the duration (Fig 10a). We then plotted a linear slope to make a decision. Since $m_{pi\ \mu sd} = 0.0587$ is smaller than $m_{Web\ \mu sd} = 0.412$ (Table 5), as it is seen here, we have obtained the result that PiCam has given more favorable results.

a. Raspi3 with micro sd, Picam vs Webcam

b. Raspi3 with RAM, Picam vs Webcam
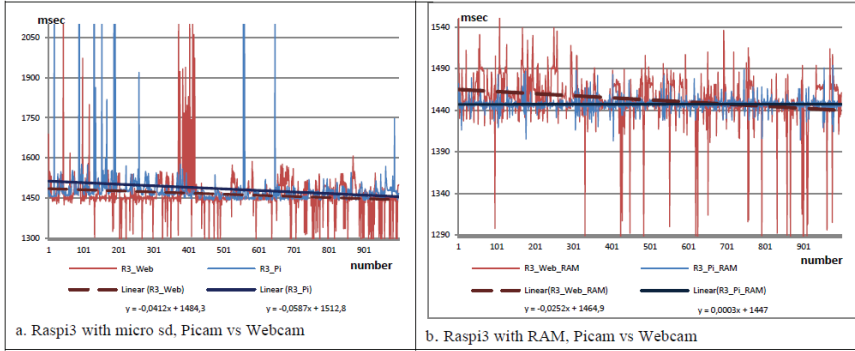
Fig 10 **Raspi 3 PiCam vs WebCam**

Same way For Raspi 3, we wrote the images from the webcam and PiCam to the RAMdrive and measured the duration (Fig 10b). We then plotted a linear slope to make a decision. Since $m_{pi\ RAM} = 0.0003$ is smaller than $m_{Web\ RAM} = 0.0252$, as it is seen here, we have obtained the result that Picam has given more favorable results.

However, $m_{pi\ RAM} = 0.0003$ and $mean = 1447$ msec (Fig 9b) are smaller than others, this means that for Raspi 3 we can achieve the result of Pi-Cam's faster and more stable operation in RAMDrive. In addition, if we compare r2 picam_ram with R3_picam_ram, the stability in R3 is obviously seen (Fig.11).
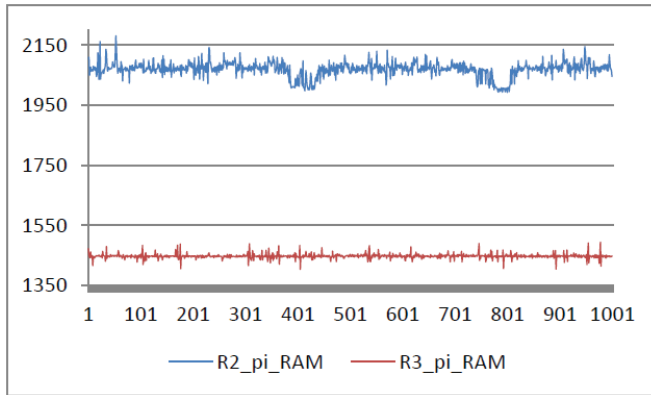
Fig 11 **R2 picam with RAM vs R3 picam with RAM**

7   CONCLUSIONS

In this paper, a system that works by itself, recognizes the plate, and controls the barrier is aimed to be developed. First, the system recognizes plate recognition at a certain distance without error when the necessary teaching steps are applied. As a result of repeating experiments thousands of times, it has been decided that the best choice for reading at fast and constant speed is the following configuration:

- Embedded system: Raspi 3

- Camera: raspberry PiCam

- Auxiliary memory: 1MB RAM disk

- Operating System: Linux pi01 4.4.26-v7

- Compiler: Python 2.7.9

- Library: opencv2 2.4.9.1

The developed system can be traded and widely used by the fees that a normal home user can take. In addition, the program is a smart program so other country plates can be read easily by making small adjustments. Also, since it is an intelligent system, measurements can be made for various angles by making appropriate samples. For example, accurate measurements can be made in the processes performed for vehicles approaching at angles up to ± 30 degrees.

In the continuation of the work, firstly the system can be tested for different weather condition such as in fog, cloudy, sunny, snowy, rainy, daylight, evening time etc. It is thought that it is possible to make a variety of evaluations by translating a plate in a traffic flowing in a later stage into an ASCII code and sending this code to a central database to see if it is

listed in the black list. It is also envisaged to recognize vehicle plates that move in highway speed limits during further studies.

8   ACKNOWLEDGEMENT

REFERENCES

[1],Lijuan Qin and Ting Wang. 2016. Design and research of automobile anti-collision warning system based on monocular vision sensor with license plate cooperative target, *Multimedia Tools and Applications*, (Oct. 2016), 1–14. DOI:10.1007/s11042-016-4042-6

[2],M. Wang, L. Jiang, W. Lu and A. Fang. 2016. Component-model based detection and recognition of road vehicle, In *Progress in Informatics and Computing (PIC), 2015 IEEE International Conference*, (Dec. 2015), DOI:10.1109/PIC.2015.7489887

[3],Ş. Öztürk, B. İnan and Y. Artan. 2016. Color based vehicle classification in surveillance videos, In *Signal Processing and Communication Application Conference (SIU), 2016 24th*, (May. 2016), DOI:10.1109/ SIU.2016.7496076

[4],Noppakun Boonsim and Simant Prakoonwit. 2016. Car make and model recognition under limited lighting conditions at night, *Pattern Analysis and Applications*, (May 2016), 1-13. DOI:10.1007/s10044-016-0559-6

[5],R. Yang, H. Yin and X. Chen. 2016. License Plate Detection Based On Sparse Auto-Encoder, In *Computational Intelligence and Design (ISCID), 2015 8th International Symposium*, (Dec. 2015), DOI:10.1109/ISCID.2015.151

[6],X. Yan, Q. Shen and X. Liu. 2016. Super-resolution Reconstruction for License Plate Image in Video Surveillance System, In *Communications and Networking in China (ChinaCom), 2015 10th International Conference*, (Aug. 2015), DOI:10.1109/CHINACOM.2015.7498016

[7],C. Paunwala and S. Patniak. 2010. An Improved License Plate Extraction Technique Based on Gradient and Prolonged Haar Wavelet Analysis, In *ICWET '10 International Conference and Workshop on Emerging Trends in Technology*, (Feb. 2010), DOI:10.1145/1741906.1742047

[8],Zhang Meng. 2013. PPCA-Based License Plate Detection Algorithm, *ACM SIGSOFT Software Engineering Notes* 38, 3 (May 2013), 1-4. DOI:10.1145/2464526.2464541

[9],V. Shapiro , D. Dimov, S. Bonchev, V. Velichkov , and G. Gluhchev. 2003.Adaptive License Plate Image Extraction, In *CompSysTech '04 Proceedings of the 5th international conference on Computer systems*

and technologies, (Jun. 2004), DOI:10.1145/1050330.1050364

[10], C.Y. Wen, T.S. Sheng, C.C. Tseng, and S.S. Huang. 2016. License Plate Localization and Recognition under Different Illumination Conditions, In *Consumer Electronics-Taiwan (ICCE-TW), 2016 IEEE International Conference*, (May. 2016), DOI:10.1109/ICCE-TW.2016.7520917

[11], H. Samma, C.P. Lim, J.M. Saleh and S.A. Suandi. 2016. A memetic-based fuzzy support vector machine model and its application to license plate, *Memetic Computing* 8, 3 (Sep 2016), 235-251. DOI:10.1007/s12293-016-0187-0

[12], Tiange Li and Song Yu. 2016. Parallel License Plate Recognition Scheme based on Image Splicing for Intelligent Transportation System, In *Computer Science and Network Technology (ICCSNT), 2015 4th International Conference*, (Dec. 2015), DOI:10.1109/ICCSNT.2015.7491009

[13], N. Thai-Nghe, and N. Chi-Ngon. 2014. An Approach for Building an Intelligent Parking Support System, In *SoICT '14 Proceedings of the Fifth Symposium on Information and Communication Technology*, (Dec. 2014), 192-201. DOI:10.1145/2676585.2676594

[14], Ahmed El - said. Shaimaa. 2014. Shadow aware license plate recognition system, *Soft Computing* 19, 1 (Jan 2015), 225-235. DOI:10.1007/s00500-014-1245-5

[15], P. Liu, G. Li and D. Tu. 2016. Low-quality License Plate Character Recognition Based on CNN, In *Computational Intelligence and Design (ISCID), 2015 8th International Symposium*, (Dec. 2015), DOI:10.1109/ISCID.2015.153

[16], V. Jain , Z. Sasindran, A. Rajagopal, S. Biswas , H.S. Bharadwaj and K.R. Ramakrishnan. 2016. Deep Automatic License Plate Recognition System, In *ICVGIP '16 Proceedings of the Tenth Indian Conference on Computer Vision, Graphics and Image Processing*, (Dec. 2016), DOI:10.1145/3009977.3010052

[17], M. Mohandes, M. Deriche, H. Ahmedi, M. Kousa and A. Balghonaim. 2016. An Intelligent System for Vehicle Access Control using RFID and ALPR Technologies, *Arabian Journal for Science and Engineering* 41, 9 (Sep 2016), 3521-3530. DOI:10.1007/s13369-016-2136-0

[18], S. Kumari, D.K. Guptar, and R.M. Singh. 2016. A Novel Methodology for Vehicle Number Plate Recognition Using Artificial Neural Network, In *VisionNet'16 Proceedings of the Third International Symposium on Computer Vision and the Internet*, (Sep. 2016), 110-114. DOI:10.1145/2983402.2983432

[19], Y. Jia, T. Gonnot and J. Saniie. 2016. Design Flow of Vehicle License Plate Reader Based on RGB Color Extractor, In *Electro Information Technology (EIT), 2016 IEEE International Conference*, (Aug. 2016),

DOI:10.1109/EIT.2016.7535290

[20], R. Baran, T. Rusc, and P. Fornalski. 2015. A smart camera for the surveillance of vehicles in intelligent transportation systems, *Multimedia Tools and Applications* 75, 17 (Sep 2016), 10471-10493. DOI:10.1007/s11042-015-3151-y

[21], S. Lawlor, T. Sider, N. Eluru M. Hatzopoulou, and M.G. Rabbat. 2016. Detecting Convoys Using License Plate Recognition Data, *IEEE Transactions on Signal and Information Processing over Networks* 2, 3 (Sep 2016), DOI:10.1109/TSIPN.2016.2569426

[22], V. Khare, P. Shivakumara, P. Raveendran, L.K.. Meng and H.H. Woon. 2015. A New Sharpness based Approach for Character Segmentation in License Plate Images, In *Pattern Recognition (ACPR),* 2015 3rd IAPR Asian Conference, (Jun. 2016), DOI: http://dx.doi.org/10.1109/ACPR.2015.7486562

[23], Lining Xu and Yongxu Wu. 2016. New Challenge of Protecting Privacy due to Stained Recognition, In *Computer Software and Applications Conference (COMPSAC), 2016 IEEE 40th Annual,* (Aug. 2016), DOI:10.1109/COMPSAC.2016.232

[24], Rahim Panahi and Iman Gholampour. 2016. Accurate Detection and Recognition of Dirty Vehicle Plate Numbers for High-Speed Applications, *IEEE Transactions on Intelligent Transportation Systems* PP, 99 (Aug. 2016), DOI:10.1109/TITS.2016.2586520

[25], S. Kaur, and S. Kaur. 2014. An Efficient Approach for Number Plate Extraction from Vehicles Image under Image Processing, *(IJCSIT) International Journal of Computer Science and Information Technologies* 5, 3 (Jan. 2014), 2954-2959

[26], Anu Agarwal and Sudhir Goswani. 2014. An Efficient Algorithm for Automatic Car Plate Detection & Recognition, *Advanced Science and Technology Letters 54, (Aug. 2016)*, 13-16 DOI:10.14257/astl.2014.54.04

[27], V.D. Mai, D. Miao and R. Wang. 2012. Building a License Plate Recognition System for Vietnam TollBooth, In *SoICT '12 Proceedings of the Third Symposium on Information and Communication Technology*, (Aug. 2012), 107-114. DOI:10.1145/2350716.2350734

[28], M. Ashourian, N. Daneshmandpoura. O.S. Tehrania and P. Moallemb. 2013. Real Time Implementation of a License Plate Location Recognition System Based on Adaptive Morphology, *International Journal of Engineering IJE TRANSACTIONS B: Applications* 26, 11 (Nov. 2013), 1347-1356

[29], N. Bellas, S.M. Chai, M. Dwyer and D. Linzmeier. 2006. FPGA implementation of a license plate recognition SoC using automatically generated streaming accelerators, In *Parallel and Distributed Processing Symposium, 2006. IPDPS 2006. 20th International*, (Apr.

2006), DOI:10.1109/IPDPS.2006.1639437

[30],T. Duy Ta , D. Anh Le, M. Thi Le, T. Van Tran, T. Trong Do, V. Duc Nguyen, C. Van Trinh, and B. Jeon. 2015. Automatic Number Plate Recognition on Electronic Toll Collection Systems for Vietnamese Conditions, In *IMCOM '15 Proceedings of the 9th International Conference on Ubiquitous Information Management and Communication*, (Jan. 2015), DOI:10.1145/2701126.2701187

[31],D. Lavanya, C.V. Keerthi latha, and Nirmala. 2015. License Plate Extraction Of Images Using Raspberry Pi, *International Journal of Advanced Research in Computer Engineering & Technology (IJARCET)* 4, 1 (Jan. 2016), 183-189

[32],M. Jyorthirmayee, and S. Aruna. 2016. An Implementation of Automatic Vehicle License Plate Recognition for Security System, *International Journal & Magazine of Engineering, Technology, Management and Research* 3, 10 (Oct. 2016), 552-556

Chapter 4

A DECISION MAKING MODEL BASED CASE STUDY TO PREDICT AND PREVENT POTENTIAL CRIMINAL BEHAVIOUR TENDENCY: THE GENOM-IST PROJECT

İnci ZAİM GÖKBAY[1]

1   Asst.Prof., İstanbul University, Informatics Department, inci.gokbay@istanbul.edu.tr

1. Introduction

Individual, becomes human with the society and substantiates his/her existence. He/she learns social behaviors with interactive relations in society and this society's culture decides for him/her what to learn. Regarding to Plato; society's mission is to designate and educate child's potential to have good behavior. Patriot, peaceful, jovial, good hearted, qualified individuals can only grow up with the healthy and egalitarian society which has powerful, tenacious community life. Well-being behavior outputs are strongly related with the inputs of good living, equal and high skilled education, high socio-economic and cultural conditions. However economic and technological developments in recent years has first draw a socio-economic statu difference line than grew it to a gap between society members. Depending upon this gap; high rates of migration, poverty, inequalities in education, unequal employment opportunities and earnings, health risks, inadequacy in family relations, and all insufficient enclosing living conditions occured and play important role in child's behaviors. With the industrial revolution, the mission of supporting child's well-being has begun to transform into different forms of child abuse. Different abuse types of society have evolved child's cognitive and perceptual forms to be a warrior rather than being healthy happy social human.

To develop a prediction model of human behavior, system of input-output relations, process units and mathematical model of processing principle should be defined. Mind can be defined as complex adaptive system, because of its flexibility and can improve its performance by monitoring and adjusting its own configuration and operations in response to feedback from surrounding environment. As can be seen in Figure 1 an adaptive system is an evolving network of relationships. Behavior is the impulse response of this adaptive filter (or in other words mind).

Diversity of environment forces mind to make many experiment and gain different experiences. As epigenetic studies show in recent years' genetic predispositions are related to genetic digestion and all other genetic histories (Riddihough & Zahn, 2010), (Bell, 2011). From this point of view, we do not only have information in our life time experience we also have genetic experience information in our cells from our family tree. Complex Adaptive Systems (CAS) are sensitive due to their dependence on initial conditions. Here the very first initial conditions are, genetic information's, the information baby has recorded during gestation and basal metabolism needs.
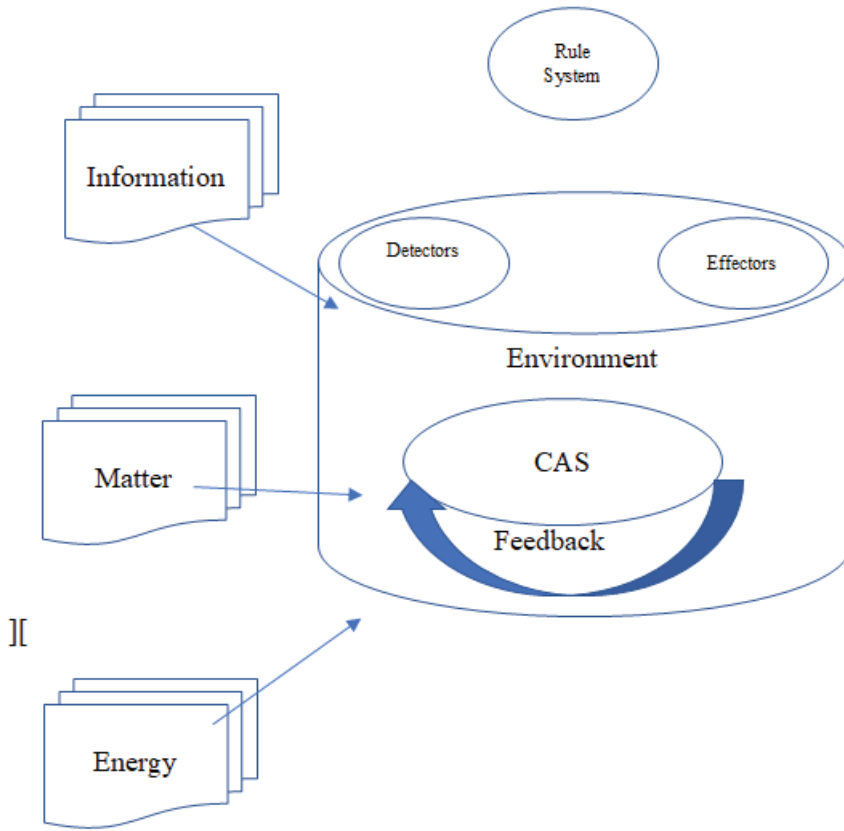
Figure 1: Complex Adaptive System (CAS) (as mind model)

Comparing to a fully-grown adult a newborn infant brain has a similar number of neurons. It can easily be shown to have behavioral and electrophysiological responses to a variety of external stimuli. But has yet to establish and refine the many connections that underlie human behavior in later life (Paus et al., 2001), (Nowakowski, 2006). As time passes newborn builds up its own CAS and initial conditions are updated with inputs coming from family environment. During growth process environment and its inputs updates the boundaries of CAS. So briefly we can say that experiences offer infinite number of information and every information is composed of infinite number of data. Every data entrance to CAS updates the boundaries, changes the initial conditions and builds up a new processing model inside (Figure 1).

To do this; every experience opens another transmission line in adaptive system (in mind). Transmission Line is any physical structure that will guide an electromagnetic wave. So, from this point of view every transmission line carries the environment input data as forward information and experience response of individual is carried as backward information. The

summation of this two information will create the updated boundary conditions. Boundary conditions – called in this work as Personality - which we may call as individual's response are made up of statements about behavior patterns that are stable over time and across situations (Figure 2). According to Costa and McCrae (Costa, 1989), personality is defined as the stable pattern of variation in individual acting, thinking, and experiencing. In stable systems, every bounded input produces a bounded output which we before called as forward and backward information.
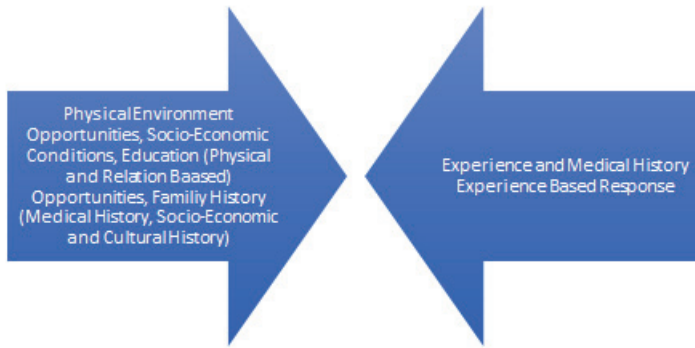
Figure 2: Transmission Lines: Forward Information and Backward Information

Personality arises from interactions between forward information that carries the situation in which the individual is placed and backward information processes that take place inside the individual. Incoming information is processed with the sum of initial conditions which has epigenetic, neurological information and previous experience. From this CAS description, it can be clearly seen tahat "Personality" is the intersection of two main headings: Temperament and Character. Temperament reflects the biological and innate part whereas character, modeled by experience and learning.

$$\sum_{i=0}^{N} Temperament + \sum_{l=0}^{P} Character = Personality \tag{1}$$

In literature temperament is described as a neurobiological element of the individual that differs from person to person in emotions, sociability, and self-control. Temperament is epigenetic, originating in genes but also affected by child-rearing practices. According to the psychobiological model, temperament represents constitutionally based individual differences in emotional and motor reactivity, as well as self-regulation, dem- onstrating consistency across situations and relative stability over time (Rothbart, 1981).

$$\sum_{i=0}^{N} \text{Family Relation Experience}$$

$$+ \sum_{j=0}^{M} \text{School Environment Experience}$$

$$+ \sum_{k=0}^{O} \text{Peer Relation and Community Relation Experience}$$

$$= \sum_{l=0}^{P} \text{Character} \tag{2}$$

Conservation of energy theory states that the total energy of an isolated system remains constant. Here isolated system refers to human and the surrounded relations as formulated in (1). Also the law means that the created energy can not be destroyed but it can be transformed or transferred from one form to another. Thus, if we have chance to predict risk behaviors (created energy) then we'll have another chance to prevent children to be criminal (transformed energy). With this hypothesis, we aimed to develop a prevention services model based on predicting the risk behaviors of children. From 2014 to 2018 we did a field study with Genomist Project team. Project was funded by İstanbul Kalkınma Ajansı (Project Code: YEN-112, ÇGE-143, www.hayatvecocuk.net). Here in this book chapter, based on my field experience I'm going to introduce the importance of data, in child's welfare and the quality of life.

2. Attributes and Weights Of Stochastic Approach

Piaget proposed that infants construct knowledge through their interactions and their own motor activity instead of observing (Piaget, 1952). All environments that child is interacted with (including family, educational and physical environment that surround) acts on their intelligence level, temperament and characteristic features. Temperament involves individual differences in emotional, motor, and attentional reactivity and self-regulation of behavior and attention (Putnam, Sanson, & Rothbart, 2002). Character describes the differences of individual in self-object relationships, beginning with parental attachments in infacy, then self object differentiation in toddlers, and continue to mature. Briefly, temperarement refers to the way a human is born, character refers to what they make themselves intentionally. Researchers commonly agree that personality is a product of innate heritable dispositions and interactions with environmental influences as formulated in equation (1). Mentioned features develop the processing algorithm of CAS where the impulse response is behavior. From this point of view, as mentioned above and also in figure 2 temperament or initial val-

ues may be called as reference information that an individual has epigenetic, neurological and initial health condition information. Existing studies shows the important links between environmental exposures, epigenetic alterations, and shifts in behavioral outcomes relevant to temperament. And multiple adversities exposure during gestation results in temperament profiles marked by high levels of negative behavioral inhibition and risk for anxiety, with these effects mediated by epigenetic processes.

It was a common belief in ancient times that the emotional state of a mother may affect the child she is carrying (Ferreira, 1965). Unfortunetly people dont think like that any longer, studies indicate that 4 to 8 percent of pregnant women experience abuse during pregnancy (Adams Hillard, 1985; Helton, McFarlane, & Anderson, 1987). And unfortunaletly if a woman is depressed, anxious, or stressed while she is pregnant, this will increase the risk for her child having a wide range of adverse outcomes, including emotional problems or impaired cognitive development (O'connor, 2002). In conclusion, prenatal stress effects early motor and mental development of the child.

$$Reference\ Initial\ Conditions = \begin{bmatrix} X_{0_1} & X_{0_2}, X_{0_3} \end{bmatrix}$$

Where;

$X_{0_1} = Epigenetic\ Information$

$X_{0_2} = Prenatal\ Information$

$X_{0_3} = Attachment$

(3)

As newborn grows up initial condition information vector in Eq. (3) become updated and feedbacks the processing algorithm with family relationships. Especially unstressed pregnancy and after healthy mother-child attachment plays an important role in personality development.
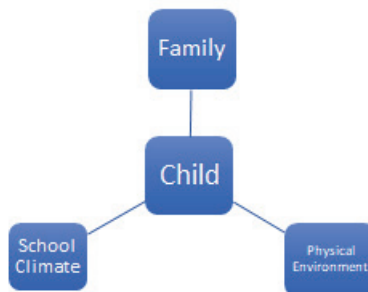
Figure 3: Defined Universe for Mathematical Model: Family Relations, School and Physical Environments

2.2. Family Relations Attributes and Weights Of Stochastic Approach

Sigmund Freud described the influence of traumatic experiences on the development of depression and major disorders more than 100 years ago. And it has been nearly 50 years that studies described Transgenerational transmission of trauma (TTT). Transgenerational transmission of trauma (TTT), is the process of which a trauma that happened to the first generation is passed on to the second generation (N. P. Kellermann, 2009). According to TTT we can briefly say that epidemic illness, wars, slavery, torture and torment history lefts its visible and invisible marks not only on the survivors, but also on their children. Kellermann (N. P. Kellermann, 2001)suggested four major theorethical approaches to understand trauma transmission: (i) psychodynamic relational models; (ii) sociocultural and socialization models; (iii) family systems and communication models; and (iv) biological or genetic models. According to these theories, Kellermann (N. P. Kellermann, 2009) explains unconsciously displaced parental emotions, inadequate parenting behavior, family enmeshment, and/or a hereditary predisposition, as a function of trauma transmission. The cycle of violence posits that victimized/ traumatized children grow up with the tendency of impulsive aggression behavior. And they will potentially be harmful and will have disposition to aggrieve the others.

Prenatal substance addiction or exposure to substances (nicotine, alcohol, or illegal drugs) is an established risk factor for poor fetal growth, preterm birth and neurodevelopmental impairment (such as attention deficit disorder or poor cognitive and language development). Domestic violence is a traumatizing experience that often is chronic and repetitive and has a myriad of negative consequences for its victims. Especially violence during pregnancy represent serious threats to the physical and emotional health of woman and the child   before and after birth. Some studies showed that preschool-age children exposed to domestic violence have more behavior problems, social difficulties, posttraumatic-stress symptoms, greater trouble developing empathy, and less-developed verbal abilities than non-witnesses (Fantuzzo et al., 1991; Graham-Bermann & Levendosky, 1998; Hinchey & Gavelek, 1982; Huth-Bocks, Levendosky, & Semel, 2001).

Ainsworth (M. D. S. Ainsworth, Bell, S. M., & Stayton, D. ; M. D. S. Ainsworth, Blehar, M. C., & Waters, E. , 1978) and Bowlby (M. D. S. Ainsworth & Bowlby, 1991) defined the attachment as a deep and enduring emotional bond that connects one person to another across time and space. And (Bowlby, 1969) has assumed that the attachment relationship with the parents is to be a central basis for development in other areas of the child's life, such as cognitive functioning and learning. For future cognitive development quality of attachment is supposed to have some

consequences. (Hazen & Durrett, 1982), in a longitunal research observed that a 2-year-old child who is securely attached have been more active in exploring the environment. They have also been more disposed to learn (Waters, Wippman, & Sroufe, 1979) and more enthusiastic when solving problems (Matas, 1978). There are studies which concludes that expectations for problem-solving situations the performance securely attached children compared to anxiously attached children are to be better. Some works reported that there is a significant direct association between pathologic family environments and substance use, depression, disordered eating, lower self-esteem, and suicidality (Allen, Hauser, Eickholt, Bell, & Oconnor, 1994; Aydin & Oztutuncu, 2001; Delaney, 1996; Fergusson, Woodward, & Horwood, 2000; Hollis, 1996; King, 2001; Neumark-Sztainer, 2001; O'Donnell, Stueve, Wardlaw, & O'Donnell, 2003; Sale, Sambrano, Springer, & Turner, 2003).

In our project, initial condition attributes are obtained in two steps. In the first step a psychiatrist and a criminal psychologist made semi-structured interviews with the convicted individuals in penal institutions and based upon their experiences and interview results we developed a questionnaire including structered and semi-structured interview parts. Main topics (or main attributes of the system) are summarized in Figure 4. As it will be explained later from this event set (So called Initial Condition Event Set-ICES) we obtained weight coefficients (w_i) and attributes (X_i).

$$ICES = \sum_{i=0}^{N} w_i X_i$$

(4)

Figure 4: Family Universe of Mathematical Model (Summary)

2.2. School Environment Attributes and Weights Of Stochastic Approach

Second important environment that has influence on child after his/her family is school environment. School is a complex environment with many participants and stakeholders–children, parents, teachers, school leaders, staff, community partners and more. It is the first environment, without family protection, that children are alone in society. School has socializing agent function for children, in addition to children's intellectual school has mission to increase social, behavioral and academic development. Unfortunately, in recent years' school environment turned to a place which chilhood bullying and victimization by peers ocur (Olweus, 1978). School bullying creates a fear climate and decreases the quality of life for all participants. But admittedly there is a strong relationship between parenting factors.

As we did to find initial condition attributes we again in the first step a psychiatrist and a criminal psychologist made semi-structured interviews with the teachers, guidance counselors and other partners at schools and based upon their experiences and interview results a questionnaire including structered and semi-structured interview parts developed. Main topics (or main attributes of the system) are summarized in Figure 5. As it will be explained later from this event set (So called School Climate Event Set-SCES) we obtained weight coefficients (w_{ij} and attributes (X_i).

$$SCES = \sum_{i=0}^{N} w_i X_i$$

(5)

Figure 5: School Universe of Mathematical Model (Summary)

2.3. Physical Environment and Community Relation Attributes and Weights Of Stochastic Approach

Every city has unsafe neighborhoods where the chances of being a part of crime are dramatically higher than in the rest of the city. The spatial concentration of crime is a consequence of poverty, race and ethnicity, immigration, the labor market, age composition, family structure, homeownership, and residential stability. Crime and violence have been associated with the low socioeconomic status (SES). Demographic structure, culture and SES of neighborhood influences the child's character.

Being in relation with the individuals that has tendency to be a criminal, growing at the places where violence and crime is a daily activity constitutes violence. These children plays with weapons instead of swing. Their idols are gang related. Their dreams are about being a powerful hero such as them. The characteristics of healthy social development are associated family, school and with external stimulus.

Main topics (or main attributes of the system) are summarized in Figure 6. As it will be explained later from this event set (So called **Physical Environment and Community Relation** Event Set-PECRES) we obtained weight coefficients (w_i) and attributes (X_i).

$$PECRES = \sum_{i=0}^{N} w_i X_i$$

(6)

Figure 6: *Physical Environment-Community Relation Universe of Mathematical Model (Summa*

3. Linear Systems

In this prediction model, CAS is assumed as a linear system process [S] that generates a behavior. Here behavior is an event [E] set as the response to n independent real input variables $\{X_1, X_2, X_3, \ldots, X_n\}$ as shown in Figure 3.
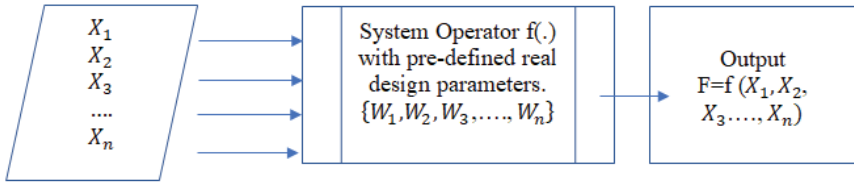
Figure 7: Mathematical Model for Human Behavior Related with Environment described as n-Dimensional System

Let F designates the utility function for the event set E. Let $\{W_1,W_2,W_3,\ldots, W_n\}$ be the pre-assigned real system parameters then, the linear utility function is given by

$$F = f(X_1, X_2, X_3\ldots, X_n) = \sum_{i=0}^{n} W_i X_i \qquad (7)$$

In vector notation

$$F = [W]^T [X]$$

$$\text{Here } [W]^T = [W_1\ W_2\ W_3 \ldots W_n] \text{ and } [X]^T = [X_1\ X_2\ X_3 \ldots X_n] \qquad (8)$$

For a CAS operating as a linear system [S], the system parameters $\{W_i; i=1,2,3,..,n\}$ may be processed as weighting coefficients on the input variables $\{X_i; i=1,2,3,..,n\}$. The input vector [X] will vary dynamically and over a period of time will conduct a fixed state.

Actually, once the model [S] is built, the performance of the system may be measured by assigning proper scores to that state of the input variables. At that state, let the input variables be measured with the scores designated by $\{x_1,x_2,x_3,\ldots, x_n\}$ and the weight coefficients $\{w_1,w_2,w_3,\ldots, w_n\}$ Then, the performance score of linear system F is given by

$$F = \sum_{i=0}^{n} w_i x_i \qquad (9)$$

As before mentioned initial values and boundaries of CAS will be updated depending upon individual's environmental interactions. So, then it will be appropriate to bound both input variables and the weight factors over some intervals satisfying the following inequalities.

$$X_{min} \leq X_i \leq X_{max}$$

$$W_{min} \leq W_i \leq W_{max}$$

$$(10)$$

In above descriptions, the min and max subscripts refers to lower bound (the initial condition's and boundary's lowest experience) and upper bound (the initial condition's and boundary's highest experience) of individual, respectively. With the notations above, it will be accurate to assess the maximum and minimum value of the performance score as;

$$F_{max} = W_{sum}X_{max}; where\ W_{sum} = \sum_{i=0}^{n} W_i$$

$$F_{min} = W_{sum}X_{min}; where\ W_{sum} = \sum_{i=0}^{n} W_i$$

$$(11)$$

For many practical implications, the system performance can be expressed as the efficiency η and can be defined in percentage as follows.

$$\eta = \frac{F}{F_{max}} = \sum_{i=1}^{n} \left[\frac{W_i}{W_{sum}}\right]\left[\frac{X_i}{X_{max}}\right]$$

$$(12)$$

System failure can be described as

$$\mu = 1 - \eta$$

$$(13)$$

These definitions can lead us to describe and predict risk behavior pattern that will tend individual to have criminal act with stochastic systems employing the random input-variables.

4. Stochastic Approach to Describe Pattern of Risk Behavior Tendency

The event under consideration is described by means of an n-dimensional vector and its performance is measured using a utility function which is expressed as the weighted-linear sum of. In other words, if the event vector is given by

$$[X] = \begin{bmatrix} x_1 \\ x_2 \\ x_3 \\ \cdots \\ x_n \end{bmatrix}$$

(14)

Then, its linear weighted sum is defined as

$$X_w = w_1 x_1 + w_2 x_2 + w_3 x_3 + \cdots + w_n x_n = [W]^T[X] = [X]^T[W] \quad (15)$$

In (15), is called the weight matrix. For the present case, is given by

$$[W] = \begin{bmatrix} w_1 \\ w_2 \\ w_3 \\ \cdots \\ w_n \end{bmatrix}$$

(16)

with non-negative entrees $w_i \geq 0$. The non-negative real scalar X_w is called the performance measure of Stochastic Random Event (SRE). If all the random variables $\{x_i, w_i\}$ are properly normalized then, X_w may be called as a utility score, probability of occurrence or a figure of merit of stochastic random event. For many applications, entrees of SRE vector [X] and weight vector [W] are normalized in such a way that they satisfy the following inequalities.

$$0 \leq x_i \leq 1$$
$$0 \leq w_i \leq 1$$
$$w_{sum} = w_1 + w_2 + w_3 + \cdots + w_n = 1$$

(17)

such that

$$i = 1,2,3,\ldots,n$$

As far as the measure of risk behavior (RBM-risk behavior measure) concept is concerned, X_w is generically defined as the risk behavior measure of an individual. It may be normalized with respect to the individuals whom are convicted.

For example, if we compare the risk behavior life map tends to be a criminal of m different convicted individual, and if the most powerful map optimized from the set of convicted individual maps $\{X_w\}_{rbc}$ is set to unity (i.e. $\{X_w\}_{rbc}=1$), then for all individuals that has a life map similar to convicted individauls set composed of criminal' life map, X_w must satisfies the

following inequality.

$$0 \leq X_w \leq 1 \tag{18}$$

In general, we may consider the risk behavior vector [X] (-that has tendency to act as a criminal) as a stochastic random event set $\{X\}$. Further, we presume that X is composed of n-mutually exclusive sets $\{X_i\}$ such that

$$\{X\} = \{x_1, x_2, \dots, x_n\} = \{x_1\} \cup \{x_2\} \cup \{x_3\} \dots \cup \{x_n\} \tag{19}$$

or in general we can express as

$$\{X\} = \{X \cap x_1\} \cup \{X \cap x_2\} \cup \{X \cap x_3\} \cup \dots \cup \{X \cap x_n\} \tag{20}$$

For example, risk behavior life map may be described by means of the following main attributes (or main variables)

$$\{x_1\} = \{Neurological\ Information\}$$
$$\{x_2\} = \{Epigenetic\ Information\}$$
$$\{x_3\} = \{Medical\ Information\}$$
$$\{x_4\} = \{Family\ Relation\ Experience\}$$
$$\{x_5\} = \{School\ Environment\ Experience\}$$
$$\{x_6\} = \{Peer\ Relation\ Experience\}$$
$$\{x_7\} = \{Physical\ Environment\ Experience\}$$
$$\{x_8\} = \{Neighborhood\ Environment\ Experience\}$$

In the above formulation, one can properly select the weight coefficients W_i and normalize each attribute group with respect to its maximum score $(x_i)_{max}$ so that inequalities given by (17) is satisfied.

5. Conclusion

From all experiences in field we had in 4 years, proved us that the usage of mathematical models to predict the risk behavior life map patterns will be helpful tools to prevent criminal actions for children. We had the chance to screen, make surveys and analysis to 10.000 individual. From that population; we had chance to deep analyse, follow the prediction model based prevention system success on them. 300 children have been serviced including prediction model analysis, rehabilitation process, follow up process. And till now those population, despite they live in same risk map environment, has the ability to decide their own dream's life map. They have the ability to create a safe zone inside the risk zones. They know their rights and where to go if they feel they are danger. In this chapter, I

introduced only a short outline of a huge project. Figure8-9 and 10 shows a short summary flow diagram of project.
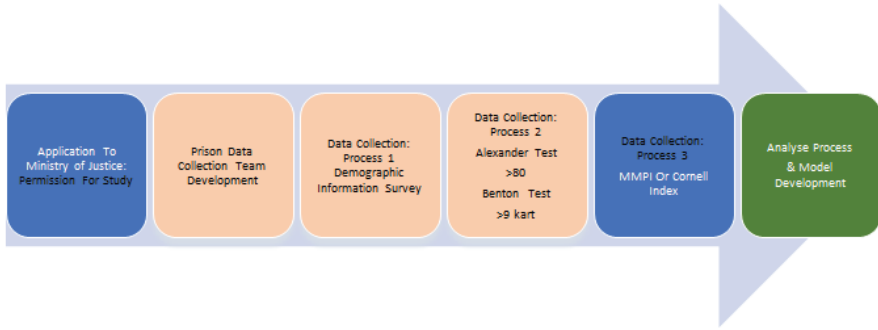
Figure 8: Prediction Model Development and Analysis Process Regarding Prison Data

Figure 9: Prediction Based on Prediction Model Developed in Step 1
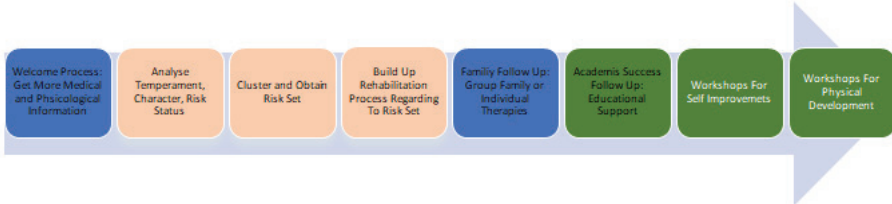
Figure 10: Prevention System Based on Prediction Model 1 &2

Acknowledgemets

References

Adams Hillard, P. J. (1985). Physical abuse in pregnancy. *Obstet Gynecol, 6*(2), 185-190.

Ainsworth, M. D. S., Bell, S. M., & Stayton, D. . Infant-mother attachment and social development. . In *The introduction of the child into a social world* (In M. P. Richards (Ed.) ed., pp. 99-135). London: Cambridge University Press. .

Ainsworth, M. D. S., Blehar, M. C., & Waters, E. . (1978). *Patterns of Attachment: A Psychological Study of the Strange Situation*: Hillsdale, Lawlence Erlbaum Associates.

Ainsworth, M. D. S., & Bowlby, J. (1991). An Ethological Approach to Personality-Development. *American Psychologist, 46*(4), 333-341. Retrieved from <Go to ISI>://WOS:A1991FG02600025. doi:Doi 10.1037/0003-066x.46.4.333

Allen, J. P., Hauser, S. T., Eickholt, C., Bell, K. L., & Oconnor, T. G. (1994). Autonomy and Relatedness in Family Interactions as Predictors of Expressions of Negative Adolescent Affect. *Journal of Research on adolescence, 4*(4), 535-552. Retrieved from <Go to ISI>://WOS:A1994QL36700006. doi:DOI 10.1207/s15327795jra0404_6

Aydin, B., & Oztutuncu, F. (2001). Examination of adolescents' negative thoughts, depressive mood, and family environment. *Adolescence, 36*(141), 77-83. Retrieved from <Go to ISI>://WOS:000169175900006.

Bell, J. T., & Spector, T. D. . (2011). A twin approach to unraveling epigenetics. *Trends in Genetics, 27*(3), 116-125. Retrieved from https://www.ncbi.nlm.nih.gov/pubmed/21257220. doi:10.1016/j.tig.2010.12.005

Bowlby, J. (1969). *Attachment and loss* (Vol. 1). New York: Basic Books. .

Costa, P. T., & McCrae, R. R. . (1989). NEO five-factor inventory (NEO-FFI). *Odessa, FL: Psychological Assessment Resources, 3*.

Delaney, M. E. (1996). Across the transition to adolescence: Qualities of parent/adolescent relationships and adjustment. *Journal of Early Adolescence, 16*(3), 274-300. Retrieved from <Go to ISI>://WOS:A1996VB97000002. doi:Doi 10.1177/0272431696016003002

Fantuzzo, J. W., DePaola, L. M., Lambert, L., Martino, T., Anderson, G., & Sutton, S. (1991). Effects of interparental violence on the psychological adjustment and competencies of young children. *J Consult Clin Psychol, 59*(2), 258-265. Retrieved from https://www.ncbi.nlm.nih.gov/pubmed/2030186.

Fergusson, D. M., Woodward, L. J., & Horwood, L. J. (2000). Risk factors and life processes associated with the onset of suicidal behaviour during adolescence and early adulthood. *Psychol Med, 30*(1), 23-39. Retrieved from https://www.ncbi.nlm.nih.gov/pubmed/10722173.

Ferreira, A. J. (1965). Emotional factors in prenatal environment. A review. *J Nerv Ment Dis, 141*(1), 108-118. Retrieved from https://www.ncbi.nlm.nih.gov/pubmed/5320604.

Graham-Bermann, S. A., & Levendosky, A. A. (1998). Traumatic stress symptoms in children of battered women. *Journal of interpersonal violence, 13*(1), 111-128.

Hazen, N. L., & Durrett, M. E. (1982). Relationship of Security of Attachment to Exploration and Cognitive Mapping Abilities in 2-Year-Olds. *Developmental psychology, 18*(5), 751-759. Retrieved from <Go to ISI>://WOS:A1982PF48000014.

Helton, A. S., McFarlane, J., & Anderson, E. T. (1987). Battered and pregnant: a prevalence study. *Am J Public Health, 77*(10), 1337-1339. Retrieved from https://www.ncbi.nlm.nih.gov/pubmed/3631370. doi:10.2105/ajph.77.10.1337

Hinchey, F. S., & Gavelek, J. R. (1982). Empathic responding in children of battered mothers. *Child abuse & neglect, 6*(4), 395-401.

Hollis, C. (1996). Depression, family environment, and adolescent suicidal behavior. *J Am Acad Child Adolesc Psychiatry, 35*(5), 622-630. Retrieved from https://www.ncbi.nlm.nih.gov/pubmed/8935209. doi:10.1097/00004583-199605000-00017

Huth-Bocks, A. C., Levendosky, A. A., & Semel, M. A. (2001). The direct and indirect effects of domestic violence on young children's intellectual functioning. *Journal of family violence, 16*(3), 269-290. Retrieved from <Go to ISI>://WOS:000170468900004. doi:Doi 10.1023/A:1011138332712

Kellermann, N. P. (2001). Perceived parental rearing behavior in children of Holocaust survivors. *Isr J Psychiatry Relat Sci, 38*(1), 58-68. Retrieved from https://www.ncbi.nlm.nih.gov/pubmed/11381587.

Kellermann, N. P. (2009). *Holocaust trauma: Psychological effects and treatment. . New York*: iUniverse.

King, R. A., Schwab-Stone, M., Flisher, A. J., Greenwald, S., Kramer, R. A., Goodman, S. H., ... & Gould, M. S. . (2001). Psychosocial and risk behavior correlates of youth suicide attempts and suicidal ideation. *Journal of the American Academy of Child & Adolescent Psychiatry, 40*(7), 837-846. Retrieved from https://www.ncbi.nlm.nih.gov/pubmed/11437023. doi:10.1097/00004583-200107000-00019

Matas, L., Arend, R. A., & Sroufe, L. A. . (1978). Continuity of adaptation in the second year: The relationship between quality of attachment and later competence. . *Child development*, 547-556.

Neumark-Sztainer, D. M. A. D. (2001). Family mealtime while growing up: Associations with symptoms of bulimia nervosa. Eating Disorders, . *9*(3), 239-249.

Nowakowski, R. S. (2006). Stable neuron numbers from cradle to

grave. *Proceedings of the National Academy of Sciences, 103*(33), 12219-12220. Retrieved from https://www.ncbi.nlm.nih.gov/pubmed/16894140. doi:10.1073/pnas.0605605103

O'connor, T. G., Heron, J., Golding, J., Beveridge, M., & Glover, V. . (2002). Maternal antenatal anxiety and children's behavioural/emotional problems at 4 years: Report from the Avon Longitudinal Study of Parents and Children. . *The British Journal of Psychiatry, 180*(6), 502-508.

O'Donnell, L., Stueve, A., Wardlaw, D., & O'Donnell, C. (2003). Adolescent suicidality and adult support: The reach for health study of urban youth. *American Journal of Health Behavior, 27*(6), 633-644.

Olweus, D. (1978). *Aggression in the schools: Bullies and whipping boys*: Hemisphere.

Paus, T., Collins, D., Evans, A., Leonard, G., Pike, B., & Zijdenbos, A. (2001). Maturation of white matter in the human brain: a review of magnetic resonance studies. *Brain research bulletin, 54*(3), 255-266.

Piaget, J. (1952). The origins of intelligence in children (M. Cook, Trans.). New York, NY, US. In: WW Norton & Co. http://dx/. doi.org/10.1037/11494-000.

Putnam, S. P., Sanson, A. V., & Rothbart, M. K. (2002). Child temperament and parenting. *Handbook of parenting, 1*, 255-277.

Riddihough, G., & Zahn, L. M. (2010). What is epigenetics? In: American Association for the Advancement of Science.

Rothbart, M. K. (1981). Development of individual differences in temperament. *Advances in developmental psychology, 1*, 37-86.

Sale, E., Sambrano, S., Springer, J. F., & Turner, C. W. (2003). Risk, protection, and substance use in adolescents: a multi-site model. *Journal of drug education, 33*(1), 91-105.

Waters, E., Wippman, J., & Sroufe, L. A. (1979). Attachment, positive affect, and competence in the peer group: Two studies in construct validation. *Child development*, 821-829.

Chapter 5

THE ROLE OF FOOD CHAIN ON THE RISING OF ANTIBIOTIC RESISTANT BACTERIA

Mevhibe TERKURAN[1]

1 Ass. Prof., Department of Gastronomy and Culinary Arts, Kadirli School of Applied Sciences, Osmaniye Korkut Ata University,mevhibeterkuran@windowslive.com

1. Introduction

In recent years, there has been a rapid increase in the number of anti-biotic-resistant (AR) and multidrug-resistant (MDR) bacteria worldwide. There is a wide range of studies regarding the presence of multidrug-resistant bacteria in various countries, both in humans and in food animals and fruit and vegetables. In addition to this, the report of the World Health Organization in 2014 reported that this problem is an increasingly serious threat to public health. In several studies, higher antibiotic resistance levels have been reported in various bacteria such as *Salmonella* spp., *E. coli*, *Campylobacter* spp., *Staphylococcus aureus*, and *Enterococcus* spp. causing infection disease or intoxication in the public. According to the WHO; both surveillance programs and strategies should be used together to prevent and reduce antimicrobial-resistant bacterial dissemination among the World (World Health Organization, 2014). Besides, these aforementioned bacteria may cause serious diseases that may result in morbidity and mortality in the patients as well as financial effects due to more costly drugs and long staying periods in the hospitals (Caniça et al., 2019). According to some reports; if the drug resistance process is not controlled carefully the death rate attributable to antimicrobial resistance is considered to exceed 10 million deaths per year by 2050, compared to the current 0.7 million death estimate. Thus, a person will die every three seconds because of a resistant microorganism (O'Neil, 2014).

The term of MDR has been considered as some bacterial strains are now resistant to three or more classes of antimicrobial agents. XDR (Extensive Drug Resistance) has been defined as if the bacteria are susceptible to drugs in only one or two antimicrobial categories. Another resistance mechanism is PDR (Pan Drug Resistance) which is defined as antimicrobial resistance to all agents in all available antimicrobials (Magiorakos et al., 2012).

The food chain has an important role in the dissemination of antibiotic-resistant bacteria. In veterinary medicine, the massive use of antibiotics for prophylaxis or treatment of the food animals has the main source of antibiotic-resistant bacteria. In food animals due to digestive tract bacteria, they may gain antibiotic-resistant genes and disseminate them to some pathogens or environmental opportunistic bacteria(Capita and Alonso-Calleja, 2013; O'Neill, 2014).

Foods have been consistent with lots of bacteria because of their natural structure. Nutritional components, high water capacities, and suitable pH value as well as the appropriate temperature of them providing bacterial proliferation easily in the food products. Besides, perishable foods such as meat, chicken meat, dairy products, fruit, and vegetables may also be the

source of these bacteria. Among the important reasons for the presence of ARB / MDR bacteria in meat and meat products; improper antimicrobial use in food animals, for instance; there may be conditions such as prophylaxis when treating their infections. Food handlers can also play a key role in the contamination of MDR bacteria. They can do this in two ways; first, they can cause cross-contamination in the food processing area during; storing, cutting, transferring and other food handling activities. The second way is by carrying these bacteria themselves and by contacting food and transmitting these bacteria. To reduce MDR bacteria in foods, all potential sources of AR/MDR bacteria should be considered and strategies devised widely in the world. Some information about antimicrobial resistance and the problems for the food sectors have been reported by various studies (Hur et al., 2012; Doyle et al., 2013). Fruit and vegetables have been another antibiotic-resistant bacteria route because of antibiotic agents-contaminated irrigation water/organic fertilization. Food animals have been the main sources of spreading AR/MDR bacteria especially the poultry production sector. During the production of poultry, antibiotic-resistant bacteria can be selected in the animal microbiota due to the addition of low concentration antimicrobials to the animal feed and these bacteria can be transmitted to the environment with animal waste. Another important factor in the selection of resistant bacteria in the environment is manure usage in agricultural fields. The pond bacteria may also be gained antibiotic-resistant genes because of antibiotic usage in the aquaculture industry (Nonaka et al., 2012).

Urban wastewater from drug production wastes and healthcare facilities and habitats are another important way to spread resistant bacteria to the environment. These sites play an important role in the selection of antimicrobial-resistant bacteria, including antimicrobial agents and their derivatives (Marathe et al., 2013; Michael et al., 2013). To reduce the growing epidemic of drug-resistant infections in the community depends on well-coordinated studies in the multidisciplinary field and different sectors to transfer of cross-cutting issues in animal and human health, agriculture/ aquaculture, food industry, and environment (O'Neill,2014).

In this chapter, some AR/MDR foodborne bacteria, the mechanism of gaining and dissemination of antibiotic resistance and preventive strategies including new methods will be summarised.

2. Antibiotic Resistance Mechanisms of Foodborne Bacteria

It is considered that two types of mechanisms have an important role to create and spread the resistant bacterial population in the environment. These mechanisms are vertical and horizontal gene transfer. Vertical gene transfer occurs during the evolution phase, and genetic errors accumulate

in the plasmid or chromosome of bacterial cells. This mechanism is also defined as intrinsic resistance. On the other hand, in horizontal gene transfer, in other words, changes in acquired resistance, plasmids on mobile genetic elements, insertion sequences, phage-related elements and integers of bacteria, and transposons are among the types of bacteria they acquire (Holmes et al., 2016). Bacterial cells can continue to be exposed to antibiotics that interfere with cell wall synthesis, protein synthesis, or other activities by strongly reducing their metabolic activity. Several bacteria are naturally resistant to some antibiotics. The main reason for this; is that they have thick, lipid-rich cell walls that many antibiotics cannot pass into the cell. Some bacteria may cover some specific genes that break down modified proteins and antibiotics that do not bind to antibiotics, inhibit entry into cells, or actively encode enzymes that excrete antimicrobial compounds from the cells. ATP-powered flow systems may also be related to multiple resistance mechanisms (Mueller et al. 2013; Wood et al. 2013). Antibiotic-resistant bacteria can use various resistant mechanisms against antimicrobial agents. Some of them are explained below:

2.1. Structural Changes in the Bacterial Cell Wall

Antibiotics bind to macromolecules to enter the bacterial cells. Some resistant bacteria may change cell wall structure to prohibit the antimicrobials entering the cell. For example; (VRE) Vancomycin-Resistant Enterococci species prevent antibiotic binding by using cell wall structural changes (Çetinkaya et al., 2000; Aktaş & Derbentli, 2009). The same mechanism has been seen in Methicillin-resistant *Staphylococcus aureus* (MRSA) strains reduce antibiotics uptake by synthesizing methicillin-low affinity modified cell wall proteins (Robinson & Enright, 2004).

2.2. The Enzymes to Inactivate the Antibiotics

Antibiotic molecules can be less effective or ineffective because of the enzymes produced by the bacteria can break down or alter antimicrobial molecules. For example; most beta-lactam antibiotics are inactivated by beta-lactamase (*bla*) enzymes synthesized by Gram-positive and Gram-negative bacteria (Aktaş, 2004). These types of enzymes are synthesized through transferable genetic elements are defined as chromosomes, plasmids or transposons (Sun et al. 2009).

2.2.A. resistance to Penicillin-Type Drugs

It is a type of resistance that occurs through beta-lactamase enzymes. Beta-lactamases may be of chromosomal or plasmid origin and show their effects by breaking down the amide bonds of the beta-lactam ring of penicillin, cephalosporin, and similar beta-lactam group antibiotics. In the ear-

ly days, bacterial resistance genes encoded enzymes that could break down only a few penicillin variants as more effective and modified penicillin drugs were produced, some bacteria developed resistance against them. It synthesized Expanded Spectrum β-Lactamases (ESBLs), which can attack a wide variety of third-generation beta-lactams, including cephalosporins by some bacteria. Frequent exposure to antibiotics has led to mutations in the beta-lactamase enzymes synthesized by bacteria and has resulted in widening their area of action against new-generation antibiotics. Today, the development of resistance against beta-lactam antibiotics, especially in *Enterobacteria*, is a serious problem that spreads and becomes more complex (Akalın 2004; EFSA 2011; Castanheira et al., 2014; Shaikh et al. 2015).

2.2.b.A Zinc-Containing Enzyme, New Delhi Metallo-β-Lactamase (NDM)

NDM genes were first identified in 2008. These genes encode enzymes that can inactivate any type of penicillin, cephalosporin, and carbapenem group drugs. These genes have spread to many *Enterobacteriaceae* species and other bacteria in various countries of the world through environmental factors. In the USA, this gene was detected in some bacteria from livestock and some *E. coli* strains from companion animals (Goettig et al., 2013; Woodford et al., 2014; Shoma et al., 2014).

2.3.Efflux Pomps

Extraction pumps are membrane transport proteins responsible for the excretion of exogenous or endogenous substances. They are found in all living cells, from bacteria to eukaryotic cells. While some of them (e.g.Tet A and CmlA) are specific for a single substrate, most pump systems (e.g MexAB-OprM, NorA, and BmrA) can recognize multiple compounds in various structures. Examples of these compounds are biocides, detergents, disinfectants, antimicrobial peptides, cancer chemotherapy drugs used and various antibiotics. Various efflux systems have been detected in several bacterial strains (Ferna´ndez and Hancock, 2012; Aygül, 2015). Some efflux pumps have specific properties against certain molecules. However, most efflux pumps can interact with many molecules, for example, dyes and detergents, as well as antibiotics. According to some studies, *Salmonella typhimurium* cells may carry more or less 10 types of efflux pumps. Similarly, the first efflux pump CmeABC, which is related to multidrug resistance, was first found in *Camplobacter jejuni* species, then it was also identified in four other species in *Camplobacter* spp. (Guo et al., 2010; Yamasaki et al., 2013). Efflux pumps change the place of compounds that are toxic to the bacterial cell, including antibiotics, by replacing them with protons. For example, the AdeABC efflux pump is

well-defined in *A.baumannii* strains. Aminoglycosides are pumped out cefotaxime, tetracycline, erythromycin, chloramphenicol, trimethoprim, and fluoroquinolones. Besides, the growing expression of the AdeABC efflux pump supplies high levels of carbapenem resistance, accompanied by carbapenem hydrolyzing oxacillinase (Magnet et al., 2001; Marque et al., 2005).

3.Resistance Gene Transfering Mechanisms of Foodborne Bacteria

Fruit and vegetables are the main routes of acquired ARB because of direct raw consumption of them and some food preservation techniques such as freezing, drying, cooling, acidification, pasteurization, UV irradiation, modified- atmosphere condition..etc. can reduce to foodborne bacteria and maybe the potential of bacterial contamination. For instance; UV irradiation and freezing techniques can damage or stress effects on bacterial cells and kill or inactivate the bacteria. The cell-wall of dead bacteria is lysed due to cell-wall damage. Then bacterial-DNA including possible ARGs are released into the environment. This transformation of DNA has been an important role of the dissemination of ARGs in the environment by a horizontal gene transfer mechanism (Levy- Booth et al., 2007; Nielsen et al., 2007; Rico et al., 2007). Antimicrobial resistance genes in bacteria can generally be inserted into chromosomes or mobile genetic elements such as plasmids, DNA, transposons, integrons and genomic islands. In addition, resistance genes can be transferred between the bacteria using three mechanisms. These mechanisms are defined as conjugation, transduction, and transformation (Beutlichet al., 2011; Stokes and Gillings, 2011; Domingues et al., 2012).

3.1. Dissemination of Antibiotic-Resistance Due to Food Chain (Animals, Food Handlers and Irrigation)

The effects of food processing steps, food handlers, and other food-related factors have been so important in the rising AR/MDR bacteria in the food industry. For instance; the soil is a crucial source of AR/MDR bacteria because of the bacteria that can live for a long time on its surface. Moreover, organic fertilization can also help to contribute to creating more resistant bacteria on the soil. Therefore, fruit and vegetables may be contaminated and accumulated more resistant microorganisms from the soil. Harvesting, transporting, handling, cutting, cooking, packaging, storing and other food processing activities may be effective contamination factors of the spreading of AR/MDR bacteria in the food industry (Huijbers et al, 2015; Bengtsson-Palme, 2017). Thus, preventing activities of the resistant bacteria should be planned and implemented in each step of food-produc-

ing processes.

In the environmental field, commensal bacteria and pathogens spread their genetic material to the environment through mobile genetic elements, as they circulate in a wide variety of their hosts. This provides great convenience for MDR types to appear in a short time. This occurs universally in different reservoirs (Table 1). In other words, it is seen in the food chain, in the gastrointestinal tract of animals and humans as well as in the environment where globalization plays an important role (Jones-Dias et al., 2016).

The genetic transfer elements of the bacteria, for example, transposons, plasmids, insertion sequences as well as bacteriophages increase the gain of pathogenicity factors in bacteria. Thus, the ability to adapt to new places in bacteria enhancements. This situation can lead to increasing the number of bacterial diseases (Ghaly et al., 2017; Jones-Dias et al., 2016).

Some important antibiotic-resistant foodborne bacteria and their resistance against antibiotics that have been summarized below:

1. *Campylobacter* **spp.:** According to some studies*, Campylobacter* spp. were found resistant to some important antibiotics such as *β*-lactams, cotrimoxazole,macrolides, quinolones, ampicillin, chloramphenicol,lincosamides, tetracycline, aminoglycosides, and tylosin, (Alfredson et al., 2007; Koluman et al., 2013).

2. *Salmonella* **spp.:** *Salmonella* spp. have indicated multidrug resistance against to some antimicrobials such as tetracyclines, sulfonamides, kanamycin chloramphenicol, streptomycin, cephalosporins as well as penicillins (Olsen et al., 2004).

3. *Staphylococcus aureus***:** These bacteria are generally considered pathogens for both animals and humans (Huttner et al., 2013). Antibiotic-resistant *Staphylococcus aureus*strains arecrucial in the dairy product as well as cooked meals are generally contaminated by these bacteria and may cause foodborne diseases in the catering sector.   In a study conducted in Turkey; antibiotic-resistant *Staphlococcus aureus* and *Salmonella* spp. were found in raw and ready –to eat meat products. In this study; *S. aureus* was found resistant to Penicillin G, Oxytetracycline, Sulfamethoxazole, Tetracycline, Erythromycin, and Ampicillin. In addition, *Salmonella* spp. was found resistant to Penicillin G, Sulfamethoxazole, Erythromycin, and Ampicillin (Bozkurt, 2018).

4. *Enterococcus* **spp.:** These genera are found in the intestinal tract of humans warm-blooded animals and defined as indicator bacteria for hygienic quality of food products. *Enterococcus* spp. can survive in different harsh circumstances (e.g. low or high pH, temperature and salty

water). Because of their adaptation on hard conditions made them an important bacteria of community-acquired infections and nosocomial Vancomycin-Resistant Enterococci (VRE) infections that so difficult to treat in hospital settings (Hummel et al., 2006; Werner et al., 2013; Staley et al., 2014).

5. *Yersinia* **spp.:** This genus is included in various pathogenic species, including *Y. pestis*, *Y.enterocolitica*, and *Y. Pseudotuberculosis.* These species are usually abundant in seafood. In clinical settings; *Y. enterocolitica* strains may cause some crucial infections such as septicemia, septic arthritis, pneumonia, cellulitis, meningitis, empyema, osteomyelitis, and panophthalmitis. Moreover, the resistance was reported against cefoxitin and amoxicillin or clavulanic acid by some strains of them reported (Preston et al., 1994; Pham et al., 1991; Canniel, 2002).

3.2. Reservoirs of AMR/MDR in Animals and the Environment

Various MDR bacterial strains have been found in several environmental areas including human living places, food animal production lines. Some other animals, such as livestock, pigs, poultry/chickens, turkeys, rabbits, insects, and pets, also carried antibiotic-resistant bacteria according to various studies. Various studies have documented their presence in the natural environment, including livestock, wild animals, insects, companion animals, soil and surface waters. Although these bacteria are not antibiotic-resistant, they may pose a risk because they may transfer antibiotic resistance genes to other bacteria (Chaoui., et al., 2019; Verkola et al., 2019., Brown et al., 2019; Sellera et al., 2019). Some studies on antibiotic-resistant bacteria ısolated from foods are presented in Table 1.

3.2. a. Environment

MDR bacteria can survive in manure and waste lagoons and can spread from these sources to areas outside the farms. Environmental surfaces can also accommodate MDR bacteria because of frequently used antibiotics in there such as medical and veterinary sectors. For example; a study conducted in Northern Germany and evaluated that multi-drug resistant bacteria in the surface waters. They found that 58 % of the strains isolated from surface waters were phenotypically resistant to multiple drugs. Besides, it was determined that two of the MDR isolates carried *mcr-1*, the colistin resistance gene. In addition, an *Enterobacter kobei* strain, which produces carbapenemase-enzyme and carries the *blaVIM-1* gene, was also detected in this study. Another study conducted in Japan reported that some water culture systems have also been contained MDR bacteria (Antunes et al., 2011; Nonaka et al., 2012; Walsh and Duffy, 2013; Falgenhauer et al., 2019).

4.The Strategies of Minimising AR/MDR Bacteria in Foods and Environment

Some important preventive activities should be implemented to minimize AR/MDR bacteria in foods and the environment.

Those are summarised below:

1. Legislation; some regulations should be arranged by national and international authorities to the use of antibiotic-resistant bacteria including *blaGES-5* carbapenemase, which is detected in bacteria found environment and foods such as fruit and vegetables, food animals and wastewater samples (WHO, 2014; Manageiro, et al., 2014; Carvalheira et al., 2017).

2. In the field of veterinary medicine; according to the ''*Global Action Plan*'', all necessities should be met by each part of the food production sectors. This plan has been published by FAO for 2016-2020 years, preventive usage, increasing animal densities, poor hygiene, polluted water, and cheap feed sources, which are mostly given through feed or water, should also be monitored. Besides, the ways in which antibiotic resistance genes can transfer by a direct route through soil-contaminated vegetables/crops or by irrigation with contaminated water should be clearly documented (FAO / OIE / WHO, 2016).

 3. In the field of medicine; including hygiene measures and efforts to combat MDR, TB, and MRSA in healthcare settings, including testing and isolation of infected patients, contributed to control those infections (Fournier et al., 2012; Huang et al., 2013; Suzuki et al., 2013). Besides, The European Society of Clinical Microbiology and Infectious Diseases has been published a guideline to reduce transmission of MDR Gram-negative bacteria in hospitals. Some of these applications may also be helpful in veterinary medicine areas, animal husbandry, and food processing sectors (Doyle et al., 2013; Tacconelli et al., 2014).

4. Genotypic methods; some genetic methods can be used to determine the possible relationships between food/environmental and clinical strains (logical spreading can be measured in worldwide). Pulsed Field Gel Electrophoresis (PFGE) has been successfully used to determine the genetic relationships of food and clinical species so far. PFGE has a very high discrimination power since the results are reproducible and easily interpretable, they are considered as the reference method in genotypic identification, especially in monitoring of hospital infections. On the other hand, the main disadvantages of the method are the need for expensive equipment, being time-consuming and still unable to establish standard protocols for many species (Doming et al., 2003; Singh et al., 2006; Van Belkum et al., 2007). The Multilocus Sequence Typing (MLST) method

has been used to find the variety of strains of bacterial strains, producing useful results to provide a comparative analysis between different laboratories (Sabat et al., 2013). The ability of MLST to resolve closely related strains is, in principle, limited by the absolute sequence diversity found in the locus covered by the scheme and how this sequence diversity is distributed among the population to be categorized. Since MLST schemes require protected PCR primer binding sites, targets must also be adequately protected for the method to function well, and this limits the possible results of the classic MLST (Jolley & Maiden, 2014). Also, some other genetic methods, such as meta-transcriptomic, proteomic, metabolomic, next-generation sequencing (NGS) method, whole-genome sequencing (WGS) may lead to future integration of NGS to ensure food safety (Sabat et al., 2013; Ronholm et al., 2016; Lubyet al., 2016; Moran-Gilad, 2017).

5. Conclusions

AR / MDR bacteria have become widespread in microorganisms and new MDR strains have disseminated around the world very quickly. This emerging problem is not only for developed countries using large amounts of antibiotics in human medicine and animal husbandry but also for developing countries. Eventually, developing countries have become more risky for this issue than developed countries. Because, there is not enough control mechanisms about the usage, sale, and distribution of antibiotics in these places. The extensive/massive use of antibiotics in human and veterinary medicine, agriculture and aquaculture has led to the selection of microorganisms with a higher grade of resistance. Therefore, the costs for the treatment of common infections have been significantly increased. Each part of the environment has become a possible source of dissemination of antibiotic-resistant bacteria. The source is sometimes people, sometimes farm environments, and food animals/other animals/insects, and feeding materials of them. Another source is fresh fruit and vegetables affected by antibiotic-contaminated soil or water. According to some surveillance reports; there is a rising trend in MDR in many other pathogens, although there are several reports that some multi-drug pathogens have been decreased. For example, MRSA and VRE are still important health problems in hospital settings, but their number has decreased in some healthcare institutions that have adopted strict control over antibiotic use and screening and treatment of patients coming to prevent the import of new sources.

To sum up; the strategies to provide proper/smart usage of antimicrobials should be implemented in human and veterinary medicine and agriculture as well as aquaculture sectors, and in all countries around the world.

Table 1.Some Studies about Foodborne AR/MDR Bacteria

Type of Food-borne Bacteria	Type of antibiotic resistance (Multidrug/pandrug)	Isolation Materials	**Study Area**	**Reference**
S. enterica, C. coli, and C. jejuni	• *Campylobacter* was resistant to 3 of 3 antibiotics tested • *Salmonella* was resistant to 14 of 15 antibiotics tested	Retail chicken	California (USA)	(Rahman et al., 2018)
Non-typhoidal *Salmonella enterica* (NTS) (four serovars including *infantis, muenchen, newport* and *virchow*)	• 60% from all of the poultry isolates tested ($n = 188$) were multidrug resistant, mediated by chromosomal *SNPs* and different mobile genetics elements.	Poltry	Israel	(Cohen et al., 2019)
S.typhimurium, S.agona, S.corvallis and *S.kentucky*	• Multidrug-resistance (MDR) was detected in *Salmonella* isolated from chicken (245/302, 81.1%) and pork (229/313, 73.2%). The resistance rate of different *Salmonella* serotypes varied widely. • *Salmonella* isolates were identified as ESBLs-producing, covering. six *Salmonella* serotypes Bla_{OXA-1} was the dominant ESBLs gene (9/21, 42.9%), followed by $bla_{CTX-M-55}$ (5/21, 23.8%).	Chicken and pork	China	(Zhang et al., 2018)
Shiga (Vero)-toxin producing *Escherichia coli*	• STEC strains harbored the highest levels of resistance against ampicillin (93.75%), gentamycin (93.75%), tetracycline (87.50%) and ciprofloxacin (81.25%). All of the STEC strains were resistant to at least 3 antibiotics, while the prevalence of resistance against more than 12 antibiotics were 12.50%. • *Aac* (*3*)-*IV* (100%), *CITM* (100%) and *tetA* (62.50%) were the most commonly detected antibiotic resistance genes	Raw and cooked meat (Hospital kitchen)	Iran	(Ranjbar et al., 2017)
Campylobacter coli	• The *cfr*(C)(florfenicol resistance gene) gene was detected in multiple *C. coli* (34 of 344; 10%) isolates derived from different cattle farms • /*cfr*(C) as a new multidrug resistance mechanism in *Campylobacter* species.	Faecal samples of cattle	USA	(Tang et al., 2017)

| E. coli, Enterococcus faecalis Enterococcus faecium, Campylobacter coli | • 64% (74/110) of commensal E. coli, 100% (78/78) Enterococcus faecalis and 96% (22/23) Enterococcus faecium isolates were resistant at least to one antibiotic.
• E. coli were 11.1% (20/180) with bla_{CTX-M}, bla_{TEM}, and bla_{CMY} genes identified.
• Campylobacter jejuni (12.8%, 23/180)
• Campylobacter coli (2.8%, 5/180) were the most resistant to tetracycline (61%, 14/23; 100%, 5/5) and fluoroquinolones (61%, 14/23; 100%, 5/5). | Faecal samples of calves | Latvia, | (Terentjeva et al., 2019) |

REFERENCES

1. Akalın, E.H. (2004): Beta Laktam? beta laktamaz inhibitörü antibiyotiklerin klinik kullanımı (I). amoksisilin/klavulanik asit ve ampisilin/sulbaktamın klinik kullanımları. Turkiye Klinikleri J Pharmacol-Special Topics, 2, 2, 123-127.

2. Aktaş, F. (2004): Beta laktam- beta laktamaz inhibitörü antibiyotiklerin klinik kullanımı (II). Piperasilin- tazobaktam, tikarsilin- klavulanik asit ve sefoperazon? sulbaktam'ın klinik kullanımları. Turkiye Klinikleri J Pharmacol-Special Topics, 2, 2, 123-127.

3. Aktaş, G.& Derbentli, Ş., (2009). Vankomisine Dirençli Enterokokların önemi ve epidemiyolojik özellikleri. İnfeksiyonDergisi (Turkish Journal of Infection), 23 (4), 201-209p.

4. Alfredson D.A.,&Korolik V. (2007):Antibiotic resistance and resistance mechanisms in Campylobacter jejuni and Campylobacter coli. FEMS Microbiol Lett. 277(2):123–32. doi: 10.1111/j.1574-6968.2007.00935.x

5. Aygül, A. (2015). Antibiyotik direncinde dışa atım sistemlerinin ve dirençle mücadelede dışa atım pompa inhibitörlerinin önemi. Mikrobiyol Bul, 49(2), 278-291.

6. Bengtsson-Palme, J. (2017). Antibiotic resistance in the food supply chain: where can sequencing and metagenomics aid risk assessment?. Current Opinion in Food Science, 14, 66-71.

7. Beutlich, J., Jahn, S., Malorny, B., Hauser, E., Hühn, S., Schroeter, A., & Helmuth, R. (2011). Antimicrobial resistance and virulence determinants in European Salmonella genomic island 1-positive Salmonella enterica isolates from different origins. Appl. Environ. Microbiol., 77(16), 5655-5664.

8. Bozkurt, B. (2018). Çiğ ve yarı-pişmiş bazı et ürünlerinde salmonella spp. vestaphylococcus aureus' un belirlenmesi ve antibiyotik

dirençliliklerinin araştırılması (Master's thesis, Balıkesir Üniversitesi
Fen Bilimleri Enstitüsü).

9. Brown, E.E., Cooper, A., Carrillo, C., & Blais, B. (2019). Selection
    of multidrug-resistant bacteria in medicated animal feeds. Frontiers in
    microbiology, 10.

10. Caniça, M., Manageiro, V., Abriouel, H., Moran-Gilad, J., & Franz, C.
    M. (2019). Antibiotic resistance in foodborne bacteria. Trends in Food
    Science & Technology, 84, 41-44.

11. Carniel, E. Plasmids and pathogenicity islands of yersinia. In: Hacker
    J, Kaper JB, (2002). Pathogenicity islands and the evolution of
    pathogenic microbes. Berlin, Heidelberg: Springer; 2002. p. 89-108.

12. Capita, R.,& Alonso-Calleja, C. (2013). Antibiotic-resistant bacteria:
    a challenge for the food industry. Critical reviews in food science and
    nutrition, 53(1), 11-48.

13. Carvalheira, A., Silva, J., & Teixeira, P. (2017). Lettuce and fruits as
    a source of multidrug resistant Acinetobacter spp. Food microbiology,
    64, 119-125.

14. Castanheira, M., Deshpande, L. M., Costello, A., Davies, T. A., & Jones,
    R. N. (2014). Epidemiology and carbapenem resistance mechanisms
    of carbapenem-non-susceptible Pseudomonas aeruginosa collected
    during 2009–11 in 14 European and Mediterranean countries. Journal
    of Antimicrobial Chemotherapy, 69(7), 1804-1814.

15. Center for Veterinary Medicine (2013). Antimicrobials sold or dis-
    tributed for use in food-producing animals. 2013. Available at:
    http://www.fda.   Gov/downloads/ForIndustry/UserFees/Animal
    DrugUserFeeActADUFA/UCM338170.pdf, accessed March 2020.

16. Chaoui, L., Mhand, R., Mellouki, F., & Rhallabi, N. (2019).
    Contamination of the surfaces of a health care environment by
    Multidrug-Resistant (MDR) Bacteria. International Journal of
    Microbiology, 2019.

17. Cohen, E., Davidovich, M., Rokney, A., Valinsky, L., Rahav, G., &
    Gal-Mor, O. (2020). Emergence of new variants of antibiotic resistance
    genomic islands among multidrug-resistant Salmonella enterica in
    poultry. Environmental microbiology, 22(1), 413-432.

18. Çetinkaya, Y., Falk, P. & Mayhall, C.G., (2000). Vancomycin-Resistant
    Enterococci. Clinical Microbiology Reviews, 13, 686-707p.

19. Domig J.K., Mayer H.K., &Kneifel W. (2003). Methods used for
    the isolation, enumeration, characterisation and identification of
    Enterococcus spp.2. Pheno- and genotypic criteria. International
    Journal of Food Microbiology. 88: 165–188.

20. Domingues, D. J. (2012). U.S. Patent No. 8,187,649. Washington,
    DC: U.S. Patent and Trademark Office.

21. Doyle M, Loneragan G, Scott H, &Singer R. (2013). Antimicrobial

resistance: challenges and perspectives. Comp Rev Food Sci Food Safety, 12:234–248.

22. Edwards, M., Hamilton, R., Oliver, N., Fitzgibbon, S., & Samarasekera, R. (2019). Antibiotic resistance: modelling the ımpact on mortality and morbidity.

23. EFSA. (2011): Scientific Opinion on the public health risks of bacterial strains producing extended-spectrum β-lactamases and/or AmpC β-lactamases in food and food producing animals. EFSA Journal, 9, 2322-2417.

24. Falgenhauer, L., Schwengers, O., Schmiedel, J., Baars, C., Lambrecht, O., Heß, S., & Imirzalioglu, C. (2019). Multidrug-resistant, clinically relevant Gram-negative bacteria are present in German surface water samples. Frontiers in Microbiology, 10, 2779.

25. FAO/OIE/WHO(Food and Agriculture Organization of the United Nations, World Organisation for Animal Health, World Health Organization) (2016).The FAO action plan on antimicrobial resistance 2016-2020: Supporting the food and agriculture sectors in implementing the Global Action Plan on Antimicrobial Resistance to minimize the impact of antimicrobial resistance. Rome: FAO.

26. FDA, (2011). Summary report on antimicrobials sold or distributed for use in food-producing animals. Food and Drug Administration, Department of Health and Human Services; 2011.

27. Ferna´ndez L, &Hancock REW. (2012). Adaptive and mutational resis-tance: Role of porins and efflux pumps in drug resistance. Clin Microbiol Rev, 25:661–681.

28. Fournier S, Brun-Buisson C, & Jarlier V. (2012). Twenty years of anti-microbial resistance control programme in a regional multi hospital institution, with focus on emerging bacteria (VRE and CPE). Antimicrob Res Infect Control, 1:9.

29. Goettig S, Hamprecht A.G., Christ S., Kempf V.A.J., & Wichelhaus T.A. (2013). Detection of NDM-7 in Germany, a new variant of the New Delhi metallo-beta-lactamase with increased carbapenemase activity. J Antimicrob Chemother, 68:1737– 1740.

30. Guo B, Lin J., Reynolds D.L., & Zhang, Q. (2010). Contribution of the multidrug efflux transporter CmeABC to antibiotic resistance in different Campylobacter species. Foodborne Pathog Dis., 7:77–83.

31. Holmes, A.H., Moore, L.S., Sundsfjord, A., Steinbakk, M., Regmi, S., Karkey, A., & Piddock, L.J. (2016). Understanding the mechanisms and drivers of antimicrobial resistance. The Lancet, 387(10014), 176-187.

32. Huang, Y., Zhang, L., Tiu, L., & Wang, H. H. (2015). Characterization of antibiotic resistance in commensal bacteria from an aquaculture ecosystem. Frontiers in microbiology, 6, 914.

33. Huijbers, P. M., Blaak, H., de Jong, M. C., Graat, E. A., Vandenbroucke-Grauls, C. M., & de Roda Husman, A. M. (2015). Role of the environment in the transmission of antimicrobial resistance to humans: a review. Environmental science & technology, 49(20), 11993-12004.

34. Hummel A, Holzapfel WH, &Franz CM. (2007). Characterisation and transfer of antibiotic resistance genes from enterococci isolated from food. Syst Appl Microbiol., 30(1):1–7. doi: 10.1016/j.syapm.2006.02.004.

35. Hur, J., Jawale, C., & Lee, J.H. (2012). Antimicrobial resistance of Salmonella isolated from food animals: A review. Food Research International, 45(2), 819-830.

36. Huttner, A., Harbarth, S., Carlet, J., Cosgrove, S., Goossens, H., Holmes, A., & Pittet, D. for the world healthcare-associated ınfections forum participants, (2013). Antimicrobial resistance: a global view from the 2013 world healthcare-associated ınfections forum. Antimicrob Resist Infect Control, 2(31), 2994-2.

37. Jolley, K.A.,& Maiden, M. C. (2014). Using MLST to study bacterial variation: prospects in the genomic era. Future microbiology, 9(5), 623-630.

38. Jones-Dias, D., Manageiro, V., Ferreira, E., Barreiro, P., Vieira, L., Moura, I. B., & Caniça, M. (2016). Architecture of class 1, 2, and 3 integrons from gram negative bacteria recovered among fruits and vegetables. Frontiers in microbiology, 7, 1400.

39. Koluman, A.,& Dikici, A. (2013). Antimicrobial resistance of emerging foodborne pathogens: status quo and global trends. Critical reviews in microbiology, 39(1), 57-69.

40. Levy-Booth, DJ, Campbell, RG, Gulden, R.H, Hart, MM., Powell, JR, Klironomos, JN., & Dunfield, KE. (2007). Cycling of extracellular DNA in the soil environment. Soil Biology and Biochemistry, 39(12), 2977-2991.

41. Luby, E., Ibekwe, A. M., Zilles, J., & Pruden, A. (2016). Molecular methods for assessment of antibiotic resistance in agricultural ecosystems: Prospects and challenges. Journal of environmental quality, 45(2), 441-453.

42. Magnet, S.P., Courvalin, &T. Lambert. (2001). Resistance-nodulation-cell division type efflux pump involved in aminoglycoside resistance in Acinetobacter baumannii strain BM4454. Antimicrobial Agents and Chemotherapy, 45: 3375-3380.

43. Manageiro, V., Pinto, M., & Caniça, M. (2015). Complete sequence of a blaOXA-48-harboring IncL plasmid from an Enterobacter cloacae clinical isolate. Genome Announc., 3(5), e01076-15.

44. Marque, S.L. Poirel, C. Heritier, S. Brisse, M.D. Blasco, R. Filip, G. Coman, T. Naas, &P. Nordmann. (2005). Regional occurrence of

plasmid mediated carbapenem hydrolyzing oxacillinase OXA-58 in Acinetobacter spp. in Europe. Journal of Clinical Microbiology, 43: 4885-4888.

45. Magiorakos, A. P., Srinivasan, A., Carey, R. B., Carmeli, Y., Falagas, M. E., Giske, C. G., & Paterson, D. L. (2012). Multidrug-resistant, extensively drug-resistant and pandrug-resistant bacteria: an international expert proposal for interim standard definitions for acquired resistance. Clinical microbiology and infection, 18(3), 268-281.

46. Marathe, N. P., Regina, V. R., Walujkar, S. A., Charan, S. S., Moore, E. R., Larsson, D. J., & Shouche, Y. S. (2013). A treatment plant receiving waste water from multiple bulk drug manufacturers is a reservoir for highly multi-drug resistant integron-bearing bacteria. PLoS One, 8(10).

47. Michael I, Rizzo L, McArdell CS, Manaia CM, Merlin C, Schwartz T, Dagot C, & Fatta-Kassinos D. (2013). Urban wastewater treatment plants as hotspots for the release of antibiotics in the environment: A review. Water Res, 47:957–995.

48. Moran-Gilad,J.(2017).Whole genome sequencing (WGS) for food-borne pathogen surveillance and control–taking the pulse. Euro Surveillance, 22pii=30547.

49. Mueller-Doblies D, Clouting C, & Davies RH. (2013). Investigations of the distribution and persistence of Salmonella and cipro-floxacin-resistant Escherichia coli in turkey hatcheries in the UK. Zoonoses Public Health, 60:296–303.

50. Nielsen, K.M., Johnsen, P. J., Bensasson, D., & Daffonchio, D. (2007). Release and persistence of extracellular DNA in the environment. Environmental biosafety research, 6(1-2), 37-53.

51. Nonaka, L., Maruyama, F., Onishi, Y., Kobayashi, T., Ogura, Y., Hayashi, T., & Masuda, M. (2014). Various pAQU plasmids possibly contribute to disseminate tetracycline resistance gene tet (M) among marine bacterial community. Frontiers in microbiology, 5, 152.

52. Olsen S.J., Ying M, Davis M.F., Deasy M, Holland B., Iampietro L. (2004). Multidrug-resistant Salmonella typhimurium infection from milk contaminated after pasteurization. Emerg Infect Dis. 10(5):932–5. doi: 10.3201/eid1005.030484.

53. O'Neill, J.I.M. (2014). Antimicrobial resistance: tackling a crisis for the health and wealth of nations. Rev. Antimicrob. Resist, 20, 1-16.

54. Pham J.N, Bell SM, Lanzarone JY. (1991). Biotype and antibiotic sensitivity of 100 clinical isolates of Yersinia enterocolitica. J Antimicrob Chemother, 28(1):13–8. doi: 10.1093/jac/28.1.13.

55. Preston MA, Brown S, Borczyk AA, Riley G, Krishnan C. Antimicrobial susceptibility of pathogenic Yersinia enterocolitica

isolated in Canada from 1972 to 1990. Antimicrob Agents Chemother. 1994; 38(9):2121–4. doi: 10.1128/aac.38.9.2121.

56. Rahman, G., Price, L., & Rabanes, H. G. (2018). Implications of foodborne bacteria on human health: Isolation and Antibiotic Resistance of Salmonella enterica and Campylobater spp. on Retail Chicken Sold in California, 2018.

57. Ronholm,J.,Nasheri,N.,Petronella,N.,&Pagotto,F.(2016).Navigating microbiological food safety in the era ofwhole-genome sequencing. Clinical Microbiology Reviews, 29, 837–857.

58. Ranjbar, R.,Masoudimanesh, M., Dehkordi, F.S., Jonaidi-Jafari, N., & Rahimi, E. (2017). Shiga (Vero)-toxin producing Escherichia coli isolated from the hospital foods; virulence factors, o-serogroups and antimicrobial resistance properties. Antimicrobial Resistance & Infection Control, 6(1), 4.

59. Rico, D., Martin-Diana, A.B., Barat, J.M., & Barry-Ryan, C. (2007). Extending and measuring the quality of fresh-cut fruit and vegetables: a review. Trends in Food Science & Technology, 18(7), 373-386.

60. Robinson, D. A.,& Enright, M. C. (2004). Multilocus sequence typing and the evolution of methicillin-resistant Staphylococcus aureus. Clinical microbiology and infection, 10(2), 92-97.

61. Sabat, A. J. , Budimir,A.,Nashev,D.,Sá-Leão,R.,van Dijl ,J.M., Laurent, F.,on behalf of the, ESCMID Study Group of Epidemiological Markers (ESGEM).(2013). Overview of molecular typing methods for outbreak detection and epidemiological surveillance. Euro Surveillance,18, 20380.

62. Sellera, F.P., Madec, J.Y., & Lincopan, N. (2019). Comment on: Applying definitions for multidrug resistance, extensive drug resistance and pandrug resistance to clinically significant livestock and companion animal bacterial pathogens. Journal of Antimicrobial Chemotherapy, 74(2), 535-536.

63. Shaikh, S., Fatima, J., Shakil, S., Rizvi, S.M. ve Kamal, M.A. (2015): Antibiotic resistance and extended spectrum beta-lactamases: Types, epidemiology and treatment. Saudi J Biol Sci, 22, 1, 90-101.

64. Shoma, S., Kamruzzaman, M., Ginn, A. N., Iredell, J.R., & Partridge, S.R. (2014). Characterization of multidrug-resistant Klebsiella pneumoniae from Australia carrying blaNDM-1. Diagnostic microbiology and infectious disease, 78(1), 93-97.

65. Singh A., Goering R.V., Simjee S, Foley S.L., Zervos M.J. (2006). Application of molecular techniques to the study of hospital ınfection. Clin. Microbiol. Rev. 19: 512-530.

66. Staley, C., Dunny, G. M., & Sadowsky, M. J. (2014). Environmental and animal-associated enterococci. In Advances in applied microbiology (Vol. 87, pp. 147-186). Academic Press.

67. Stokes, H.W., & Gillings, M.R. (2011). Gene flow, mobile genetic elements and the recruitment of antibiotic resistance genes into Gram-negative pathogens. FEMS microbiology reviews, 35(5), 790-819.

68. Sun, S., Berg, O.G., Roth, J.R. & Andersson, D.I. (2009): Contribution of gene amplification to evolution of ıncreased antibiotic resistance in Salmonella typhimurium. Genetics, 182, 1183–1195.

69. Suzuki, S., Ogo, M., Miller, T.W., Shimizu, A., Takada, H., & Siringan, M.A. (2013). Who possesses drug resistance genes in the aquatic environment?: sulfamethoxazole (SMX) resistance genes among the bacterial community in water environment of Metro-Manila, Philippines. Frontiers in microbiology, 4, 102.

70. Tacconelli, E., Cataldo, M.A., Dancer, S.J., De Angelis, G., Falcone, M., Frank, U., & Singh, N. (2014). ESCMID guidelines for the management of the infection control measures to reduce transmission of multidrug-resistant Gram-negative bacteria in hospitalized patients. Clinical Microbiology and Infection, 20, 1-55.

71. Tang, K.L., Caffrey, N.P., Nóbrega, D.B., Cork, S.C., Ronksley, P. E., Barkema, H. W., ... & Ghali, W. A. (2017). Restricting the use of antibiotics in food-producing animals and its associations with antibiotic resistance in food-producing animals and human beings: a systematic review and meta-analysis. The Lancet Planetary Health, 1(8), e316-e327.

72. Terentjeva, M., Streikiša, M., Avsejenko, J., Trofimova, J., Kovaļenko, K., Elferts, D., & Bērziņš, A. (2019). Prevalence and antimicrobial resistance of Escherichia coli, Enterococcus spp. and the major foodborne pathogens in calves in Latvia. Foodborne pathogens and disease, 16(1), 35-41.

73. Van Belkum A., Tassios P.T., Dijkshoorn L, Haeggman S., Cookson B., Fry N.K., Fussing V, Green J, Feil E, Gerner-Smidt P, Brisse S, Struelens M. (2007). Guidelines for the validation and application of typing methods for use in bacterial epidemiology. Clinical Microbiology and Infectious Diseases. 13: 1–46.

74. Verkola, M., Pietola, E., Järvinen, A., Lindqvist, K., Kinnunen, P.M., & Heikinheimo, A. (2019). Low prevalence of zoonotic multidrug-resistant bacteria in veterinarians in a country with prudent use of antimicrobials in animals. Zoonoses and public health, 66(6), 667-678.

75. Walsh, C.,& Duffy, G. (2013). Antibiotic resistance in foodborne pathogens.

76. WHO(WorldHealthOrganization)(2014).Antimicrobial resistance: Global report on surveillance http://apps.who. Int/iris/bitstream/handle/10665/112642/ 9789241564748_eng.pdf.

77. Werner, G., Coque T.M., Franz, C.M., Grohmann, E., Hegstad, K.,

&Jensen, L. (2013). Antibiotic resistant enterococci-tales of a drug resistance gene trafficker. Int J Med Microbiol. 303(6-7):360–79. doi: 10.1016/j.ijmm.2013.03.001.

78. Wood, F., Phillips, C., Brookes-Howell, L., Hood, K., Verheij, T., Coenen, S.,& Worby, P. (2013). Primary care clinicians' perceptions of antibiotic resistance: a multi-country qualitative interview study. Journal of Antimicrobial Chemotherapy, 68(1), 237-243.

79. Woodford, N., Wareham, D. W., Guerra, B., & Teale, C. (2014). Carbapenemase-producing Enterobacteriaceae and non-Enterobacteriaceae from animals and the environment: an emerging public health risk of our own making?. Journal of Antimicrobial Chemotherapy, 69(2), 287-291.

80. Yamasaki, S., Nagasawa, S., Fukushima, A., Hayashi-Nishino, M., & Nishino, K. (2013). Cooperation of the multidrug efflux pump and lipopolysaccharides in the intrinsic antibiotic resistance of Salmonella enterica serovar Typhimurium. Journal of Antimicrobial Chemotherapy, 68(5), 1066-1070.

81. Zhang, Y., Gu, A.Z., Cen, T., Li, X., He, M., Li, D., & Chen, J. (2018). Sub-inhibitory concentrations of heavy metals facilitate the horizontal transfer of plasmid-mediated antibiotic resistance genes in water environment. Environmental Pollution, 237, 74-82.

Chapter 6

ASSESSMENT OF THE PERCEIVABLE ENVIRONMENTAL STATUS OF ÖMERLİ DAM LAKE BASIN THROUGH THE STATISTICAL ANALYSIS OF THE LAKE POLLUTION DATA AND THE SOCIAL PROPOSAL TO CONTROL POLLUTION

Muhammed Ernur AKINER[1], Nurdan AKINER[2]

1 Dr. Öğr. Üyesi, Akdeniz University, Vocational School of Technical Sciences, Environmental Protection and Control, ernurakiner@akdeniz.edu.tr
2 Prof. Dr., Akdeniz University, Faculty of Communications, Department of Radio, Television, and Cinema, nurdanakiner@akdeniz.edu.tr

Introduction

Water has always connected people all over the world and throughout history. Historically, there had been a good relationship between civilizations and water (Priscoli, 2000). Most of the early civilizations had been developed along with the water bodies. Environmental pollution caused by urbanization and an increase in industrialization affects streams. Water pollution is a significant global problem, and it is the cause of many death and epidemic events. Fourteen thousand people a day die directly or indirectly as a result of diseases caused by water pollution (Azizullah *et al.*, 2011).

The fact that the job opportunities brought by the 19th Century Industrial Revolution intensified in the cities, which caused an intense wave of migration from villages to cities, which increased the population of their towns. Informal settlements are frequently ignored and treated by policymakers, particularly in developed nations, as an issue that one would rather not have to solve (Shatkin, 2004).

Informal settlements are also situated next to developed communities as in other areas of the world (Mohanty, 2006a, 2006b). Slums are structures that contain families that migrated from the village to the city. Slums occurred as a result of the inadequateness of accommodation in cities, and it has become one of the most significant issues of urbanization as migration from rural areas to urban. Considering the structural features of the slums, it is noteworthy that they were constructed in a short time with wood, stone, briquette, mudbrick, or cans and that they show shelter quality. Slums are also shelters close to the city center, residential areas, close to each other, in a garden, with a narrow seating area. (Tatlıdil, 1989).

The National Housing Authority (NHA) describes a slum as a polluted, humid, swampy, or unsafe environment of overpopulated houses and residences that may be detrimental to health or existence or can be an origin of illegal or unethical activity, with a minimum of 30 units every 1600 square meters. On the other side, the BMA describes a slum as an overcrowded, unorderly, and dilapidated neighborhood with a deficient climate that can be detrimental to health and existence and with at least 15 housing units per 1600 square meters (UN-Habitat, 2004).

In addition to the acute problems in developing and developed countries, studies are underway to reduce this pollution. Both the used waters of residential areas and industrial facilities and the drainage waters of agricultural fields carry nutrients such as nitrogen, phosphorus, and carbon to surface waters (Badruzzaman *et al.*, 2012). Such nutrients affect the biological, chemical, and physical events in the water sources. They enter and change the ecological structure of the system. Among the factors that threaten the use of surface waters today and in the future, the most

central place is the nutrients, especially nitrogen and phosphorus components. Water resources are also ecosystems. These sources are naturally in balance before they are contaminated. However, as explained above, if pollutants come in, there will be changes in the way of deterioration in the system. Therefore, the quality of the water deteriorates, the possibilities for its use are reduced, and the cost of treatment increases. Water becomes an increasingly important substance. And the need to protect water resources arises in terms of drinking, using, and industrial water supply. The most basic way of preventing the formation of pollution in the water basins that will avoid the use of resources is by determining the contamination profile before it is late and controlling the contamination and optimizing the resources (Laird *et al.*, 2005).

While the breakdown of complex molecules in nature continues spontaneously as biological degradation, the human can be accelerated by changes made by hand, and some harmful compounds by decomposing organic pollutants of some bacteria enable biological improvement studies. Depending on external inputs in the lake ecosystem investigation of changes that may occur as micro-level through bacteria isolated from the environment against this pollutant. It is possible by the effect of bacteria or by revealing resistance mechanisms. While the breakdown of complex molecules in nature continues spontaneously as biological degradation, the situation can be accelerated by human-made changes. Some bacteria in the lake ecosystem allow biological treatment by decomposing organic pollutants (Zhang *et al.*, 2020).

In aquatic ecosystems, nutrients play a critical role by sustaining all living plants and animals. However, without a responsible management plan, excess nutrients can fuel invasive marine plant growth. Harmful algal blooms can also develop threatening the health of a lake or pond and even the community that surrounds it (Waajen *et al.*, 2016). Also, many laundry detergents and dish soaps previously made with phosphorus and phosphate-containing fertilizers should be banned, and the production of these materials have to be regulated (Scholz *et al.*, 2014). Water pollution is a significant problem in stream basins in many countries and our country. Increasing water pollution, drinking, and potable water supply is complicated. Sources of water pollution in stream basins, agricultural activities, industrial and mining activities, settlements can be counted as pollution causes (Chelyadina, 2017). Recent studies show that streams carry most of the coastal pollution. Water pollution destroys all species and biological communities, as well as harms all living creatures in or around the basin. Water pollution is caused by the discharge of wastewater containing harmful components into the basins without undergoing adequate treatment. The connection between surface waters and groundwater is

complex. Therefore, pollution in groundwater is examined under a single heading, and the surface water pollution is not so easily classified. Among the reasons why this classification is severe, the effect of the point or non-point pollution that can occur on groundwater is uncertain and difficult to investigate. Also, some impurities in the surface soil do not always have to pollute groundwater in a water basin (Chekalin, 2017).

The main elements of lake pollution are streams and atmospheric events (Williamson *et al.*, 2008). The erosion of dissolved and suspended matter transported by streams and chemical dissolution, also acid rains, increases pollution. Water entering the lake with anthropogenic contamination deteriorates its quality gradually. Pollutants entering the lake, such as pesticides and heavy metals with degradable power, are of a non-degradable type. Suspended substances settle on the lake bottom and accumulate in the lake.

Lakes can destroy organic pollution under standard conditions. However, organic loads exceeding the lake's natural treatment capacity will consume the oxygen in the lake and cause the lake to transform into an anaerobic state (Chapra, 1991). The assimilation capacity of the lake is vital for a lake to become anaerobic. Some chemical changes are occurred due to algae growth and increased organic matter. According to the nitrogen and the phosphorus concentrations in water, the lakes are divided into three classes, oligotrophic, mesotrophic, and eutrophic (Xu *et al.*, 2001). Nitrogen and other nutrients gradually increase in aged water ecosystems. Organic material that can be converted into nutrients increases the productivity of the system. The soil that comes from the water ecosystem drifting from the land around it contains active residues. Algae and microscopic organisms collected on the water surface prevent the sun rays and absorb oxygen, which is vital for underwater life. It's essential to know that eutrophic lakes and oligotrophic lakes are natural, but oligotrophic lakes are becoming more atrophic due to human activities. Phosphates and other chemicals from fertilizer run through the groundwater and into the lake (Domagalski and Johnson, 2012). The increased nutrient level causes rapid plant growth, which leads to the lake. The decomposing plant materials at the bottom of the lake causes decreased dissolved oxygen levels and reduced recreational value. Decomposed organic material at the bottom of the lake is the reason behind the odor problem of the lakes (Huang *et al.*, 2018). The decomposing material decreases the dissolved oxygen level and therefore reduces the number of the fish population.

Drinking, using, and industrial water needs of the Istanbul metropolitan region are met by Terkos, Buyukcekmece, Kucukcekmece, Alibeykoy, Omerli, Elmali, and Darlik Dams, which are located in a sub-basin in the Marmara Basin. These dams are susceptible to pollution with the anthro-

pogenic effects mentioned above. In this research, the study will be carried out on the Ömerli Dam Lake and its basin (Figure 1), one of the dam lakes that provide water to Istanbul. Pollution loads from different points and common sources in the Ömerli basin will be calculated.
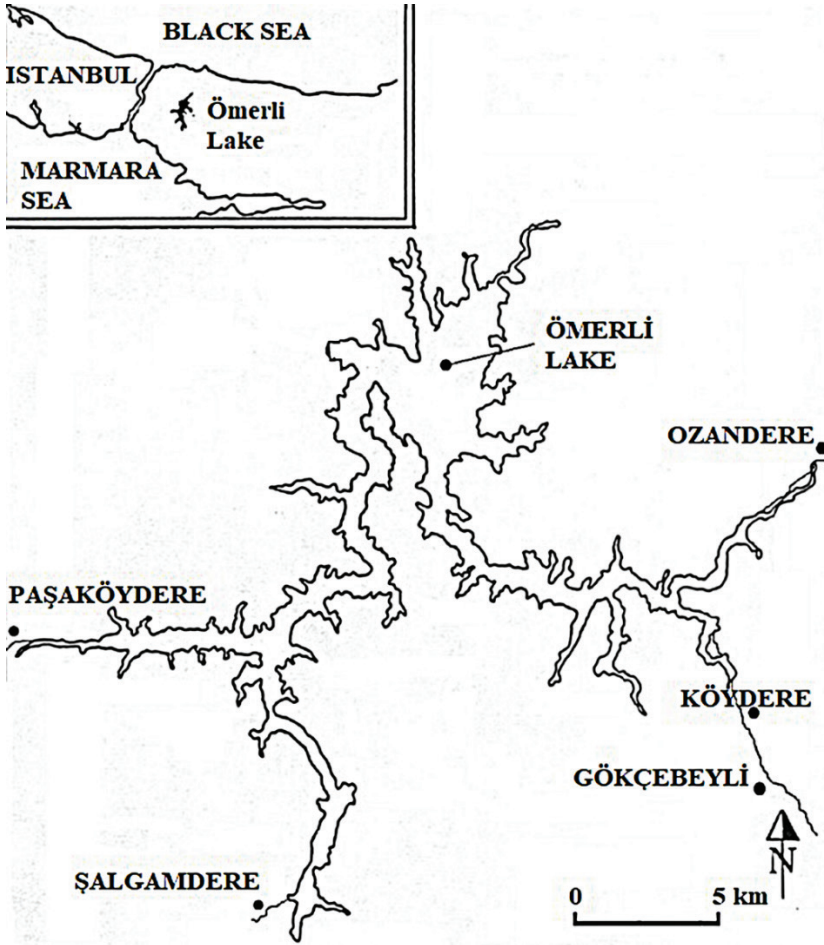

Figure 1. Ömerli Dam Lake and feeding streams in the basin.

Methodology

Water, which is one of the main elements that ensure the continuation of its natural life, is one of the essential natural resources. Population growth and industrialization and the development of agriculture have increased harmful effects on the environment and especially water resources.

A slum is typically a densely populated urban residential neighborhood that comprises largely of tightly clustered, decrepit residential units in a circumstance with inadequate or unfinished facilities, predominantly occupied by poor citizens. Naturally, the words "slum," "squatter," and "informal" are not interchangeable – commonly speaking, a slum is characterized in words of inadequate sanitation and shelter; squatting in terms of tenure legality; and informality in terms of activities beyond state regulation (Alsayyad & Roy, 2004). Even though slums are placed in urban areas, particularly in America, they may be placed in other nations, such as Europe, particularly in suburban areas and so on. It is a region of the city where the standard of accommodation is weak with inadequate living standards.

Within the globalization of the earth's towns and increasing settlement costs in developed countries' metropolitan regions, there is an increasing divide between the vulnerable and those residing in a more affluent urban lifestyle (Jones, 2012; Shatkin, 2004). David Harvey (2008), on the other hand, defines slums as the places of those who are excluded from the city. Harvey (2008) states that spatial segregation develops during the urbanization process that started with the industrial revolution. According to him, the inequality in question is a phenomenon created by the capitalist system. It is essential to democratize the right to the city and to create a massive mass movement to impose its power, if the dispossessed are to gain back ownership of the community from which they have been removed for too long and if new forms of managing capital surpluses are to be implemented while they operate through urbanization processes.

Whatever the reason behind it, there is only one truth, which is the negative impact of irregular settlements on the water quality of Ömerli Dam Lake.

A significant amount of suspended and dissolved substances carried by streams are formed as a result of erosion and chemical dissolution. Also, the traffic of contamination by the atmosphere is critical, and acid rains increase pollution. Most of the pollutants involved in the lake are due to streams. Climatic factors such as precipitation and wind, water pollution occur as a result of transportation and mixing with surface waters. Classification of quality properties of lakes, ponds, and dam reservoirs are explained in the "Classification of Continental Water Surface Waters" by Water Pollution Control Regulation (WPCR) Table: IV.2.1 (Official Gazzette, 2004). Again, according to WPCR, the table on "Receiving Environment Standards of Lake Waters": In IV.2.2, the most critical threat of lake, pond and dam reservoirs is indicated as the eutrophication event. This regulation asks control of the nitrogen and phosphorus loads (Official Gazzette, 2004). See Table 1 for the water quality classes among the Surface Water Quality Management Regulations (SWQMR) of Turkey (Official Gazzette, 2004).

Table 1. Water quality classes among the Surface Water Quality Management Regulations (SWQMR) of Turkey (Official Gazzette, 2004).

	Water Quality Class			
Parameter	1	2	3	4
Dissolved Oxygen (mg/L)	> 8	> 6	> 3	< 3
BOD_5 (mg/L)	< 4	< 8	< 20	> 20
Total Phosphorus (mg/L)	< 0.02	< 0.16	< 0.65	> 0.65
Nitrite Nitrogen (mg/L)	< 0.002	< 0.01	< 0.05	> 0.05
Nitrate Nitrogen (mg/L)	< 5	< 10	< 20	> 20

In the statistics, if the correlation value is +1 or -1, the correlation coefficient explains linear relationships, and data can be modeled with accuracy. So as the correlation value approaches -1 or +1, distribution on data can be expressed with a straight line, and data seems to be closely related to each other. If the correlation value is immense, the data (points) will be closer to the regression curve. When data move away from -1 or +1 around the line, scattering increases, and If the sample correlation coefficient equals to 0, there is no linear connection between the two variables. The one-sample t-test is used to compare a sample mean with a known value (Hazra and Gogtay, 2016). This value is generally the population average (parameter). While the sample average is the observed value, the population average is the expected value. This test is useful when we want to know if the sample is taken from a particular population (Skaik, 2015). Null and alternative hypotheses in a single sample t-test: H_0: There is no significant difference between sample average and population average. H_1: The disparity between the sample average and population average is significant. If, otherwise, Sig. < 0.05, the null hypothesis is denied. Which implies the null hypothesis is unlikely. The alternate hypothesis is presumed correct.

Assumptions for Single Sample T-Test: The variable we are interested in is continuous (Tricker, 1990). The sample is drawn randomly from the population. The variable shows a normal distribution. There is no outlier or extreme values in our data set. In this study, water quality data belongs to the lake, and feeding streams are suitable for the one-sample t-test. Hence ten years of data, gathered monthly between 2009 and 2018, were analyzed by the one-sample t-test (DSI, 2019).

Results and discussion

There are two types of lakes according to their trophic condition. An oligotrophic lake is usually extensive deep and clear, has plenty of fish,

and limited vegetation. It is a typical recreational lake. A eutrophic Lake is generally shallow, and nutrient-rich vegetation is abundant because of the nutrient loading. In a eutrophic lake, lowering elevation allows more nutrients to drain into the lake. Since the beginning of the 1970s, Ömerli Dam, located in the Ömerli Basin, meets the drinking water needs of Istanbul (Morkoç *et al.*, 2009). Illegal residences used for settlement purposes, existing rural settlements, livestock, and forestry activities primarily slummed the water quality in recent years. Five main streams are feeding the Ömerli Dam Lake. These are Gökçebeyli, Köydere, Ozandere, Paşaköydere, and Şalgamdere, respectively. Discharges belong to these streams are measured monthly, and ten years average discharges (Q) in m³/s are shown in Table 2.

Table 2. Discharges of the streams feeding the Ömerli Dam Lake (DSI, 2019).

Stream Name	Ten years average discharges (Q) in m³/s
Gökçebeyli	1.6
Köydere	0.4
Ozandere	3.4
Paşaköydere	0.8
Şalgamdere	0.5

It is observed that the surface of the lake is lush, the blur is increased, and anaerobic conditions develop. At the bottom, there is an airless, anaerobic zone as dead plant residues accumulate, and there is no water circulation. Between these two regions, sufficiently light area, but there is an airless zone where anaerobic photosynthetic bacteria break down organic residues at the bottom of the lake. Anaerobic bacteria's oxidation components use butyric acid as well as other fatty acids as photosynthesis electron donors, and hence H_2S (Sadler & Stanier, 1960). Such chemicals, which are harmful to green plants, are degraded and vanish. Natural balance is disrupted as a result of an excessive increase in the upper algae population. Although eutrophication is a naturally occurring event, its rate is increasing with anthropogenic effects (Xu, 2018). It occurs mainly from human actions, such as land use (agricultural), artificially because of factors such as sewage and industrial pollutants entering the water system. Eutrophication disrupts wetland ecosystems, causing obstacles to birds, fish, and other living things that can decline or disappear (Moyle & Leidy, 1992). Environmental pollution caused by the increase of urbanization and industrialization also affects streams and lakes (Zhang *et al.*, 2011).

In this study, Ömerli Dam Lake and feeding streams were measured monthly for Dissolved Oxygen, BOD_5, and eutrophication related parameters; Total Phosphorus, Nitrite Nitrogen, and Nitrate Nitrogen and data

belong to the years 2009 and 2018 were used for the statistical analysis. Water quality data belongs to the lake, and feeding streams were analyzed through the one-sample t-test, and results are shown in Table 3, 4, 5, 6, and 7. More precisely, coefficient of determination, R^2 value for observed vs. expected normal value, and hypothesis check ($\mu_0 \geq$ Test Value or $\mu_a <$ Test Value) for 95% Confidence Interval (CI) are depicted in Table 3, 4, 5, 6, and 7.

Results indicate that Paşaköydere and Şalgamdere streams are the main polluters of the lake. The water quality of these two streams is parallel to the water quality of the lake. Hence, lake water quality can be conserved if these two streams are protected against point and non-point sources of pollution.

Evaluation of the legal aspects of water utilization techniques and their relation to the traditions of society should also be taken into consideration.

Table 3. One-Sample T-Test findings for the observed streams and the Ömerli Dam Lake: Dissolved Oxygen pollution data.

Stream	Mean Concentration	Standard Deviation	Degree of Freedom	Test Value	Prescribed Limits (mg/L)	Level of significance: p-value	Coefficient of Determination, R^2	Hypothesis check	Result
Gökçebeyli	8.4	1.5	119	8	Concentration $\geq$ 8: WQC-I.	0.065	0.833	95% CI includes null value, accept the null hypothesis.	Water Quality Class Number 1
Köydere	7.5	2.7	119	8	Concentration $\geq$ 8: WQC-I.	0.051	0.900	accept the null hypothesis.	WQC Number 1
Ozandere	7.6	1.8	119	8	Concentration $\geq$ 8: WQC-I.	0.058	0.867	accept the null hypothesis.	WQC Number 1
Paşaköydere	7.0	3.5	119	8	Concentration $\geq$ 8: WQC-I.	0.004	0.984	95% CI excludes null value, reject the null hypothesis.	WQC Number 2

Şalgamdere	7.1	3.2	119	8	Concentration ≥ 8: WQC-I.	0.008	0.945	reject the null hypothesis.	WQC Number 2
Ömerli Dam Lake	7.3	3.4	119	8	Concentration ≥ 8: WQC-I.	0.046	0.875	reject the null hypothesis.	WQC Number 2

Table 4. One-Sample T-Test findings for the observed streams and the Ömerli Dam Lake: BOD_5 pollution data.

Stream	Mean Concentration	Standard Deviation	Degree of Freedom	Test Value	Prescribed Limits (mg/L)	Level of significance: p-value	Coefficient of Determination, R^2	Hypothesis check	Result
Gökçebeyli	4.0	2.60	119	8	8 ≤ Concentration < 20: WQC-III.	0.018	0.806	95% CI excludes null value, reject the null hypothesis.	Water Quality Class Number 2
Köydere	3.80	2.96	119	8	8 ≤ Conc. < 20: WQC-III.	0.034	0.854	reject the null hypothesis.	WQC Number 2
Ozandere	4.10	2.40	119	8	8 ≤ Conc. < 20: WQC-III.	0.036	0.835	reject the null hypothesis.	WQC Number 2
Paşaköydere	5.81	4.588	119	8	8 ≤ Conc. < 20: WQC-III.	0.058	0.860	95% CI includes null value, accept the null hypothesis.	WQC Number 3
Şalgamdere	7.602	5.57	119	8	8 ≤ Conc. < 20: WQC-III.	0.308	0.907	accept the null hypothesis.	WQC Number 3
Ömerli Dam Lake	7.905	6.32	119	8	8 ≤ Conc. < 20: WQC-III.	0.351	0.920	accept the null hypothesis.	WQC Number 3

Table 5. One-Sample T-Test findings for the observed streams and the Ömerli Dam Lake: Total P pollution data.

Stream	Mean Concentration	Standard Deviation	Degree of Freedom	Test Value	Prescribed Limits (mg/L)	Level of significance: p-value	Coefficient of Determination, R^2	Hypothesis check	Result
Gökçebeyli	0.25	0.12	119	0.65	Concentration ≥ 0.65: WQC-IV.	0.028	0.830	95% CI excludes null value, reject the null hypothesis.	Water Quality Class Number 3
Köydere	0.10	0.05	119	0.65	Conc. ≥ 0.65: WQC-IV.	0.005	0.655	reject the null hypothesis.	WQC Number 3
Ozandere	0.4	0.095	119	0.65	Conc. ≥ 0.65: WQC-IV.	0.046	0.895	reject the null hypothesis.	WQC Number 3
Paşaköydere	0.614	0.560	119	0.65	Conc. ≥ 0.65: WQC-IV.	0.316	0.891	95% CI includes null value, accept the null hypothesis.	WQC Number 4
Salgamdere	0.60	0.24	119	0.65	Conc. ≥ 0.65: WQC-IV.	0.180	0.902	accept the null hypothesis.	WQC Number 4
Ömerli Dam Lake	0.59	0.36	119	0.65	Conc. ≥ 0.65: WQC-IV.	0.308	0.920	accept the null hypothesis.	WQC Number 4

Table 6. One-Sample T-Test findings for the observed streams and the Ömerli Dam Lake: NO$_2$-N pollution data.

Stream	Mean Con-centra-tion	Standard Devia-tion	Deg-ree of Free-dom	Test Value	Prescribed Limits (mg/L)	Level of signifi-cance: p-value	Coeffi-cient of Determi-nation, R^2	Hypothe-sis check	Result
Gökçebeyli	0.038	0.023	119	0.05	Concentra-tion ≥ 0.05: WQC-IV.	0.042	0.816	95% CI excludes null va-lue, reject the null hypothe-sis.	Water Quality Class Num-ber 3
Köydere	0.045	0.041	119	0.05	Conc. ≥ 0.05: WQ-C-IV.	0.373	0.926	95% CI includes null value, accept the null hypothe-sis.	WQC Num-ber 4
Ozandere	0.014	0.021	119	0.05	Conc. ≥ 0.05: WQ-C-IV.	0.019	0.971	reject the null hypothe-sis.	WQC Num-ber 3
Paşaköydere	0.35	0.17	119	0.05	Conc. ≥ 0.05: WQ-C-IV.	0.635	0.690	accept the null hypothe-sis.	WQC Num-ber 4
Şalgamdere	0.035	0.026	119	0.05	Conc. ≥ 0.05: WQ-C-IV.	0.071	0.893	accept the null hypothe-sis.	WQC Num-ber 4
Ömerli Dam Lake	0.512	1.465	119	0.05	Conc. ≥ 0.05: WQ-C-IV.	0.799	0.708	accept the null hypothe-sis.	WQC Num-ber 4

Table 7. One-Sample T-Test findings for the observed streams and the Ömerli Dam Lake: NO_3-N pollution data.

Stream	Mean Concentration	Standard Deviation	Degree of Freedom	Test Value	Prescribed Limits (mg/L)	Level of significance: p-value	Coefficient of Determination, R^2	Hypothesis check	Result
Gökçebeyli	1.8	1.432	119	5	5 ≤ Concentration < 10: WQC-II.	0.032	0.915	95% CI excludes null value, reject the null hypothesis.	Water Quality Class Number 1
Köydere	1.85	1.41	119	5	5 ≤ Conc. < 10: WQC-II.	0.039	0.920	reject the null hypothesis.	WQC Number 1
Ozandere	1.75	1.20	119	5	5 ≤ Conc. < 10: WQC-II.	0.032	0.888	reject the null hypothesis.	WQC Number 1
Paşaköydere	4.28	3.78	119	5	5 ≤ Conc. < 10: WQC-II.	0.234	0.810	95% CI includes null value, accept the null hypothesis.	WQC Number 2
Şalgamdere	3.8	3.25	119	5	5 ≤ Conc. < 10: WQC-II.	0.238	0.725	accept the null hypothesis.	WQC Number 2
Ömerli Dam Lake	4.15	3.50	119	5	5 ≤ Conc. < 10: WQC-II.	0.270	0.943	accept the null hypothesis.	WQC Number 2

Conclusion

Ömerli Dam Lake is a vital water body for Istanbul. The lake is used for the supply of drinking and utility water in Istanbul, which has a population of twenty million. The five main streams that feed the lake have their sub-basins within the basin of the lake. The main pollution elements in the lake basin are agriculture, illegal livestock breeding, especially buffalo breeding, and informal settlements.

When looking at the informal settlements problem with a human focus, it is observed that it is not easy to change the link between the space

and the individual. The village-to-city migration, which has been continuing since the industrial revolution, is the source of the economic inequality created by capitalist social relations, rapid population growth, and cheap housing shortages.

Until today, many measures, such as demolition of slums, have been attempted to remove these contaminants. However, it has not been successful.

According to Kıray (1969), informal settlements, which is why, in Turkey, rural-urban migration is no desire to be the owner of cheaper housing. Since the people who migrate from the village to the city have meager purchasing power, they try to accommodate with a saving method: "The cheapness of the house is provided, first of all, by the unpaid labor provided by the builder himself, his friends and relatives, and then by the minimum wage paid to skilled labor. The second source of savings is to use as cheap as possible and therefore low quality building materials. The third and significant saving is the possibility of not paying any money for the land on which the house will be built or paying too little money to be considered "normal."

Moreover, close relationships such as kinship, fellowship, and friendship continue in the slums of the cities, just as a reflection of the tradition of solidarity in the village. This causes a few families from the same town or the same neighborhood to come to an empty space around the city and make a dwelling (Kıray, 1969).

Especially in the sub-basin borders formed by Paşaköydere and Şalgamdere streams, as well as agriculture and animal husbandry activities affect the water quality of the lake negatively. When we look at the one-sample t-test results, we see that this situation has been proved statistically. This condition implies that seeking a sociological answer to the issue of informal settlements is crucial.

The problem of Istanbul Ömerli Dam Lake's slum structure must be solved. For example, cheap-cost housing can be sold to people with low incomes at affordable prices. Agricultural cooperatives can be developed, and migration from the village to the city can be prevented. There may be differences in the solution, but the common point of all is human. First of all, the primary problems of people should be listened to, their needs should be learned, and solutions should be shown in the light of science. The most important source of clean water for twenty million people should be sheltered as soon as possible.

References

Alsayyad, N., & Roy, A. (2004). Urban informality: Crossing borders. Urban Informality: Transnational Perspectives from the Middle East, Latin America, and South Asia, 1-6.

Azizullah, A., Khattak, M. N. K., Richter, P., & Häder, D. P. (2011). Water pollution in Pakistan and its impact on public health—a review. *Environment International*, *37*(2), 479-497.

Badruzzaman, M., Pinzon, J., Oppenheimer, J., & Jacangelo, J. G. (2012). Sources of nutrients impacting surface waters in Florida: a review. *Journal of environmental management*, *109*, 80-92.

Chapra, S. C. (1991). Toxicant-loading concept for organic contaminants in lakes. *Journal of Environmental Engineering*, *117*(5), 656-677.

Chekalin, A., Khramchenkov, M., Konyukhov, V., Konyukhov, I., & Garaeva, A. (2017). Mathematical modeling of rainwater runoff over catchment surface and mass transfer of contaminant incoming to water stream from soil. *Journal of Fundamental and Applied Sciences*, *9*(2S), 880-889.

Chelyadina, N. S., Popov, M. A., Lisitskaya, E. V., Pospelova, N. V., & Popovichev, V. N. (2017). The ecological condition of coastal waters off the Heracles Peninsula (Crimea, the Black Sea). *Ecologica Montenegrina*, *14*, 39-47.

Domagalski, J. L., & Johnson, H. (2012). Phosphorus and groundwater: establishing links between agricultural use and transport to streams. *US Geological Survey Fact Sheet*, *3004*, 2012.

DSI (State Hydraulic Works), 2019. 2009-2018 Stream and lake pollution parameters measurements in Ömerli Dam Lake Basin; Ankara, Turkey, www.dsi.gov.tr (Unpublished report).

Harvey, D. (2008). The right to the city. The City Reader, 6(1), 23-40.

Hazra, A., & Gogtay, N. (2016). Biostatistics series module 3: comparing groups: numerical variables. *Indian journal of dermatology*, *61*(3), 251.

Huang, H., Xu, X., Liu, X., Han, R., Liu, J., & Wang, G. (2018). Distributions of four taste and odor compounds in the sediment and overlying water at different ecology environment in Taihu Lake. *Scientific reports*, *8*(1), 1-10.

Jones, P. (2012). Searching for a little bit of utopia–understanding the growth of squatter and informal settlements in Pacific towns and cities. Australian Planner, 49(4), 327-338.

Kıray, M. (1969). "Gecekondu: Az Gelişmiş Ülkelerde Hızla Topraktan Kopma ve Kentle Bütünleşememe", Ankara Üniversitesi Siyasal Bilgiler Fakültesi Dergisi, No:3.

Laird, C. D., Biegler, L. T., van Bloemen Waanders, B. G., & Bartlett, R. A. (2005). Contamination source determination for water networks. *Journal of Water Resources Planning and Management*, *131*(2), 125-134.

Mohanty, M. (2006a). Urban squatters, the informal sector and livelihood strategies of the poor in the Fiji Islands. *Development Bulletin*, *70*, 65-68.

Mohanty, M. (2006b). *Poverty, environmental hazards and vulnerability of urban poor in small island states: a case of squatter communities in Suva city, Fiji Islands*. In: Urban Dimensions of Environmental Change: Science, Exposures, Policies and Technologies. Science Press, New Jersey, pp. 231-236.

Morkoç, E., Tüfekçi, V., Tüfekçi, H., Tolun, L., Karakoç, F. T., & Güvensel, T. (2009). Effects of land-based sources on water quality in the Omerli reservoir (Istanbul, Turkey). *Environmental Geology*, *57*(5), 1035-1045.

Moyle, P. B., & Leidy, R. A. (1992). Loss of biodiversity in aquatic ecosystems: evidence from fish faunas. In *Conservation biology* (pp. 127-169). Springer, Boston, MA.

Official Gazette (2004). *Water Pollution Control Regulation*, No: 25687, Ankara, Turkey.

Priscoli, J. D. (2000). Water and civilization: using history to reframe water policy debates and to build a new ecological realism. *Water Policy*, *1*(6), 623-636.

Sadler, W. R., & Stanier, R. Y. (1960). The function of acetate in photosynthesis by green bacteria. *Proceedings of the National Academy of Sciences of the United States of America*, *46*(10), 1328.

Scholz, R. W., Roy, A. H., & Hellums, D. T. (2014). Sustainable phosphorus management: a transdisciplinary challenge. In *Sustainable phosphorus management* (pp. 1-128). Springer, Dordrecht.

Shatkin, G. (2004). Planning to forget: Informal settlements as' forgotten places' in globalising Metro Manila. Urban studies, 41(12), 2469-2484.

Skaik, Y. (2015). The bread and butter of statistical analysis "t-test": Uses and misuses. *Pakistan Journal of Medical Sciences*, *31*(6), 1558-1559.

Tatlıdil, E. (1989). Kentleşme ve Gecekondu [Urbanisation et gecekondu], Izmir: Ege Üniv. Edebiyat Fak. Yayınları, s. 16.

Tricker, A. R. (1990). The effect of rounding on the significance level of certain normal test statistics. *Journal of Applied Statistics*, *17*(1), 31-38.

UN-Habitat. (2004). The challenge of slums: global report on human settlements 2003. Management of Environmental Quality: An International Journal, 15(3), 337-338.

Waajen, G. W., Van Bruggen, N. C., Pires, L. M. D., Lengkeek, W., & Lürling, M. (2016). Biomanipulation with quagga mussels (Dreissena rostriformis bugensis) to control harmful algal blooms in eutrophic urban ponds. *Ecological Engineering*, *90*, 141-150.

Williamson, C. E., Dodds, W., Kratz, T. K., & Palmer, M. A. (2008). Lakes and streams as sentinels of environmental change in terrestrial and atmospheric processes. *Frontiers in Ecology and the Environment*, *6*(5), 247-254.

Xu, F. L., Tao, S., Dawson, R. W., & Li, B. G. (2001). A GIS-based method of lake eutrophication assessment. *Ecological Modelling*, *144*(2-3), 231-244.

Xu, Y., Zhou, S., Hu, L., Wang, Y., & Xiao, W. (2018). Different controls on sedimentary organic carbon in the Bohai Sea: River mouth relocation, turbidity, and eutrophication. *Journal of Marine Systems*, *180*, 1-8.

Zhang, L., Shen, T., Cheng, Y., Zhao, T., Li, L., & Qi, P. (2020). Temporal and spatial variations in the bacterial community composition in Lake Bosten, a large, brackish lake in China. *Scientific Reports*, *10*(1), 1-10.

Zhang, Y. N., Xiang, Y. R., Chan, L. Y., Chan, C. Y., Sang, X. F., Wang, R., & Fu, H. X. (2011). Procuring the regional urbanization and industrialization effect on ozone pollution in Pearl River Delta of Guangdong, China. *Atmospheric Environment*, *45*(28), 4898-4906.

Chapter 7

COMPUTER BASED DIGITAL GAME DESIGN AND EVALUATION FOR TEACHING CONCEPTS

Umit ALBAYRAK[1], Sakir TASDEMIR[2]

1 Instructor, Selcuk University, Department of Computer Technologies and Programming,
2 Professor Doctor, Selcuk University, Department of Computer Engineering, umitalbayrak@
selcuk.edu.tr, stasdemir@selcuk.edu.tr

INTRODUCTION

Preschool Term Concepts Education

Preschool period is the basis and the first step of the whole life of the child. During this period, all areas of development of the child are supported, it is ensured that it acquires basic habits and develops its abilities (Güvenir, 2018).

Teaching concepts in preschool children; Although it varies from child to child, it can be a long and painful process. To go through analysis, synthesis and application processes at a level that can sort in concept education; It also positively affects children's learning abilities.

Game and Digital Game in Preschool Term

The origin of the word game comes from the Latin "ludos" root.

The game is an activity of various disciplines and the field of research that defines what the games are called is called "Ludology (Science of Play)". Ludology is a science that is a Latin word derived from the words "ludik, ludus and ludere" and investigates games. Ludus stands for the meaning of "not serious" and "pretending" (Juul, 2011).

In terms of the concept of game, Huizinga's work named "Homo Ludens" has an important place. Previous studies try to determine the meaning of the game in the field of "psychology and physiology" and explain why you play the game. On the other hand, Huizinga's work emphasizes that the game is not a part of human life, but a process that reveals the culture of humanity, develops with the culture and continues with the modern age (Sağlam & Topsümer, 2019).

Looking at the literature on the definition of the concept of game;

The game is the adaptation of stimuli received from the outside world and their adaptation to one's own life (Piaget, 1962). The game allows children to grasp the life they live in, to survive in life, to distinguish between the real and the unreal about the life (Susüzer, 2006). The definition that is shared in all of these definitions is the concept of education. Because in every game, children actually learn something (Alan, 2017).

The concept of Digital Game is explained as follows in the literature;

According to Frasca, the concept of digital game briefly is a leisure activity where one or more people on the digital software can be used alone (against 10 artificial intelligence) or mutually (with a friend / acquaintance) via the online network. software (Frasca, 2001).

On the other hand, Öngen defines it as "the result of the interaction of the player with an electronic system or game tools through the display or a similar visual system" (Öngen, 2014).

Jull, on the other hand, defines digital game as an activity that is free and without any restrictions (Juul, 2011).

Ellerbrock, on the other hand, defines the concept of digital game in accordance with technological systems, as "materials used for personal entertainment, entertainment or entertainment purposes (Ellerbrok, 2011).

Although computer games are described in different ways in different sources, it can be defined as "playing games electronically". Given the classification of computer games, the classifications are made according to the type of games, the electronic environment in which they are played and the way they are played. According to the types; action, adventure, fight, puzzle, role-playing, simulation, sports and strategy games; When classified according to electronic environment; It can be specified as PC, web browser, game console, tablet and smartphone games (Navruz & Taş-demir, 2019).

Considering the main differences between traditional games and digi-tal games (Güneş, 2012);

·   While the traditional game is of interest to a wide range of disci-plines, the name of the discipline that studies digital games is Ludology.

·   While at least two people are mentioned on the basis of competi-tion and volunteering in traditional game, artificial intelligence can replace the second person in digital games.

·   Traditional games can be played in the physical field, while digital games can be played in virtual environments without physical reality.

·   While success in traditional games can be rewarded at the end of the game, success in digital games can be rewarded while playing.

·   While the game story is ready and known in traditional games, the game story can be created by the player in digital games.

·   Unlike traditional games, professional structures are seen in the production processes of digital games.

The game of biological communication with computer lies in the game. According to some researchers, it is the basic element of the game. The computer is endless and ready to play, as well as having endless pa-tience. It has an infinite capacity to entertain. John Dewey also explains the benefits of the gaming feature of computer education. It draws attention to the initiation of biological games for Piaget, is a natural biological knowl-edge theorist, he pointed out that by constructing hypotheses, you consid-ered the test and changed it when it was wrong (Şahin, 2006).

Students want to spend time and work using what they drive, use and learn in the future with whatever they want. According to Malone, it in-

creases motivation for the use of computer games in education and training (İncekara & Taşdemir, 2019; Malone, 1981). In this training, an effective and productive learning environment will be created in computer games. Computer games are not only an interesting type of game, but also improve their usable skills and help the game contain information about the prepared course. Students will learn the subject and reinforce previous options while having a pleasant time with educational computer games (İncekara & Taşdemir, 2019).

Today, there is the necessary educational game and research required on these games. It was produced by the MECC research center under the name Oregon Trail. In 1973, a project called Plato was developed and educational computer games were used for mathematics education. This project works on computer game is tested on. As a result, your eyes have positive effects on mathematics achievement and operations attitudes towards mathematics. In 1982, Rocky Boots sold 100,000 units (Navruz and Taşdemir, 2019).

It is important that computer games are in education, considering the development in computer technologies and games, computer games logs, and taking computers into a part of our daily life. With the studies you will carry out this application, the boring of the traditional methods will be overcome and you will make the education process enjoyable and more permanent learning to design (Bayırtepe and Tuzun, 2007).

Both academic fields under the digital game usage information (lieberman, Fisk, & Biely, 2009). Qualifications such as digital games, elite-eye coordination, and motor skills are supportive (Lin & Hou, 2016). It shows that supporting the problem solving, logic, analysis and decision-making skills (Kim & Smith, 2017) also supports their strategy and predictive competencies. It has been determined that the use of digital games is an important tool in acquiring the technological knowledge and skills, and especially it increases the use of technology to support the use of digital gaming tools effectively (Mesman, Kuo, Carroll & Ward, 2013), (Toran, Ulusoy, Aydın, Deveci & Akbulut, 2016).

Previous Studies on Educational Digital Games

There are many studies on the concept of game and educational digital game in the literature. Some of these studies:

Ayan and Taşdemir used the Unity 3D game platform in digital environment, inspired by today's game stories, in their game work in 2020. In the game, the player is asked to save the character defined as Falconum from where he was captured. The player will try to save My Falcon by going through exciting roads and overcoming obstacles on these roads. The

player develops different strategies while playing the game and overcoming obstacles (Ayan & Taşdemir, 2020).

İncekara and Taşdemir, during their game activities in 2019; They designed a snake game using C # programming language. The game was applied to 123 students from 3rd and 4th grade students at basic education level. The study aims to combine four topics in mathematics with the snake game to make education fun (İncekara & Taşdemir, 2019).

Navruz and Taşdemir aimed to strengthen the learning achievements of the subject of "Transformation Geometry" in the 8th grade mathematics curriculum in their game studies called Symmetry in 2019. The basic structure of the game; It is based on the automatic creation of the image after the correct click of the corners of the image resulting from the reflection of the polygons drawn on the square paper, dot paper and coordinate plane according to the determined symmetry axis (Navruz & Taşdemir, 2019).

In their study in 2015, Koçer and Albayrak developed game-based educational materials on a multi-point touchpad to learn the term "time" for children aged 5-6 in preschool education. These training materials were applied to the experimental group for 5 weeks. The findings obtained at the end of the process were compared with those of the control group who were trained with traditional methods. (Koçer & Albayrak, 2015).

In their 2008 study, Robertson and Howells present qualitative results from an eight-week discovery field where a ten-year-old class made their own computer games. Since teachers have an important role in facilitating and supporting learners while using technology, the effects of the article on classroom practice are discussed (Robertson & Howells, 2008).

Motivation of the Study

This scope of work; Based on the principle that the best way of learning is learning by playing, for a preschool period on a computer or tablet with a touch screen display; An educational digital game has been developed in order to teach big-small, long-short, heavy-light and old-young concepts.

The digital game operates in a table-top card game format with drag-and-drop logic. In this context, as it is designed to work on platforms such as smart board, touch screen computer and tablet, it also contributes to the development of hand-eye coordination in children in addition to its main purpose. Images of the game for use on the smart board are shown in Figure 1.

Figure 1. Using the Game on the Smart Board

The fact that the game is designed for touch devices can be considered as a disadvantage in terms of possibilities. But; The ability to control it with the help of a mouse in non-touch devices eliminates this disadvantage. In Figure 2, there is a screen shot in which the game is played with the help of a mouse in a non-touch device.

Figure 2. Using the Game with the Mouse on Non-Touch Devices

MATERIAL AND METHOD

Educational digital game material for concept teaching was prepared in WPF (Windows Preentation Foundation) software platform on Microsoft Visual Studio as shown in Figure 3. Microsoft Visual Studio is provided free of charge by Microsoft DreamSpark service, which provides free use for educational use by Microsoft.
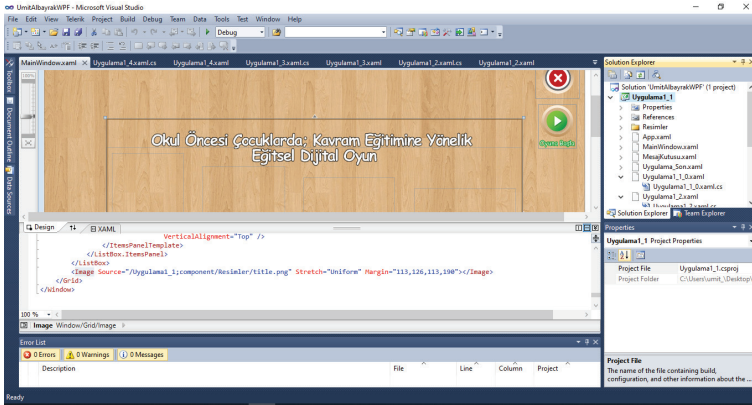
Figure 3. WPF Platform where the Game is Developed

WPF is a technology that can use all the features of the video card. It also enables the development of more performance applications using the DirectX library. Vector-based operations and advanced interfaces form the multi-point touch technology. At the same time, considering that these structures will operate simultaneously, multi-point touch applications can be developed most effectively with WPF. Multi-point touch programming is provided with WPF using StylusDevice or TouchDevice. This technology is at the Professional Developer Conference event in 2003. It was launched with the .NET Framework 3.0 family and was named with the code name Avalon when it was first announced. Technologies such as Windows Communication Foundation and Workflow Foundation were announced to developers at the 2003 Professional Developer Conference event. WPF has been a revolutionary innovation for software developers. Previously, only the developer was enough to develop a form application. This was done by the web as a result of the collaboration of the developer and designer. This was due to the design and code area being located at different places. In form applications, the whole work fell on the developer and missing designs could be revealed. When looking at WPF technology, it is striking that the design and code fields are separated from each other. Thanks to this innovation, both designer and developer will be more productive in their field (Koçer & Albayrak, 2015).

The Windows Presentation Foundation (WPF) working architecture is shown in Figure 4.
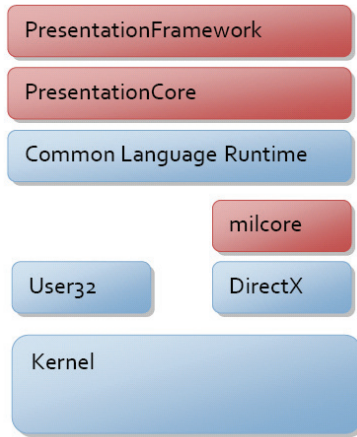
Figure 4. WPF Architecture (Microsoft, 2017)

There is a structure from bottom to top according to the structure shown in the figure. Considering the structures in WPF architecture and their functions;

Presentation Framework: This structure contains WPF tools (buttons, labels etc.).

Presentation Core: When new objects are needed other than WPF objects, objects in this layer are used.

Common Language Runtime: This structure, called common language study platform, has entered the literature with .NET and is based on the principle that programmers written in different languages can be combined under the same roof.

Milcore: It is the layer that provides viewing of WPF vehicles. In this layer, the things described in the interface creation section (using the GPU etc.) occur.

User 32: It is a structure containing user APIs in Windows platform.

DirectX: It is a structure that contains graphic elements.

Kernel: It is the core structure of the operating system. All transactions are based on this structure.

GAME DEVELOPMENT PROCESS

Educational digital game developed in children; Training of the related concepts is aimed by using the skills of grouping, comparing and sorting the images that express the big-small, long-short, heavy-light and old-young quantities and which have the right to use for free.

Educational game; It consists of two separate levels consisting of 5 stage. At the first level; children are asked to compare two different visuals according to the targeted concept (big-small, long-short, heavy-light and old-young). In the second level, 4 different visuals offered to children in each section are asked to rank by targeted concept (big-small, long-short, heavy-light and old-young).

As the target audience of the developed educational digital game is preschool children, the instructions in the whole game were made as well as written and it was ensured that illiterate preschool children did not experience any difficulties during the game.

The Welcome Screen screenshot of the educational game developed within the scope of this study. It is shown in Figure 5.
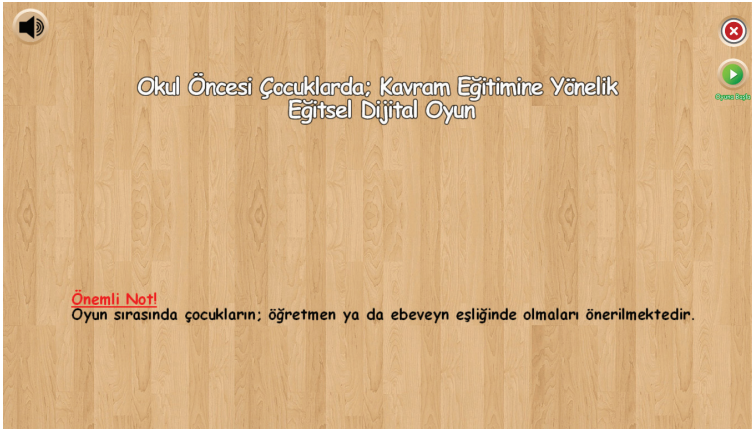
Figure 5. Game Welcome Screen Screenshot

The welcome screen also creates the main concept of the digital game that has been developed and progress is achieved in all sections with the same structure. If the basic elements on the screen are introduced;

·   Wooden table texture was chosen as the ground picture and the digital game was intended to give a real table-top card feel.

·   The black speaker icon in the upper left corner ensures that all written prompts that will appear on the screen during the game are made aloud.

·   The red close icon in the upper right corner allows the child to close the game at any stage on the screen during the game.

·   The green play icon below the close icon in the upper right allows the child to start the game on the welcome screen.

·   In the location where the start icon is in the game, the start icon is replaced by the clean icon. The clear icon allows each level to restart

during the game.

In Level 1 / Stage 1, 2 different visuals are displayed, and these visuals are compared and grouped as heavy and light. Visuals represent the heavy elephant, and light images represent the ladybug.

In Level 1 / Stage 2, 2 different visuals are displayed, and these images are compared and grouped as large and small. In the images, watermelon representing the big and grapefruit fruits were used to represent the small.

In Level 1 / Stage 3, 2 different visuals are displayed, and these visuals are compared and grouped as more or less. In the images, 9 poultry are represented, most of them are 2 horses.

In Level 1 / Stage 4, 2 different visuals are displayed, and these images are compared and grouped as old and young. In the images, the old woman representing the elderly and the girl child representing the young person were used.

In Level 1 / Stage 5, 2 different visuals are displayed, and these visuals are compared and grouped as heavy and light. The visuals bear the bear and the light representative caterpillar images. This section is also the last part of the first level.

The screenshots of the stages in Level 1 are shown in Figure 6.

Figure 6. Level 1 Screenshots

At the first level, children were asked to compare between the two

images. Those who have successfully completed all 5 levels in the first level are given the opportunity to transfer to the second level. In the second level, the number of images is 4 instead of 2 and the sections progress with a structure that requires more attention.

In Level 2 / Stage 1, 4 different visuals are displayed, and these images are compared and asked to rank from small to large. Representing from small to large in the visuals, respectively; bee, chicken, sheep and cow images were used.

In Level 2 / Stage 2, 4 different visuals are displayed, and these images are compared and asked to rank from short to long. Representing from small to large in the visuals, respectively; potted plants images are used.

In Level 2 / Stage 3, 4 different visuals are displayed, and these images are compared and asked to rank from less to more. Representing fewer to more in the images, respectively; Images of 1 raspberry, 2 apples, 3 peaches and 4 pears were used.

In Level 2 / Stage 4, 4 different visuals are displayed, and these visuals are compared and asked to rank from short to long. Representing from short to long in the visuals, respectively; crayons images of different sizes were used.

In Level 2 / Stage 5, 4 different visuals are displayed, and these images are compared and asked to be sorted from young to old. Representing young to old in the images, respectively; images of baby girls, boys, middle-aged women and old men were used. This episode is also the last part of both the second level and the game.

The screenshots of the stages in Level 2 are shown in Figure 7.

Figure 7. Level 2 Screenshots

At the second level, children were asked to compare and rank among the four images. Those who successfully complete all 5 stages in the second level have finished the game and are directed to the ending screen of the game.

If the correct answer is given at the end of the stages, the correct answer information is reported to the player visually and audibly. Visual notification is notified by the correct answer screen and voice notification is announced by the applause sound. When the correct answer is given at each stage, it is provided to go to the next stage.

In case of wrong answer at the end of the stages, wrong answer information is notified to the player visually and audibly. The warning is repeated until the correct answer is given in the game and the player is provided to learn the correct one.

DISCUSSION AND CONCLUSION

Digital play plays an increasingly decisive role in children's lives, and it also directly affects the child's physical and emotional environment. (Yaman, Dönmez, Kabakçı Yurdakul, & Odabaşı, 2013).

Preschool period; It is a period when technological devices such as phones, tablets and computers began to be used by children. Unfortunately, many parents misinterpret the use of technological devices in their children and either prohibit the use of the device or ignore uncontrolled use; They deprive their children of uncontrolled content from video sharing sites that is unclear for what purpose. But; It was observed that when the desire of children to use technological devices is supported in a controlled manner and with educational digital games, they contribute to the development of children in all aspects.

Educational games can be defined as the most suitable tool for learning. With the educational game, individuals can learn the concepts that are explained to them more easily and these concepts are not erased from memory for a long time. Learning can be said to be healthy and clear, because learning takes place with fun. In educational games, the individual faces a goal and this goal must be achieved. The aim may be to exceed a

certain point, to complete the task in a certain time (Tasdemir, Cizmeci, & Alan, 2016).

It has been observed that educational digital game, which aims to teach concept learning in preschool children with fun, teaches related concepts successfully.

Of the developed work; In addition to its primary purpose as a concept teaching, it has been observed that success is achieved in its secondary objectives such as the positive use of technological devices in children and the development of hand-eye coordination.

When the developed study is evaluated in terms of use in mobile devices; Since it is based on Microsoft Visual Studio, it does not support Android and IOS devices. It supports only Windows Mobile devices within mobile platforms. Failure of the developed study to work on all platforms can also be considered as a negative aspect of the study.

REFERENCES

Alan, D. (2017). Dijital Oyun Tabanlı Yaklaşım İle Yazılım Geliştirme Öğretimi. Retrieved January 13, 2020 from

Ayan, A., & Taşdemir, S. (2020). Computer Aided Digital Game Design and Programming: an Example Application. In A. HAYALOĞLU & A. GÜNDAY (Eds.), Academic Studies in Engineering (Mart 2020, pp. 251–272). Ankara. Retrieved April 26, 2020 from www.gecekitapligi.com

Bayırtepe, E., & Tuzun, H. (2007). The Effects Of Game-Based Learning Environments On Students' Achievement And Self-Efficacy İn A Computer Course. Hacettepe Üniversitesi - Eğitim Fakültesi Dergisi, (33), 41–54. Retrieved January 12, 2020 from http://www.efdergi.hacettepe.edu.tr/yonetim/icerik/makaleler/998-published.pdf

Ellerbrok, A. (2011). Playful biometrics: Controversial Technology through the Lens of Play. Sociological Quarterly, 52(4), 528–547. Retrieved January 13, 2020 from https://doi.org/10.1111/j.1533-8525.2011.01218.x

Frasca, G. (2001). Digital Creativity Rethinking agency and immersion: video games as a means of consciousness-raising Rethinking agency and immersion: video games as a means of consciousness-raising. Digital Creativity, 12(3), 167–174. Retrieved January 13, 2020 from https://doi.org/10.1076/digc.12.3.167.3225

Güneş, A. (2012). Dijital oyunların güvenlik bağlamında yasal ve yönetsel düzenleme sorunları. Retrieved January 13, 2020 from

Güvenir, Z. (2018). Okul Öncesi Öğretmenlerinin Fen Öğretimine Yönelik Tutumları ile Okul Öncesi Eğitim Programında Yer Alan Fen Etkinliklerini Uygulama Durumları.

İncekara, H., & Taşdemir, Ş. (2019). Matematikte Dört İşlem Becerisinin Geliştirilmesi için Dijital Oyun Tasarımı ve Öğrenci Başarısına Etkileri. Gazi Journal of Engineering Sciences, 5(3), 227–236. Retrieved January 12, 2020 from https://doi.org/10.30855/gmbd.2019.03.03

Juul, J. (2011). Half-real: Video games between real rules and fictional worlds. Retrieved January 13, 2020 from https://books.google.com/books?hl=tr&lr=&id=pyo3AgAAQBAJ&oi=fnd&pg=PR5&dq=Jill,+J.+(2011),+Half-Real:+Video+Games+Between+Real+Rules+and+Fictional+Worlds,+The+M%C4%B0T+Press+Cambridge,+Massachusetts+London,+England.&ots=kT5x4OM7LU&sig=9444V1tW-1rATt3PoIp8qWHkm-U

Kim, Y., & Smith, D. (2017). Pedagogical and technological augmentation of mobile learning for young children interactive learning environments. Interactive Learning Environments, 25(1), 4–16. Retrieved January 12, 2020 from https://www.tandfonline.

com/doi/abs/10.1080/10494820.2015.1087411?casa_token=DwG_
NPNgVOEAAAAA:OVx2I17EC_dA1La5Ddk-twM4cggTD-2WK6
useXuJzhWIAI1nrx06WszNmJrFwT1zgIRW13lyurfRdw

Koçer, H. E., & Albayrak, U. (2015). Measuring the Effect of Multi-touch Panel Based Education for Pre-school Students. Procedia - Social and Behavioral Sciences, 191, 1560–1570. Retrieved January 12, 2020 from https://doi.org/10.1016/J.SBSPRO.2015.04.623

Lieberman, D. A., Fisk, M. C., & Biely, E. (2009). Digital games for young children ages three to six: From research to design. Computers in the Schools, 26(4), 299–313. Retrieved January 12, 2020 from https://doi.org/10.1080/07380560903360178

Lin, Y., & Hou, H. (2016). Exploring young children's performance on and acceptance of an educational scenario-based digital game for teaching route-planning strategies: a case study. Interactive Learning Environments, 24(8), 1967–1980. Retrieved January 12, 2020 from https://www.tandfonline.com/doi/abs/10.1080/10494820.2015.1073745?-casa_token=aLVroDlMEwMAAAAA:lKfCtCLU58sdU6sRClBGr-YGU7ojIA3i0ObBnkSloir_N0oBV_rzJSEi_mD8w7hqBUdUhiG-cUScDU7w

Malone, T. (1981). What makes things fun to learn? A study of intrinsically motivating computer games. Dissertation Abstracts International, 41(5B), 1955. Retrieved January 12, 2020 from https://elibrary.ru/item.asp?id=7302452

Mesman, G., Kuo, D., Carroll, J., & Ward, W. (2013). The impact of technology dependence on children and their families. Elsevier, 27(6), 451–459. Retrieved January 12, 2020 from https://www.sciencedirect.com/science/article/pii/S0891524512001034

Microsoft. (2017). WPF Mimarisi | Microsoft Docs. Retrieved January 12, 2020, from https://docs.microsoft.com/tr-tr/dotnet/framework/wpf/advanced/wpf-architecture

Navruz, M., & Taşdemir, Ş. (2019). Design and development of an educational digital game based on mathematics course transformation geometry. International Journal of Applied Mathematics Electronics and Computers, 7(4), 88–95. Retrieved April 26, 2020 from https://doi.org/10.18100/ijamec.597156

Öngen, Y. (2014). Kişilerarası iletişim açısından sanal gerçeklik olarak bilgisayar oyunları: world of warcraft örneği. Retrieved January 13, 2020 from http://dspace.marmara.edu.tr/handle/11424/38177

Piaget, J. (1962). Play, Dreams and Imitation in Childhood. W W Norton & Co. Retrieved January 13, 2020 from

Robertson, J., & Howells, C. (2008). Computer game design: Opportunities for successful learning. Computers & Education, 50(2), 559–578. Retrieved April 26, 2020 from https://doi.org/10.1016/J.COMPEDU.2007.09.020

Sağlam, M., & Topsümer, F. (2019). Dijital Oyunlar Ve Öznel İyi Oluş İlişkisi: Muğla Sıtkı Koçman Üniversitesi Örneği, 14(2), 31–50. Retrieved January 13, 2020 from https://doi.org/10.12739/NWSA.2019.14.2.4C0230

Şahin, B. (2006). Okul öncesi dönemde bilgisayar destekli fen öğretimi ve etkilerinin incelenmesi. Retrieved January 12, 2020 from https://tez.yok.gov.tr/UlusalTezMerkezi/tezSorguSonucYeni.jsp

Susüzer, K. (2006). Oyun Yoluyla Fransızca Öğretimi. Retrieved January 13, 2020 from

Tasdemir, Ş., Çizmeci, H. İ., & Alan, D. (2016). Learning Mathematics With Educational Digital Game Programming. Research Highlights in Education and Science. Retrieved January 13, 2020 from

Toran, M., Ulusoy, Z., Aydın, B., Deveci, T., & Akbulut, A. (2016). Çocukların Dijital Oyun Kullanımına İlişkin Annelerin Görüşlerinin Değerlendirilmesi. Kastamonu Eğitim Dergisi, 24(5), 2263–2278.

Yaman, F., Dönmez, O., Kabakçı Yurdakul, I., & Odabaşı, H. F. (2013). Dijital Ebeveynlik ve Değişen Roller. Retrieved January 13, 2020 from https://www.researchgate.net/publication/271209011

Chapter 8

DESIGN AND REALIZATION OF A MULTI LAYER DIELECTRIC LENS STRCUTURES VIA THE USE OF 3D PRINTING TECHNOLOGY

Aysu BELEN[1]

1 Yüksek Mühendis, Hybrid and Electric Vehicle Technology, Iskenderun Vocational School of Higher Education, Iskenderun Technical University, aysu.yldrm07@gmail.com

Antenna designs with high gain features are one of the most important elements of today's wireless communication systems. Although antenna arrays are a common solution for high gain applications, they have disadvantages. Increase of loss the main items of these are: the loss in the feeding network is increased with the increasing number of array elements that would make the design more complex. Another solution to meet the high gain demand is the usage of dielectric lens structures. Dielectric lens structure are being used for focusing the incoming electromagnetic waves into the aperture of the antenna. Thanks to the wide operation band features of dielectric lens structures, these designs are also being extensively used in fields of military RADAR applications, Intelligence transportation, automobile RADAR and Satellite communications [1-8]. Another usage of dielectric lens structures is to create antennas with multi beams [9-10].

One of the methods for performance enhancement of dielectric lens structures is to have a design with multi layers. By this mean a matching circuit would be formed with layers of dielectric lens structures to have a better transmission performance with lesser reflection losses over a wide operation band [11]. Some of the commonly used dielectric lens structures in literature can be named as: Luneburg, Einstein, dielectric stick, and Fresnel lens designs.

These designs usually have a complex and difficult 3 dimensional architectures to be prototyped with traditionally dielectric materials. However, with the recent advances in 3Dprinting technology, design of such complex architectures had become more feasible especially in field of manufacturing of high frequency antenna designs [12-14]. Furthermore, with the reduced manufacturing cost, having high accuracy, being fast and ability of realization of complex designs are the main reasons of trending applications of 3D printing technology in antenna design applications [15-21]. It should be also mentioned that 3D printing technology not only being a trending manufacturing method in field of microwave engineering but it's being extensively used in other fields such as biomedical, civil engineering, architecture etc. [22-28].

The main concept of 3D printing technology is based on dividing the targeted structures in forms of layers. Each layer will be formed by using either melted metallic or plastic based materials to be the base of the other layers. Due to be the fastest and most cheapest between other methods of 3D printing, this method is the most commonly used 3D printing technology which is named as Fused Deposition Modelling (FDM). In this method usually two main materials are being used (i) Acrylonitrile Butadiene Styrene (ABS), (ii) PolyLactic Acid (PLA). The designs that being manufactured with this materials are tend to have a high mechanical strength, high tempter, and high chemical reaction resistance. By using these materials

realization of high frequency stages that either being high cost or infeasible had become a solvable problem such as design of lens antenna, Ku band horn antennas, Frequency Selective Surfaces, Array Antennas and waveguide structures [29-43].

In this work, design realization of a multilayer dielectric lens design for X band applications had been achieved via the use of 3D printing technology. For 3d manufacturing PLA had been used as a commonly and easy to found material. During the prototyping process, the infill rate of each layers are separately calculated in order to have different dielectric constant values. The simulated and experimental results of the proposed multilayer dielectric antenna had been compare alongside of performance results of counterpart works in literature. Thus, by this mean, an efficient, low cost and fast prototyping method for manufacturing of high performance complex dielectric lens antennas had been achieved via the use of 3D printing technology.

Lens antenna

The main concept of optical lens and radio frequency (RF) lenses are similar, in both of them the incoming waves are directed with respect to the geometry of the lens designs either for focusing or giving a certain requested pattern. Lens structures are usually preferred in high frequency applications. The operation frequency of lens structures are proportional to their size, with increasing the operation frequency the size of design is reduced and vice versa. These designs have their own advantages and disadvantages with respect to their applications.

Advantages of Lens Antenna

-   Can be used in wide band applications,

-   Can be used for performance enhancement of existing structures,

-   To achieve a planar EM wave, in short distances, which is a very important aspect in small size research laboratories.

-   In lens antennas, feed and feed support, do not obstruct the aperture.

-   It has greater design tolerance.

-   Larger amount of wave, than a parabolic reflector, can be handled.

-   Beam can be moved angularly with respect to the axis.

Disadvantages of Lens Antenna

-   Need of complex designs with increase operation frequency,

-   Having a material that can be formed in the requested design

alongside of having the requested dielectric constant,

- Lenses are heavy and bulky, especially at lower frequencies,

- Costlier compared to reflectors, for the same specifications,

With the recent advances in 3Dprinting technology, prototyping of complex designs had become low cost and faster compared to traditionally methods. As it mentioned before in 3D printing technology the main concept of manufacturing is based on dividing the targeted structures in forms of layers. Fused Deposition Modelling (FDM) is the most commonly used prototyping method. Herein, CEL Robox® Micro manufacturing platform (Fig. 1) had been used for 3D prototyping of the proposed Lens antenna design using PLA thermoplastic material. With CEL Robox® Micro design of structures with layer accuracy of 400 micron to 20 micron is possible. Here in order to have a smooth surface for lens design the layer accuracy should be selected with care, but it also should be noted that with increase layer accuracy the total number layers is also increased that might extended the total prototyping process.

Fig. 1. *CEL Robox® Micro manufacturing platform [44]*

It is possible to have different infill rates, ratio of material to the total volume which mean in %50 infill rate the design is filled %50 material and %50 air, of designs during the 3D prototyping process. With this unique feature, it is possible to create designs with different dielectric constant values. A design that had been prototyped with %100 PLA material infill rate would have a dielectric constant value of 2.7 while a design with %18 infill rate would have dielectric constant value of 1.2 [45]. In Table 1 and [45], experimental results of designs with different infill rate of PLA had been presented. Equation (1) had been obtained via interpolation methods to have a analytical formulation to calculate the dielectric constant of material with respect to the infill rate. The equation can provide a dielectric range variation of 1.2-2.7.

Table 1. *PLA Effect of infill rate of PLA on dielectric constant vale of design [45]*

Infill rate %	Dielectric constant ε_r	Loss tangent
18	1.24	0.002
33	1.6	0.004
73	2.53	0.006
100	2.72	0.008

$$\varepsilon_r = -1.3x10^{-6}x^3 + 0.0374x + \frac{6.42}{x} + 0.217 \tag{1}$$

Here x represent designs infill rate value in (%) [46].

Prototyping of Multilayer lens antenna with 3D printer

In design of dielectric lens structures there are some critical aspects that designer should take into the consideration. If the dielectric constant of material is high the wave lengths inside the lens would reduce however this would also cause unwanted reflection between the lens structure and air environment or other layers of design. These reflection would have a great impact on overall performance of antenna and would cause a great efficiency loss [47]. Herein, a multilayer lens antenna design aimed for X band applications had taken into the consideration. In fig. 2 the geometrical design of the proposed multilayer lens antenna had been presented. The optimal designs of antenna are given in Table 2.

(a)

(b)
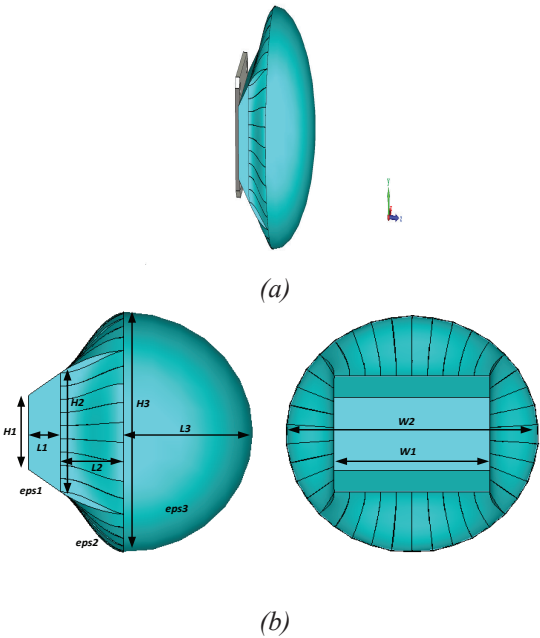
Fig. 2. *(a) Perspective, (b) schematic, view of the proposed multilayer lens antenna.*

Table 2. *Parameters of proposed multilayer lens antenna in (mm).*

H1	25	L1	10mm
H2	50	L2	20mm
H3	82	L3	42mm
W1	50	W2	82mm
ε_1	1.5	Infill rate in %	29%
ε_2	2.1	Infill rate in %	52%
ε_3	2.4	Infill rate in %	66%

3D EM simulator tools had been used for simulation performance measures of the proposed multilayer lens antenna design. In Figs. 3-4, the simulated electric field distribution of the multilayer lens antenna at 10 GHz, and far field radiation pattern for different operation frequencies had been presented.
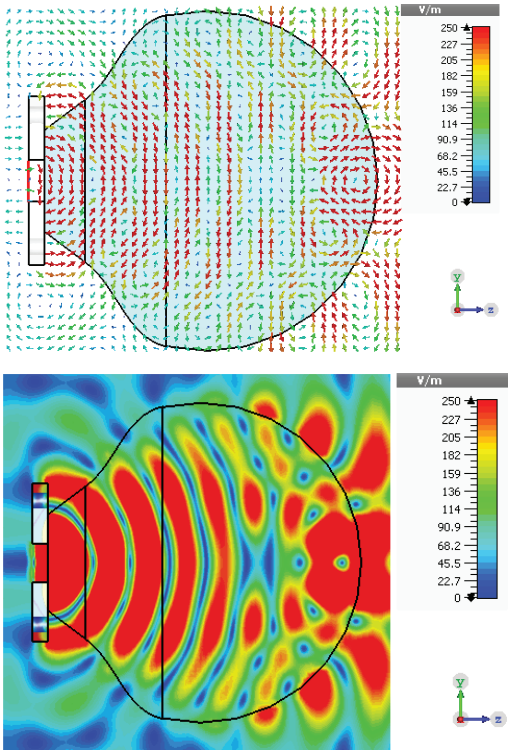
Fig. 3. *Simulated E-field distribution of antenna @ 10 GHz.*
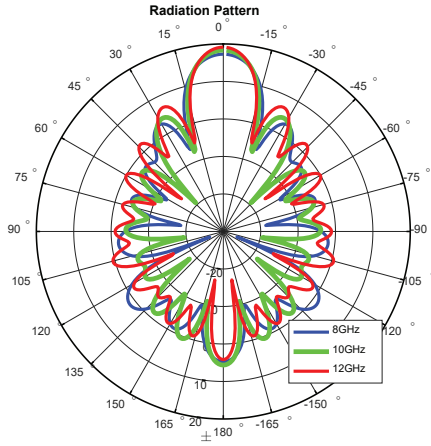
Fig. 4. *Simulated far field radiation pattern of the multilayer lens antenna*

3D printing and measurements

The first step of 3D manufacturing is to convert the design into a ".stl" file format. 3D printers use this file to create a G-code to calculate the roads and timing of adding materials and layers to optimally prototyped the aimed design. The proposed multilayer lens antenna is consist of 3 different layers where infill rate of each is determined by using equation (1) and table 2. Thus by having a variant dielectric constant in each layer a matching between the antenna and air environment had been achieved for reducing the reflections. The manufacturing sensitivity of layers are set as 0.2mm using PLA material. In fig. 5, the 3D prototyped multilayer lens antenna feed with a WR90 waveguide had been presented.
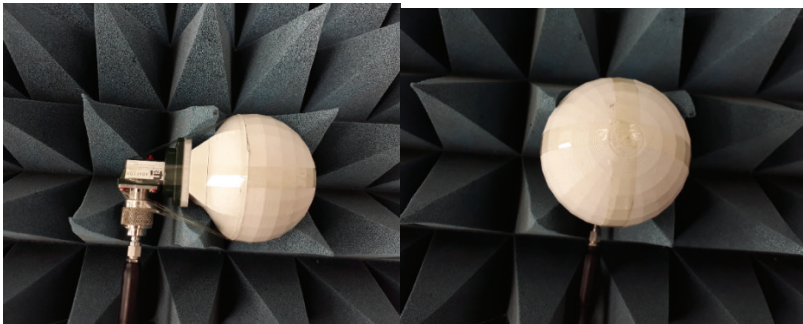
Fig. 5. *3D printed proposed multilayer lens antenna.*

The measurement results of S_{11} and gain are obtained using the measurement setup given in Fig. 6 [48]. A Network Analyzer with a measurement bandwidth of 9 kHz to 13.5 GHz, and two identical antennas "Rohde—Schwarz RS Zvl13 and LB8180 0.8 to 18 GHz" have been used for measurement of the 3D printed Dielectric Lens antenna.
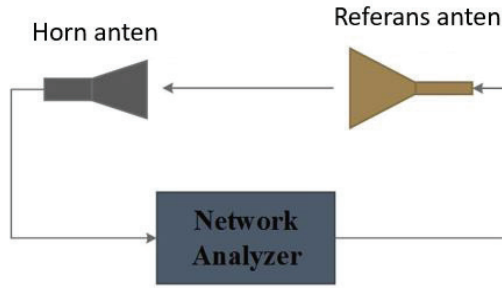
(a)
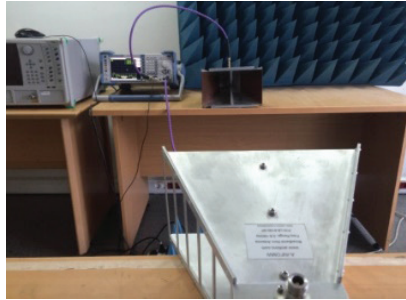
(b)

Fig. 6. *(a) Schematic view, (b) Laboratory view of the measurement setup [49].*

In Fig. 7, both simulated and measured Return loss characteristics of the proposed multilayer lens antenna had been presented. as it can be seen from the figure, the measured performance of antenna at X band is hand to hand with simulated results and S_{11} is less than -6dB.
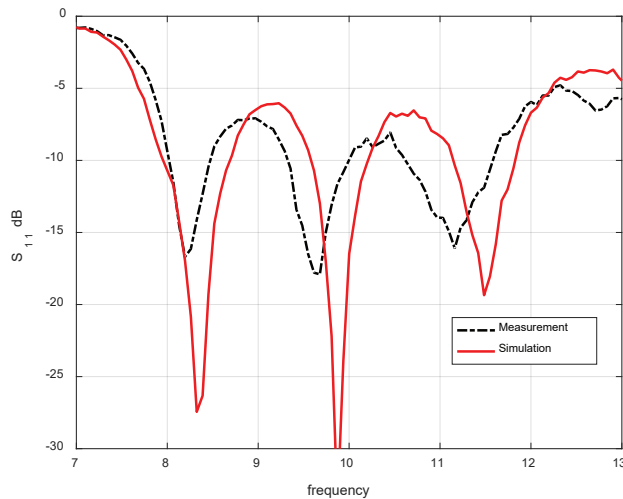
Fig. 7. *Simulated and measured Return loss characteristics of 3D printed Multi-layer lens antenna.*

The simulated and measured radiation pattern of the proposed antenna are given in Fig. 8. The antenna achieves a measured gain characteristics of 16dBi, 17.2dBi, 17.9dBi at 8, 10, 12 GHz operation frequencies respectively. Again similar to S_{11} characteristics the simulated and measured results are hand to hand in radiation pattern characteristics. In Table 3, the simulated and measured results of radiation characteristics are tabulated.

(a)

(b)
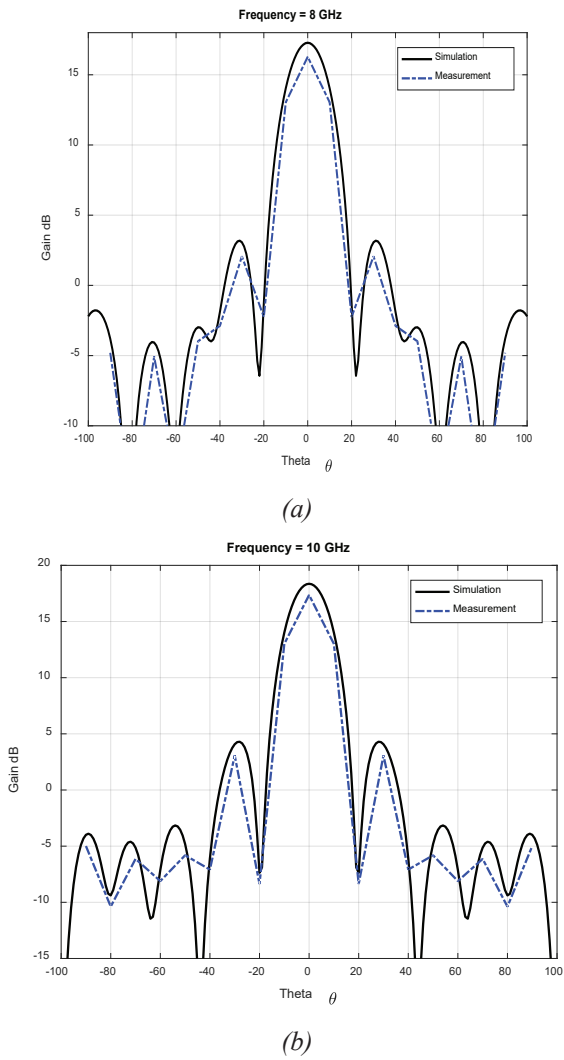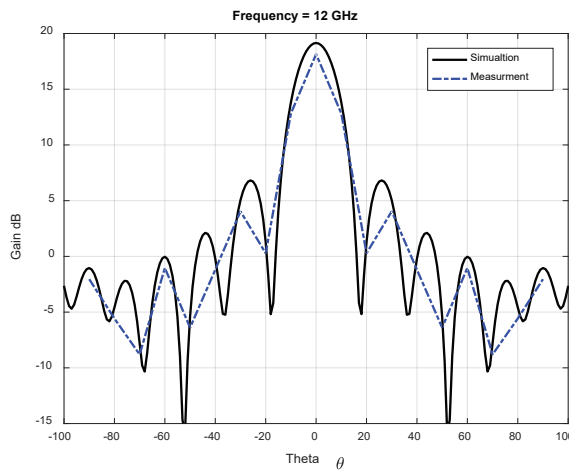
(c)

Fig. 8. *Simulated and measured radiation patterns of the antenna @ (a) 8 GHz, (b) 10 GHz, (c) 12 GHz.*

Table 3. *Comparison of simulated and measured gain results.*

Frequency (GHz)	Simulated (dBi)	Measured (dBi)
8	17.28	16.1
9	17.90	16.8
10	18.36	17.2
11	18.68	17.5
12	19.15	17.9

Furthermore, a performance comparison of the proposed 3D printed multilayer lens antenna design with counterpart designs in literature had been done and presented in Table 4. As it can be seen form the table, the proposed design achieves a better performance results over the x and operation frequencies with less size compare to counterpart designs.

Table 4. *A comparison of proposed antenna design with counterpart designs in literature*

	Size (mm)	Operation band (GHz)				
		8	9	10	11	12
Here	82x82x72	16.1	16.8	17.2	17.5	17.9
[50]	279x244x159	16	18	14.8	17	15
[51]	85.1x30.8x15.9	8.5	9	9	9	10

| [52] | 90.7x210x210 | --- | --- | 17 | --- | --- |
| [53] | 87.4x59.3x80 | 14 | 15.5 | 16.5 | 15 | 17 |

Conclusion

In this work design and realization of a high performance multilayer lens antenna via the use of 3D printing technology had been achieved. Here in order to have a design with high efficiency a design with layers that have different dielectric constant values are designed. Variant dielectric constant value had achieved with the usage of 3D printer's infill rate features. Design and simulation of proposed multilayer lens antenna had been done in 3D EM simulator environment. Then, the experimental results of 3D printed antenna are compared with simulated results and found to be agreeable over the aimed operation band. Furthermore, the experimental performance results of propose multilayer lens antenna are compared with counterpart designs in literature. The proposed designs not only achieves higher gain performance but it is also is smaller size in size with most of the counterpart designs. Thus, in this work design and realization of high performance multilayer lens antenna designs are achieved in a fast, low cost way via the use of 3D printing technology. In features works it is possible to achieve designs with higher layers and more complex designs of lens structures.

References

[1] Risser, J. R. 1949. Microwave Antenna Theory and Design. New York, NY, USA: McGraw-Hill.

[2] Chantraine-Bares, B., Sauleau, R., Coq, L.L. and Mahdjoubi, K. 2005. A new accurate design method for millimeter-wave homogeneous dielectric substrate lens antennas of arbitrary shape. IEEE Trans. Antennas Propag., vol. 53, no. 3, pp. 1069–1082.

[3]   Kock, W. E. 1948. Metallic delay lens." Bell System Tech. J., vol. 27, pp. 58–82.

[4]   Kock, W. E. 1946. Metal lens antennas," Proc. IRC, vol. 34, no. 11, pp. 826–836.

[5]   Schoenlinner, B., Wu,X., Ebling, J.P., Eleftheriades, G.V. and Rebeiz, G.M. 2002. Wide-scan spherical-lens antennas for automotive radars. IEEE Trans Microwave Theory Tech 50, 2166–2175.

[6] Fuchs, B., Lafond, O., Rondineau, S., Himdi, M., and Le Coq, L. 2007. Off-axis performances of half Maxwell fish-eye lens antennas at 77GHz. IEEE Trans Antennas Propag 55, 479–482.

[7] Costa, J.R., Fernandes, C.A., Godi, G., Sauleau, R., Le Coq, L. and Legay,H. 2008. Compact Ka-band lens antennas for LEO satellites. IEEETrans Antennas Propag 56, 1251–1258.

[8] Fernandes, C.A. 1999. Shaped dielectric lenses for wireless millimeter-wave communications. IEEE Antennas Propag Mag 41, 141–150.

[9] Lafond, O., Caillet, M., Fuchs, B. , Palud, S., Himdi, M., Rondineau, S. and Le Coq, L. 2008. Millimeter wave reconfigurable antenna based on active printed array and inhomogeneous lens, Eur Microwave Conf,Amsterdam, Holland, 147–150.

[10] Fuchs, B., Palud, S., Lafond, O., Himdi, M. and Rondineau, S. 2007. Sys-te`me antennaire dont le diagramme de rayonnement est reconfigura-ble parmi des diagrammes de rayonnement sectoriels et directifs, etdispositifs e´metteur et / ou re´cepteur correspondant, French Patent0756664.

[11] Nguyen, N. T., Sauleau, R., Pérez, C. J. 2009. Very Broadband Extended Hemispherical Lenses: Role of Matching Layers for Bandwidth Enlargement. IEEE Transactions on Antennas and Propagation, vol. 57, no. 7, pp. 1907 – 1913.

[12] Belen, M. A., Mahouti, P. 2018. Design and realization of quasi Yagi antenna for indoor application with 3D printing technology. Microw Opt Technol Lett. 60 (9):2177-2181. https://doi.org/10.1002/mop.31319.

[13] Toy, Y.C., Mahouti, P., Güneş, F. and Belen, M.A. 2017. Design and Manufactering of an X-Band Horn Antenna using 3-D Printing Technology", 8th International Conference on Recent Advances in Space Technologies, İstanbul, TURKEY

[14] Adams, J. J. , Duoss, E. J., Malkowski, T., Motala, M., Ahn, B. Y., Nuzzo, R. G., Bernhard, J. T. and Lewis, J. A. 2011. Conformal Printing of Electrically Small Antennas on Three-Dimensional Surfaces. Advanced Materials, 23 [11], pp. 1304-1413.

[15] Shaker, G., Ho-Seon, L., Safavi-Naeini, S., Tentzeris, M. 2011. Printed electronics for next generation wireless devices. IEEE Antenna and propagation conference (LAPC), pp. 1-5.

[16] Mei, J., Lovell, M. and Mickle, M. 2005. Formulation and processing of novel conductive solution inks in continuous inkjet printing of 3-D electric circuits. IEEE Transactions on Electronics Packaging Manufacturing, vol. 28, no. 3, pp. 265- 273.

[17] Shaker, G., Safavi-Naeini, S., Sangary, N., Tentzeris, M. M 2011. Inkjet Printing of Ultrawideband (UWB) Antennas on Paper Based Substrates. Antennas and Wireless Propagation Letters, IEEE, Vol. 10, pp. 111-114.

[18] Hester J. et al. 2015. Additively manufactured nanotechnology and origami-enabled flexible microwave electronics. Proc. IEEE, vol. 103,

no. 4, pp. 583–606.

[19] Kimionis, J., Georgiadis, A., Isakov, M., Qi, H. J. and Tentzeris, M. M. 2015. 3D/inkjet-printed origami antennas for multi-direction RF harvesting. IEEE MTT-S Int. Microw. Symp. (IMS), Phoenix, AZ, USA, pp. 1–4.

[20] Martinez, R. et al. 2015 "Planar monopole antennas on substrates fabricated through an additive manufacturing process," in 9th Eur. Conf. Antennas and Propag. (EuCAP), Lisbon, Portugal.

[21] Tehrani, B., Cook, B. S. and Tentzeris, M. M. 2015. Post-process fabrication of multilayer mm-wave on-package antennas with inkjet printing. 2015 IEEE Int. Symp. Antennas and Propag. (APSURSI), Vancouver, BC, Canada.

[22] Butscher A., Bohner M., Doebelin N., Hofmann S., Müller R. 2013. New depowdering-friendly designs for three-dimensional printing of calcium phosphate bone substitutes, Acta Biomaterialia, volume 9, Issue 11, 9149-9158s, ISSN 1742-7061.

[23] Xu T., Zhao W., Zhu J. M., Albanna MZ, Yoo J. J., Atala A. 2013. Complex heterogeneous tissue constructs containing multiple cell types prepared by inkjet printing technology, Biomaterials, volume 34, Issue 1, pages 130-139, ISSN 0142-9612.

[24] Wang K., Ho C. C. , Zhang C., Wang B. 2017. A Review on the 3D Printing of Functional Structures for Medical Phantoms and Regenerated Tissue and Organ Applications, Engineering, volume 3, Issue 5, pages 653-662, ISSN 2095-8099,

[25] Yagnik D. 2014. Fused deposition modeling - a rapid prototyping technique for product cycle time reduction cost effectively in aerospace applications, IOSR Journal of Mechanical and Civil Engineering, 62-68.

[26] Sivadasan M, Singh, K. and Sood A. K. 2013. Use of fused deposition modeling process in investment precision casting - a viable rapid tooling, International Journal of Conceptions on Mechanical and Civil Engineering, 1(1).

[27] Satyanarayanaa B., Prakash K. J. 2015. Component replication using 3D printing technology, Procedia Materials Science, 10, 263 – 269.

[28] Malaeb Z., Hachem H., Tourbah A., Maalouf T., Zarwi N.E., Hamzeh F.2015. 3D Concrete Printing: Machine and Mix Design. International Journal of Mechanical Engineering and Technology, 6(6), pp. 14–22.

[29] Zhang, S., Arya, R. K., Pandey, S., et al. 2016. 3D-printed planar graded index lenses. Microw. Antennas Propag., 10, (13), pp. 1411–1419, doi: 10.1049/iet-map.2016.0013

[30] Ghazali M. I. M., Karuppuswami S., Kaur, A. 2017. 3-D printed air substrates for the design and fabrication of RF components. Trans. Compon. Packag. Manuf. Technol., 2017, 7, (6), pp. 982–989, doi:

10.1109/TCPMT.2017.2686706

[31] Jun S., Sanz-Izquierdo B., Heirons J., 2017. Circular polarised antenna fabricated with low-cost 3D and inkjet printing equipment', Electron. Lett. 53, (6), pp. 370–371, doi: 10.1049/el.2016.4605

[32] Wang S., Zhu L., Wu W. 2018. '3-D printed inhomogeneous substrate and superstrate for application in dual-band and dual-CP stacked patch antenna', Trans. Antennas Propag. doi: 10.1109/ TAP.2018.2810330

[33] Wu J., Kodi A., Kaya S. 2017. Monopoles loaded with 3-D-printed dielectrics for future wireless IntraChip communications', Trans. Antennas Propag. 65, (12), pp. 6838–6846, doi: 10.1109/ TAP.2017.2758400

[34] Belen M.A., Mahouti P. 2018. Design and realization of quasi Yagi antenna for indoor application with 3D printing technology. Microw Opt Technol Lett. 60:2177–2181.

[35] Toy Y. C., Mahouti P., Güneş F., Belen M. A. 2017. Design and manufactering of an X-band horn antenna using 3-D printing technology. 8th International Conference on Recent Advances in Space Technologies (RAST), Istanbul, pp. 195-198. doi: 10.1109/ RAST.2017.8002988

[36] Garcia C. R., Rumph R. C., Tsang H. H., Barton J. H. 2013. Effects of extreme surface roughness on 3D printed horn antenna, Electron Lett 49, 734–736.

[37] Chieh J. C. S., Dick B., Loui S., Rockway J. D. 2014. Development of a Ku-band corrugated conical horn using 3-D print technology, IEEE Antennas Wireless Propag Lett 13, 201–204.

[38] Junping S., Wei-Jiang Z., Xinrong L., Xiuhan J. 2015. 75-500 MHz quadruple-ridged horn antenna with dual polarisation, Electron Lett 51, 597–598.

[39] Auria M., Otter W.J., Hazell J., Gillatt B.T.W., Long-Collins C., Ridler N.M., Lucyszyn S. 2015. 3-D printed metal-pipe rectangular waveguides, IEEE Trans Compon Packag Manuf Technol 5, 1339–1349.

[40] Sage G. P. 2016. 3D printed waveguide slot array antennas, IEEE Access 4, 1258–1265.

[41] Arbaoui Y., Laur V., Maalouf A., Queffelec P., Passerieux D., Delias A., Blondy P. 2015. Full 3-D printed microwave termination: A simple and low-cost solution, IEEE Trans Microwave Theory Tech 64, 271–278.

[42] Moscato S., Bahr R., Le T., Pasian M., Bozzi M., Perregrini L., Tentzeris M.M., 2015. Additive manufacturing of 3D substrate integrated waveguide components, IET Electron Lett 51, 1426–1428.

[43] Barton J. H., Garcia C. R., Berry E. A., Salas R., Rumpf R. C. 2015. 3- D printed all-dielectric frequency selective surface with large

bandwidth and field of view, IEEE Trans Antennas Propag 63, 1032–1039.

[44] CEL Robox® Micro üretim platformu, http://cel-uk.com/3d-printer/rbx01-480.html. Available on [21.11.2018]

[45] Zhang S. , Njoku C, C., Whittow, W. G. and Vardaxoglou, J. C. 2015. Novel 3D printed synthetic dielectric substrates. Microw. Opt. Technol. Lett., 57: 2344-2346. doi:10.1002/mop.29324

[46] Mahouti P. 2019. 3 Boyutlu Yazıcı Teknolojisi ile Bir Mikros¸erit Yama Antenin Maliyet Etkin Üretimi. J Eng Sci Des. 7:473-479.

[47] Nguyen, N. T., Sauleau, R., Pérez, C. J., 2009. Very Broadband Extended Hemispherical Lenses: Role of Matching Layers for Bandwidth Enlargement. IEEE Transactions on Antennas and Propagation, vol. 57, no. 7, pp. 1907 – 1913.

[48] A-info, lb8180, 0.8-18 Ghz broad band horn antenna available at: http://www.ainfoinc.com/en/p_ant_h_brd.asp

[49] Belen M. A. 2018. Ultra Geniş Band Uygulamaları için Düzlemsel Hat Beslemeli Mikroşerit Anten Tasarımı, Gazi Üniversitesi Fen Bilimleri Dergisi Part C: Tasarım ve Teknoloji,

[50] Türk, A.S., Keskin, A. K., Şentürk, M. D. 2015. Dielectric loaded TEM horn-fed ridged horn antenna design for ultrawideband ground-penetrating impulse radar. Turkish J Elec Eng & Comp Sci. 23: 1479 – 1488, 2015.

[51] Bauerle, R. J., Schrimpf, R., Gyorko, E., Henderson, J. 2009. The Use of a Dielectric Lens to Improve the Efficiency of a Dual-Polarized Quad-Ridge Horn from 5 to 15 GHz. IEEE Transactions on Antennas and Propagation, Vol. 57, No. 6.

[52] Tak, J., Kang, D. G. and Choi, J. 2017. A Lightweight Waveguide Horn Antenna Made via 3D Printing And Conductive Spray Coating. Microwave and Optical Technology Letters / Vol. 59, No. 3.

[53] Ain, M. F., Othman, A. and Ahmad, A. A. 2013. Hybrid Dielectric Resonator Integrated Pyramidal Horn Antenna. Microwave and Optical Technology Letters. vol. 55, no. 6.

Chapter 9

REFLECTION CHARACTERISTICS OF MICROSTRIP REFLECTARRAY ANTENNAS VIA THE FULL WAVE EM SIMULATION BASED ARTIFICIAL NEURAL NETWORKS

Aysu BELEN[1], Filiz GÜNEŞ[2]

1 Yüksek Mühendis, Hybrid and Electric Vehicle Technology, Iskenderun Vocational School of Higher Education, Iskenderun Technical University, aysu.yldrm07@gmail.com
2 Prof. Dr., Department of Electronic and Communication, Yıldız Technical University, fgunes51@gmail.com

1. Introduction

Reflectarray antennas (RA) have been of high interest due to the unique advantage of combining the best features of both reflectors and phased array antennas especially in antenna gain that can be achieved without using any complicated feeding network. Microstrip RAs have both electromagnetically and mechanical advantages: From an electromagnetic perspective, they are high gain antennas, low side-lobes, capable of beam steering, and from a mechanical perspective, they have light weight structures, easy to fabricate and manufacture and also robust [1-3].
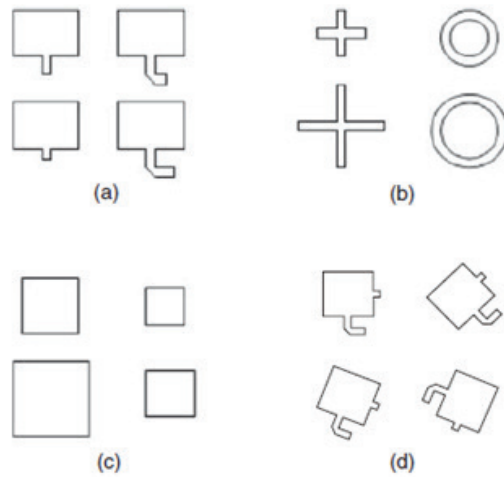
Fig. 1. *Typical RA unit elements with phase compensation reflection w.r.t variable (a) transmission line lengths, (b) dipoles' and rings' sizes, (c) patch's size, (d) elements' rotations[3].*

Microstrip RAs are composed of many isolated patches elements on a substrate (ε_r, tanδ, h) which are various forms such as square, circle, rings (Fig.1) and able to reflect the incident wave independently with a phase compensation proportional to the distance from phase centre of the feed-horn to form a pencil beam in a specified direction (Θ_0, φ_0) as is well-known from the classical array theory. Thus "Phasing" is a very important process in designing reflectarray. In literature different approaches of compensating the phase of each element have been proposed (Fig.1).

In Fig. 1, typical patch forms used in the microstrip RA designs are presented with their phase compensation methods. One of the methods for the reflection phase compensation is to add with a variable stub length in a microstrip patch [4-5]. Another method which is often used is to change the sizes or rotation angle with certain degrees of the unit elements such

as rings or dipoles [6-8], and thus the reflection phase characteristics of a RA can be built up [9]. In Fig.2, a traditional planar RA design is presented alongside of its feeding antenna. In Fig. 3, a traditional large scale planar RA with variant transmission line patches had been presented.

Fig. 2. *A traditional RA design with the Feeding [3]*
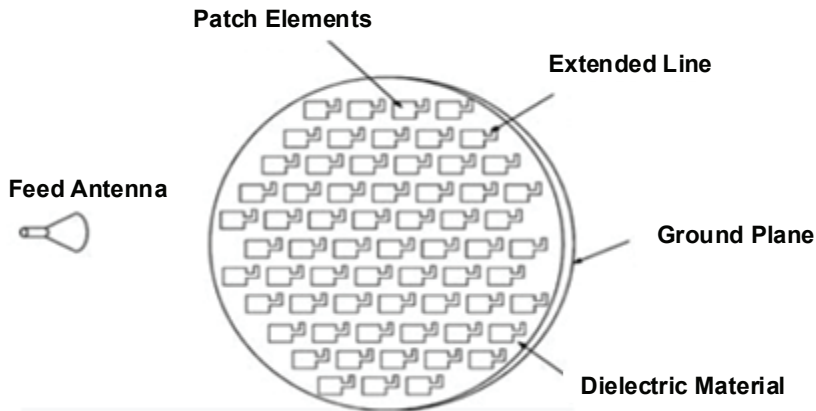
Fig. 3. *A traditional large scale planar RA with variable stub length patch element [3].*

Since RA designs are simply hybrid of a reflector antenna and a planar phased array antenna in a compact size and low profile design [10-14],

they are mostly preferred in applications such as satellite communication where the designs can be folded and reshaped easier to traditionally designs.

However, microstrip RA designs usually suffer with a narrow bandwidth characteristic caused by intrinsic narrow bandwidth of a microstrip patches and spatial phase delays between the feed and unit cell elements [15]. Some of the methods for enlarging the operation band of microstrip RA designs are: (i) Utilization of dielectric substrates with high thickness, (ii) Having unit element designs with multilayers [16-17]. By using these methods it is possible to increase the bandwidth up to %15.

For design of a MRA, in order to satisfy requirements as the capability to radiate a shaped beam or multi-beams, also to enhance the frequency behavior and bandwidth, novel, complicated patch configurations on multi-layers are needed. Thus, the MRA design problem becomes a massive multi- objective multi- dimensional optimization problem that is not computationally efficient and feasible due to its high mesh size that might take days of simulations even for a few iterations [18]. Therefore first of all for a computationally efficient optimization process, an accurate and rapid model for the reflection characteristic of a unit element is needed to establish as a continuous function within the input domain of the patch geometry and substrate variables, then it could be convenient to carry this model out adopting a hybrid "global + local" optimization method to find the best solution among all the possible solutions [19-22].

A commonly used novel method for creating an accurate and fast numerical models of microwave devices is Artificial Neural Networks (ANN) which is a simplified mathematical model of the biological neural network. Particularly Multi - Layer Perceptron type of Neural Network (MLP NN) has found a lot of microwave modelling and optimization applications [23-35]. A MLP NN is composed of a collection of interconnected neurons taken place in the input, output and hidden layers where neurons have activation functions to be used in the mapping process between the input and output domains. A MLP NN architecture matrix consists of weighting coefficients belonging to the interconnections and the bias values, which are determined by an optimization process called the training process using the simulated or measured data sets as the target data. Then validation of the ANN model is made by the prediction process via the defined test criteria and data. Thus the ANN is ready for the regression process consisting of accurate and rapid prediction of the outputs corresponding to any given input vector within the input domain. In the other words, the outputs are obtained numerically as continuous functions of the input variables expressing nonlinear mapping between the input and output domains. In the applications of modelling of microwave devices, these inputs may be

geometry   and substrate parameters of a microstrip patch antenna or DC bias conditions and operation frequency of a microwave transistor, etc, where the outputs may be gain and resonance frequency, the Scattering parameters, respectively, of the related devices [26-33].

In this work, using a feed forward MLP, which is one of the most commonly used ANN type in literature, reflection phase characteristics of a double-layer planar MRA unit with respect to its geometrical parameters on a chosen substrate in the frequency domain have been studied   to be utilized in building up X- band MRA.

In next section design process of the proposed unit element and creation of its data set will be presented. In section III, a study case is given where MLP NN models are built up with different architectures and the best MLP NN case will be chosen comparing performance regressions of the models by applying the commonly used error metric Mean Absolute Error (MAE). Finally the paper ends with a brief conclusion section.

2. Unit Element Designs and Creation of Dataset

In this section, obtainment of the training and testing data set for the ANN model of the double–layer planar microstrip RA unit element and its design will be studied. The design presented in Fig. 4 is taken as an RA unit element model to suitable to be used for design large scale RA design. The design variables of the proposed unit element and their constraints are given in Table 1.
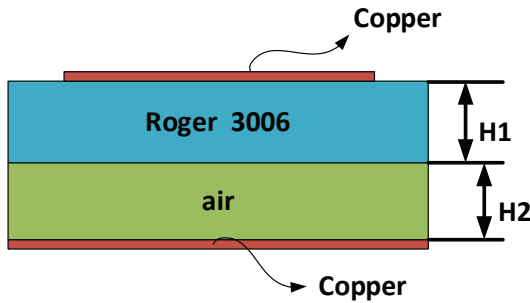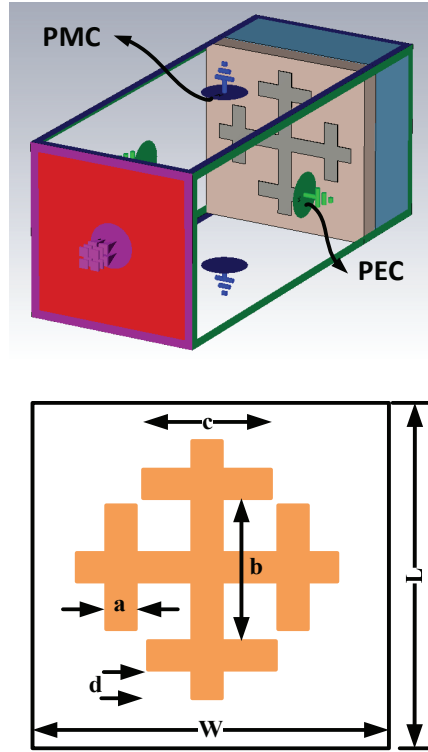
Fig. 4. *Proposed Multilayer planar RA element and the H-wall waveguide simulator*

All the data given in Table 1 has been obtained by using 3D EM simulation tool CST via the H-wall waveguide simulator subject to the transverse electromagnetic (TEM) mode propagation boundary conditions to determine the amplitude and phase of the reflected wave from the proposed double-layer planar RA unit cell (Fig.4). Also in Fig. 5, the reflection phasing characteristic distribution of the data is given, as it can be seen the phase reflection has a large range between -480 and 120 degree which is a suitable range for design of a large scale RA design. However, as it can be seen the data set (Fig. 5) has a nonuniform distribution which causes a challenging and complicated regression in the generalization process of the MLP model.

Table 1. *Ranges of the RA Unit Element parameters for the ANN modelling*

Parameter	Range	Step size
a (mm)	0.5-1.5	0.25
b (mm)	4-8	0.5
d (mm)	0.5-1.5	0.25
Frequency (GHz)	8-12	0.05
Total Sample	18225	
H2 (mm)	5	
H1	Roger 3006 eps6.15 h1: 1.52mm	
c (mm)	b*0.5	
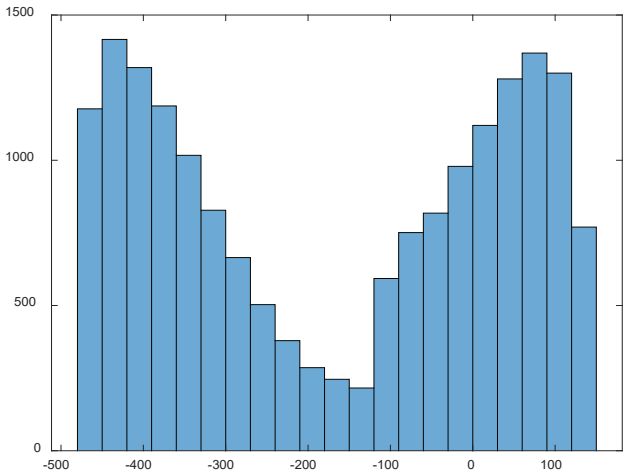
Fig. 5. *Histogram graphic of the reflection phase*

In this work, a MLP NN based black box modelling (Fig. 6) process is studied in order to obtain an accurate, fast and reliable regression model of the proposed multilayer planar RA element. In order to determine the optimal architecture parameters of MLP model, MLP models with different architecture parameters of hidden layer and neurons are taken into consideration. The studied MLP models are defined in Table 2. In next section, the regression performance evaluation of MLP models is presented.
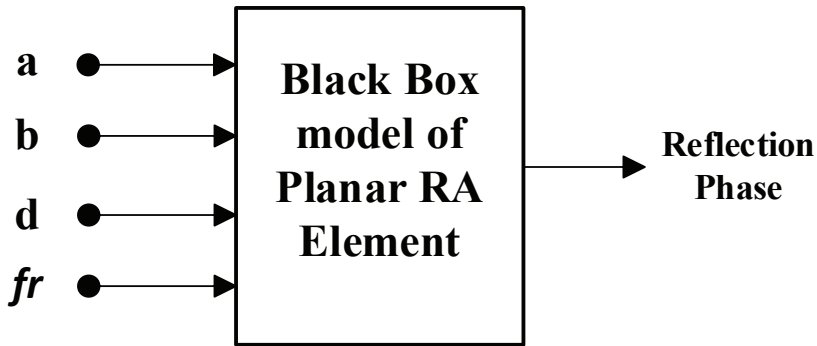
Fig. 6. *Black box model of the Multilayer MRA unit element*

Table 2. *User defined parameters of MLP NN Architectures*

MLP Model	User Defined Parameters	MLP Model	User Defined Parameters
Case 1	1 hidden layer, with 5 neurons	Case 2	1 hidden layer, with 10 neurons
Case 3	1 hidden layer, with 15 neurons	Case 4	1 hidden layer, with 20 neurons
Case 5	1 hidden layer, with 30 neurons	Case 6	2 hidden layer, with 5 and 10 neurons
Case 7	2 hidden layer, with 10 and 15 neurons	Case 8	2 hidden layer, with 15 and 20 neurons
Case 9	3 hidden layer, with 5, 10 and 15 neurons	Case 10	3 hidden layer, with 10, 15 and 20 neurons
Case 11	3 hidden layer, with 15, 20 and 30 neurons	Case 12	4 hidden layer, with 5, 10, 15 and 20 neurons,

* Bayesian regularization back-propagation are used for updating the weight and bias values of the models, all other parameters are taken as default.

3. Study Case

Herein, 18225 samples that have been obtained in previous section, are shuffled and divided into two equal parts within the search domain (Table 1) for training and testing of these 12 different MLP models given in Table 2. MATLAB 2019B version is used as coding environment. The commonly used error metric Mean Absolute Error (MAE) is used as main metrics for determination of the optimal architecture parameters. Due to the randomly initialization of a MLP model, the same architecture achieves the different performance measures at each run. Thus, in this study, the performance of each model is measured determining the worst and best case regression performance after 10 different runs. In Table 3, the best, worst, mean and standard deviation of MAE metric alongside of best case scenarios Relative Mean Error (RME) results of ANN models defined in the previous section are calculated:

$$MAE = \frac{1}{N}\sum_{i=1}^{N}|T_i - P_i| \qquad (1)$$

$$RME = \frac{1}{N}\sum_{i=1}^{N}\frac{|T_i - P_i|}{|T_i|} \qquad (2)$$

where T_i: the target value, P_i: the corresponding predicted value, n: number of the samples for each output.

Table 3. *Performances of the MLP models obtained after 10 different runs*

Case	MAE			Standard deviation	Best RME
	Worst	**Best**	**Mean**		
1	135.8	18.2	72.7	54.49	0.085
2	125.7	17.7	41.1	43.35	0.083
3	53.32	8.5	17.0	13.24	0.039
4	132.5	9.3	26.6	38.43	0.043
5	115.6	10.5	25.5	31.9	0.049
6	10.3	3.7	7.72	2.76	0.017
7	10.8	4.0	8.21	2.803	0.018
8	11.0	2.3	8.93	2.82	0.010
9	10.5	1.74	5.42	4.11	0.008
10*	**10.1**	**0.740**	**2.93**	**3.17**	**0.0034**
11	10.1	0.636	2.83	3.92	0.0029
12	171.3	0.812	24.55	51.7	0.0038

* Model with the Best overall performance

As it can be seen from Table 3, the MLP models with a few number of neurons has a high MAE error both in the worst and best cases. With the increase in number of neurons and hidden layers, not only the standard deviation of 10 runs is reduced but the best obtainable regression MAE also decreases significantly that can be seen in the models specifically with 3 hidden layers. However with the increase in number of layers and hidden neurons the training process becomes complicated and takes more time. After a certain threshold (here 4 layer model), the stability (divergence between best and worst performance) is also reduced as it can be observed in the model 12 with 4 hidden layers, the standard deviation is significantly increased compared to 3 layers models. Here, the model 10 is taken as the optimal MLP architecture design where both best MAE and standard deviation are low and its training time is shorter to the similar designs. In Fig. 7, the performance results of proposed MLP based RA unit are given for the different variable geometrical parameters over operation band of 8-12 GHz. As it can be seen the proposed model has an outstanding regression performance where the MLP based predicted reflection phase values coincides with the 3D simulated reflection phase values of unit element.

(a)

(b)

(c)
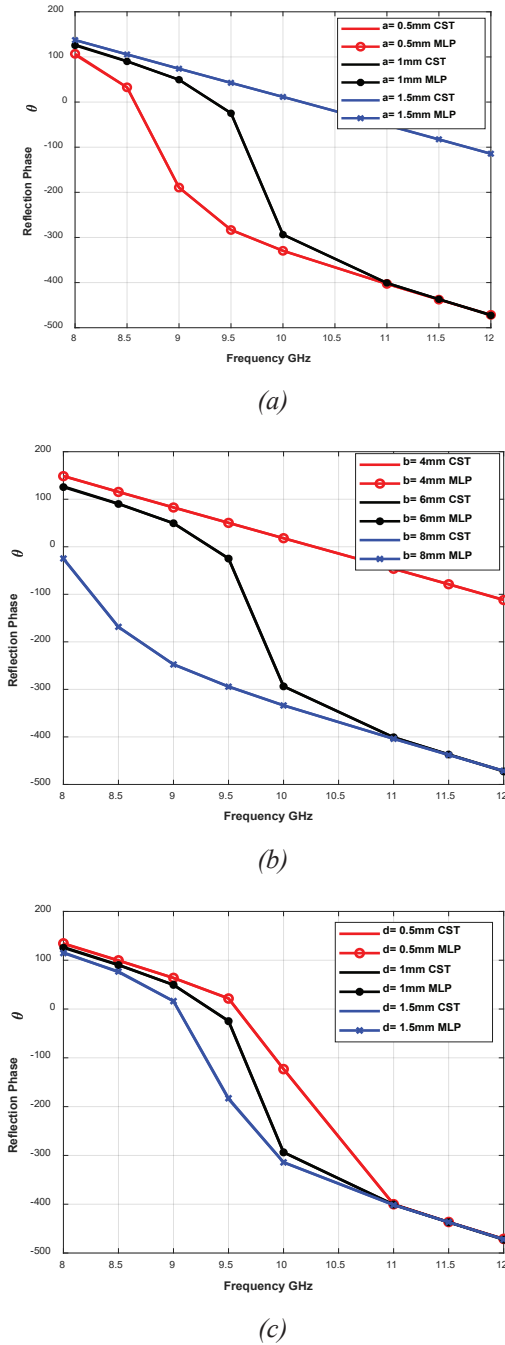
Fig. 7. *Reflection Phase response of proposed MLPNN based model for: (a) a is variable, b=6mm, d=1mm; (b) b is variable, a=1mm, d=1mm; (c) d is variable, a=1mm b=6mm, over frequency range of 8-12 GHz.*

4. CONCLUSION

In this work, a single, accurate and fast MLP NN model is completed for the reflection characteristic of a MRA double-layer unit element with the novel complicated patch configuration, based on the 3-D CST simulation to be employed in both design and analysis of the complete MRA. All the stages of building the MLP NN model are given in details as a general systematic method. It can be concluded that this method can be applied as a robust method for accurate, fast modelling for the reflection characteristics of the arbitrarily shaped multi-layer unit elements in design and analysis of a MRAs.

Acknowledgements

References

1. Berry, D. G., Malech, R. G., Kennedy, W. A., 1963. The Reflectarray Antenna. IEEE Trans. Antennas Propag., vol. 11, no. 6, pp. 645–651.
2. Phelan, H. R., 1977. Spiral phase Reflectarray for Multitarget Radar. Microw. J., vol. 20, pp. 67–73.
3. Huang, J., Encinar, J. A., 2007. Reflectarray Antennas. IEEE Press.
4. Munson, R. E., Haddad, H., 1987. Microstrip Reflectarray for Satellite Communication and RCS Enhancement and Reduction. U.S. Pat. 4684952, Washington, D.C.
5. Huang, J., 1991. Microstrip Reflectarray. IEEE AP - S/URSI Symp. London, Canada, pp. 612–615.
6. Pozar, D. M., Metzler, M., 1993. A. Analysis of a Reflectarray Antenna Using Microstrip Patches of variable Size. Electron. Lett., vol. 29, no. 8, pp. 657–658.
7. Kelkar, A., 1995. FLAPS: Conformal Phased Reflecting Surfaces. Proc. IEEE Natl. Radar Conf., Los Angeles, Calif., pp. 58 – 62.
8. Guo, Y. J., Barton, S. K., 1995. Phase Correcting Zonal Reflector Incorporating Rings. IEEE Trans. Antennas Propag., vol. 43, no. 4, pp. 350–355.
9. Huang, J., Pogorzelski, R. J., 1998. A Ka - Band Microstrip Reflectarray with Elements having variable Rotation Angles. IEEE Trans. Antennas Propag., vol. 46, no. 5, pp. 650–656.
10. Huang, J., Encinar, J. A., 2007. "Reflectarray Antennas", Wiley-IEEE Press, ISBN: 978–0470–08491–4.

11. Güneş, F., Nesil, S., Demirel, S., 2013. Design and Analysis of Minkowski Reflectarray Antenna Using 3-D CST Microwave Studio-Based Neural Network Model with Particle Swarm Optimization. International Journal of RF and Microwave Computer-Aided Engineering, vol.23, no.2, pp.272-284.

12. Güneş, F., Demirel, S., Nesil, S. 2014. A Novel Design Approach to X-Band Minkowski Reflectarray Antennas using the Full-Wave EM Simulation-based Complete Neural Model with a Hybrid GA-NM Algorithm. Radioengineering, vol. 23, No. 1.

13. Pozar, D. M., Targonski, S. D., Pokuls, R., 1999. A Shaped-Beam Microstrip Patch Reflectarray. IEEE Trans. Antennas Propag., vol. 47, no. 7, pp. 1167–1173.

14. Encinar, J. A., Zornoza, J. A., 2004. Three-Layer Printed Reflectarrays for Contour Beam Space Applications. IEEE Trans. Antennas Propag., vol. 52, pp. 1138–1148.

15. Pozar, D. M., 2003. Bandwidth of Reflectarrays. Electron. Lett., vol. 39, no. 21, pp. 1490 – 1491.

16. Encinar, J. A., Zornoza, J. A., 2003. Broadband Design of Three-Layer Printed Reflectarrays. IEEE Trans. Antennas Propag., vol. 51, pp. 1662–1664.

17. Encinar, J. A., 2001. Design of Two-Layer Printed Reflectarray Using Patches of Variable Size," IEEE Trans. Antennas Propag., vol. 49, pp. 1403–1410..

18. Mahouti, P., 2020. Application of artificial intelligence algorithms on modeling of reflection phase characteristics of a nonuniform reflectarray element. International Journal of Numerical Modelling: Electronic Networks, Devices and Fields, 33(2), e2689.

19. Pozar, D., Metzler, T., 1993. Analysis of a reflectarray antenna using microstrip patches of variable size. Electronics Letters 29(8): 657–658.

20. Berry, D., Malech, R., Kennedy, W., 1963. The reflectarray antenna. IEEE Transactions on Antennas and Propagation. 11(6): 645–651.

21. Huang, J. 1990. Microstrip reflectarray antenna for the SCANSCAT radar application.

22. Pozar, D. M., Targonski S. D., 1997. Syrigos H. Design of millimeter wave microstrip reflectarrays. IEEE transactions on antennas and propagation 45(2): 287–296.

23. Giannini, F., Leuzzi, G., Orengo, G., Albertini, M, 2002. Small-signal and large-signal modeling of active devices using CAD-optimized neural networks. Int J RF Microwave Computer-Aided Eng 12, 71–78.

24. Marinkovic, Z. D., Markovic, V. V., 2005. Temperature-dependent models of low-noise microwave transistors based on neural networks.

Int J RF Microwave Computer-Aided Eng 15, 567–577.

25. Krishna, D., Narayana, J., Reddy, D. 2008. ANN Models for Microstrip Line Synthesis and Analysis. World Academy of Science, Engineering and Technology, International Science Index 22, International Journal of Electrical, Computer, Energetic, Electronic and Communication Engineering, 2(10), 2343 - 2347.

26. Güneş F., Nesil S., Demirel S., 2013. Design and Analysis of Minkowski Reflectarray Antenna Using 3-D CST Microwave Studio-Based Neural Network Model with Particle Swarm Optimization. Int J RF Microwave Computer-Aided Eng, vol.23, pp.272-284.

27. Güneş F., Demirel S., Nesil S., 2014. A Novel Design Approach to X-Band Minkowski Reflectarray Antennas using the Full-Wave EM Simulation-based Complete Neural Model with a Hybrid GA-NM Algorithm. Radioengineering, vol.23, No.1, pp.144-153.

28. Güneş F., Torpi H., and Gürgen F., 1998. A multidimensional signal-noise neural network model for microwave transistors", IEE Proc Circ Devices Syst. 145, 111–117.

29. Zhang, Q.J., Gupta, K.C., 2000. Neural Networks for RF and Microwave Design. Artech House, Boston.

30. Suntives, A., Hossain, M. S., Ma, J., Mittra, R. Veremey, V., 2001. Application of artificial neural network models to linear and nonlinear RF circuit modeling. Int J RF and Microwave Comp Aid Eng, 11: 231-247. doi:10.1002/mmce.1028.

31. Hammoodi, A.I., Milanova, M., Raad, H., 2018. Elliptical Printed Dipole Antenna Design using ANN Based on Levenberg–Marquardt Algorithm. Advances in Science, Technology and Engineering Systems Journal, vol. 3, no. 5, pp. 394-397.

32. Karaboga, D., Guney, K., Sağiroğlu, S., Erler, M., 1999. Neural computation of resonant frequency of electrically thin and thick rectangular microstrip antennas. IEE Proc Microwave Antennas Propag 146, 155–159.

33. Mishra, R.K., Patnaik, A., 1998. Neural network-based CAD model for the design of square patch antennas, IEEE Trans Antennas propag. 46, 1890–1891.

34. Rosenblatt, F., 1961. Principles of Neurodynamics: Perceptrons and the Theory of Brain Mechanisms. Spartan Books, Washington DC.

35. Rumelhart, D E., Geoffrey E. H., Williams, R. J. 1986. Learning Internal Representations by Error Propagation".

Chapter 10

NEW APPROACHES FOR KNIT-DENIM FABRIC DESIGN

B U Nergis, C Candan[1], S Yazıcı, D Soydan, C İpek

1 Prof. Dr. Öğretim Üyesi, İstanbul Technical University, Faculty of Textile Technologies and Design, candance@itu.edu.tr

1. Introduction

From the 17th century to the present, denim has been in use in the clothing industry, initially being used in the manufacture of durable trousers for hard labour, used for the sails of Columbus' ships; and worn by American cowboys. Today, denim can be identified as an indicator of fashion wear that can match with the ever-changing fashion trends and expectations of people. According to TS 2791 Textiles-cotton denim fabric standard, this is a strong twill fabric that is made of entirely cotton yarns or a blend of cotton and synthetic yarns. The most typical characteristics of denim fabric is its indigo dyed warp and white weft yarns, together with the appearance of diagonal ribbed fabric created by 3/1 Z (right hand) or 2/1 Z (right hand) twill weave. According to Morder Intelligence Report (2019) and Warren (2019) globalization of fashion trends, increasing casualization of clothing, growing trend of customization, rising availability of high-quality, cost-effective denim products are the major factors propelling the growth of the denim market and the jeans market is expected to register at a CAGR of 6.7% during the forecast period of 2020-2025.

On the other hand, consumer preferences are shifting towards wrinkle resistant, flexible, soft, and comfortable textiles. Manufacturers and designers need to adapt and meet these demands to keep consumers satisfied. Recently, the denim fashion trend has been moving towards stretch denim, which usually incorporates an elastic component into the fabric to allow a degree of stretchability in garments (Kumar, Chatterjee, Padhye, and Nayak, 2016). Application of knitted fabric in denim garments has also been increasing since these fabrics are elastic on all sides, comfortable and aesthetic to wear (Grand View Research, 2019).

Although Knit Denim related works are in scarcity, there are some patented inventions for knitted denim structures and production processes (U. S. Patent No: 4613336, 1984; U.S. Patent No: 7185405, 2001; U.S. Patent No:0172982, 2004; U.S. Patent No. 7,530,241 B2, 2009) and, studies reported on achieving denim-like look by the knitting process. Table 1 provides an overview of the content of the publications in terms of fabric structures and the yarns used.

Table 1: *The content of the publications in terms of fabric structure and yarn type studied.*

References	Knit denim structures (with needle diagrams where available)	Yarns employed	Tested properties
(Değirmenci Z., 2013; Değirmenci Z., Çelik N., 2014.)	Fleece Knitted fabrics were produced on single jersey circular knitting machine. 	Face of the fabrics: Ne 30/1 indigo rope dyed 100 % cotton yarn. Back side (inner side) of the fabrics: Ne 30/1 and Ne 20/1 cotton, tencel, modal, bamboo, viscose, polyester, modal-cotton (65-35), polyester-cotton (65-35) and polyester-viskon (65-35) vortex yarns.	The samples were tested for their thermal comfort, dimensional and physical properties.
(Jamshaid H., et.al., 2020)	The denim effect in knitted fabric was produced on single jersey circular machine. 	100% cotton yarn with linear densities of Ne 10/1, Ne 11, Ne 12, Ne 14, Ne 16, Ne 18.	The samples were tested for their comfort properties.

(Didar S.A., Patwary S.U., Kader S., Akter M.K., Ahmed T., 2015)	"Knit denim" and "Tuck denim" structures were produced on a single jersey circular knitting machine. Knit denim: | Row	Needle Diagram | |---|---| | 1 | | | 2 | | | 3 | | | 4 | | Tuck Denim | Row	Needle Diagram | |---|---| | 1 | | | 2 | | | 3 | | | 4 | |	Ne 24/1 100% cotton combed yarn.	The samples were tested for their dimensional and fastness (washing and rubbing) properties.
(Akbar A.R., Su S., Khalid J., Cai Y., and Lin L.; 2017)	Knitted denim with twill effect was designed by using cross terry structure on a circular knitting machine. 2/1 and 3/1 cross terry structures were obtained with 2 and 3 floats and with 3 and 4 tracks repeat.	Cotton, polyester, flax and polypropylene yarns were used.	Comfort properties and bursting strength of knitted denim were tested. The samples were also tested for their inherent anti-microbial properties.
(Gokarneshan N., 2010)	Float plated, 2 thread fleece and interlock plated structures were produced. Of these structures, it was not possible to achieve denim effect by the Interlock structure.	Ne 30 indigo dyed and white cotton yarns were used.	The samples were tested for their fastness and structural properties.

The results obtained from the studies given in Table 1 suggested that:

1. Knitted denim structures can provide a variety of designs.

2. Knit denims have higher stretching, drapebility and softness pro-

perties and provide overall better comfort values compared with woven denims.

3. Knit denims are easy to use and care depending on their wrinkle resistant structures.

4. Knit denim seems to be a promising alternative to the woven ones.

Additionally, the price of knitted denim fabrics is cheaper. The twist of knitted denim yarn is smaller and no sizing is needed for the yarn. Knitting is a one step process in manufacturing of fabric from yarn. Therefore, knit denim production requires much less complicated process (Didar S.A., 2013)

Based on the literature survey, the study presented in this chapter was conducted such that several types of denim like knit structures designed and produced using knitting yarns colored by indigo dyes in the form of packages, which is one of the unique differences of the work. Moreover, different washes were also tried out in different knit structures in an attempt to achieve much heavier faded looks in the structures.

2. Experimental Work

2.1. Material

The yarn details used for the work are given in Table 2. In addition to the cotton and polyester yarns, elastane yarn of 70 denier is also utilized for the denim like knit structures developed. In doing so, it was aimed to enhance wear comfort as well as dimensional stability of the fabrics.

Table 2: *Yarn details*

Yarn Types	Fiber Type	Yarn Count	Indigo Dyed/ Undyed
Combed ring spun	Cotton	Ne 24/1	Indigo Dyed
Combed ring spun	Cotton	Ne 30/1	Indigo Dyed
Combed ring spun	Cotton	Ne 30/1	Undyed
Synthetic spun	Polyester	100 Den	Undyed
Synthetic spun	Polyester	150 Den	Undyed

2.2 Method

The parameters that are most effective in obtaining denim appearance are the type of dye, the yarn type, yarn count, fiber content, and finally knit

structure itself. The various combinations of these parameters may help design denim like knit structures of different appearance, texture, dimensional stability, and durability.

In traditional woven denim fabric production process, indigo dyeing is realized in the form of ropes. This process takes time and requires high amount of material. For knitting process, however, there is no need for that amount of yarn, and accordingly in order to save time and material the yarns were colored using indigo dyes in the form of packages (bobbins). The details of the circular knitting machines on which the developed knit designs were produced are given in Table 3.

Table 3: *Machine Details*

	Diameter (Inch)	**Machine Gauge (E)**	**Fabric Models**
Machine 1	32	28	Model 2, 3, 4 & 5
Machine 3		22	Model 1 only

The fabric properties were measured in accordance with the Standards given as follows:

1. Weight of the fabrics: ASTM D3776 / D3776M

2. Abrasion resistance of the fabrics: EN ISO 12947-2

3. Pilling of the fabrics: TS EN ISO 12945-1

4. Fabric Thickness: TS 7128 EN ISO 5084

The knit structures developed, together with the corresponding needle and cam arrangements, are presented in Figure 1.

Denim like knit structures	Design details
Model 1	
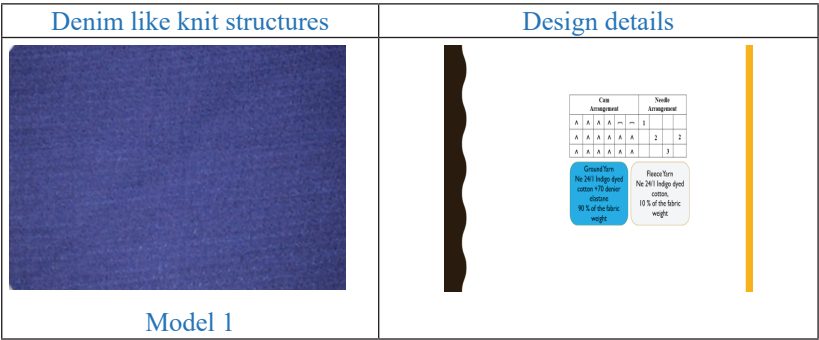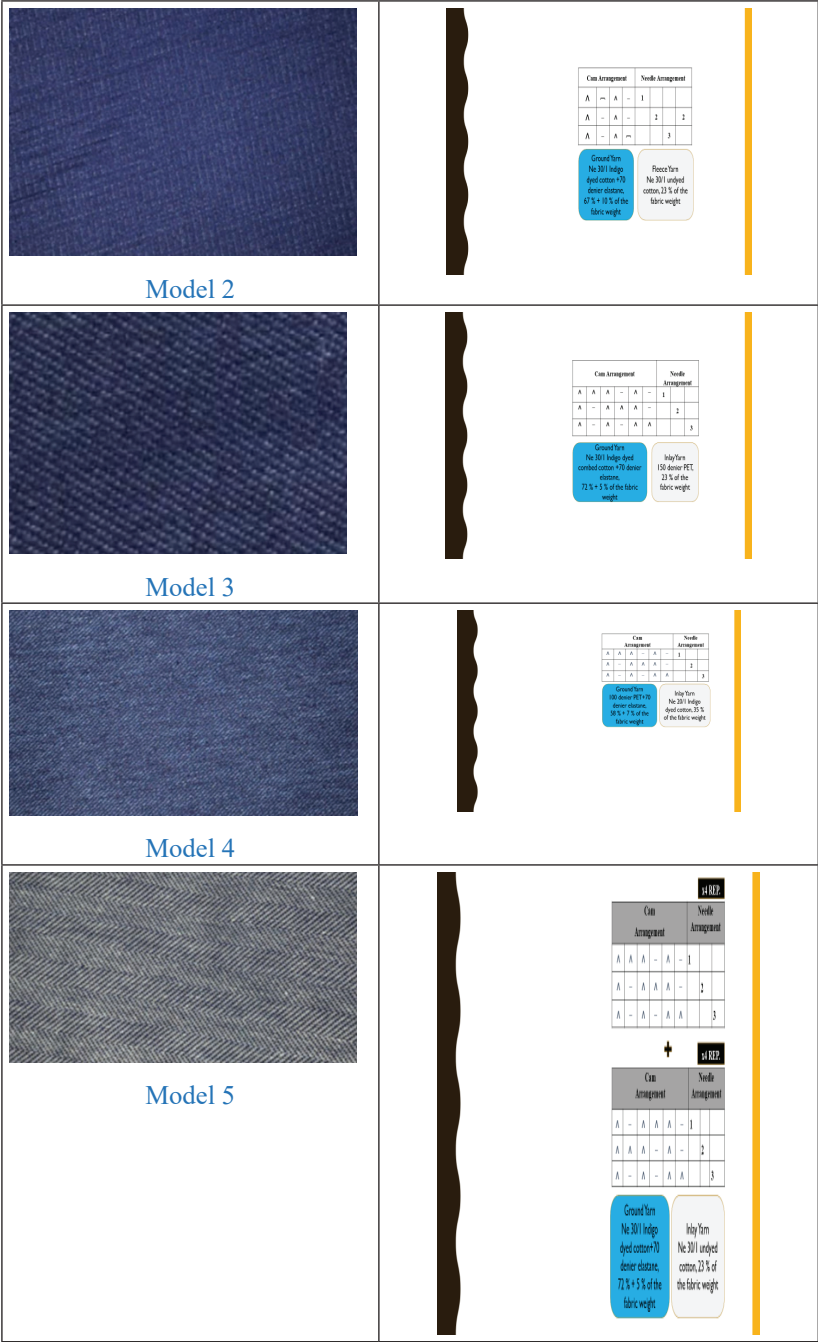
Figure 1: *The denim like knit structures*

With the help of a focus group of 8 people formed for the work, the fabric samples were visually rated in terms of denim like appearance, and accordingly three models namely Model 3, 4, and 5 were selected to turn

them into the pairs of pants. In order to enhance the denim like effect further, the pants from these fabrics were subjected to the special washinging processes, namely eco-stone (Model 3), sponge random (Model 4), and enzyme (Model 5) washing under the commercial conditions. The steps of the process are given in Table 4.

Table 4: *Washing Processes*

ECOSTONE WASHING	SPONGE RANDOM WASHING	ENZYME WASHING
Rinse Washing	Random Sponge application	Enzyme application
Cold Rinse	Neutralization	Cold Rinse
Stone Random	Cold Rinse (twice)	Softening
Cold Rinse	Softening (twice)	
Neutralization		
Cold Rinse		
Detergent Washing		
Cold Rinse		
Softening		

Finally, multi-criteria desicion approach was adopted in order to be able to offer the best option from all of the feasible alternatives suggested with the work. To do so, the combination of AHP and TOPSIS methods were used to determine the best possible option among the fabrics developed (Majumbar, A., Sarkar, B., Majumbar, P.K., 2005; Shyjith, K., Ilangkumaran, M., Kumanan, S., 2008).

3. Results and Discussion

The measurement results of the knitted fabrics are given in Table 5 in which the abrading results are not presented as no yarn breakage was observed in any of the fabrics at the end of the test. A comparative study of the results revealed that in general, Model 3, 4, and 5 show better performance than Model 1 and 2 (Table 5). The denim effect of float plated structures (i.e. Model 3, 4, and 5) appears better, when compared to the other structures (i.e. Model 1 and 2) because the float plated have more stiffness and relatively heavier. The faded looks obtained for the relevant models through the ecostone washing are, however, given in Figure 2.

PANTS FROM MODEL 3, ECOSTONE WASHING	PANTS FROM MODEL 4, SPONGE RANDOM WASHING	PANTS FROM MODEL 5, ENZYME WASHING

Figure 2: *The faded looks obtained for the relevant models*

As may be seen from the figure, the faded looks of the pants are not as heavy as the ones which could be achieved for woven denims. The most satisfactory appearance is rated, by the aforementioned focus group above, for the Model 3 pants treated using the ecostone washing process.

Table 5: *Performance Results of the Fabrics*

Model No	Thickness (mm)	Fabric Width (cm)	Weight (g/m²)	Dimensional Stability (%)		ICI Pilling (7.000 rev.)
				Widthwise	Lengthwise	
Model 1	0.58	190	200	-6	-2.5	3
Model 2	0.86	185	265	-5	-1.5	4
Model 3	0.69	185	270	-4.5	-1.5	4.5
Model 4	0.66	188	310	-3.5	-2	4
Model 5	0.69	185	250	-5	-2.5	3.5

The dimensional stability of the float plated structures (i.e. Model 3, 4, and 5) are also better than the others. This is partly due to the structures themselves. The presence of PET yarns in the structures (i.e. Model 3, 4, and 5) has a positive impact on dimensional stability of the fabrics, as is expected. When it comes to pilling behavior of the fabrics, Model 3 shows the best performance, which is followed by Model 2 and 4. (Table 5)

Finally, the hybrid AHP-TOPSIS evaluation indicated that in Model 3 is the best alternative wheares the Model 1 one is the worst one. Accordingly, it may be concluded that Model 3 fabric may be a good choice so far as people seeking for the wear comfort of a knit fabric in pants, without compromising over denim look.

Acknowledgement

The authors would thank to Islandenim Tekstil A.Ş. headquartered in Adana for their invaluable help in producing the samples.

References

Akbar A.R., Su S., Khalid J., Cai Y., and Lin L. (2017). Investigation of Comfort Properties of Knitted Denim. *IOP Conf. Series: Materials Science and Engineering, 275,* 1-6.

Değirmenci Z. (2013). İndigo Boyalı Pamuk İpliğinden Yazlık Kullanıma Uygun Örme Denim Kumaş Özelliklerinin Araştırılması. (Doktora tezi). https://tez.yok.gov.tr/UlusalTezMerkezi/tezSorguSonucYeni.jsp. (343353)

Değirmenci Z., Çelik N. (2014). An Investigation On The Influence of Laundering On The Dimensional Stability of The Denim-Like Knitted Fabrics. *Tekstil ve Konfeksiyon, 24(4),* 363-370.

Didar S.A. (2013). Prospect of knitted denim. Available from **https://www.textiletoday.com.bd/prospect-of-knitted-denim/**

Didar S.A., Patwary S.U., Kader S., Akter M.K., and Ahmed T. (2015). Development of Different Denim Effect on Knitted Fabric and Comparative Analysis with Conventional Woven Denim on the Basis of Physical and Dimensional Properties. *Research Journal of Engineering Sciences, 4(4)*, 9-15.

Gokarneshan N., Kumar M.K., Devan P., DineshK. , Kumar P.A, Saranya G. and Subhash K. (2010). Denim-like effect in knitted fabrics. Available from https://indiantextilejournal.com/articles/FAdetails.asp?id=2682

Grand View Research. (2019). Knitted Fabric Market Size, Share & Trends Analysis Report By Product (Weft-knit, Warp-knit), By Application (Technical, Household), By Region, And Segment Forecasts, 2019–2025. Available from https://www.grandviewresearch.com/industry-analysis/knitted-fabric-market on 03.03.2020

Jamshaid H., Rajput W.A., Zahid B., Asfand N., Basra S.A., and Ali A. (2020). Comparison of Functional Properties of Woven and Knitted Denim Fabrics. *Industria Textila*, *71(1),* 3-7.

Kumar S., Chatterjee K., Padhye R., and Nayak R. (2016). Designing and Development of Denim Fabrics: Part 1 - Study the Effect of Fabric Parameters on the Fabric Characteristics for Women's Wear. *J Textile Sci Eng, 6,*. doi: 10.4172/2165-8064.1000265

Majumbar, A., Sarkar, B., Majumbar, P.K. (2005). Determination of Quality Value of Cotton Fibre Using Hybrid AHP-TOPSIS Method of Multi-Criteria Desicion-Making. *The Journal of The Textile Institute, 96(5)*, 303-309.

Mordor Intelligence. (2019). Jeans Market - Growth, Trends, and Forecast (2020-2025) Available from https://www.mordorintelligence.com/industry-reports/jeans-market on 05.03.2020

Quinnen M. (1984). *Knitted Fabric Produced From Indigo Dyed Yarn* United States Patent No: 4613336.

Rastogi B. L., Oswal J. L. (2001). *Process for the preperation of indigo dyed yarn for use in the manufacture of knitted fabric*. United States Patent No: 7185405.

Shin J. C. (2004). *Knitted fabric for producing indigo-dyed cotton denim jeans*. United States Patent No:0172982.

Shih L. (2009). *Method For Knitting Denim.* Patent No. US 7,530,241 B2

Shyjith, K., Ilangkumaran, M., Kumanan, S. (2008).Multi-criteria desicion making approach to evaluate optimum maintance strategy in textile industry. *Journal of Quality in Maintance Engineering, 14(4),* 375-386.

Warren L. (2019). Global Denim Industry to Grow by $14M by 2024, Thanks to One Innovation Available from https://sourcingjournal.com/denim/denim-business/technavio-report-denim-organic-cotton-market-growth-182319/ 05.05.2020.

Chapter 11

VENTILATION OF DANGEROUS GASES FOR CHEMICAL INDUSTRIES SAFETY

Didem SALOGLU[1]

1 Doç. Dr., Yalova University, Engineering Faculty, Department of Chemical Engineering, didemsalogludertli@gmail.com

INTRODUCTION

Gases and vapours in industrial processes can be described to be flammable, explosive, toxic, and asphyxiating. Furthermore, there are additional risks associated with the use of pressurised gas systems.

Gases and vapours relased from chemical processes in industrial facilities seriously affect the ambient air. In industrial processes, the concentration of gases and vapours in the workplace can be decreased with turbulence of the ambient air. This diffusion process of transport of gases and vapours is obtained by ventilation. Suitable ventilation procedures reduce the permanence of the gases and vapours in the workplace, and they are released to the atmosphere by diffusion, therefore, the explosion limit is lowered. Ventilation replaces the explosive atmosphere with fresh air, and circulation moves the air without renewal (Fang et al., 2016). Ventilation and air movement have two main functions: increasing dilution value in order to reduce the coverage limit of the danger zone and reducing type of the danger zone. Normally, as the ventilation rate increases, the coverage limit of the danger zone decreases. However, some obstacles such as embankments, walls, and ceilings prevent ventilation and increase the hazard zones. Increasing the air movement can cause evaporation on open liquid surfaces. However, the benefit of increased air movement is greater than the rate of discharge (Sasmito et al., 2013).

TYPES OF VENTILATION

Ventilation is achieved by moving air by wind, temperature differences, and by equipment such as fans.

Therefore, there are two basic types of ventilation:

a. Natural ventilation

b. Mechanical (forced) ventilation

In closed or open areas, if the replacement of air with flammable and combustible gases by fresh air is not sufficient using natural ventilation, it should be carried out using fans through ventilation openings of suitable dimensions on the walls and roofs (Gil-Baez et al., 2017). Doors and windows that are not specifically designed as ventilation openings are not used as industrial ventilation openings.

In the ambient atmosphere, fresh air is circulated using a fan, while exhaust gas is expelled using an aspirator. In some cases, a fan is provided to take fresh air into the ambient air, while the explosive gases can be discharged using natural ventilation. This is called a 'hybrid' system. Hybrid ventilation systems are preferred for reducing the investment and operating costs of the enterprise.

NATURAL VENTILATION

The ambient air temperature and concentration of ambient air can be controlled by air flow passing through the windows, doors, or openings for ventilation. The ambient air is kept at the desired temperature with airflow from opened windows, doors, and natural ventilation openings, and furthermore, hazardous gases and vapours can be ventilated from the ambient atmosphere.

Natural ventilation is an environmentally friendly method in which a building can be ventilated without using energy and is also very important for sustainable development (Demir, 2017; Saloglu & Demir, 2016).

Usability Criteria of Natural Ventilation

In the case of natural ventilation, the worst-case scenario is considered in determining the degree of ventilation. After such a scenario, the level of usability of the ventilation improves. It is clear that when using natural ventilation, there are both a lower and a higher level of ventilation available. The forecasting procedure of the degree of ventilation is open to errors arising from optimistic assumptions. Especially in some cases, the degree of ventilation is predicted by evaluating all the negative conditions of natural ventilation applied in closed areas. For example, the wind at two different temperatures causes air flow; the external temperature may be above the internal temperature, in which case, the buoyancy of the air is effective (stack effect), and the wind is easily pointed in a certain direction. On the other hand, the wind factor can eliminate the effects of buoyancy of ventilation and reduce its availability (Gil-Baez et al., 2013).

Natural Ventilation Caused by Wind

The driving force of natural ventilation in a closed area is the pressure difference between the air inlet opening and the air outlet opening. The volumetric air flow rate caused by wind is expressed in Eq. (1):

$$Q_{vol} = C_d A_e u_w \sqrt{\frac{\Delta C_p}{2}} \tag{1}$$

Q_{vol}	Volumetric flow rate (m³/s)
C_d	Surface pressure coefficient depending on the characteristic features of the inlet and outlet openings, turbulence, and viscosity
A_e	Equivalent impact area of air (air inlet (m²) and air outlet opening (m²)) effects in a closed area
U_w	Wind speed at the reference height (m/s)
ΔC_p	Pressure coefficient according to the characteristic features of the building

If there is more than one opening in a closed area, the equivalent effect area of the air is expressed in Eq. (2):

$$A_e = \sqrt{\frac{2\,A_1^2\,A_2^2}{A_1^2+A_2^2}}$$
(2)

A_e Equivalent impact area of air (air inlet (m²) and air outlet opening (m²)) effect in closed area

A_1 Air inlet opening (m²) effect in closed area

A_2 Air outlet opening (m²) effect in closed area

According to the characteristic features of the building, the pressure coefficient is shown by the pressure coefficients formed in the building according to the wind direction (Figs. 1 & 2) (Demir, 2017).

Surface pressure coefficient (ΔC_p) according to the angle at which the wind overlaps is given as:

If the direction of the wind reaches the openings at an angle of 90°: $\Delta C_p = 0.9$,

If the direction of the wind reaches the openings at an angle of 45°: $\Delta C_p = 0.4$,

If the direction of the wind reaches the openings at less than an angle of 90°: $\Delta C_p = 0.2$.
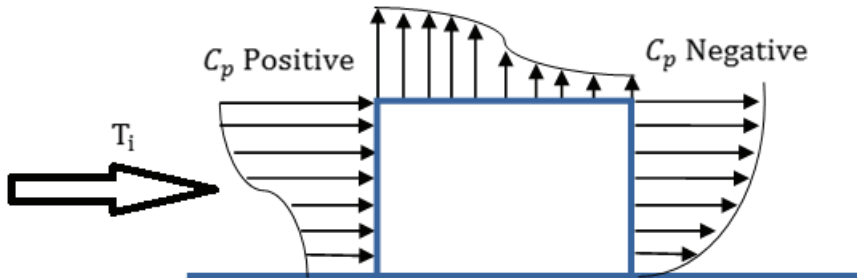
Figure 1. *Effect of local pressure*
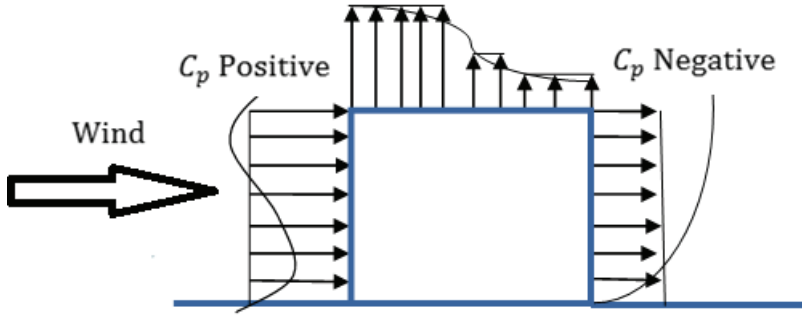
Figure 2. *Effect of global pressure*

Natural Ventilation Caused by Stack Effect

The 'stack effect' ventilation caused by buoyant force is air movement caused by the difference between internal and external temperature. Due to this difference, air density is formed and provides the driving force. The pressure obtained by the air movement creates unilateral or cross ventilation in the interior according to the structure and plan of the building (Spengler et al., 2001; Saloglu & Demir, 2016). Cross ventilation is provided with openings on opposite surfaces in the same plane by taking advantage of wind pressure (Fig. 3).
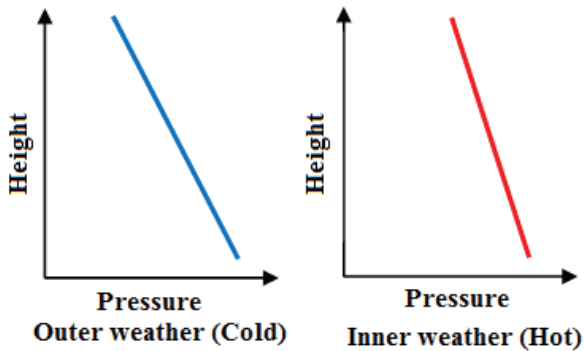
Figure 3. *Pressure differences occurring according to internal and outdoor temperature difference*

At the design stage, the decisions taken regarding the shapes, dimensions, and locations of the openings required for ventilation determine the speed, distribution, and amount of fresh air to be taken into the building (Ok, 2005). The chimney effect is based on the principle that 'heated air rises'. This effect occurs with different air densities, which are formed by the temperature differences between the outside and the inside of buildings. The imbalance in the pressure directions of the internal and external air causes a pressure difference. If the air temperature inside the building is more than the outside air temperature, the air inside rises and goes out

through the openings in the upper areas, and thus the outside air enters the structure through the openings in the lower areas. If the internal temperature of the building is lower than the outside temperature, the current occurs in the opposite direction (Spengler et al., 2001). This effect may be insufficient for the formation of the desired air movement in the interior of the building (Darcin, 2008).

In Fig. 4, the upper opening air inlet air pressure is greater than the external air pressure, and the air flows from the internal environment to the external environment. In the lower opening, the internal air pressure is lower than the outdoor air pressure, and the air flows from the outdoor environment to the internal environment. Neutral pressure occurs near the middle of the lower and upper openings (Kolderup, 2008).

Outer weather (Cold)   Inner weather (Hot)
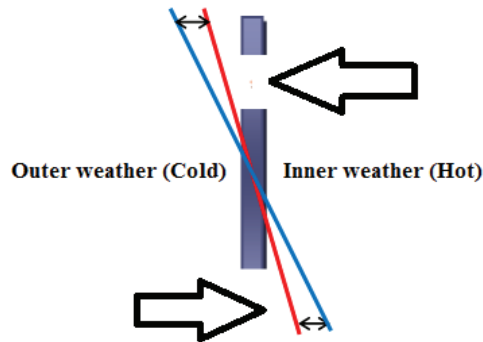
Figure 4. *Graphical representation of the pressure difference in the upper and lower openings*

In Fig. 5, the height of the neutral pressure level depends on the size of the lower and upper openings. The neutral pressure level is close to the large opening.

Neutral Pressure
Inner weather (Hot)
Outer weather (Cold)
Outer weather (Cold)
Inner weather (Hot)
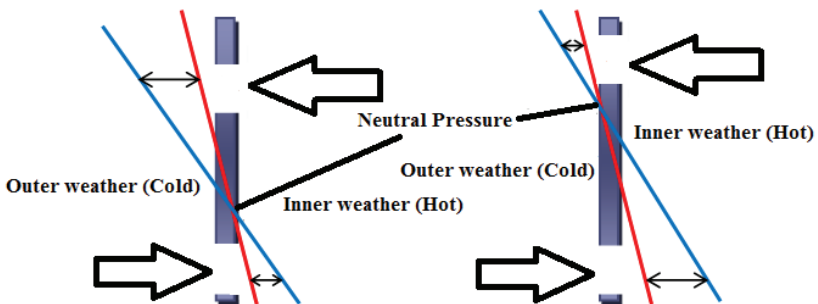
Figure 5. *Graphical representation of the neutral pressure*

In Fig. 6, the lower openings should be smaller than the others, and the upper opening should be large enough to create an equal flow of air towards the upper floors (Kolderup, 2008).
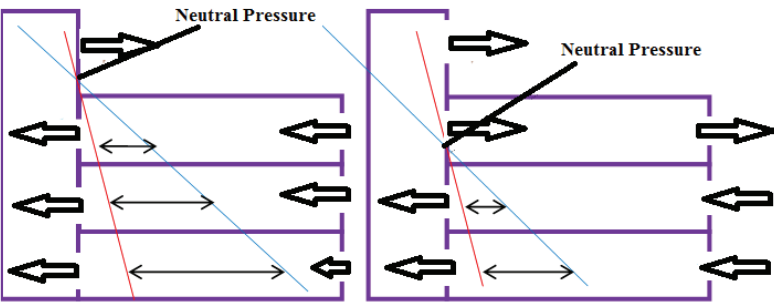
Figure 6. Graphical representation of the neutral pressure according to internal and external air movements

The internal temperature may increase due to natural reasons, by mechanical heating systems, or by the increase in heat caused by the process. Internal temperature buoyancy should be higher than outdoor temperature for effective ventilation (Demir, 2017). In a temperature change, the internal temperature arising from the lower opening and the temperature air flow from the upper opening are calculated by the following Eq. (3):

$$Q_{vol} = C_d A_e \sqrt{\frac{\Delta T}{(T_{in} + T_{out})} gH} \tag{3}$$

ΔT	Temperature difference (°C)
T_{in}	Internal temperature (°C)
T_{out}	External temperature (°C)
g	Gravity (m²/s)
H	Difference between two openings (m)

Eq. (3) gives good results for closed areas with entrance and exit openings on the walls. If there are no obstructions to the air flow (Fig. 7), free air volumetric flow rate can be used in the calculations. In addition, if the distance between the lower and upper openings' mid-point is small, and the horizontal distance between the openings is high, effective ventilation decreases.
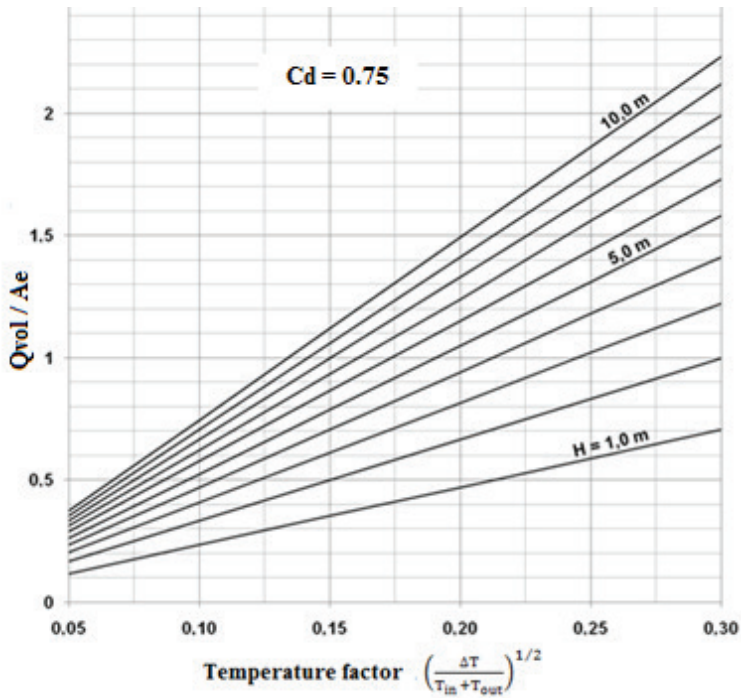
Figure 7. *Temperature effect of the flow rate*

NATURAL VENTILATION CAUSED BY BOTH WIND AND STACK EFFECT

Although wind and stack effect usually occur separately, they are also likely to occur together. Due to the pressure difference created by the wind, a windy and hot day can be the driving force, while the thermal buoyancy can be the driving force on a cold day without wind. These forces complement each other according to wind direction and wind inlet and outlet openings (Fig. 8).
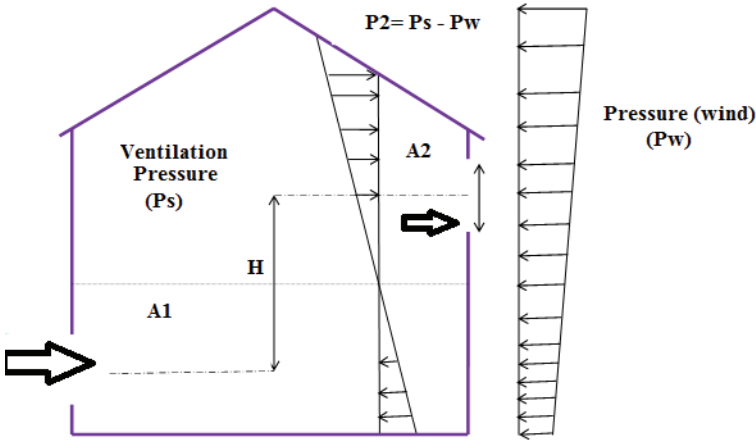
Figure 8. *Wind and chimney effect on the neutral ventilation*

The design should work in harmony with the wind and chimney effects, and these should not interfere with each other. For good natural ventilation, it is necessary to use pressure distribution properly and design the openings in the most appropriate way. Fig. 8 shows schematically the wind effect and the principle of the chimney effect working together. Pressure differences or temperature differences due to wind can also be calculated from Eq. 4-9 (Amini et al., 2013; Saloglu & Demir, 2016).

$$Q_{mass} = \frac{\Delta m}{\Delta t} = \rho Q_{vol} \tag{4}$$

Q_{mass} — Mass flow rate (kg/h)

Δm — Mass (kg)
Δt — Time (h)
ρ — Density (kg/m³)

To find the mass flow of air from the density and volumetric flow of air in Eq. (4-7):

$$\rho = \frac{Q_{mass}}{Q_{vol}} \tag{5}$$

$$Q_{mass} = \rho \, Q_{vol} \tag{6}$$

Volumetric flow rate can be expressed as below if the pressure $P_1 > P_2$:

$$Q_{vol} = V \, A \tag{7}$$

Q_{vol} — Volumetric flow rate (m³/h)
V — Air rate (m/s)
A — Area (m^2)

From Bernoulli equation (Eq. (8)):

$$P_1 - P_2 = \frac{1}{2}\rho_1 V^2 \tag{8}$$

P_1 Internal pressure (kg/m^2)
ρ_1 Internal density (kg/m^3)
V Air rate (m/s)
P_2 External pressure (kg/m^2)

Volumetric flow rate can be calculated from Eq. (9):

$$Q_{vol} = A_e \left(\frac{2(P_1 - P_2)}{\rho_1}\right)^{0.5} \tag{9}$$

The actual airflow rate is smaller than the theoretical airflow rate. Actual flow rate is 2-40% lower than the calculated value. The reason for this is the geometry of the opening where the flow is happening. This tolerance is corrected by the C_d surface pressure coefficient (Demir, 2017; Saloglu & Demir, 2016).

Volumetric flow rate (Q_{vol*}) is corrected by the surface pressure coefficient (Eq. 10):

$$C_d < 1$$

$$Q_{vol*} = C_d Q_{vol} \tag{10}$$

When the internal air pressure is greater than the external air pressure, Eq. 11 can be used:

$$Q_{vol} = C_d A_e \sqrt{\frac{2\Delta p}{\rho_a}} \tag{11}$$

ΔP Pressure difference $(\Delta p = P_1 - P_2)$ (kg/m^2)
ρ_a Density (kg/m^3)

Natural Ventilation by Single and Double Passes

If the air outlet path is not defined, the propulsions may have low values, and insufficient ventilation may occur (Fig. 9).
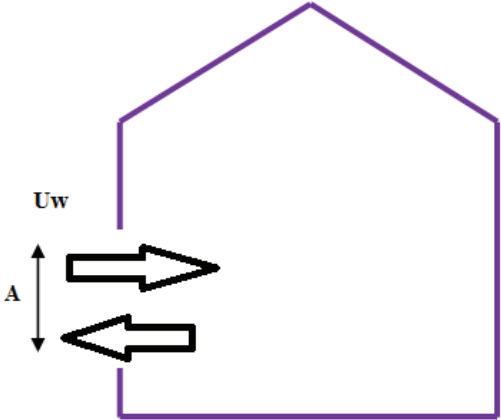
Figure 9. *Natural ventilation by single pass*

Ventilation rate is expressed in Eq. (12):

$$Q = 0.25 \, A \, u_w \tag{12}$$

Volumetric flow rate is expressed in Eq. (13), and double-pass ventilation with temperature effect is shown in Fig. 10:

$$Q_{vol} = C_d A_e \sqrt{\frac{\Delta T}{(T_{in} + T_{out})} gH} \tag{13}$$
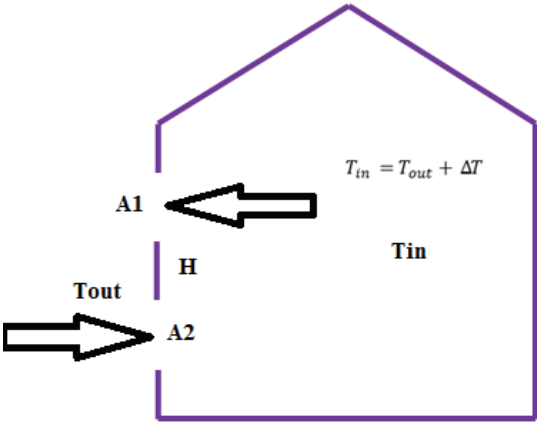
Figure 10. *Natural ventilation by double-pass and temperature effect*

Ventilation with single pass and temperature effect is shown in Fig. 11, and volumetric flow rate is expressed in Eq. (14).
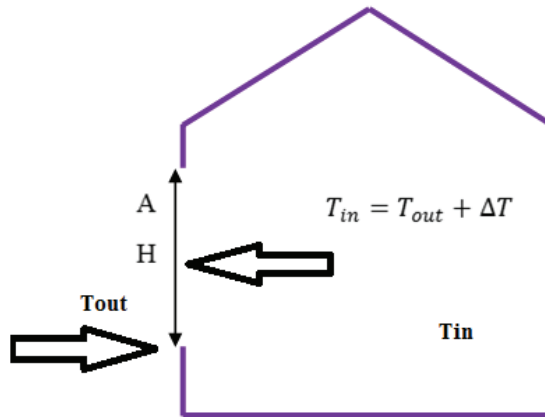
Figure 11. *Ventilation with single pass and temperature effect*

$$Q_{vol} = C_d \frac{A}{3} \sqrt{\frac{2\,\Delta T}{(T_{in}+T_{out})} gH}$$

(14)

Air inlets and outlets as well as wind and thermal ventilation conditions create the driving force as shown in Figs. 12-14; volumetric flow rate can be calculated from Eqs. 15 and 16.
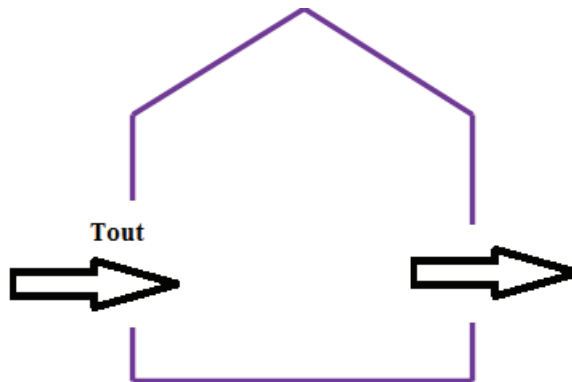
Figure 12. *Natural ventilation by double-pass*
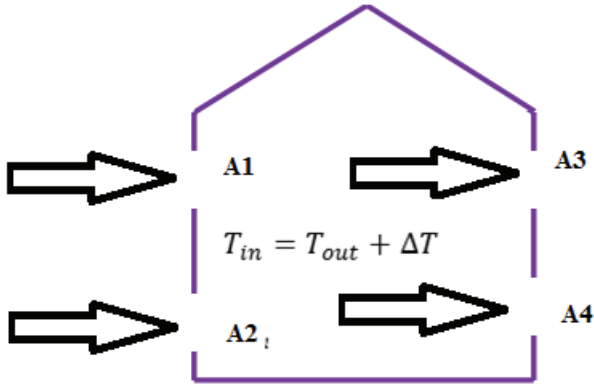
Figure 13. *Natural ventilation under the effect of bilateral wind and temperature differences*

$$Q_{vol} = C_d A_w u_w \sqrt{\Delta C_p} \qquad (15)$$

$$\frac{1}{A_w^2} = \frac{1}{(A_1 + A_2)^2} + \frac{1}{(A_3 + A_4)^2} \qquad (16)$$

MECHANICAL (FORCED) VENTILATION

In cases where natural ventilation is not sufficient, ventilation using air evacuation devices to accelerate ventilation by interfering with natural circulation is used; this is called 'mechanical (forced) ventilation' (Fig.14) (Dogan, 2012).
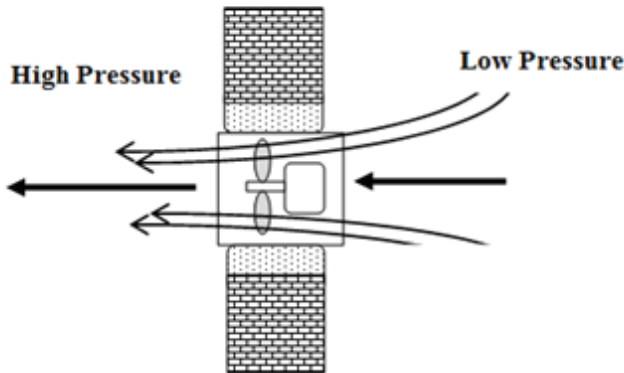
Figure 14. *Air flow through the fan*

This provides fresh air to the closed area by ventilation. In these types of buildings/areas, the air is pushed to the closed area mechanically by the fan. With the compressed air, internal pressure increases. Since the outer pressure is lower than the internal pressure when the fan operates, dirty air goes out through the opening where it is located (Dogan, 2012). Ambient air is diluted with this type of ventilation system in closed areas where there is an explosive atmosphere.

Suction of Air from the Closed Area

The explosive atmosphere formed inside is carried to the external area using fans (aspirators). Thus, due to the pressure difference between inside and outside, fresh air enters through the openings in the closed area. Furthermore, dangerous gases are transported by a fan (aspirator) with local suction nozzles (Dogan, 2012).

Suction of Air and Compression to the Closed Area

Suctioning air and pushing it outside is a method mostly used for ventilation of large volumes. While flammable and combustible air is expelled from the closed area with fans (aspirators), clean and fresh air is fed to the closed area, also with the help of fans (Dogan, 2012). It is a ventilation system where fresh air is taken mechanically from the outside using an aspirator, and exhaust air is pushed into the atmosphere using a fan. Although mechanical (forced) ventilation is used in closed areas, it can also be used in areas open to the atmosphere if natural ventilation is restricted or prevented by obstacles.

In mechanical (forced) ventilation systems, the amount of air exchange depends on the selected fan, the distribution network of the designed system, and the losses in the distribution network. If these parameters are not selected properly during system design, the amount of air supplied to the building will be different from the desired amount. Mechanical ventilation often emerges as a system of choice for the health and comfort of residents and employees, providing the minimum amount of air needed for large buildings. The initial investment and operating costs of mechanical ventilation, which is a complex system, are high (Torno et al., 2013).

Mechanical (forced) ventilation can be general or local, and different degrees of air movement and air exchange may be appropriate.

With mechanical (forced) ventilation:

a. Explosive atmosphere zone type and zone coverage can be reduced,

b. Duration time of the explosive gas atmosphere can be reduced,

c. The formation of an explosive gas atmosphere can be prevented.

Usability Criteria of Mechanical (Forced) Ventilation

When evaluating the level of usability of mechanical (forced) ventilation, reliability of the equipment and the presence of spare fans should be considered. In order to obtain a good ventilation level, spare fans should be automatically activated in case of failure. However, if precautions are taken to prevent the discharge of flammable and explosive gases in case of failure of the ventilation, the classification made while the ventilation is in operation does not need to be changed, that is, the availability level of the ventilation is considered to be good (Torno et al., 2013).

The air movement created by the ventilation systems within the structure can be examined in three groups according to the type of ventilation. Accordingly, systems can be classified as air suction systems, air conditioning systems, and air mixing systems. In air suction systems, the air is sucked in with an aspirator. With this suction, since the pressure inside the space decreases, fresh air equal to the absorbed air is transferred to the space through designed openings (Darcin, 2008). The air conditioning system is actually a group of systems under a general name. Each system has a separate task in creating the desired climatic conditions, that is, they are separate parts in the heating, cooling, and humidifying system in the air conditioning plant, consisting only of separate units. Therefore, the entire air conditioning system can be evaluated in five different categories. The air conditioning plant and its side elements consists of air transport channels, blowers, and automatic control elements (Dogan, 2012).

Regardless of the ventilation rate in the narrowly confined space in the arrangement of a ventilation system, when spraying from the discharge source, it is not diluted below the lower explosive limit value (LEL) (Gurel & Ketez, 2010). When the degree of dilution cannot be reduced to the desired level with natural ventilation, mechanical (forced) ventilation is needed (Fig. 15).
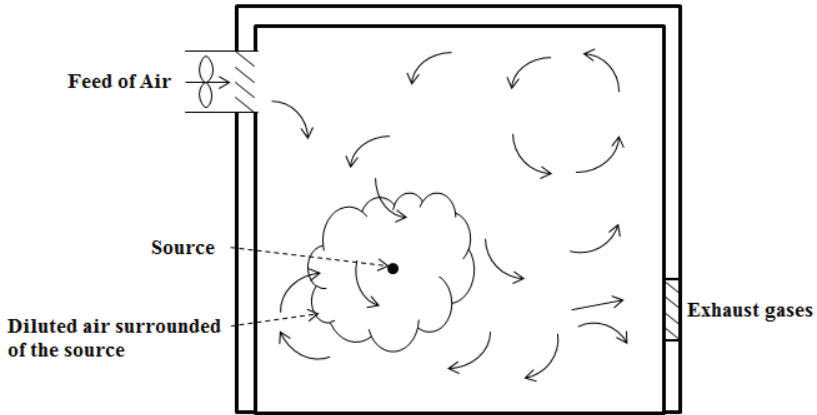
Figure 15. *Natural ventilation system*

In the ventilation system in Fig. 16, the air exchange per unit time is high, ensuring that the concentration level is high.
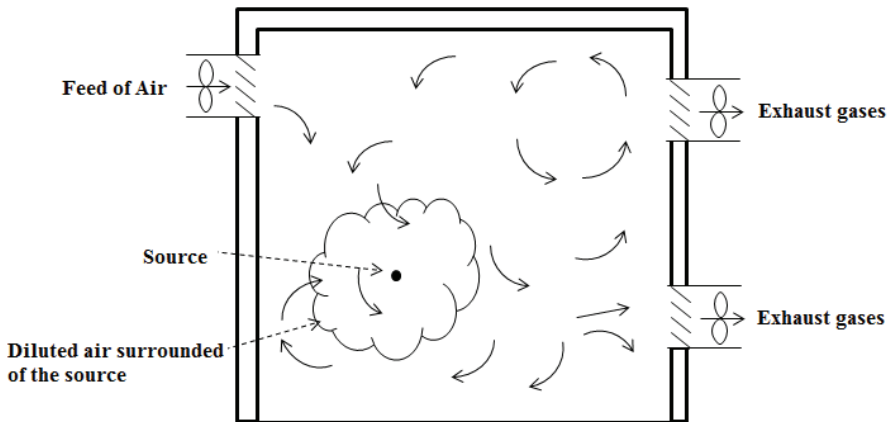
Figure 16. *Mechanical ventilation system*

In Fig. 16, mechanical (forced) ventilation, feeding, and exhaust are used together. In the case of gas emitting from the source of injection by spraying, although the concentration efficiency in the environment is high, it may be affected by negative effects of environmental conditions, and the concentration efficiency may decrease. In this case, a degree of dilution, moderate or high, may occur (Toraño et al*.,* 2011).

Local mechanical (forced) ventilation, being close to the source of spreading, increases the dilution degree. More importantly, as shown in Fig. 17, the gas and vapor discharge is controlled by removing gas and va-por discharged from the source. The degree of dilution around the spread-ing source is medium (Zhang et al., 2013). Local mechanical (forced) ven-tilation should be placed as close to the source of danger as possible. If

the rate of propagation from this source is low, this ventilation system is effective. For local mechanical (forced) ventilation to be effective in evacuation, the ventilation rate must be higher than the discharge rate. In order to keep the source of emission under control, the ventilation speed should be at least 0.5 m/s.
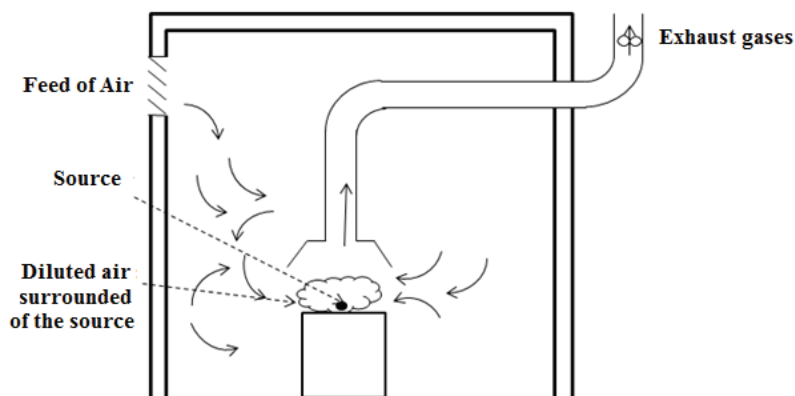
Figure 17. *Local ventilation*

Conclusion

Operational safety and sustainable success cannot be considered separately in business life. Process safety is carried out to prevent major industrial accidents. Chemical plants carry various risks. These risks include mechanical hazards, fire and explosion hazards, and reactivity and toxic hazards that cause workers to suffer accidents. These hazards not only harm the facility and its employees, but they also affect the residential areas around the facility. Although it is not possible to eliminate these risks, they can be reduced to an acceptable level by using ventilation systems. Safety processes must be studied in all areas of the facility to ensure process safety in chemical plants with combustible and explosive substances and to predict danger levels by making necessary mathematical models. In this way, risks should be minimized.

REFERENCES

Amini, E., Nayeri, F.S., Hemati, A., Esmaeilinia, T., Nili, F., & Dalili, H. (2013). Comparison of high frequency positive pressure mechanical ventilation (HFPPV) with conventional method in the treatment of neonatal respiratory failure. *Iranian Red Crescent Medical Journal, 15*(3), 183-186.

Darçın, P. (2008). *Yapı içi hava kirliliği giderilmesinde doğal havalandırma ilkeleri.* (Yüksek Lisans Tezi). Yıldız Teknik Üniversitesi, Fen Bilimleri Enstitüsü.

Demir, A. (2017). *Kimyasal proseslerin güvenliğinde parlayıcı, patlayıcı kimyasal ortalmaların etki analizi ve saha uygulamaları.* (Yüksek Lisans Tezi). Yalova Üniversitesi, Fen Bilimleri Enstitüsü.

Dogan, P.D. (2012). *Uygulamalı havalandırma ve iklimlendirme esasları.* Ankara: Seçkin Yayıncılık.

Fang, Y., Fan, J., Kenneally, B., & Mooney, M. (2016). Air flow behavior and gas dispersion in the recirculation ventilation system of a twin-tunnel construction. *Tunnelling and Underground Space Technology*, *58*, 30-39.

Gil-Baez, M., Barrios-Padura, A., Molina-Huelva, M., & Chacartegui, R. (2017). *Natural ventilation systems to enhance sustainability in buildings: a review towards zero energy buildings in schools.* International Conference on Advances in Energy Systems and Environmental Engineering (ASEE17), https://doi.org/10.1051/e3sconf/20172200053.

Gurel, A., & Ketez, M. (2010). Havalandırma sistemlerinde kanal çapları ve basınç kayıplarının bilgisayar destekli hesaplanması. *Makine Teknolojileri Elektronik Dergisi*, *7*(4), 83-90.

Kolderup, E. (2008). *Saving Energy with Natural Ventilation Strategies*, AEE Meeting. http://www.aee-sf.org/meetings/AEE_Presentation_9-24-08_twoperpage.pdf

Ok, V. (2005). Yapma çevre tasarımında rüzgar etkileri. *Tasarım*, *157*, 70-74.

Saloglu, D., & Demir, A. (2016). Endüstriyel tesislerdeki yanıcı gaz ve sıvıların yayılma hızlarının teorik olarak belirlenmesi. *Kimya ve Sanayi, Türkiye Kimya Derneği-Turkish Chemical Society, 2*(7), 53-56.

Sasmito, A.P., Birgersson, E., Ly, H.C., & Mujumdar, A.S. (2013) Some approaches to improve ventilation system in underground coal mines environment - a computational fluid dynamic study. *Tunnelling and Underground Space Technology, 34*, 82-95.

Spengler, J.D., Samet, J.M., & McCarthy, J.F. (2001). *Indoor air quality*

handbook. McGraw-Hill Education.

Torano, J., Torno, S., Menendez, M., & Gent, M. (2011). Auxiliary ventilation in mining roadways driven with road headers: validated CFD modelling of dust behavior. *Tunnelling and Underground Space Technology, 26*, 201-210.

Torno, S., Toraño, J., Ulecia, M., & Allende, C. (2013). Conventional and numerical models of blasting gas behaviour in auxiliary ventilation of mining headings. *Tunnelling and Underground Space Technology, 34*, 73-81.

Zhang, X., Fang, Y., Peng, P., & Zhao, Z. (2015). Study on regularity of gas emission and diffusion at heading face during tunnel construction. *Journal of Highway and Transportation Research and Development, 32*(2), 119-126.

Chapter 12

MECHANICAL PERFORMANCE OF ENGINEERED CEMENTITIOUS COMPOSITES (ECC) / ASPHALT CONCRETE COMPOSITE SYSTEMS

Hasan Erhan YÜCEL[1]

1 Asst. Prof. Dr., Department of Civil Engineering, Faculty of Engineering, Nigde Ömer Halisdemir University, heyucel@ohu.edu.tr

1. INTRODUCTION

Asphalt pavements often need to repair 8 to 12 years after production due to the reasons such as increased traffic density and increased vehicle carrying capacity. These reasons generally cause extra stresses on asphalt pavements and when the stresses exceed the structural capacity of asphalt pavements, distresses/deteriorations occur. There are several types of distresses formed on asphalt pavements like ravelling, bleeding, polishing, settling, cracking (transverse, reflective, slippage, longitudinal, block, fatigue), rutting and rippling. Overlays are used to repair most of these distresses occuring on the asphalt pavements (Hicks et al., 2000).

There are basically three types of overlay applications to rehabilitate asphalt pavements as asphalt concrete overlays, unbonded Portland cement concrete overlays and bonded ultra-thin Portland cement concrete overlays (Fwa, 2005). After examining the deteriorated asphalt pavement, it is decided which type of overlay must be used. Moreover, the most economical and effective overlay type must be selected for long service life according to material properties. Therefore, Portland cement concrete overlays highly preferred because of their high mechanical and durability properties. In the application, an additional material generally used to provide bonding or unbonding between the overlay and existing asphalt concrete to produce Portland cement concrete/asphalt concrete composite system. The easiest way to produce bi-layer composite system is directly casting the overlay material on existing asphalt concrete. However, this situation may only be possible with the use of high performance concretes as overlay material.

In recent years, concrete technology has been rapidly improved and Engineered Cementitious Composites (ECC) was invented. ECC, which is a type of high performance fiber reinforced cementitious composites, has a great energy absorption capacity thanks to its very high ductility feature, 300-500 times higher than conventional concrete (Li, 1998, 2003; Li et al., 2001). The fibers contained in ECC work as bridges after the formation of first crack on the ECC. Thus, the load is transferred to a different point of the member and multiple micro cracks occur unlike conventional concrete. Therefore, ECC shows strain-hardening behaviour like a metal material. ECC has superior mechanical and durability properties such as compressive strength, flexural strength, tensile strength and permeability, frost resistance, respectively (Şahmaran et al., 2011; 2012a; 2012b; Özbay et al., 2013a). Moreover, ECC has a self-healing behaviour after the formation of multiple micro cracks and can be acceptable as crack-free material for limited crack widths (Özbay et al., 2013b; Özbay et al., 2013c).

These high performance features of ECC showed that it could be an

overlay material and it led to research on this subject. The studies (Lim and Li, 1997; Kamada and Li, 2000; Zhang and Li, 2002; Lepech and Li, 2010; Yücel et al., 2013) proved that ECC has a superior performance in terms of both bond strength and interfacial properties between the two concrete layers, when ECC is used as overlay material on existing concrete layer. Therefore, in the light of these studies, the usability of ECC as an overlay material on concrete has been determined. This situation brings to mind the availability of ECC also for asphalt pavements.

As mentioned in previous paragraphs, after the application of overlay material, the asphalt pavement structure do not have a single layer. Therefore, the service life of the pavement is not only depended on the properties of the materials used in, but also the performance of the overlay material/ asphalt concrete composite as a whole system (Huang et al., 2015). Moreover, it is well known that the weakness section of the composite system is the interfacial zone between new overlay material and existing pavement layer (Bonaldo et al., 2005; Tayeh et al., 2012, An et al., 2014). In many researches, it has been determined that a large part of the pavement overlay defects are due to poor bonding conditions (Collop et al., 2009; Hu and Walubita, 2011; Peattie,1980; Shaat, 1992; Lepert et al., 1992; Hachiya and Sato, 1997). For this reason, the flexural behaviour and the bond properties of the interfacial section must be determined.

In this chapter, the flexural and bond strength performance of the composite obtained by rehabilitation of an asphalt pavement with ECC will be explained. A binder layer, which has been subjected to heavy traffic load and therefore the wear layer has been damaged and completely separated, has been chosen as the asphalt pavement to be repaired. ECC mixtures were used as overlay material for this binder layer that was disassembled and brought to the laboratory. As the overlay material, two different ECC mixtures (Fly-ash-ECC and Slag-ECC) classified in terms of mineral admixtures in their content were determined and compared to Silica-fume Modified Concrete (SMC) mixture which is known as one of the most preferred cement-based overlay material in the literature due to its high performance and easy application (Sprinkel and Moen, 1999; Özyıldırım and Gomez, 1999; Sprinkel, 2004; Alhassan, 2007 and Mokarem et al., 2008; Issa et al., 2008). Therefore, Overlay Material/Asphalt Concrete composite systems were produced and four-point bending test and direct pull-off test were applied on these composite samples to determine the flexural and bond strength parameters.

2. EXPERIMENTAL STUDY

2.1 Materials

Three overlay mixtures (Fly-ash-ECC, Slag-ECC and SMC) were prepared for this research. CEM I 42.5 R type normal Portland cement was used for all overlay mixtures. The ECC mixtures consist of Class-F type fly ash, granulated blast furnace slag (Slag), quartz sand with 0-400µm grain size, polyvinyl-alcohol (PVA) fibers with the length of 8 mm, water and polycarboxylate ether based high range water reducing admixture (HRWR). River sand and crushed stone with maximum aggregate size of 5 mm and 12 mm respectively, silica fume, water, HRWR and air entraining admixture (AEA) as chemical admixtures were used to produce SMC. Mix proportions of all overlay mixtures are presented in Table 1.

Table 1. *Mix proportions of overlay mixtures by weight*

Materials	Fly-ash-ECC	Slag-ECC	SMC
Portland cement	1.00	1.00	1.00
Fly ash	1.20	-	-
Slag	-	1.20	-
Silica fume	-	-	0.10
Quartz sand	0.58	0.58	-
River sand	-	-	1.54
Crushed stone	-	-	2.35
Water	0.58	0.58	0.33
HRWR	0.010	0.011	0.012
AEA	-	-	0.00095
PVA (%)	2	2	-

*All ingredient proportions by weight except for fiber.

The asphalt pavement, used as the existing asphalt concrete to create overlay material/asphalt concrete composite specimens, is the binder layer obtained by spalling out the wear layer as a result of the use of the asphalt pavement in the field prepared in accordance with the Highway Technical Specifications of Turkey (2013).

2.2 Four-point Bending Test

Overlay materials/asphalt concrete composite beams were designed with the thickness of 50mm/30mm respectively. Firstly, the deformed asphalt concrete pavement was removed from the construction site and was brought to the construction materials laboratory. After that, the asphalt concrete was separated into beam specimens with the dimensions of 400 x 75 x 30 mm by cutting with a diamond saw. During this process, care was taken to ensure that the asphalt pavement surface was not cut and damaged. Then, the surface of asphalt concrete specimens were cleaned by

using brush, water and compressed air. Thus, beam specimens were made ready to use as substrate asphalt concrete layer in 400 x 75 x 30 mm dimensions and under the same surface conditions. Finally, the prepared asphalt concrete beam specimens were placed into the molds with the dimensions of 400 x 75 x 80 mm and the overlay mixtures (Fly-ash-ECC, Slag-ECC and SMC) were directly cast over the asphalt concrete beam specimens as seen in Figure 1-a. All specimens were demoulded after 24 hours as seen in Figure 1-b, and moisture cured in plastic bags at 95±5% RH, 23±2°C for 7 days, and then air cured at 50±5% RH, 23±2°C until the day of testing.

(a)   (b)

Figure 1. *Production of the overlay material/asphalt concrete composite beam specimens*

To specify the flexural performance of layered overlay material/asphalt concrete composite beams, four-point bending tests were performed with Fly-ash-ECC, Slag-ECC and SMC overlay layers on the bottom (in tension) and asphalt concrete layer on the top (in compression) to simulate field conditions. Four-point bending test was carried out on a closed-loop controlled material testing device with the overlay material/asphalt concrete composite beam specimens at the age of 7 and 28 days. The mid-point deflection of the composite beams were recorded with LVDTs to determine the relative displacement between the top of the beam and the loading fixture. For each test age and overlay material, six overlay material/asphalt concrete composite beam specimens were tested.

2.3 Direct Pull-off Test

Direct pull-off tests were applied according to ASTM D 4541 standard. Firstly, the deteriorated asphalt concrete pavement taken from existing road were cut with the dimensions of 50×35 cm. Also, the surface conditions of asphalt concrete was protected during this cutting process. After that, the asphalt concrete was cleaned by using brush, water and compressed air. After this application, one of the overlay materials (Fly-ash-ECC, Slag-ECC and SMC) was cast over the existing asphalt concrete with the thickness of 30 mm and without any bonding agent (Figure 2-a).

When the casting of new materials is finished, layered systems were completely covered by plastic sheets to protect from the outdoor environment just before the core drilling process. The cores were started to be drilled two hours before testing as seen in Figure 2-b. In this study, diameter of the cores was 50 mm with the drilling depth into the asphalt concrete of nearly 15±5 mm., which are generally used values to be applied (Austin et al., 1995; Yıldırım et al., 2015). Care was taken to keep suitable distance when drilling the cores since the vibration caused due to cutting drill tool can be influential on the bond strength results of adjacent cores. After the completion of core drilling procedure, the core samples were dried and cleaned by compressed air. Metal disks were then sticked over the separate core specimens with the use of an epoxy based material . Direct pull-off tests were performed at the age of 7 and 28 days and for each date and type of overlay material eight core specimens were tested. Application of the tensile load was made at a constant pace rate until the failure of specimens. Finally, bond strength results and fracture modes of the specimens were noted.

(a) (b)

Figure 2. *Production of the direct pull-off test specimens*

3. RESULTS AND DISCUSSION

3.1 Four-point Bending Test

Four-point bending test was performed to evaluate the flexural behaviour of overlay material/asphalt concrete composite systems. Table 2 and Figure 3 shows the flexural strength and mid-span beam deflection values and flexural performance of overlay material/asphalt concrete composite beams, respectively. The SMC test results serve as a reference for assessing the flexural performance of ECC overlaid specimens. Test results show that ECC overlaid specimens are superior to SMC overlaid specimens according to flexural strength. Among the ECC specimens, it is easily seen that the composite beam incorporated Slag-ECC as overlay material has the highest flexural strength for each testing age. Moreover, the use of ECC layer can also result in significant ductility improvement for the lay-

ered beams. Strain-hardening behaviour is observed for Fly-ash-ECC and Slag-ECC / asphalt concrete composite beams. Conversely, SMC/asphalt concrete composite beams show the behaviour of brittle material.

Crack formation of overlay material/asphalt concrete composite beams after four-point bending test are shown in Figure 4.When the layered composite beams were analyzed in terms of crack formation, there is only one major crack was observed on SMC/asphalt concrete composite beams (Figure 4-c). For Slag-ECC and Fly-ash-ECC composite beams, firstly multiple micro cracks were occured in the ECC layer (Figure 4-a and Figure 4-b). As a result, one of these multiple micro cracks opened more widely than the others, and propagate into the concrete layer. Multiple cracking permits large straining in the ECC layer until its failure, therefore leading to a higher ultimate deflection value and a ductile failure mode. Similar results were obtained from the previous studies by using ECC/conventional concrete composite systems (Kamada and Li, 2000; Lim and Li, 1997; Zhang and Li, 2002; Yücel et al., 2013).

Table 2. *The flexural strength and mid-span beam deflection values of overlay material/asphalt concrete composite beams*

Overlay Material	Flexural Strength, MPa		Mid-span Beam Deflection, mm	
	7 days	28 days	7 days	28 days
Fly-ash-ECC	8,94	10,84	7,65	5,18
Slag-ECC	10,25	11,46	5,31	3,93
SMC	6,12	6,94	0,76	0,67
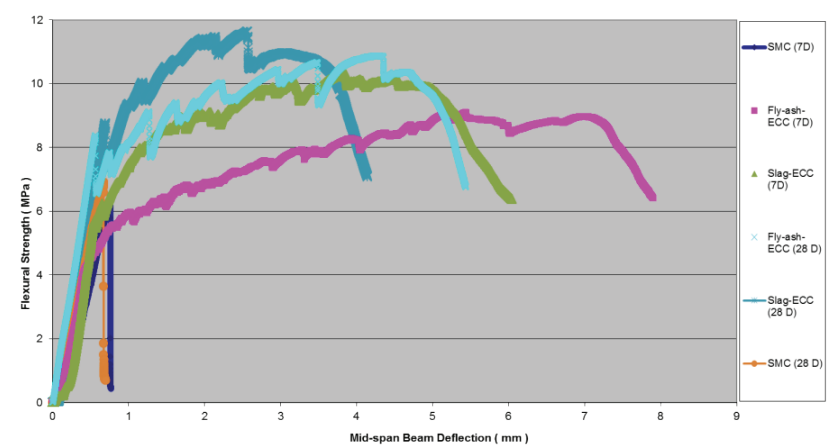
Figure 3. *The flexural performance of overlay material/asphalt concrete composite beams*
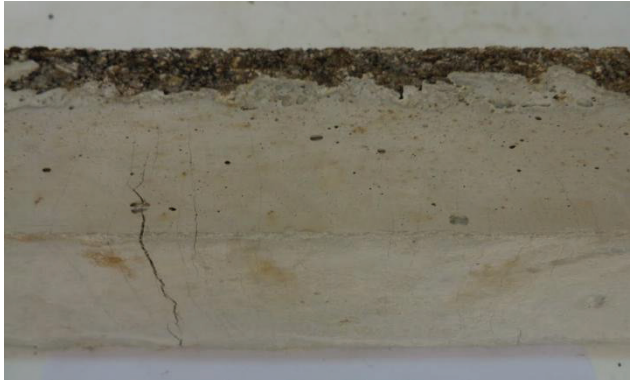
(a)Slag-ECC/asphalt concrete composite beam
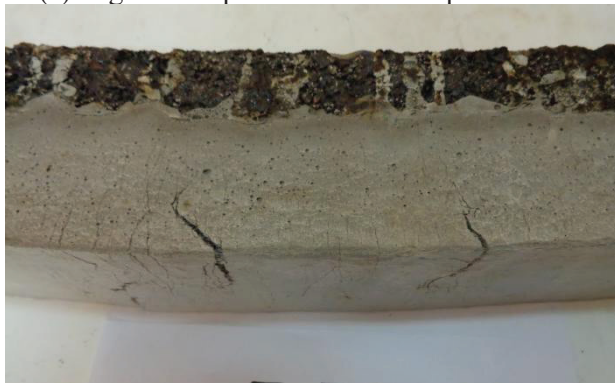
(b)Fly-ash-ECC/asphalt concrete composite beam

(c)SMC/asphalt concrete composite beam

Figure 4. *Crack formation of overlay material/asphalt concrete composite beams after four-point bending test*

3.2 Direct Pull-off Test

Direct pull-off test was conducted on overlay material/asphalt concrete composite systems to determine the bond performance of overlay materials. The bond strength values and the failure modes of core specimens obtained as a result of direct pull-off tests conducted at the age of 7 and 28 days are given in Table 3. In addition, the failure modes of Fly-ash-ECC, Slag-ECC and SMC specimens at the end of 28 days as a result of direct pull-off tests were presented in Figure 5. According to bond strength values, Slag-ECC showed highest performance as overlay material for all test ages. However, SMC has the lowest bond strength values for the ages of 7 and 28 days. Moreover, a slight improvement was assigned on the bond strength values with the increase of test age. When the direct pull-off test results evaluated from failure mode point of view, a sharp difference was observed. As seen in Table 3 and Figure 5, Slag-ECC showed superior performance like bond strength and no failure on interfacial plane was observed. However, 2 and 3 specimens failed from interface over 8 specimens was determined for Fly-ash-ECC and SMC, respectively.

Table 3. *The bond strength values and failure modes between overlay material and asphalt concrete*

Overlay Material	Bond Strength(MPa)	Failure Mode	Bond Strength(MPa)	Failure Mode
	7 days		28 days	
Fly-ash-ECC	0,817	5 through substrate and 3 through interface	0,935	6 through substrate and 2 through interface
Slag-ECC	0,880	6 through substrate and 2 through interface	1,006	All through substrate
SMC	0,786	4 through substrate and 4 through interface	0,868	5 through substrate and 3 through interface

(a)Slag-ECC/asphalt concrete composite

(b)Fly-ash-ECC/asphalt concrete composite

(c)SMC/asphalt concrete composite

Figure 5. *Specimen examples of the failure modes of Fly-ash-ECC, Slag-ECC and SMC/asphalt concrete composites for direct pull-off tests after 28 days*

4. CONCLUSIONS

This chapter focus on the performance of ECC as overlay material over an existing asphalt concrete. To determine the overlay performance of ECC, the flexural and bond behaviour of overlay material/asphalt concrete composite systems, which are the most important parameters for overlay materials, were assigned. SCM, one of the most preferable and high performance overlay material according to the literature, was also used as

overlay material to compare the performance of ECC.

According to the results of four-point bending test and direct pull-off test, both Fly-ash-ECC and Slag-ECC showed superior flexural and bond properties compared to SCM. Especially, it is very important to achieve such a high bond strength and no delamination failure without applying a bonding agent between the layers unlike conventional methods.

Although, it has been determined that the superior characteristics of ECC on the use of asphalt concrete as an overlay material, it should be remembered that these studies were carried out under laboratory conditions. Therefore, it is considered important to test ECC on an asphalt concrete with full-scale in construction site.

5. REFERENCES

Alhassan MA (2007) Performance-based Aspects and Structural Behavior of High Performance Fibrous Bonded Concrete Overlays. PhD thesis, University of Illinois, USA.

An, J, Nam, B and Kim, J. (2014) Numerical Analysis of Reflective Cracking in an Asphalt Concrete Overlay over a Flexible Pavement. Design, Analysis, and Asphalt Material Characterization for Road and Airfield Pavements, 67-74.

Austin, S., Robins, P. and Pan, V. (1995) "Tensile bond testing of concrete repairs", Materials and Structures, V. 995, No. 28, 249–59.

Bonaldo E, Barros JAO and Lourenço PB (2005) Bond characterization between concrete substrate and repairing SFRC using pull-off testing. International Journal of Adhesion and Adhesives 25: 463–474.

Collop, AC, Sutanto, MH, Airey, GD and Elliott RC. (2009) Shear bond strength between asphalt layers for laboratory prepared samples and field cores. Construction and Building Materials, 23, 2251–2258.

Fwa T.F., (2005) The Handbook of Highway Engineering, CRC Press.

Hachiya T, Sato K. (1997) Effect of tack coat on bonding characteristics at interface between asphalt concrete layers. In: 8th International conference on asphalt pavements. Seattle.

Hicks, RG, Seeds, SB and Peshkin, DG. (2000) Selecting a Preventive Maintenance Treatment for Flexible Pavements. Report FHWA-IF-00-027. Foundation for Pavement Preservation (FP[2]), Washington, DC, and FHWA, U.S. DEpartment of Transportation.

Highway Technical Specifications (2013). General Directorate of Highways, Ankara, Turkey.

Hu, X and Walubita, LF (2011) Effects of Layer Interfacial Bonding Conditions on the Mechanistic Responses in Asphalt Pavements. Journal of Transportation Engineering, Vol. 137, No.1, 28-36.

Huang, W, Lv, Q and Tian, J. (2015) Effects of Tack Coat Type and Surface

Characteristics on Interface Bond Strength, International Symposium on Frontiers of Road and Airport Engineering.

Issa, MA, Alhassan, MA and Shabila, H (2008) High-Performance Plain and Fibrous Latex-Modified and Microsilica Concrete Overlays. ASCE Journal of Materials in Civil Engineering, 20(12): 742-753.

Kamada T and Li VC (2000) The effects of surface preparation on the fracture behavior of ECC/concrete repair system. Cement and Concrete Composites 22(6): 423–431.

Lepech MD and Li VC (2010) Sustainable pavement overlays using engineered cementitious composites. International Journal of Pavement Research and Technology 3(5): 241–250.

Lepert P, Poilane JP, Villard-Bats M. (1992) Evaluation of various field measurement techniques for the assessment of pavement interface condition. In: 7th International conference on asphalt pavements; 3. p. 224–37.

Li VC (1998) ECC – tailored composites through micromechanical modeling. Fiber Reinforced Concrete: Present and the Future (Banthia N, Bentur A and Mufti A (eds)). CSCE, Montreal, Canada, pp. 64–97.

Li VC (2003) On engineered cementitious composites (ECC) – a review of the material and its applications. Advanced Concrete Technology 1(3): 215–230.

Li VC, Wang S and Wu C (2001) Tensile strain-hardening behavior of PVA-ECC. ACI Materials Journal 98(6): 483– 492.

Lim YM and Li VC (1997) Durable repair of aged infrastructures using trapping mechanism of engineered cementitious composites. Cement and Concrete Composites 19(4): 373–385.

Mokarem DW, Lane DS, Özyıldırım HÇ and Sprinkel MM (2008) Measurement of Early Age Shrinkage of Virginia Concrete Mixtures. Final Report, VTRC 08-R9. Virginia Transportation Research Council, Charlottesville, Virginia, USA.

Özbay E., Şahmaran, M., Lachemi, M. and Yücel, H. E. (2013a) "Effect of Microcracking on the Frost Durability of High Volume Fly Ash and Slag Incorporated ECC," ACI Materials Journal, 110 (3), 259-268.

Özbay E., Şahmaran, M., Lachemi, M. and Yücel, H. E. (2013b) "Self-Healing of Microcracks in High Volume Fly Ash Incorporated Engineered Cementitious Composites" ACI Materials Journal, 110 (1), 33-44.

Özbay E., Şahmaran, M., Yücel, H. E., Erdem, T.K., Lachemi, M. and Li, V.C. (2013c) "Effect of Sustained Flexural Loading on Self-Healing of Engineered Cementitious Composites" Journal of Advanced Concrete Technology, 11 , 167-179.

Özyıldırım Ç and Gomez JP (1999) High-Performance Concrete in a Bridge in Richlands, Virginia. Final Report, VTRC 00-R6. Virginia

Transportation Research Council, Charlottesville, Virginia, USA.

Peattie KR. (1980) The incidence and investigation of slippage failures, the performance of rolled asphalt road surfacings. London: The Institution of Civil Engineers; p. 3–15.

Şahmaran M., Özbay, E., Yücel, H. E., Lachemi, M. and Li, V.C. (2011) "Effect of Fly Ash and PVA Fiber on Microstructural Damage and Residual Properties of Engineered Cementitious Composites Exposed to High Temperatures" ASCE Journal of Materials in Civil Engineering, 23 (12), 1735-1745.

Şahmaran M., Özbay, E., Yücel, H. E., Lachemi, M. and Li, V.C. (2012a) "Frost Resistance and Microstructure of Engineered Cementitious Composites: Influence of Fly Ash and Micro Poly-Vinyl-Alcohol Fiber" Cement and Concrete Composites, 34 (2), 156-165.

Şahmaran M., Yücel, H. E., Demirhan, S., Arık, M.T. and Li, V.C. (2012b) "Combined Effect of Aggregate and Mineral Admixtures on the Tensile Ductility of ECC" ACI Materials Journal, 109 (6), 627-638.

Shaat AA. (1992) Investigation of slippage of bituminous layer in overlaid pavement in Northern Ireland. Consultancy report submitted for the DOE in Northern Ireland.

Sprinkel M (2004) Performance Specification for High Performance Concrete Overlays on Bridges. Final Report, VTRC 05-R2. Virginia Transportation Research Council, Charlottesville, Virginia, USA.

Sprinkel, M.M., and Moen, C. (1999) Evaluation of the Installation and Initial Condition of Latex-Modified and Silica Fume Modified Concrete Overlays Placed on Six Bridges in Virginia. VTRC 99-IR2. Virginia Transportation Research Council, Charlottesville.

Tayeh BA, Bakar BHA, Johari MAM and Voo YL (2012) Mechanical and permeability properties of the interface between normal concrete substrate and ultra high performance fiber concrete overlay. Construction and Building Materials 36: 538–548.

Yıldırım, G. , Şahmaran, M. , Al-Emam, M. K. M., Hameed, R. K. H., Al-Najjar, Y. and Lachemi, M. (2015) 'Effects of Compressive Strength, Autogenous Shrinkage and Testing Methods on the Bond Behavior of HES-ECC' ACI Materials Journal, 112 (3), 409-418.

Yücel, H. E., Jashami, H., Şahmaran, M., Guler, M. and Yaman, I.O. (2013) "Thin ECC Overlay Systems for Rehabilitation of Rigid Concrete Pavements" Magazine of Concrete Research, 65 (2), 108-120.

Zhang J and Li VC (2002) Monotonic and fatigue performance in bending of fiber reinforced engineered cementitious composite in overlay system. Cement and Concrete Research 32(3): 415–423.

Chapter 13

A PERSPECTIVE ON HYDROGELS AND TECHNOLOGICAL APPLICATIONS

Nil ACARALI[1]

1 Doç. Dr., Yildiz Technical University, Davutpasa Campus, Department of Chemical Engineering, nbaran@yildiz.edu.tr, nilbaran@gmail.com

1. HYDROGELS

Hydrogels are polymers that are capable of absorbing water and/or biological fluids, crosslinked by physical or chemical bonds [1], [2]. The materials are in three-dimensional mesh structure consisting of water-absorbing polymer chains. Network structures can consist of homopolymers or copolymers. Hydrogels are insoluble in water due to cross-links in their structures; however, they show swelling behaviour with the presence of water absorbing groups. The water absorption system is shown in Figure 1 [1].
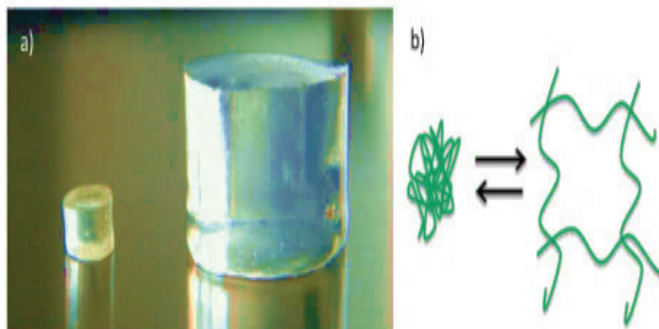
Figure 1. a) Dry and swollen gel, b) Schematic view of gel swelling [1]

By keeping their shape and mechanical stability, they can keep water up to 20-100% of their own weight. This type of hydrogel is called xeorogel. Hydrogels that exceed 100% swelling capacity are called superabsorbent hydrogels [2], [3].

Physical cross-linked gels are known to be more susceptible to any changes due to the external environment than to other attachment types. In hydrophobic interactions, it affects the swelling of the gel since there are molecular interactions like physical cross-linking [3].

Hydrogels are generally used in biomedical, biotechnological, pharmaceutical, technology and agricultural fields thanks to their ability to respond in a controlled manner by increasing and decreasing their volumes by increasing their volumes by hundreds of times [4-6].

Nowadays, one of the important topics in biotechnological field is the studies on the use of hydrogels as a carrier in enzyme and cell immobilization [7]. Various applications have been developed in which hydrogels act as carriers for controlled drug release [8]. In these systems, the hydrogel, the swelling-shrinkage response proportional to the stimulus size is used to adjust the drug delivery rate from the release system. One of the places where hydrogels in the controlled drug delivery area play a big role are self-adjusting insulin delivery systems [9]. The best example for this is insulin release systems discovered and developed for diabetics. This sys-

tem is the membrane that surrounds the insulin reservoir and consists of an action-response hydrogel [10].

Hydrogels to be used in various applications must have properties that can react to external effects similar to real systems [11, 12]. These hydrogels produced from polymers are classified according to the type of action as follows pH, temperature, magnetic, electric field sensitive hydrogels etc.

2. CLASSIFICATION OF HYDROGELS

Hydrogels can be grouped according to the source used, the method of preparation, the structure of cross-linking, the structure of the side groups they possess, their physical structure, the methods of preparation, their water content, their chemical stability, their reactions to environmental conditions and many more features [2].

2.1. Source Based Classification

Hydrogels can be divided into two classification based on sources as natural, synthetic and a combination of two species. Proteins among hydrogel-forming natural polymers, collagen, gelatine and polysaccharides include polysaccharides [13].

2.2. Classification by Polymeric Composition

(a) Homopolymeric hydrogels represent the polymer network from which a single type of monomer is derived; this is a basic structural unit.

(b) Copolymer hydrogels include two or more different types of monomers consisting of at least one hydrophilic component arranged randomly, alternatively.

(c) Multipolymer Interpenetrating polymeric hydrogel (IPN) is a significant hydrogel group, consisting of two independent cross-linked polymer components [13].

2.3. According to Physical Structures

The hydrogels can be grouped according to their physical structure as amorphous (non-crystalline), crystalline and semi-crystalline. Semi-crystalline is a complex mixture of amorphous and crystalline phases [13].

2.4. Cross-Linking Classification

Hydrogel can be classified in two groups according to the properties of crosslinkers according to their connection interactions. Chemically cross-linked nodes have permanent connections, although physical nodes have temporary junctions resulting from polymer chain circulation [13].

2.5. Classification by Physical Properties

The hydrogels that do not contain a reversible covalent bond; can be formed by temporary bonds arising from physical interactions in physical networks or polymer chains. Alginate, gelatine and chitosan (forming a polymer-polymer complex) are examples of such polymers [2].

2.6. Classification Based on Physical Appearance

The appearance of hydrogels such as matrix, film or microsphere depends on the polymerization method involved in the synthesized process. Hydrogels can be divided into four classifications based on the presence or absence of electric charge in cross-linked chains:

(a) Neutral

(b) Ionic

(c) Amphoteric electrolyte

(d) Zwitterionic [2].

3. USE OF HYDROGELS

Hydrogel technologies in 1954 with the creation of the first synthetic hydrogels are used in agriculture, sealing, hygienic products, drug release systems, coal removal, artificial snow, food additives, biomedical applications, drugs, regenerative drugs and tissue engineering, barrier materials, dressing and biosensor applications. In addition, the increasingly functional monomers and macromer spectrum extend their applicability. It was used in the first absorption of biopolymer based agricultural water. Acrylamide is the basic ingredient used in the preparation of agricultural hydrogel products [13]. Due to the biocompatibility of hydrogels, ease of transport and biodegradability, they have found use in controlled drug release systems and medical equipment production. The first application of hydrogels to biomaterials is contact lenses [14]. Eye drops are diluted with the effect of tears, causing flow in a very short time. Hydrogel, developed as an eye drop, becomes viscous under the influence of temperature in the eye, although it is administered as a liquid. Due to its sliding sensitivity feature, it becomes liquid when the eye is blinked; It provides the gel to spread all over the eyes homogeneously. Like eye drops, it can also be used in nasal sprays [15].

It is also used in burn treatment. They are used in burn treatment because of their flexible structure, mechanical resistance, antimicrobial properties, water vapor and metabolites [14].

4. TECHNOLOGIES USED IN HYDROGEL PREPARATION

Hydrogels are usually prepared on the basis of hydrophilic monomers, while hydrophilic monomers are used in hydrogel synthesis to design properties. Generally, hydrogels can be synthesized from polymers as natural and synthetic. These polymers need to be functionalized with groups that have suitable functional groups or can be radically polymerized [16].

Monomers are used to ensure that hydrogel has the desired physical properties. With the high concentration effect of the monomer, high polymerization rate and degree of polymerization. Dispersion polymerization is an alternative method as polymers are synthesized as powder or microspheres by using many technologies. To develop the mechanical specifications for a hydrogel, it can be grafted onto the coating. The method is covalently applied to the support. Various supports as polymeric have been used with grafting techniques for the synthesis of hydrogen [13].

5. APPLICATIONS OF HYDROGELS IN WOUND HEALING

In history, hydrogels were used to heal wounds. It absorbs water in hydrogel structure; therefore, it acts as a moist wound dressing material. The angiogenesis process of the wound provides sufficient amount of oxygen and nutrients, allowing the granulation tissue to grow. Hydrogels are usually supported on surface with support such as a film. The advantages of hydrogels for this application are appropriate rheological properties, good tissue compatibility, easy of application increasing the compliance of the patient, haemostatic movement environment for minor bleeding etc [16].

6. SWELLING OF HYDROGELS

Swelling is the sudden change of a certain volume in the polymer structure and the absorption of a small molecule liquid by a polymer with a change in the polymer structure. As molecules enter structural spaces, they open up between the super molecular structures of the polymer. This is called interstructure swelling. If the solvent molecules enter the structures, the macromolecules are forced open. This is called internal swelling. As the solvent content increases, the polymer structure gradually separates from each other and a volatile polymeric network structure with solvent is formed in the solution [17].

Swelling is one-way mixing because the polymer molecules are very large. The swollen polymer, a solution of a small molecule liquid in the polymer, coexists with the layer of pure small molecule liquid for a certain period of time. When the polymer chains are sufficiently removed from each other, the solvent molecules begin to diffuse slowly into the polymer. Here, a more concentrated solution layer and a more dilute solution layer are combined. After a while more, the concentrations of these two layers

become equal and a single-phase homogeneous system is formed.

Swelling can occur limited or unlimited. Unlimited swelling automatically turns into solution. This phenomenon is called dissolution. The main feature observed in the dissolution of a polymer is that the polymer and solvent molecules differ in size and therefore have different mobility. The mobility of a small molecule fluid is very high, and the mobility of macromolecules is very low. Therefore, large molecule structures have difficulty in transitioning to the solvent phase, and before a polymer dissolves, it swells by absorbing a large amount of liquid [18].

Swelling is a characteristic feature of polymeric mesh structures. Depending on the amount of crosslinking, polymeric structures can absorb a large amount for liquid without dissolving [19]. A polymeric gel determines the swelling ability of groups as functional that interact with each other and solvent. Chains push and pull are affected by non-covalent electrostatic, hydrophobic effects. Hydrophobic interactions are such physical crosslink-like interactions, which affect the swelling behaviour of the gel [20-22].

7. HYDROGELS IN DRUG DELIVERY FOR SWELLING-CONTROLLED SYSTEMS

A hydrogel is known as a polymeric structure that has the ability to absorb >20% of water weight. The hydrophilicity of the product applies water-attracting specifications. The basic water-insoluble behaviour helps to the presence of cross-links. Hydrogels have an elastic form in nature due to the memorized property. They consist of polymers with water to form a solid with water like specifications [23]. Taking advantage of all these features, it has been seen that hydrogels can be used in the field of drug release for swelling-controlled systems.

8. IMPROVEMENT OF DRUG DELIVERY FOR HYDROGEL-BASED SYSTEMS

Synthesis of hydrogel-based drug contains cross-linking of linear polymers or polymerization of monofunctional monomers. The poor mechanical property of cross-linked hydrogels can be improved with different methods. Polymers from various sources can be obtained for synthesizing hydrogels. Generally, polymers with amine, amide, carboxylate etc. groups in their side chains are utilized in studies [18].

9. APPLICATION AREAS OF SMART POLYMER

Hydrogels are utilized in biological applications, drug release and tissue degeneration because:

• Hydrogels provide a semi-wet 3-D medium suitable for biological

interactions at the molecular level.

• It creates an inert surface that prevents non-specific adsorption of many hydrogel proteins (anti fouling feature).

• Biological molecules can be covalently involved in the structure of hydrogels.

• Hydrogels have high adjustable mechanical properties.

• Hydrogels respond to the target with external applications.

Apart from the application areas, it is used in artificial muscles, micro-electro-mechanical-system instruments such as micro valves and micro fluidity controllers. In addition, diapers, watering and smart windows can be given as examples in daily life. With the rapid development and advancement in recombinant DNA technology, a wide variety of protein and peptide drugs have been developed for use in the treatment of diseases that are weak and difficult to control. Due to the high molecular weight and precise spatial structure of proteins, combined controlled release techniques are more challenging [23].

Hydrogels can control drug release by changing the gel composition depending on the surrounding stimulus. Heat sensitive hydrogels attract significant attention in the pharmaceutical area because of their swelling or shrinkage properties according to the change of the surrounding liquid temperature. Hydrogels contribute greatly to the improvement of drug delivery systems with their excellent tissue compatibility, ease of use. Heat sensitive polymers show a low/high critical solution temperature in environments. In cases where polymers show low critical temperature, these polymers have water-soluble properties at temperatures below low critical temperature. However, they show less water solubility or water insolubility at temperatures above this critical temperature [23] Schematic illustration of mesh size in hydrogel is shown in Figure 2.
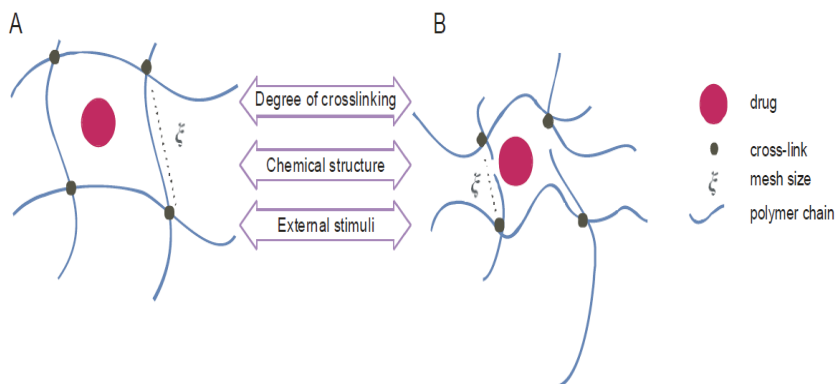
Figure 2. Schematic representation of mesh size in hydrogel at (A) swollen state and (B) deswollen state [24]

10. PROTEIN DRUG RELEASE SYSTEMS IN HYDROGEL STRUCTURE

Protein release from hydrogel is complex due to environmental factors. Hydrophilic polymers utilized in controlled release systems can be collected in three main classes as nonporous, microporous and macroporous hydrogels. Protein-releasing hydrogel systems are shown in Figure 3 as a schematic representation.
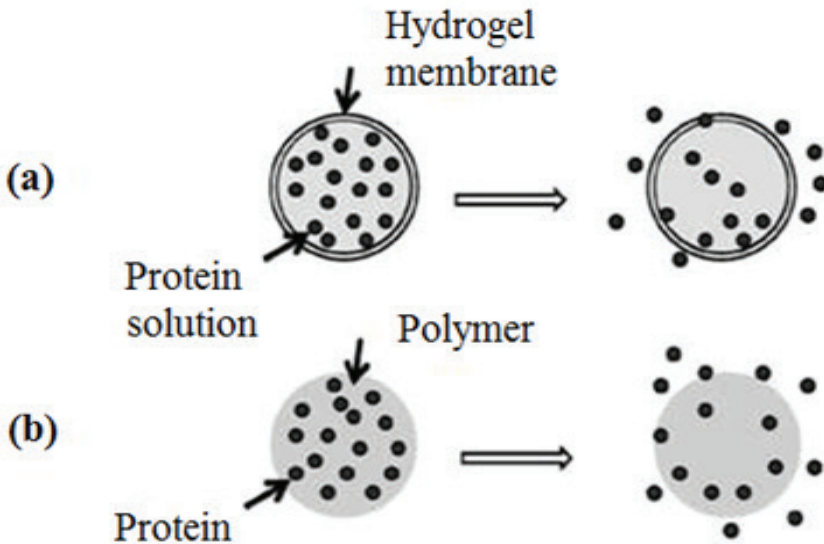
Figure 3. Protein-releasing hydrogel systems (a) Reservoir system containing protein in aqueous state (b) Anhydrous release device (matrix system) created by compression of the powder mixture of protein and hydrophilic polymer [25]

Porous hydrogels contain three-dimensional covalent or ionic cross-linked macromolecular chains and are characterized by pore sizes. Pore size is equivalent to macromolecular connection length and is between 10 and 100 A°. In general, protein release from this type of hydrogel occurs through networks where polymer chains are heavily blocked. One of the methods used to prepare a non-porous hydrogel is polymerization with the level of solvent below equilibrium value. Microporous hydrogels contain pores larger than the macromolecular connection length. Protein release occurs through the combination of diffusion and convection, where water passes through the pores and the solute is carried. Macroporous hydrogels, on the other hand, generally have large pores with diameters greater than

0.1 µm value. The mass transfer mechanism is in the form of diffusion and convection from water-filled pores. In porous systems, release models that define protein diffusion are based on the classical hydrodynamic basis. Macroporous hydrogels can be formed with solvent in excess of equilibrium value. One of the ways to achieve large pore sizes is to perform polymerization without solvent [25].

REFERENCES

[1] Baker, Ş.B., (2012). Controlled Drug Release Hydrogel Systems and Application Studies, Master Thesis, Eskisehir Osmangazi University, Institute of Science, Eskisehir.

[2] Brahima, S., (2016). Synthesis of pH and Temperature Sensitive Hydrogels and Modelling of Drug Release Behaviours, Master Thesis, İnönü University, Institute of Science, Malatya.

[3] Tan, N., (2008). Investigation of the Effect of IPN Type Hydrogels Containing Chitosan-Poly (Acrylic Acid) -Poly (Acrylamide) on Swelling Behaviours and Wound Healing, Master Thesis, Gazi University, Institute of Science and Technology, Ankara.

[4] Peppas, N.A., Bures, P., Leobandung, W. and Ichikawa, H., (2000). "Hydrogels in Pharmaceutical Formulations", European Journal of Pharmaceutics and Biopharmaceutics, 50: 27-46.

[5] Hoffman, A.S., (2002). "Hydrogels for Biomedical Applications", Advanced Drug Delivery Reviews, 54: 3-12.

[6] Taşdelen, B., Kayaman, N., Güven, O. and Baysal, B.M., (2005). "Anticancer Drug Release Poly (N-Isopropylacrylamide/Itaconic Acid) Copolymeric Hydrogels", Radiation Physics and Chemistry, 73: 340-345.

[7] Roseman, T.J. and Carderelli, N.F., (2001). "Monolithic Polymer Devices", Control. Release Technology, Florida, 11: 46-49.

[8] Bayhan, M., (1997). "Effect of Kem-Chymotrypsin Immobilization and Reactor Conditions on Immobilized System Performance on Temperature Sensitive Hydrogel Matrices", Master Thesis, Hacettepe University, Ankara.

[9] Qui, Y. and Park, K., (2001). "Environment-Sensitive Hydrogels for Drug Delivery", Advanced Drug Delivery Reviews, 53: 321-339.

[10] Arı, A., (1998). "Synthesis and Biological Characterization of Temperature and pH Sensitive Poly (vinyl ether) Hydrogels", Master Thesis, Hacettepe University, Ankara.

[11] Bajpai, A.K. and Giri, A., (2002). "Swelling Dynamics of a Macromolecular Hydrophilic Network and Evaluation of Its Potential for Controlled Release of Agrochemicals", Reactive and Functional

Polymers, 53: 125-141.

[12] Kim, S.J., Park, S.J. and Kim, S.I., (2004). "Properties of Smart Hydrogels Composed of Poly (Acrylic Acid) / Poly (Vinyl Sulfonic Acid) Responsive to External Stimuli", Smart Materials and Structures, 13: 317-322.

[13] Ahmed, E.M., (2015). "Hydrogel: Preparation, Characterization, and Applications: A Review", Journal of Advanced Research, 6: 105–121.

[14] Akay, P., (2014). Enzymatic Modification and Characterization of Chitosan Based Hydrogels, Master Thesis, Yalova University, Department of Chemical and Process Engineering, Yalova.

[15] Gümüşderelioğlu, M. and Kesgin, D., (2001). "Smart Polymers", Science and Technology, 52-55.

[16] Thirumaleshwar, S., Kulkarni, P.K. and Gowda, D.V., (2012). "Liposomal Hydrogels: A Novel Drug Delivery System for Wound Dressing", Current Drug Therapy, 7: 212-218.

[17] Basan, S., (2001). Polymer Chemistry, Cumhuriyet University Press, Sivas, 1-57.

[18] Gupta, P., Vermani, K. and Garg, S., (2002). "Hydrogels from Controlled Release to pH-Responsive Drug Delivery", Drug Discovery Today, 7: 569-578.

[19] Tanaka, T., (1985). "Phase Transition in Polymer Gels", Scientific American, 7: 110-112.

[20] Atta, A.M. and Arndt, K.F., (1994). "New Crosslinkers to Synthesize pH and Temperature-Sensitive Ionic Hydrogels", Macromolecules, 14: 671-674.

[21] Zhang, X.Z., Yang, Y.Y., Chung, T.S. and Ma, K.X., (2001). "Preparation and Characterization of Response Macro porous poly (N-Isopropyl Acrylamide) Hydrogels", Langmuir, 17: 6094-6099.

[22] Kim, J.J., Lee, M.Y. and Kim, S.X., (2003). "Preparation and Characterization of Thermosensitive Poly (N-Isopropylacrylamide) / Poly (Ethylenoxide) Semi-interpenetrating Polymer Networks", Journal of Applied Polymer Science, 90: 3032-3036.

[23] Sozmen, N.N., (2008). "Intelligent Polymer Using in Biomedical Applications and Developing the Characterization Method with Quartz Crystal Micro-Balancing Systems", Master Thesis, Başkent University, Science Institute, Ankara.

[24] Hydrożeli, U.L.Z., (2010). "Drug Release From Hydrogel Matrices", Ecological Chemistry and Engineering, 17(2): 117-135.

[25] Fu, Y., and Kao, W.J., (2010). "Drug Release Kinetics and Transport Mechanisms of Nondegradable and Degradable Polymeric Delivery Systems", Expert Opinion on Drug Delivery, 7(4): 429–444.

Chapter 14

ECOLOGICAL PRINTING: SURFACE DESIGN OF LEATHERS TANNED WITH DIFFERENT TANNING MATERIALS

Selime MENTEŞ ÇOLAK[1], Neslihan Fatoş ARĞUN[2],
Meruyert KAYGUSUZ[3]

1 Prof. Dr., Pamukkale University, Denizli Vocational School of Technical Sciences, Traditional Handcrafts Department, Denizli, TURKEY, scolak@pau.edu.tr
2 Lecturer, Pamukkale University, Denizli Vocational School of Technical Sciences, Traditional Handcrafts Department, Denizli, TURKEY, fargun@pau.edu.tr
3 Assoc. Prof., Pamukkale University, Denizli Vocational School of Technical Sciences, Textile, Garment, Footwear and Leather Department, Denizli, TURKEY, meruyertk@pau.edu.tr

1. INTRODUCTION

Dyes are coloring agents that have an affinity to the substrate and give color to the material on which they are applied (Deb et al., 2017). Today, the widespread use of synthetic dyes consisting of harmful chemical compounds started to endanger human health and the environment. Synthetic dyes are of petrochemical origin, and some of them in particular may have toxic and carcinogenic effects due to a number of chemical groups in their structure. For example, it is claimed that some azo dyes can produce carcinogenic aromatic amines under certain conditions, and it is expressed that, in case of skin contact for a long time, it can cause serious health problems through the skin absorption. For this reason, the use of 22 types of aryl amines is prohibited by the European Union (Erdem et al., 2018).

Although synthetic dyes are highly preferred in the early years due to their advantages such as production speed, production continuity and wide color range, etc., recently a gradually growing awareness has begun to arise among the people toward the essentiality of less use of chemicals, with the emerge of their harms such as environmental pollution, increase in cancer cases and allergic skin conditions. Along with this awareness rising against chemical dyes, the growing interest attracts attention in the use of natural dyes, which are renewable, cause minimum environmental pollution and generally have no harmful effects on human health (Özkan Tağı, 2018). The increased use of natural dyes contributes to the reduction of environmental pollution, health problems associated with synthetic dyes and harmful waste water problems.

Recently, it is seen that people are tend towards ecological life in order to live healthier and reduce environmental problems. Natural dyes obtained from plants, animals and soil are compatible with nature (Enes, 1987). The use of natural dyes has long been known, and they are obtained from natural sources such as plants, insects, animals and minerals (Nattadon and Rattanaphol, 2012). These dyestuffs, which are abundant in nature, are easy and cheap to provide. Natural dyes are increasingly used today because they are non-toxic or less toxic, not allergic and environmentally friendly. Surface paints and prints can be done with natural dyes (Bilir, 2018). With the global warming of the world, to prevent environmental pollution, for a more livable environment, concepts such as sustainable fashion, ecological printing (eco-print), natural dyes, green environment, environmentally friendly designs have been revealed (Öztürk and Yılmaz Ege, 2019).

2. ECOLOGICAL PRINTING

The patterning process of the textile surface, that spreading rapidly around the world in recent years, by using natural materials such as flow-

ers, leaves, rusty metals is called ecological printing (eco-printing) (Özkan Tağı, 2018). Ecological printing means patterning the fabric surface with completely natural materials and various mordants. In ecological printing, it is possible to use the fabric's own color, as well as to give the image depth in plants by coloring the ground (Akpınarlı and Tambaş, 2019). Ecological printing is a printing method that is used to transfer natural colors and shapes to the surface of materials such as fabric, special paper, leather, etc., with materials from nature having colorant features. It is the transfer or release of the shapes of plants parts such as leaves, stems, barks, etc. to the fabric by boiling in water. Eggs called "Pisanka" in Poland are obtained via staining through covering with various plants. For the dyeing process, onion bark (brown), oak, alder or walnut bark (black), rye sprouts (green), hibiscus flower petals (violet), marigold and young apple tree bark (golden yellow) are used. Introduction of the natural dyeing and ecological printing technique with the application of India Flint on fabric in 1986 took an important place in the world textile industry. Protein, iron, copper, aluminum solutions are used as solutions in ecological printing, and alum ($KAl(SO_4)_2$), aluminum sulfate ($Al_2(SO_4)_3$), iron sulfate ($FeSO_4$), cream tartar ($KC_4H_5O_6$), sea water, tea, ash, yogurt, whey are used as mordants in fabrics (Akpınarlı and Tambaş, 2019a). Terms such as eco-printing are used to describe the direct use of plants in natural dyeing without extraction. In eco-printing or contact printing, the pattern/design is transferred to the fabric surface. Chemical bonding of dye molecules to the textile fibers occurs in both methods (Ismal, 2016).

Ecological Printing Techniques

Ecological printing applications can be done with different techniques. Main ecological printing techniques are classified as:

- Hitting (hapa zome),

- Hot rolled eco-printing,

- Cold roll eco-printing (cold bundled eco prints),

- Rust dyeing,

- Solar dyeing (Flint, 2008).

Plants Used in Ecological Printing

In ecological printing technique; leaves of eucalyptus, maple, sycamore tree, acorn, rose, geranium, basil, mint, fern and calendula flower, lupine, onion peel, leaves, branches, roots and flowers of olive, pomegranate, lemon, pine tree, fig, maple, bonito, walnut, vine, laurel, black pepper, ornamental plum (Japanese plum), sumac, and valonia plants, leaves and flowers of alder, apple tree, wild apple and blueberry, blackberry, marigold,

head and root parts of carrot, flowers and leaves of dahlia, dandelion, iris flower, lilac, and plants as oak, pansy, purple cabbage, safflower are used (Bozacı, 2016; Aydoğan Bayram, 2017; Oyman and Can, 2017).

In this printing technique, the plants must be chosen attentively. Some plants are not suitable for eco-print due to the release of toxic gases. It is dangerous to use plants that are unknown or not identified. Indeed, there are many plant species, which are lethal poisonous. Some of the plants found in gardens and by the roads contain certain levels of poison. Fulya flowers and leaves, Narcissus, Lilium flower, Blue halberd, Poinsettia, *Aconitum napellus*, Oleander, Crocus flower, Mountain tulip, Castor oil plant are some of the poisonous plants (Bozacı, 2016).

During eco print applications, leafy plants are mordanted, but flowers and plant roots do not need to be mordanted. The roots are used as peeled. Plants, roots, stems, leaves and flowers can be used as dried or fresh in dyeing. In ecological printing method, sometimes, plants collected from the same tree do not exhibit the same result even if the same conditions are provided. This makes the printing with plants exclusive and unique. There are many parameters in printing with the plants such as providing suitable conditions, wetness or dryness of plants, picking time etc. (Oyman and Can, 2017).

The climatic condition of the region where the plants are collected affects the amount of water in the plant and differs in its shape and color (Bozacı, 2016; Oyman and Can, 2017; Akpınarlı and Tambaş, 2019a). Plants in printing are for a single use. Even if two same treatments are made with the same kind of plants, the same ecological printing is not achieved. Since no synthetic and chemical substances that could be harmful are used in its application, textile products prepared with completely natural materials are obtained (Bayram, 2017).

Significant Parameters in Ecological Printing Applications

The fact that the material, such as the fabric etc. to be used, is mordanted before starting the "water boiling" technique (in hot rolled eco-printing) increases the color and shape permanence (Oyman and Can, 2017). The substances which are added to the textile material to be dyed before the plants are applied to the fabric in order to keep the dye better are called mordants (Menet Kırmızı, 2008). Mordants are metallic salts, natural compounds containing metal ions, or other complexing agents used for to improve the dye uptake and fixation, color tone and fastness properties. Mordants are substances that fix the dyestuff to the substrate (IUPAC, 2019). Color strength and chromaticity coordinates vary significantly depending on three different mordanting methods and mordant type (İşmal and Yıldırım, 2019). Each mordant produces different dye complexes lead-

ing to completely different colors and fastness properties. Mordant can be applied in three ways: before, during and after dyeing (Anonymous, 1991).

However, in ecological printing techniques, mordanting method is generally applied first. Mordanting is performed to keep the dyes on the fabric longer or to change the colors. Bonding between the fabric and the dye is taken place with the mordant process so that the dye can be hold onto the fabric (Karadağ, 2007). Mordanting increases the affinity between the dye and the textile surface, thus wise, more vivid colors, better fastness and wider color spectra can be obtained (Kadolph and Casselman, 2004; Shahid et al., 2013). Water-soluble metal salts are used as mordant substances, as well as the substances with weak acid or base properties. The most important mordant substances are: alum $[KAl(SO_4)_3.12H_2O]$, iron sulfate $(FeSO_4.7H_2O)$, copper sulfate $(CuSO_4.5H_2O)$, $SnCl_2.2H_2O$ and wine stone. The majority of natural dyes are in mordant dyeing class (Karadağ, 2007).

The fabrics used in the ecological printing process should be completely natural as linen, cotton, silk and wool. There are many parameters in application like the frequency of wrapping the fabric, the yarn and pipe used for wrapping, boiling time and the pH of the water (Oyman and Can, 2017). It is stated that when the boiling time is under 1.5 hours, the shape of the plant is formed, but it is observed that it does not fully encolour (Bozacı, 2016; Oyman and Can, 2017; Akpınarlı and Tambaş, 2019a).

3. ECOLOGICAL PRINTING ON LEATHERS TANNED WITH DIFFERENT TANNING MATERIALS

Painting and decorating of the leather surface is a procedure that has been applied since ancient times. Production steps in the leather industry consist of processes consuming a lot of water, having high energy inputs, and possessing high levels of waste disposal potential. The dyeing and surface patterning techniques and technologies counted in in these processes are progressing day by day towards the more eco-friendly applications with the innovative perspectives.

Due to the reasons such as appealing to the eyes, being an organic material, and being compatible with modern items, leather is used in making many articles and accessories. Since their existence, people have developed various techniques, by using different materials, and created leather crafts and decorative arts. Today, ornamented leather goods are becoming more important and continue to be used in all areas of our lives. In the surface decorations of leather products; techniques such as dyeing, printing, carving, applique, cutting, burning, wet forming, sewing and processing are used (Odabaşı and Özdemir, 2018).

The first thing that attracts attention or affects the consumers in the

preference of leather products is color and surface design. That's why the color and surface design are important in leather production. In the process called finishing in practice, different patterns can be created on the leather surface with the help of patterned printing rollers. The dyeing and finishing processes in traditional leather production are made to increase the attractiveness of leather products, so that the amount of water and energy used and environmental pollution are increased. In order to protect the environment and human health, recently, studies conducted on sustainable fashion and ecological printing (eco-pint) have gained importance. Although ecological printing on textiles is widely used abroad, there are very few studies about ecological printing on leather. Few designers use this method in our country. In this study, the applicability of ecological printing technique on different tanned leather was investigated.

Important Issues in Ecological Printing of Leathers

There are situations to be considered during ecological printing applications;

1. Temperature

Leather is a material with protein structure. Protein-based materials such as leather, wool and silk have low resistance to temperature. For this reason, the temperature should not be high as for cellulose based materials such as cotton, linen and jute in eco-print applications. Tanning is done to make the leather resistant to temperature (shrinkage resistance) and microorganisms, and to improve some physical and chemical properties of the leather. Strengthening the leather structure and turning it into non degradable form by providing chemical bonding with reactive groups of collagen fibers and tanning agents of various types and properties is called tanning. Different tanning methods are used, so depending on the tanning agent and tanning method, the properties and color of the leather can vary. For example, the color of the chrome tanned leather becomes green blue without any additional dyeing, while the color of aldehyde tanned leather is beige, and the color of vegetable tanned leather varies from beige to brown tones according to the used vegetable tanning agent. These colors are converted to the desired color with subsequent dyeing processes.

The shrinkage temperature is an indication of the tanning. The tanning process increases the hydro-thermal stability of the leather which is measured by the shrinkage temperature. When the raw leather is left in boiling water at 100°C, a volumetric and areal decrease occurs in the leather. On the other hand, as the tanning process and collagen fibers are isolated from each other according to the type of the tanning agent, the shrinkage temperature of the leather increases and shows resistance to hot water. The shrinkage temperatures of the leather go up to 70-100°C degrees. The be-

havior and strength of different tanned leathers against temperature also differ. For this reason, it is of great importance to work at the temperatures appropriate for the tanning type of the leather used during eco-print applications. In cases where these temperatures are exceeded, changes and contractions occur in the leather structure. This changes the handle properties of the leather, causing hardening and decreases in its mechanical properties. In ecological printing on the leather, in order to avoid loss of area and structural change in the leather, application should be performed within the maximum working temperature ranges. (Table 1).

Tablo 1. *Shrinkage and maximum working temperatures of the leathers tanned with different tanning agents*

Leather Type	Shrinking temperature, ⁰C	Maximum working temperature, ⁰C
Raw leather (untanned leather)	62-64	37-38
Chrome tanned leather	100	60-70
Vegetable tanned leather	70-85	45
Aluminum tanned leather	70-75	45
Aldehyde tanned leather	80-90	55
Chamois (Oil-tanned leather)	65-70	40

2. Washing

Before the eco-print application, it is necessary to wash the leathers and remove the unbound tanning substances and chemicals on and between its collagen fibers. Another point to be considered in eco-print on the leather is that no matter what kind of tanned leather is chosen, it is necessary to tighten the leather before removing the plants on the leather material and remove the water between the collagen fibers as much as possible. In addition, the water remaining on the used plants after mordanting should be thoroughly removed with a paper towel. The excess of water remaining on the leather and plants causes dissolution of the plant colors and cloudy appearance of the plant patterns and colors. In this study, ecological printing on different types of tanned leathers is performed and the obtained patterns and shapes on the leather are examined.

4. MATERIALS AND METHOD

In the study, chromium-tanned crust sheepskin, vegetable tanned vaketa (calfskin), undyed sheepskin tanned with aldehyde and chrome tanned and dyed sheepskin were selected as materials. The leathers were first wetted to introduce water between the collagen fibers and to remove the residues of the unbound tanning agents and chemicals on the leather and between the leather fibers. Later, the leathers were mordanted for 1.5 h in the

solution containing aluminum sulfate and white vinegar. In addition, cotton fabric was used to cover the leathers (blankets). The cotton fabric was washed before use and the finishing layer on it was removed. The cotton fabric was mordanted with iron sulfate solution. After these processes, the leathers and cotton fabric were tightened and water was removed as much as possible, but the leather and cotton fabric were kept moist. Different plant flowers and leaves such as thuja leaves, rose leaves, lavender flowers, sycamore leaves, walnut leaves, chrysanthemum flowers, hibiscus, American ivy leaves, gerbera flowers, ornamental plum leaves, cloud tree leaves were used in the study (Fig. 1).

To prepare the plants for eco printing, they are kept in iron sulfate solution for 15-20 seconds, and then placed on a paper towel to get rid of the excess of water. For ecological printing, the plants dipped in iron sulfate solution and removed from excess of water are placed in certain compositions on the leather with the petal facing towards the leather surface, rolled up with a cotton cloth (blanket), wrapped in rods, and fixed with a rope.

Figure 1. *Some plants used in eco-print study of different tanned leathers*

The prepared rolls were placed in the water in the pot and the process was carried out for 2 hours in a controlled manner so that the temperature does not exceed 50-55ᵒC. At the end of the process, the rolls were removed from the pot, kept to cool, the rolls were opened, vegetable waste was removed and the shade was left to dry completely in an airy place. After drying, the leather is ironed and ecological printing is completed.

The ecological printing obtained from the experimental study, the points to be considered and their visual evaluation are given below (Fig. 2).
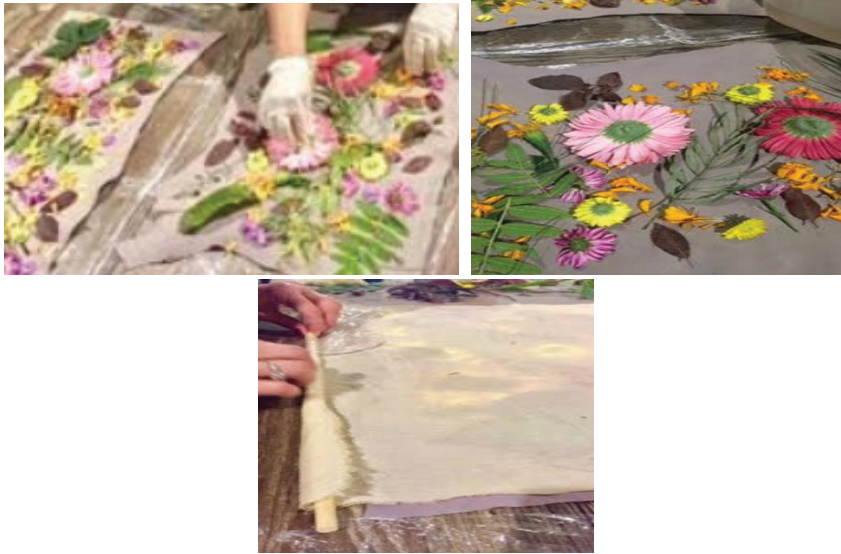
Figure 2. *Placing the plants on chrome leather and placing and wrapping (wrapping) the cotton fabric (blanket) on it*

In eco print applications, packaging, wrapping should be done very smoothly, slowly and carefully without any folding (Fig. 3 and Fig. 4). The parts folded during the packaging cause the pattern to deteriorate and streak images in these regions.

Figure 3. *Aqueous iron sulfate solution, tightly binding the wrapped leather with the rope and dyeing-patterning process in hot water*

Figure 4. *Vegetable tanned leather: soaking, placement of plants and hot roll process*

5. RESULTS AND DISCUSSION

1. Chrome Tanned Leather Samples

Chrome tanning is the most common tanning type in the world. Hydrothermal stability (shrinkage temperature in aqueous medium) of it is the highest tanning type among other tanning types. It gives softer leathers than vegetable tanned leathers. Due to the unique color of the tanning agent, the chrome tanned leather has a blue-green appearance. Although large and small cattles are used in tanning process of all leathers, they are mainly used in the production of garment leathers because they give soft leather. Chrome tanned leather is thinner than vegetable tanned leather.

Eco print can be applied to both sides of the leather, either grain or flesh. However, since the collagen fibers of the grain and flesh sides are different from each other and the collagen fibers on the grain are thinner and the collagen fibers are thicker towards the flesh, there are small differences in the appearance of the two sides after ecological printing (Fig. 5).

Figure 5. *1) Unpacked package with dyeing process finished (plants on it have not been removed yet) 2, 3, 4) Chromed leather samples with all processes finished, 5) Pattern on cotton fabric blanket*

In the study, plants were placed on both grain and flesh sides of chrome tanned leather and it was examined how to dye and pattern. It was observed

that the application of eco print applied to the flesh side in chrome skin gives similar results to the grain, but the pattern obtained on the grain side is clearer than the flesh side (Fig. 6).

Figure 6. *Eco print performed on the flesh side of chrome tanned leather*

In the study, it was observed that plant patterns appeared more clearly than other tanning methods in the application made on chrome tanned leathers. It is believed that this may originate due to the binding of the chromium tanning agent to the carboxyl groups of the leather collagen and the fact that the amino groups of leather are free to react with the dyestuffs consisting in these plants to form a compound.

2. Vegetable Tanned Leather Samples

Vegetable tanned leathers; mimosa, valeks, kebrako, tara, etc. They are tanned leather with tannins obtained from tanning plants. The leathers show colors ranging from light brown to dark brown according to the color of the vegetable tannin used in the tanning process. It is the most used tanning method after chrome tanning method. It has a lower thermal stability than chrome tanned leather. It is very suitable for printing and shaping, they take shape more easily than chrome tanned leather. They are hydrophilic, air and water vapor permeable. At the end of its lifetime, it is biodegradable in the medium term. It is mostly used for tanning cattle or bovine leathers. Generally, it is used in the production of shoe upper, leathercraft and sole leather etc. It gives leather that is firm, hard and inelastic. The leather obtained is thicker than the chrome tanned leather types.

In this study, eco-print applications on vegetable tanned leather are shown in Figure 7.

Figure 7. *Patterns formed on vegetable tanned leather by ecological printing*

3. Aldehyde Tanned Leather Samples

Aldehyde tanning is another tanning agent used for tanning leathers.

Aldehyde tanning gives the leather fullness, softness, thin leather, resistance to rubbing, sweat and washing fastness.
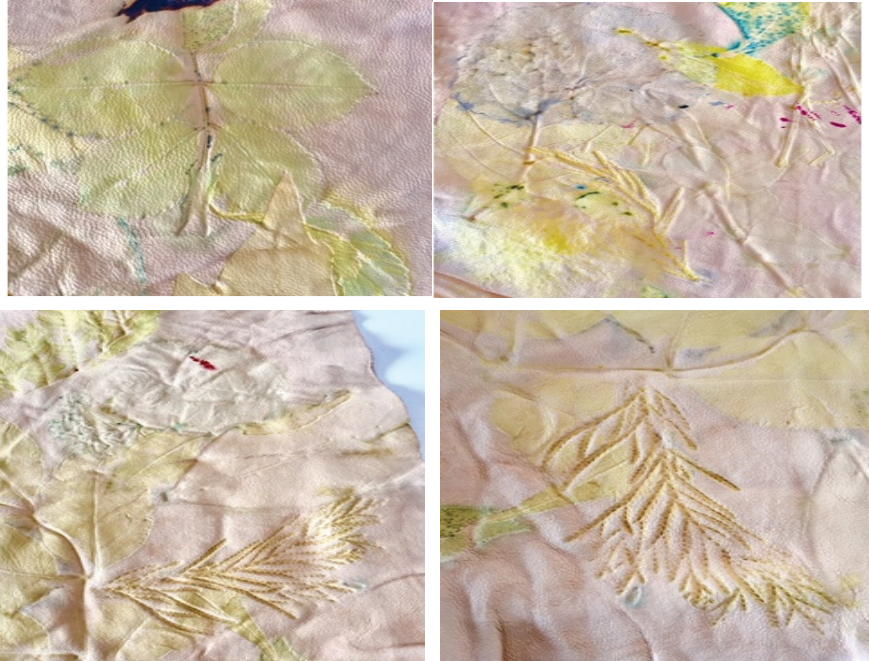
Figure 8. *Patterns formed on aldehyde tanned leather by ecological printing*

It has been determined that the patterns in vegetable tanned and aldehyde tanned leather are not well-defined as in chrome tanned leather.

The selected plants were also found to be important. It has been observed that some plants appear very well with some colors and patterns, while others appear slightly cloudy. In addition, a very interesting result was encountered in hibiscus application. While the hibiscus plant does not create a negative result in other leathers, it has been seen that there are holes in the skin of the aldehyde tanned leather where the hibiscus is. It is believed that a different reaction takes place between the hibiscus and the aldehyde tanned leather, and a compound that is effective enough to form a hole in the leather appears.

Figure 9. *The parts where hibiscus flowers affect the aldehyde tanned leather*

4. Eco print on the finished leather

Ecological printing application was made on the dyed leather. It was observed that the patterns and shapes did not come out in the eco-print tests on the dyed leather (Fig. 10). This is thought to be due to the fact that the bonds to which the plant dye should be bonded are occupied by the dyestuffs used during the dyeing process of leather.

Figure 10. *Eco-print application on the dyed leather*

After and eco print processes, the leathers are stretched and dried. Ironing process is made. (ironing temperature should be paid attention). A colorless polish can be applied on the leather to protect the pattern and color formed on the leather.

With this study, patterns were obtained with different plants and flowers on the leather with an environmentally friendly application. For this purpose, different tanned leather samples were successfully brought into contact with wet leaves and flowers; different pattern effects and color tones were obtained.

As a result of the study, it is concluded that the following issues should be taken into consideration.

1. Tanning type; Depending on the type of tanning, the properties of the reactive groups of the leather, the attitude of the leather, its behavior against the temperature and its color vary. Accordingly, it differs in the design created by ecological printing on the leather.

2. Temperature; Depending on the type of the tanning agent, the maximum operating temperatures should be taken into account. Otherwise, leather losses, shrinkage and structural deterioration are seen.

3. Thickness: Depending on the type of tanning agent and the type of raw material used, the thickness of the leathers varies. However, after tanning, the thickness of the leather can be adjusted to the desired size. In ecological printing studies, it is recommended to work with leathers which of their thickness is around 1 mm, regardless of which type of tanned leather is chosen due to the difficulties encountered during the removal of the water of the thick skins and their rollings and wrapping-bonding. In eco print applications, leather thickness is important. For this reason, it is recommended to work with thin leathers.

4. The moisture consisting in leather, plants and flowers; In applications where the water is not removed sufficiently, there are dispersions in pattern and dyeing during ecological printing.

5. Plant selection; The rate of dye contained in plants and flowers in nature is different. Some flowers give good color, while others flow. The right plant must be chosen. It is important that the plant does not react differently with the leather, while hibiscus flowers in the study did not show any negative situation in other types of tanning and cotton fabric (blanket), but caused holes on the leather tanned with aldehyde.

6. Placement of plants; Plant leaves can be placed flat or inverted on the leather. The pattern effects and color tones differences can be seen depending on the plant leaves being placed upside down or straight.

7. Time; Sufficient time must be applied for the ecological printing to take place, in this study it has been observed that 2 hours is sufficient. Since the ecological printing process can be reached with high temperatures as 100°C with cellulosic-based materials, the process should be carried out by keeping it for a long time as it increases the temperature of the leather while working with it, even though ecological printing takes place in 1-1.5 h.

8. The condition of the leather; In ecological printing applications, (drum dyed) or finishing affects ecological printing negatively. Regardless

of which tanning agent is tanned for the ecological printing application, it is important that the leathers are not dyed and finished.

9. The side of the leather; Ecological printing application can be applied to the grain and flesh sides of the leather. But it gives better results on the grain side.

The production of synthetic dyes depends on the petrochemical source, and the application of these dyes causes serious health hazards and negatively affects the ecological balance of nature. Natural dyes are considered environmentally friendly as they are obtained from renewable sources compared to synthetic dyes from non-renewable oil sources. Plant leaves, roots, and flowers are potential natural sources of dye due to their easy availability. These are biodegradable and the residual vegetable material remaining after removal of the dyes can be easily composted and used as fertilizer.

In the last two decades, consumer awareness about environmentally friendly textile materials has increased, as well as environmental protection laws have started to increase the demand for natural dyes and natural prints. In addition, as the combination and interaction of art and technique; unpredictable results, patterns, colors and visual effects are possible with ecological printing, and this provides unlimited creative power to designers/artists.

With the widespread use of this environmentally friendly application, it is thought that environmental pollution caused by dye and chemicals used in other printing techniques will decrease its harm on human health.

References

Akpınarlı, F.H., Tambaş, C. (2019), Ekolojik Baskı 3 Boyut Etkisi, https://ekolojik kasaba.com/ekolojik-baski, ulaşım tarihi 24.05.2020

Akpınarlı, F. H., Tambaş, C. (2019a). Pamuklu-İpekli Kumaşlara Ekolojik Baskı Uygulaması ve Haslık Düzeylerinin Belirlenmesi, İdil, 62(8), 1295-1311.

Anonymous, (1991). Bitkilerden Elde Edilen Boyalarla Yün Liflerinin Boyanması. T.C Sanayi ve Ticaret Bakanlığı, Küçük Sanatlar ve Sanayi Bölgeleri ve Siteleri Genel Müdürlüğü, Ankara.

Aydoğan Bayram, M. (2017). Eco Printing Tekniği İle Çevre Dostu Ekolojik Tekstil Baskısı. II. Uluslararası Akdeniz Sanat Sempozyumu, Akdeniz Üniversitesi Yayınları, Antalya, s.163-170.

Bilir, M. Z. (2018). Ekolojik Boyama Esaslı Çok Renkli Yüzey Tasarımı, Yedi: Sanat, Tasarım ve Bilim Dergisi, 20, 63-73.

Bozacı, B. (2016). Doğanın Şarkısı Ekolojik Baskı, İzmir.

Deb, A. K., Shaikh, A. A., Sultan, M. Z., Rafi, I. H. (2017). Applıcatıon of Lac dye In Shoe Upper Leather Dyeing, Leather and Footwear Journal, 17(2), 97-106.

Dikmelik, Y. (2013). Deri Teknolojisi, Sepici Kültür Hizmeti Yayınları, Hürriyet Matbaası, İzmir.

Enez, N. (1987). Doğal Boyamacılık Anadolu'da Yün Boyamacılığında Kullanılmış Olan Bitkiler ve Doğal Boyalarla Yün Boyamacılığı, Fatih Yayınevi Matbaası, İstanbul.

Erdem, R., Aydoğan Bayram, M., Bilge, G., Atak, O. (2018). İpek Kumaşların Bitki Yaprakları ile Bölgesel Desenlendirilmesi, Süleyman Demirel Üniversitesi Fen Filimleri Ensititüsü, 22(2), 1058 - 1065.

Flint, I. (2008). Eco Colour Botanical Dyes For Beautiful Textiles. U.S: Interweave, 154-165.

Ismal, Ö. E. (2016). Patterns from Nature: Contact Printing, Journal of the Textile Association, 77(2), 81-91.

Işmal, Ö.E., Yıldırım, L. (2019). Metal mordants and biomordants, The Impact and Prospects of Green Chemistry for Textile Technology.

IUPAC, (2019). Compendium of Chemical Terminology, 2nd ed. (the "Gold Book"). Compiled by A. D. McNaught and A. Wilkinson. Blackwell Scientific Publications, Oxford (1997). Online version (2019) created by S. J. Chalk.

Kadolph, S. J., Casselman, K. D. (2004). In The Bag: Contact Natural Dyes. Cloth. Text. Res. J., 22, 15-47.

Karadağ, R. (2007). Doğal Boyamacılık. Geleneksel El Sanatları ve Mağazalar İşletme Müdürlüğü Yayınları, Ankara.

Menet Kırmızı, G. (2009). Japon Tekstil Boyama ve Desenlendirme Teknikleri Üzerine Bir Araştırma. Yüksek Lisans Tezi, Dokuz Eylül

Üniversitesi Güzel Sanatlar Enstitüsü, İzmir. s.23.

Nattadon, R., Rattanaphol, M. (2012). Eco-friendly of Textiles Dyeing and Printing with Natural Dyes, RMUTP, International Conference: Textile & Fashion, Bangkok, Thailand.

Odabaşı, E., Özdemir, M. (2018). Deri Yüzey Süslemede Kullanılan Dival İşi Tekniği ile Yapılmış Bazı Deri Ürünler, Vocational Education (NWSAVE), 13(3), 32-51.

Özkan Tağı, S. (2018). Tekstil Tasarımında Alışılmadık Bir Ekolojik Baskı Yöntemi "Pas Baskı", İdil, 7(43), 327-333.

Öztürk, F., Yılmaz Ege, J. (2019). Sürdürülebilir Moda'nın, Ekolojik Baskı Tekniği İle Değerlendirilmesi ve Bir Örnek Uygulama, Avrasya Sosyal ve Ekonomi Araştırmaları Dergisi (ASEAD), 6(5), 394-406.

Oyman, N. R., Can, D. İ. (2017). Okaliptüs Bitkisiyle İpek ve Pamuklu Kumaş Üzerine Eko-Baskı Uygulamaları. II. Uluslararası Akdeniz Sanat Sempozyumu, Akdeniz Üniversitesi Yayınları, Antalya, s.191.

Shahid, M., Shahid-ul-Islam, Mohammad, F. (2013). Recent Advancements In Natural Dye Applications: A Review. Journal of Cleaner Production, 53, 310-311.

Chapter 15

USING PERMANENT MAGNETS FOR BIOELECTROMAGNETIC APPLICATIONS

Serhat KÜÇÜKDERMENCİ[1]

1 Dr. Öğr. Üyesi , Balıkesir University Faculty of Engineering Department of Electrical and Electronics Engineering, kucukdermenci@balikesir.edu.tr

1. INTRODUCTION

Magnetic fields produced by both electromagnets (Do et al., 2015; Kastner et al., 2015) and permanent magnets (Roth et al., 2016; Garraud et al., 2015) are widely used in bioelectromagnetic applications. Permanent magnets containing rare earth alloys produce higher magnetic field strength and gradient than approximate size electromagnets (Erni et al., 2013). Magnets made of Neodymium-Iron-Boron (NdFeB) and Samarium-Cobalt (SmCo) alloys are commonly used permanent magnets. NdFeB and SmCo magnets show stronger magnetic properties compared to traditional magnets and price performance ratios are satisfactory (Mahadi et al., 2003). Electromagnets produce Foucault parasitic currents. They need voltage sources sometimes they also need cooling systems. Permanent magnets differ from electromagnets because they do not have these disadvantages. Equation (1) is Gauss's law for magnetism and defines the magnetic flux density for permanent magnets. In linear materials, the relationship between magnetic flux density B and magnetic field intensity H is given by Equation (2). H from equations (1) and (2) can be expressed as the gradient of the magnetic scalar potential (see Equation (3)). In Equation (4), the relationship between B and H is given. This equation can be used in some nonlinear materials such as permanent magnets. Here B_r is remnant magnetic flux density which represents magnetic flux density without magnetic field source (Kraus et al., 1973; Comsol, 2013)

$$\nabla \cdot \mathbf{B} = 0 \tag{1}$$

$$\mathbf{B} = \mu_0 \mu_r \mathbf{H} \tag{2}$$

$$\mathbf{H} = -\nabla V_m \tag{3}$$

$$\mathbf{B} = \mu_0 \mu_r \mathbf{H} + \mathbf{B}_r \tag{4}$$

Magnetic nanoparticles (MNP) release heat energy into the environment when exposed to alternative magnetic fields (AMF). This AMF is generally in the range of kilohertz to megahertz. This thermal energy can be used in various applications such as shape memory materials (Mohr et al., 2006), drug release (Liu et al., 2014), magnetic hyperthermia (MHT) (Hergt et al., 2006). MHT is a medical procedure in which cancerous cells are heated to a temperature between 42 and 46 ° C (Deatsch et al., 2014). In MNP studies, the heating properties of MNPs are expressed in SAR (see Equation (5)).

$$SAR = \frac{P}{m} \tag{5}$$

where P is the power expended and m is the mass of MNPs. SAR is defined as the power expended per unit mass of MNPs. SAR is experimentally expressed as Equation (6);

$$SAR = \frac{C}{m_p} \frac{dT}{dt}$$ (6)

where C is the heat capacity of the sample, m_p is MNP mass and dT / dt is the derivative of the temperature difference over time.

While there is no magnetic field in the environment, the total magnetization is zero due to the random orientation of the MNPs. When applying the magnetic field, the magnetic moments of the MNPs tend to align in the direction of the outer magnetic field. When all moments are aligned, saturation is achieved. It is important that the temperature rise in the treated area does not exceed 46 ° C, so as not to damage healthy tissues during MFH. Therefore, various approaches are being studied to control the temperature rise. Some studies show that the application of static magnetic field (SMF) can reduce or suppress the heating properties of MNP (Cantillon et Murphy et al., 2010). In a study, (Bauer et al., 2016) MNPs were exposed to the static magnetic field of the neodymium magnet, a decrease in the specific absorption rate (SAR) was observed.

Hensley et al. (Hensley et al., 2017) created a region with zero magnetic field in the center using a pair of neodymium magnets with opposite magnetization directions. This region is called field free region (FFR). The particles in the FFR show a high SAR value as they remain under the influence of AMF. Since MNPs out of the FFR are in saturation state, that is, the effect of AMF is blocked, no temperature increase is observed.

The same principle can be applied using a pair of coils (Tasci et al., 2009). Tasci et al. observed that only MNPs in the FFR warmed up. Similarly, Murase et al. (Murase et al., 2013) exposed MNPs to different SMF values using the coil pair. They observed that the value of the applied SMF was inversely proportional to the SAR value of the MNP.

2. USING PERMANENT MAGNETS FOR SAR REDUCING

Sebastian et al. set up an experiment setup to control the heating properties of MNP with SMF. In the experiment setup, the SMF is produced by a pair of neodymium magnets (see Figure 1).
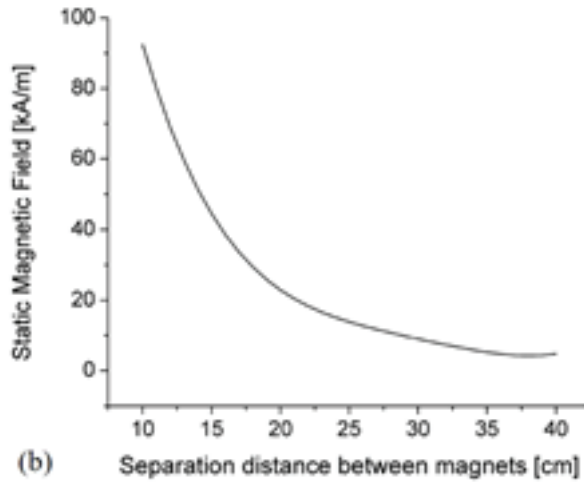
Figure 1. Distance between magnets and SMF curve (Sebastian et al, 2019)

In order to apply variable SMF, the distance between the magnets has been changed. The temperature rise, specific absorption rate (SAR) and SMF correlation of MNPs exposed to an alternative magnetic field (AMF) were analyzed. In the experimental setup, SMF was produced using a pair of N35 neodymium magnets. SMF magnetization directions are aligned to be the same and perpendicular to the AMF generated by the excitation coil. The dimensions of the magnets used are 4 x 4 x 10 cm^3 and the residual magnetic flux density is B$_r$ = 1170 mT. By setting the distance between the magnets from 40 cm to 12 cm, SMF of 4-90 kA/m was obtained. The magnetic field produced by magnets was analyzed by COMSOL simulation. Figure 2 shows the magnetic field distribution when the distance between the magnets is 25 cm.
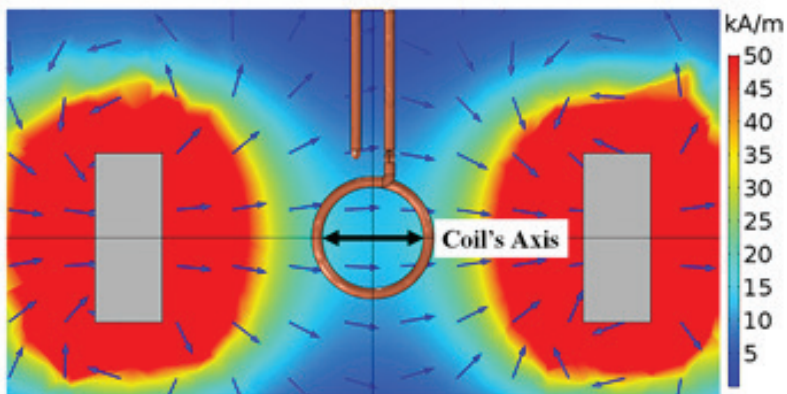
Figure 2. Magnetic flux density simulation when the distance between the magnets is 25 cm. (Sebastian et al, 2019)

It was observed that the increase in SAR and temperature was maximum for the situation without SMF (see Figure 3.a). SAR and temperature decrease inversely as the SMF value increases. As MNPs approach the saturation value, the warming contribution disappears. When $H_{AMF} = 9.6$ sin (ωt) kA/m, the effect of SMF on temperature was investigated. For example, when $H_{SMF} = 32$ kA/m, the temperature increase is 9 K and $H_{SMF} = 4$ kA/m temperature increase is 55 K (see Figure 3.b).
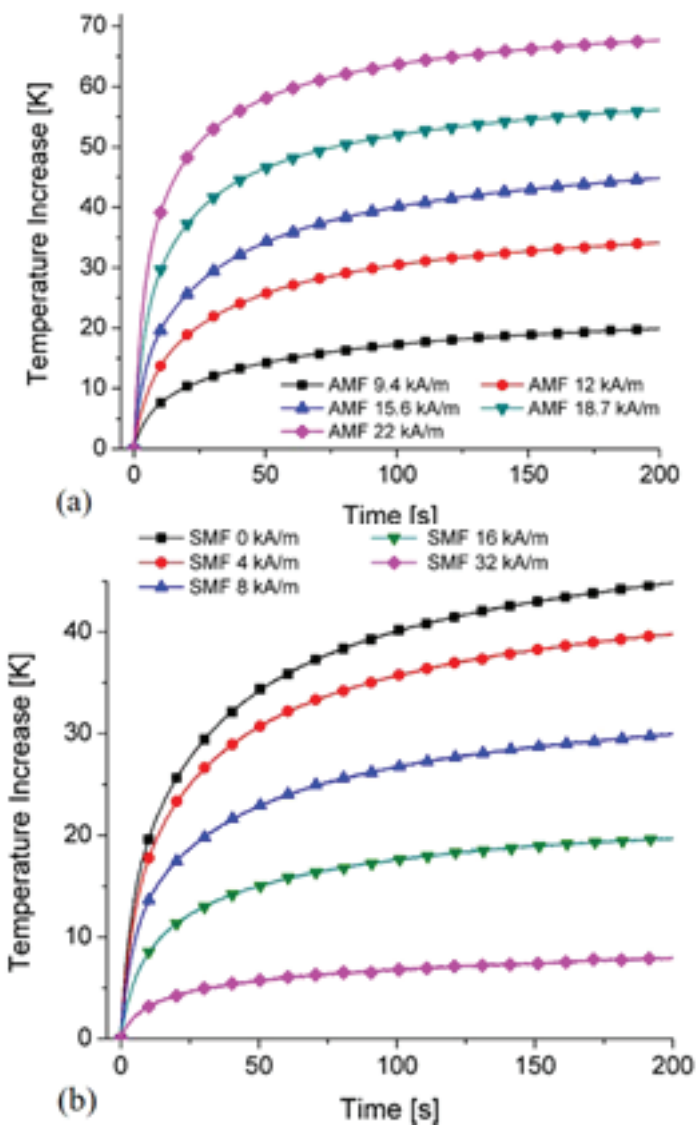
Figure 3. The effect of applied AMF on MNP's temperature rise
(a) $H_{SMF} = 0$ kA/m (b) $H_{SMF} = 15.6$ kA/m. (Sebastian et al, 2019)

3. USING PERMANENT MAGNETS FOR SAR FOCUSING

The typical problem in MFH applications is the difficulty of selectively localizing the heat without damaging healthy tissues. Static magnetic field application has been proposed to reduce overheating of healthy tissues (Hensley et al., 2017). Also, Murase et al. investigated the use of a static magnetic field to target MNPs in specific areas deep within the body (Murase et al., 2013). There are theoretical studies showing that static magnetic field can affect MPH behaviors (Murase et al., 2016; Dhavalikar et al., 2016). A magnetic field close to 40 mT was found to be sufficient to eliminate the heating effect of MNPs.

Myrovali et al. created a test setup by adding a static magnetic field source to the typical MPH system (see Figure 4). The positions of permanent magnets are shown in broken lines in Figure 4. NdFeB magnets can be placed in the experimental setup as 2 or 4. The SMF direction is indicated by straight line arrows in Figure 4a. In the graphic, 2-way rectangular permanent magnets represent green and 4-way cubic magnets represent red. The area where there is no SMF in the center is called field free region (FFR). It is possible to change the FFR by changing the number, size and direction of the permanent magnets. With the simultaneous application of AMF and SMF, the thermal distribution in the study area can be addressed in two regions: (1) FFR area without static magnetic field and (2) saturation region (SR area) where MNPs are blocked. In the FFR region, MNPs are directly exposed to AMF, producing SAR and heating that area (Figure 4b). Because the static magnetic field in the FFR region is close to zero and there is no obstacle to the oscillation of MNPs with the effect of AMF. In the SR area, where MNPs are far from the FFR region and closer to permanent magnets, MNPs are blocked by the effect of SMF and vibration does not occur (Figure 4c). SMF is strong enough to keep MNPs immobile under AMF effect. This results in near zero SAR production by MNPs.
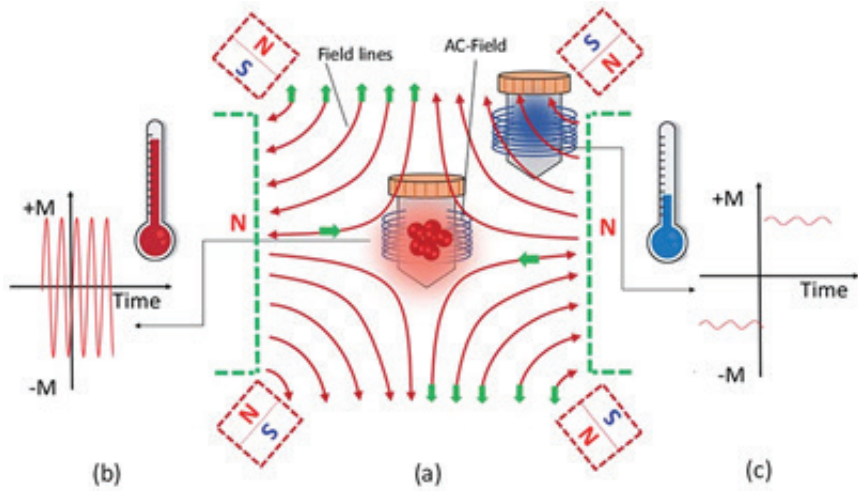
Figure 4 Schematic representation of the experimental setup for AMF and SMF.

(a) SMF is shown in red lines. Permanent magnets can be placed in two different positions, cubic-red or rectangular-green, (b) MNPs producing SAR in the field free region (FFR), (c) Blocking the movement of MNPs with the effect of SMF.

A finite element method was used to evaluate and visualize the FFR parameters of two different experimental setups. 3D geometric models were created in the simulation program with two rectangular permanent magnets 4.5 x 3 x1 cm3 and four cubic magnets 2 x 2 x2 cm3 placed opposite each other (see Figure 5).
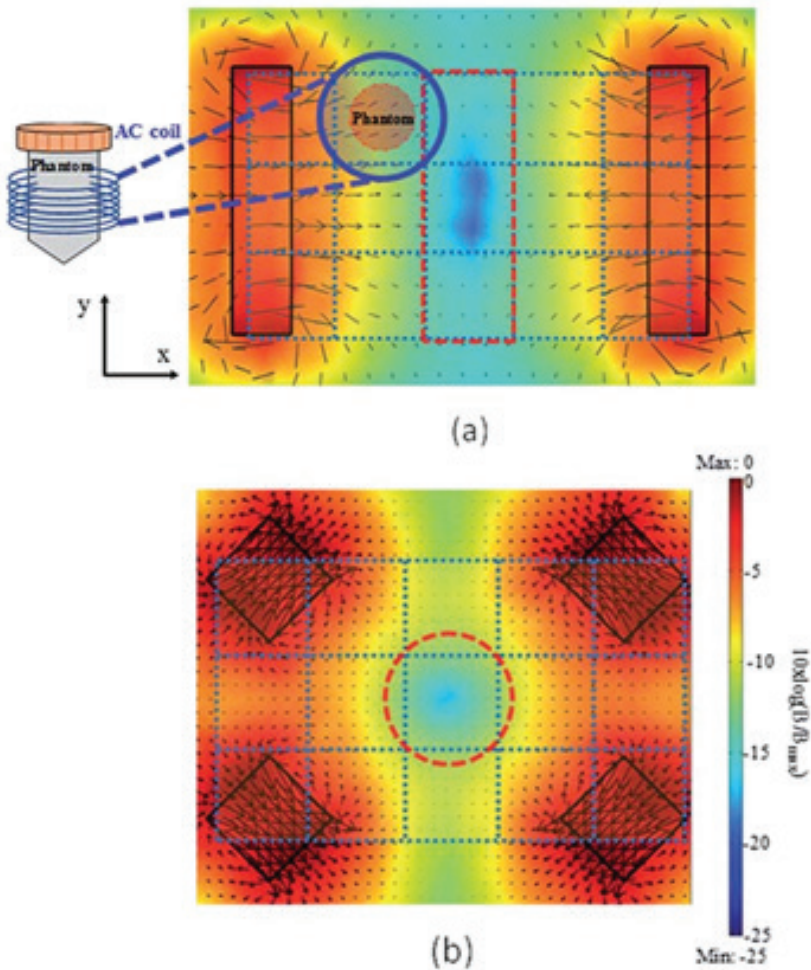
Figure 5. Creation of FFR a) with a pair of permanent magnets b) with double pair of magnets (Myrovali et al. 2020)

Focusing effect: The hyperthermia curves formed when 3 different samples of 10, 40 and 80 nm are under the effect of 70 mT / 375 kHz, respectively, are shown in Figure 6. In the first part of the curve, the heating phase for the 10, 40 and 80 nm sample is shown. The cooling curve was then recorded. The red stripe in the figure shows the hyperthermia border between 41 and 45 ° C. Blue curves indicate that the static magnetic field ranges from 0 to 10 mT; the orange curves correspond to the region between 10 and 75 mT and the red curves to the region between 75 and 200 mT.

Figure 7 shows the heating efficiency dependency between SMF and SAR. The horizontal color scale bar indicates the static magnetic source size. It is observed that in the FFR region where the static magnetic field size is close to zero, MNPs reach maximum heating efficiency and SAR value increases. SAR values vary with the AMF amplitude between 40 and 70 mT in the following ranges; 25 to 85 W g-1 for 10 nm sample, 82 to 315 W g-1 for 40 nm sample and 135 to 555 W g-1 for 80 nm sample. According to these results, it has been observed that where there is no SMF, MNPs vibrate freely under the effect of AMF and produce SAR.
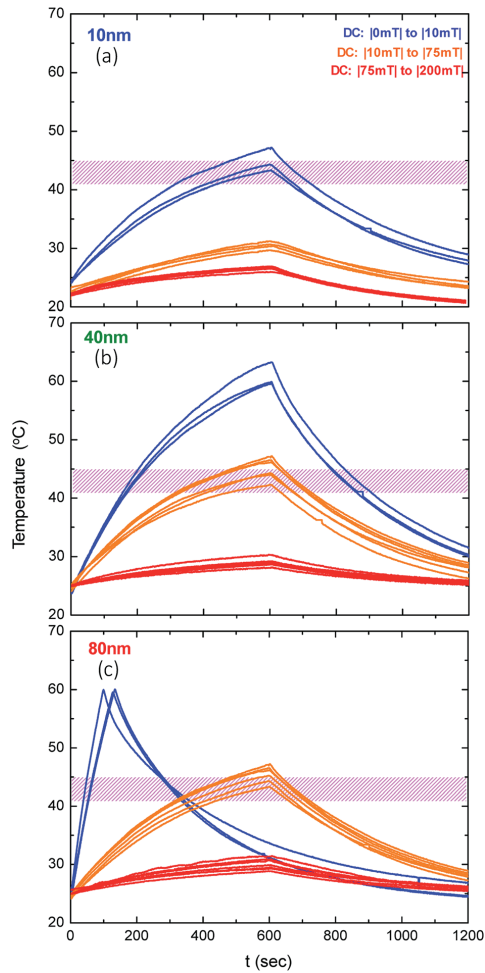
Figure 6. Warming and cooling curves of 3 different samples in different states of SMF and AMF. (Myrovali et al. 2020)
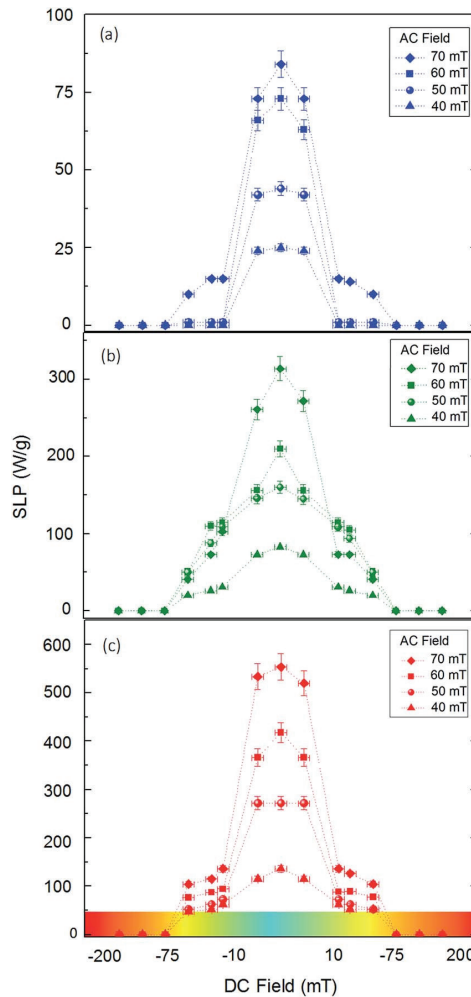
Figure 7. SAR values as a function of SMF for MNPs of different diameters
(a) 10 (b) 40 and (c) 80 nm
(Color scale bar shows SMF power density)
(Myrovali et al. 2020))

4. CONCLUSION

As magnetic field sources, permanent magnets and electromagnets are frequently used in bioelectromagnetic applications. Different designs can be created by changing coil geometries, numbers and distances between them. Permanent magnets, unlike electromagnets, do not produce parasitic currents, they do not need voltage sources and sometimes cooling systems. With these features, permanent magnets are more advantageous than elec-

tromagnets. Also, permanent magnets containing rare earth alloys produce very high magnetic field strength and gradient relative to their size.

Various experiments have been conducted in MFH, which is one of the bioelectromagnetic applications, to examine the effect of SMF on SAR and temperature increases in MNPs. The results show that it is possible to control the temperature increase in MFH with SMF. As future applications, new situations can be observed by checking various parameters such as examining the effect of the angle between AMF and SMF. By using electromagnets and permanent magnets together, SMF is among the options to improve controllability. Different FFRs can be created by changing the magnets in shape and size in the experimental setup.

Studies to use permanent magnets to dampen SAR and focus SAR can be used in clinical applications with necessary modifications. With these new approaches, MFH can be transformed into a modern cancer treatment method by protecting healthy tissues.

5. ACKNOWLEDGMENTS

6. REFERENCES

Bauer, L. M., Situ, S. F., Griswold, M. A., & Samia, A. C. S. (2016). High-performance iron oxide nanoparticles for magnetic particle imaging–guided hyperthermia (hMPI). Nanoscale, 8(24), 12162-12169.

Cantillon-Murphy, P., Wald, L. L., Zahn, M., & Adalsteinsson, E. (2010). Proposing magnetic nanoparticle hyperthermia in low-field MRI. Concepts in Magnetic Resonance Part A: An Educational Journal, 36(1), 36-47.

COMSOL Multiphysics, "AD/DC Module User's Guide," 2013.

Deatsch, A. E., & Evans, B. A. (2014). Heating efficiency in magnetic nanoparticle hyperthermia. Journal of Magnetism and Magnetic Materials, 354, 163-172.

Dhavalikar, R., & Rinaldi, C. (2016). Theoretical predictions for spatially-focused heating of magnetic nanoparticles guided by magnetic particle imaging field gradients. Journal of magnetism and magnetic materials,

419, 267-273.

Do, T. D., Noh, Y., Kim, M. O., & Yoon, J. (2015, October). An electromagnetic steering system for magnetic nanoparticle drug delivery. In 2015 12th International Conference on Ubiquitous Robots and Ambient Intelligence (URAI) (pp. 528-531). IEEE.

Erni, S., Schürle, S., Fakhraee, A., Kratochvil, B. E., & Nelson, B. J. (2013). Comparison, optimization, and limitations of magnetic manipulation systems. Journal of Micro-Bio Robotics, 8(3-4), 107-120.

Garraud, A., Velez, C., Shah, Y., Garraud, N., Kozissnik, B., Yarmola, E. G., ... & Arnold, D. P. (2015). Investigation of the capture of magnetic particles from high-viscosity fluids using permanent magnets. IEEE Transactions on Biomedical Engineering, 63(2), 372-378.

Hensley, D., Tay, Z. W., Dhavalikar, R., Zheng, B., Goodwill, P., Rinaldi, C., & Conolly, S. (2017). Combining magnetic particle imaging and magnetic fluid hyperthermia in a theranostic platform. Physics in Medicine & Biology, 62(9), 3483.

Hergt, R., Dutz, S., Müller, R., & Zeisberger, M. (2006). Magnetic particle hyperthermia: nanoparticle magnetism and materials development for cancer therapy. Journal of Physics: Condensed Matter, 18(38), S2919.

Kastner, E. J., Reeves, R., Bennett, W., Misra, A., Petryk, J. D., Petryk, A. A., & Hoopes, P. J. (2015, March). Alternating magnetic field optimization for IONP hyperthermia cancer treatment. In Energy-based Treatment of Tissue and Assessment VIII (Vol. 9326, p. 93260M). International Society for Optics and Photonics.

Kraus. J. D. and Carver Keith R., Electromagnetics, 2d ed. McGraw-Hill New York, 1973.

Liu, J., Detrembleur, C., De Pauw-Gillet, M. C., Mornet, S., Vander Elst, L., Laurent, S., ... & Duguet, E. (2014). Heat-triggered drug release systems based on mesoporous silica nanoparticles filled with a maghemite core and phase-change molecules as gatekeepers. Journal of Materials Chemistry B, 2(1), 59-70.

Mahadi, W. W., Adi, S. R., & Nor, K. M. (2003, December). Application of the rare earth permanent magnet in linear generator driven by an internal combustion engine. In Proceedings. National Power Engineering Conference, 2003. PECon 2003. (pp. 256-261). IEEE.

Mohr, R., Kratz, K., Weigel, T., Lucka-Gabor, M., Moneke, M., & Lendlein, A. (2006). Initiation of shape-memory effect by inductive heating of magnetic nanoparticles in thermoplastic polymers. Proceedings of the National Academy of Sciences, 103(10), 3540-3545.

Murase, K. (2016). A Simulation Study on the Specific Loss Power in Magnetic Hyperthermia in the Presence of a Static Magnetic Field. Open Journal of Applied Sciences, 6(12), 839.

Murase, K., Takata, H., Takeuchi, Y., & Saito, S. (2013). Control of the

temperature rise in magnetic hyperthermia with use of an external static magnetic field. Physica Medica, 29(6), 624-630.

Myrovali, E., Maniotis, N., Samaras, T., & Angelakeris, M. (2020). Spatial focusing of magnetic particle hyperthermia. Nanoscale Advances.

Roth, H. C., Prams, A., Lutz, M., Ritscher, J., Raab, M., & Berensmeier, S. (2016). A High-Gradient Magnetic Separator for Highly Viscous Process Liquors in Industrial Biotechnology. Chemical Engineering & Technology, 39(3), 469-476.

Sebastian, A. R., Kim, H. J., & Kim, S. H. (2019). Analysis and control of heating of magnetic nanoparticles by adding a static magnetic field to an alternating magnetic field. Journal of Applied Physics, 126(13), 134902.

Tasci, T. O., Vargel, I., Arat, A., Guzel, E., Korkusuz, P., & Atalar, E. (2009). Focused RF hyperthermia using magnetic fluids. Medical physics, 36(5), 1906-1912.

Chapter 16

HELMHOLTZ COIL DESIGN COMPARISONS AND NEW GENERATION COIL APPROACHES FOR BIOELECTROMAGNETIC APPLICATIONS

Serhat KÜÇÜKDERMENCİ[1]

1 Dr. Öğr. Üyesi , Balıkesir University Faculty of Engineering Department of Electrical and Electronics Engineering, kucukdermenci@balikesir.edu.tr

1. INTRODUCTION

Bioelectromagnetic applications such as magnetic fluid hyperthermia, magnetic drug delivery and magnetic particle imaging may require controlled and uniform magnetic fields (Smith et al., 2011; Khalil et al., 2014; Go et al., 2014). Permanent magnets (Sakellariou et al., 2010; Hoff et al., 2013) and air core coils are the most commonly used devices to produce uniform magnetic fields.

The most important limitation of permanent magnets is to change or move their size to change the static magnetic field. Coils, on the other hand, can produce variable static magnetic fields with current change regardless of movement (Cvetkovic et al., 2007). These coils are in different numbers (Nouri et al., 2013; Modi et al., 2016; Koss et al., 2017), in different geometric shapes (Merritt et al., 1983; Jensen et al., 2002) and at different separation distances (Azpurua, et al., 2012). The Helmholtz configuration has the ability to generate highly uniform magnetic fields in a free space region. Circular and square coils in the Helmholtz configuration mathematical analysis calculation models are well defined in the literature, unlike other geometries such as equilateral triangles (Li, et al., 2004; Restrepo et al., 2014; Beiranvand et al., 2013). There are also other polygonal geometries studied by Restrepo (Restrepo et al., 2016) or Petkovic (Petković et al., 2015). However, these isolated studies lack at least a comparative study of the most common geometries.

In biomedical applications, new magnetic coil models are being studied by using different geometries to obtain different magnetic fields for different needs. Accordingly, electromagnets can be in geometric shapes such as circles, squares and rectangles. Coils can be stacked in two or more. 1D, 2D, 3D magnetic fields can be created axially along the x, y and z axes. The Helmholtz coil is one of the most widely used configurations due to the very uniform magnetic field generation.

2. METHODOLOGY AND SYSTEMS

Invented by Hermann Von Helmholtz in the middle of the 19th century, the Helmholtz coil is ideal for producing smooth magnetic fields. Two conjugate coils are placed with a distance of radius. (Restrepo et al., 2016; Shirzadfar et al., 2019)

Structure of the Helmholtz coil consists of two identical coils located opposite one axis. If the distance between the coils is equal to the radius of the coil, it can create a very smooth magnetic field in the center region (Figure 1). The magnetic field produced by the Helmholtz coils can be calculated using the Biot-Savart law using Equation (1) and Equation (2);

$$d\vec{B} = \frac{\mu_0}{4\pi}\left(\frac{I\overrightarrow{dl}\times\hat{r}}{r^2}\right) \qquad (1)$$

Here; dl differential length, I winding current, μ_0 is the magnetic permeability of the gap, r is the distance between source and target, and r̂ is the unit vector in the same direction, and dB is differential magnetic flux density produced by the differential current element.

$$B = \nabla \times A = \nabla \times \frac{\mu_0 I}{4\pi}\int\frac{ds}{R} \qquad (2)$$

Here; A is magnetic vector potential, B is magnetic flux density, μ_0 is magnetic field permeability of space ($4\pi * 10\text{-}7$ H / m), I is coil currents (Amper), R is the distance between source and target points, ds is an infinite small current element.

The magnetic field homogeneity can be compared for circular, square and equilateral triangle Helmholtz coils. Two approaches can be considered for magnetic field homogeneity analysis. One of them is when the radius of the circular coil is equal to half of the side length of the square and equilateral triangle coils, and the other is that their circumference is equal.

2.1. The situation where the circular coil radius is equal to half the length of the square and equilateral triangle coils

The correlation between the length of the coils in different geometry and the magnetic field can be done by Taylor series approach.

Circular Helmholtz coil

Using the Biot-Savart law (Bell et al., 1989), for the circular Helmholtz coil, the magnetic flux density generated by the single coil at the target point and the superposition of two can be calculated. Magnetic flux density B (Kędzia et al., 2013) at point P generated by a single coil can be calculated by equation (3) (Beiranvand et al., 2013) (see Figure 1);
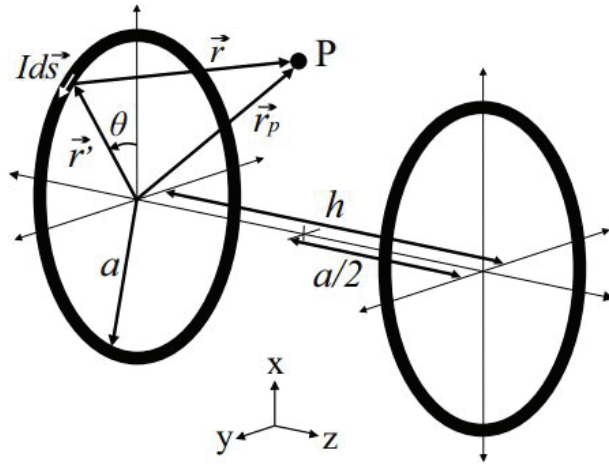
Figure 1. Circular Helmholtz coil. (Restrepo et al., 2017).

$$\vec{B}(x,y,z) = \frac{\mu_0}{4\pi} \oint \frac{Id\vec{s} \times \vec{r}}{|\vec{r}|^3} = B_x\hat{i} + B_y\hat{j} + B_z\hat{k} \qquad (1)$$

$$B_x = aB_{Z0} \int_0^{2\pi} z\cos\theta \, \frac{d\theta}{F_z^{3/2}}$$

$$B_y = aB_{Z0} \int_0^{2\pi} z\sin\theta \, \frac{d\theta}{F_z^{3/2}} \qquad\qquad (3)$$

$$B_z = aB_{Z0} \int_0^{2\pi} (a - x\cos\theta - y\sin\theta) \, \frac{d\theta}{F_z^{3/2}}$$

Where

$$F_z = z^2 + (x - a*\cos\theta)^2 + (y - a*\sin\theta)^2$$

$$B_{Z0} = \frac{\mu_0 NI}{4\pi}$$

Here; μ_0 is called the magnetic permeability of the gap. ds is the differential current element, r_p is the distance from the starting point to the point P, r^1 is the distance from the starting point to ds, and r is the distance from ds to P.

The superposition of the magnetic flux densities produced by each circular coil (CH) and the total magnetic flux densities produced in the z-direction are presented by equation (4):

$$\vec{B}(z) = 2\pi a^2 B_{Z0} \left[\frac{1}{\left(a^2 + \left(z + \frac{h}{2}\right)^2\right)^{3/2}} + \frac{1}{\left(a^2 + \left(z - \frac{h}{2}\right)^2\right)^{3/2}} \right] \hat{z} \quad (2) \qquad (4)$$

The separation distance h which provides the Helmholtz condition for the CH coil is equal to h = a.

The equation (5) is the approximation of the Taylor series of equation (4) for | z | ≤ a /2.

$$B_z(z)\big|_{|z|\leq a/2} \approx \frac{32\pi B_{Z0}}{5\sqrt{5}a}\left[1 - \frac{144}{125}\left(\frac{z}{a}\right)^4\right] \tag{5}$$

Square Helmholtz coil

The equation (6) for square Helmholtz coil geometry gives the magnetic flux density produced by a single square coil (see Figure 2).
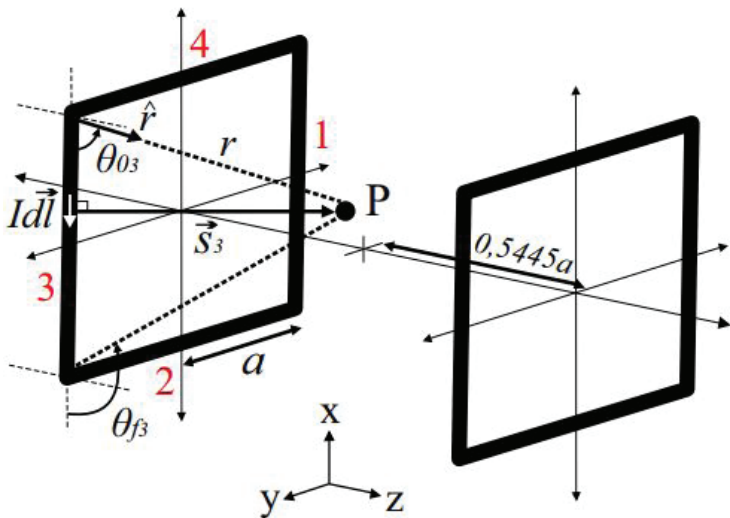
Figure 2. Square Helmholtz coil (Restrepo et al., 2017).

where dl is the differential length, r is the unit vector, r is the distance from the end point of the loop to P, θ_o and θ_f are the angles created from the ends of the current loop to the projection lines from P, s is the right distance from the loop axis to P.

$$\vec{B}(x, y, z) = B_{Z0} \sum_{i=1}^{4} \int_{\theta_{o_i}}^{\theta_{f_i}} \frac{sin\theta}{s_i} d\theta = B_x \hat{\imath} + B_y \hat{\jmath} + B_z \hat{k} \quad (4)$$

$$B_x = B_{Z0} \sum_{i=1}^{2} (-1)^i z F_{2i}$$

$$B_y = B_{Z0} \sum_{i=1}^{2} (-1)^{i-1} z F_{2i-1}$$

$$B_z = B_{Z0} \sum_{i=1}^{2} ((-1)^{i-1} x + a) F_{2i} + ((-1)^i y + a) F_{2i-1}$$

$$(6)$$

Where

$$F_i = \frac{(cos\theta_{o_i} - cos\theta_{f_i})}{s_i^2}$$

$$s_{1,3} = \sqrt{(y \mp a)^2 + z^2}$$

$$s_{2,4} = \sqrt{(x \pm a)^2 + z^2}$$

The superposition of the magnetic flux densities produced by each square coil (SH) and the total magnetic flux intensity generated in the z-direction are presented by equation 7:

$$\vec{B}(z) = 8a^2 B_{Z0} \left[\frac{1}{\left(a^2 + \left(z + \frac{h}{2}\right)^2\right) \left(2a^2 + \left(z + \frac{h}{2}\right)^2\right)^{1/2}} + \frac{1}{\left(a^2 + \left(z - \frac{h}{2}\right)^2\right) \left(2a^2 + \left(z - \frac{h}{2}\right)^2\right)^{1/2}} \right] \hat{z}$$

$$(7)$$

The separation distance h which provides the Helmholtz condition for the SH coil is equal to h = 1.089a (Piergentili, et al., 2011).

The equation (8) is the approximation of the Taylor series of equation (7) for $|z| \leq 0.5445a$.

$$B_z(z)|_{|z| \leq 0.5445a} \approx \frac{16 B_{Z0}}{1.2965\sqrt{2.2965}a} \left[1 - 0.8068 \left(\frac{z}{a}\right)^4\right] \quad (8)$$

Equilateral triangle Helmholtz coil

The equation (9) for the equilateral triangle Helmholtz coil geometry gives the magnetic flux density produced by a single equilateral triangle coil (see Figure 3),
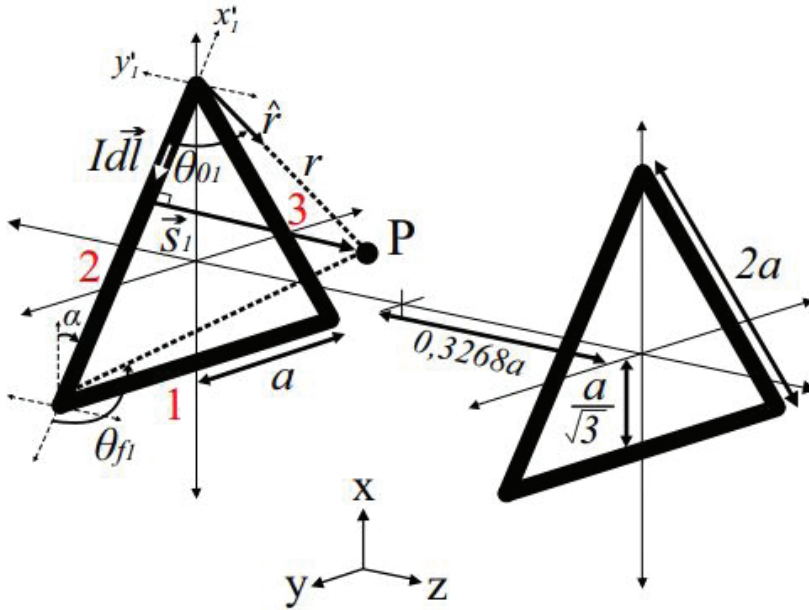
Figure 3. Equilateral triangle Helmholtz coil. (Restrepo et al., 2017).

$$\vec{B}(x,y,z) = B_{Z0} \sum_{i=1}^{3} \int_{\theta_{o_i}}^{\theta_{f_i}} \frac{\sin\theta}{s_i} d\theta = B_x\hat{i} + B_y\hat{j} + B_z\hat{k} \quad (7)$$

$$B_x = B_{Z0}\left(zF_1 + \sum_{i=2}^{3} -\frac{1}{2}zF_i\right)$$

$$B_y = B_{Z0}\sum_{i=2}^{3}(-1)^{i-1}\frac{\sqrt{3}}{2}zF_i$$

$$B_z = B_{Z0}\left(\left(-x+\frac{a}{\sqrt{3}}\right)F_1 + \sum_{i=2}^{3}\left((-1)^i y_i' + \frac{a}{\sqrt{3}}\right)F_i\right)$$

$$(9)$$

Where

$$F_1 = \frac{1}{s_2^2}\left(\frac{y+a}{\sqrt{(y+a)^2 + s_2^2}} - \frac{y-a}{\sqrt{(y-a)^2 + s_2^2}}\right)$$

$$F_{2,3} = \frac{1}{s_{2,3}^2}\left(\frac{x_{2,3}' + a}{\sqrt{(x_{2,3}' + a)^2 + s_{2,3}^2}} - \frac{x_{2,3}' - a}{\sqrt{(x_{2,3}' - a)^2 + s_{2,3}^2}}\right)$$

$$s_1 = \sqrt{(x - a/\sqrt{3})^2 + z^2}$$

$$s_{2,3} = \sqrt{(y_{2,3}' \pm a/\sqrt{3})^2 + z^2}$$

The superposition of the magnetic flux densities produced by each square coil (ETH) and the total magnetic flux intensity generated in the z-direction are presented by equation 10.

$$\vec{B}_z(z) = 2\sqrt{3}a^2 B_{Z0} \left[\frac{1}{\left(\frac{a^2}{3} + \left(z + \frac{h}{2}\right)^2\right)\left(\frac{4a^2}{3} + \left(z + \frac{h}{2}\right)^2\right)^{1/2}} \right.$$
$$\left. + \frac{1}{\left(\frac{a^2}{3} + \left(z - \frac{h}{2}\right)^2\right)\left(\frac{4a^2}{3} + \left(z - \frac{h}{2}\right)^2\right)^{1/2}} \right] \hat{z} \qquad (10)$$

The separation distance h which provides the Helmholtz condition for the ETH coil is equal to h = 0.6536a (Restrepo et al., 2016). The equation (9) is the approximation of the Taylor series of equation (8) for $|z| \le$ 0.3268a.

Comparison of normalized magnetic flux densities

Normalized magnetic flux density (B_z/B_{max}) and z-axis plot for CH, SH and ETH coils are given in figure 4.
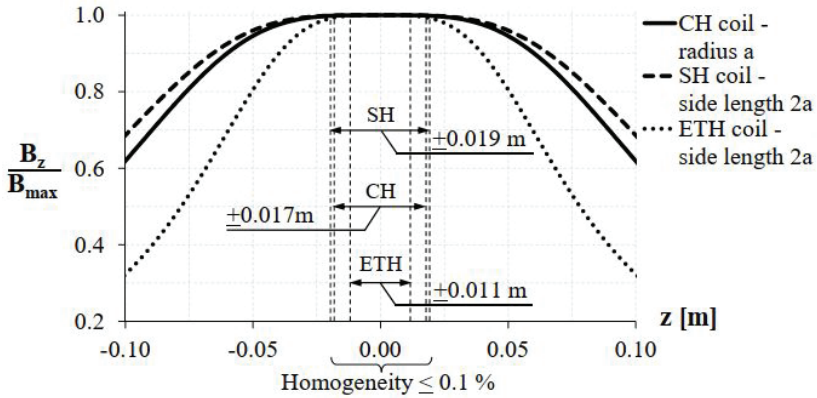
Figure 4. Normalized magnetic flux densities of CH SH and ETH coils (for the case where the radius of the circular coil is equal to half the side length of the square and equilateral triangle coils). (Restrepo et al., 2017).

Considering the homogeneity $\le$ % 0,1, it is seen that the SH coil has a greater magnetic flux density homogeneity than the others for the CH coil radius a and the side lengths 2a of the other coils.

Considering the side length of SH and ETH coils as in Figure 5, magnetic flux density homogeneity produced by square geometry was observed better than circular and equilateral triangle geometries.
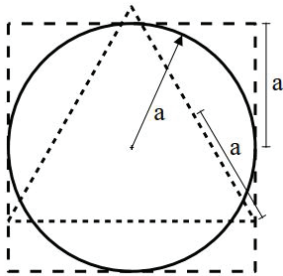
Figure 5. The situation where the radius is equal to half of the side length for circular, square and equilateral triangle coils. (Restrepo et al., 2017).

2.2. The situation where the coil circles are equal

As shown in Figure 6, the magnetic flux density homogeneity can be compared by taking the circumference of all geometries equally.
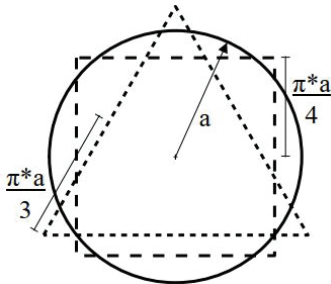
Figure 6 Circular, square and equilateral triangular coils have equal circumference.(Restrepo et al., 2017).

The circumference of the CH coil with a radius "a" is taken as reference to 2πr, and the corresponding side lengths of the SH and ETH coils are shown in Figure 6. Normalized magnetic flux densities (Bz/Bmax) of CH, SH and ETH coils are shown in Figure 7.
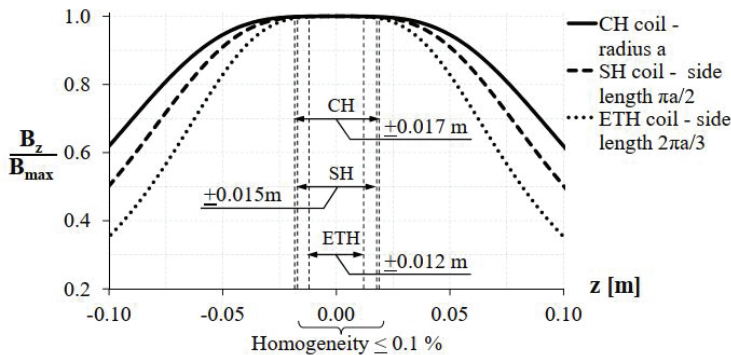
Figure 7. Normalized magnetic flux densities of CH SH and ETH coils (For coil circumference lengths equal). (Restrepo et al., 2017).

Considering the homogeneity ≤ %0,1, it is seen that the CH coil has a greater magnetic flux density homogeneity than the others for the same circumference in the coils.

3. NEW GENERATION COIL APPROACHES

Circular coils have some limitations for medical research such as drug delivery and MRI (Shirzadfar et al., 2015). Especially in biomedical applications requiring weak magnetic field, new generation coil approaches can be tried. Some examples of new generation coil approaches are presented below.

Three circular coils with triangular configuration: In this configuration, three circular coils form the edges of an equilateral triangle. The radii of the coils are 10 cm (see Figure 8.a). With simulation, the magnetic flux density can be seen to be homogeneous along the x and y axes. The homogeneity deteriorates for the z axis. (see Figure 8.b).

a)   b)
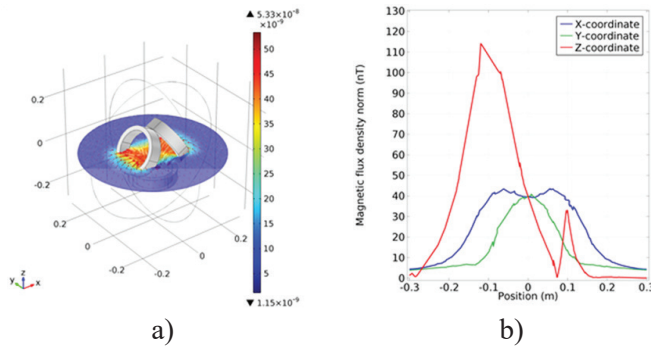
Figure 8. a) Simulation of three circular coils with triangular configuration
b) 1D plots of magnetic flux density according to x, y, z axes (Shirzadfar et al.,
2019).

Six circular coils with hexagonal configuration: In this configuration, six circular coils form the edges of an equilateral hexagon. The radii of the coils are 5 cm (see Figure 9.a). With simulation, it can be seen that the magnetic flux density is approximately homogeneous along the x axis. For the z-axis, the magnetic-free zone in the center is outstanding. These features can be evaluated for different applications (see Figure 9.b).

a)   b)
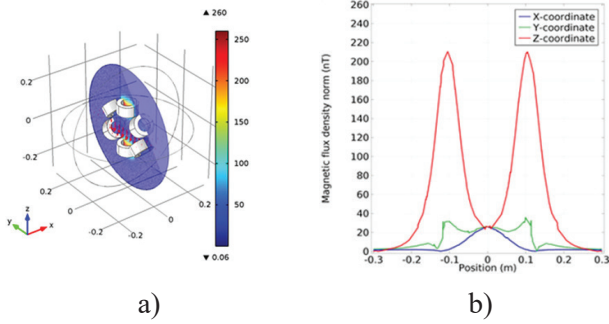
Figure 9. a) Simulation of six circular coils with hexagonal configuration b) 1D plots of magnetic flux density according to x, y, z axes (Shirzadfar et al., 2019).

Three circular coils with nested configuration: Three circular coils of different diameters are nested in this configuration. The radii of the coils are 21cm, 16cm and 10cm, respectively. The angle between the coils is 90 degrees (see Figure 10.a). With simulation, it can be said that the magnetic flux density is homogeneous in a narrow region along the x axis. The homogeneity deteriorates for the y and z axes. (see Figure 10.b).

a)   b)
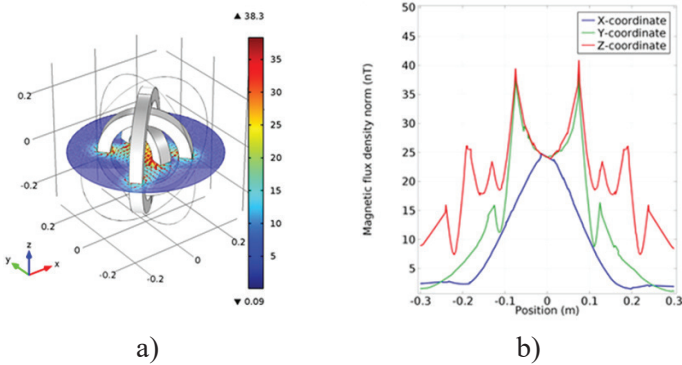
Figure 10. a) Simulation of three circular coils with nested configuration b) 1D plots of magnetic flux density according to x, y, z axes (Shirzadfar et al., 2019).

Three triangular coils with array configuration: In this configuration, a linear array is created with triangular coils. The bases of the coils are 40 cm, their height is 35 cm and the distance between them is 12 cm. (see Figure 11.a). It is quite homogeneous along the y axis of magnetic flux density by simulation. The homogeneity deteriorates for the x and z axes. (see Figure 11.b)

a)   b)
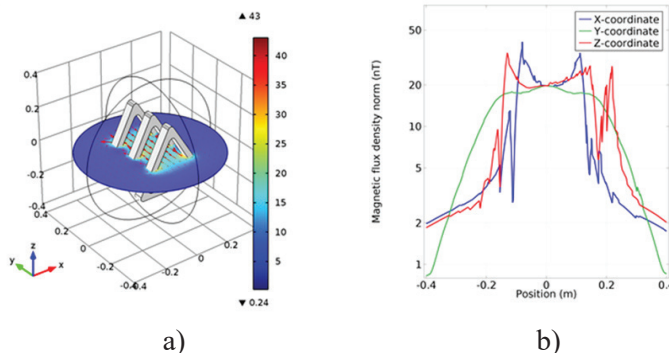
Figure 11. a) Simulation of three triangular coils with array configuration b) 1D plots of magnetic flux density according to x, y, z axes (Shirzadfar et al., 2019).

Two trapezoidal coils: The bottom bases of trapezoidal coils are 15 cm, the top bases are 30 cm and the height is 15 cm. (see Figure 12.a). With the simulation, the magnetic flux density appears to be homogeneous along the x, y, and z axes (see Figure 12.b).

a)   b)
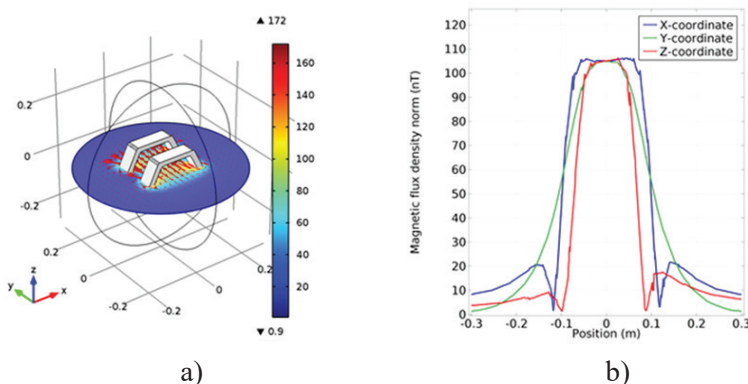
Figure 12. a) Simulation of two trapezoidal coils b) 1D plots of magnetic flux density according to x, y, z axes (Shirzadfar et al., 2019).

In smart drug delivery, which is one of the bioelectromagnetic applications, the drug plays an important role in the treatment of cancer by working only in the affected area. Thus, complications do not occur in healthy parts of the body. The patient facing side of the trapezoidal coil has more useful area when compared to normal circular coils used in medical applications and trapezoid coils. This property can provide technicians or doctors with ease of movement during application. Thus, it can help to increase patient comfort. In addition to these advantages, the homogeneity of the magnetic flux density created by the trapezoidal coil continues.

4. CONCLUSION

Many bioelectromagnetic applications require magnetic flux densities of various properties. Permanent magnets and electromagnets are frequently used as sources of magnetic fields. Coils can generate variable static magnetic fields with current change without changing the position of the coil. In magnets, this is related to the magnet's size. This is the most important limitation of permanent magnets. Different designs can be created by changing coil geometries, numbers and distances between them. Here, normalized homogeneous magnetic flux densities of Helmholtz coils formed from circular, square and equilateral triangles were compared. One of these situations is when the radius of the circular coil is equal to half the length of the square and equilateral triangle coils, and the other is that the circumference of all coils is equal. Which Helmholtz coil type to choose can be related to the needs of the application to be made. In general, the CH coil offers the best performance in relation to the test volume and coil sizes. SH coil offers the best homogeneity when side length 2a is taken. Compared to other geometries, the ETH coil allows a greater magnetic field density to be created, both by taking the side lengths 2a and when the circumference of the coil is equal.

The states of the magnetic flux densities produced by the new generation coils on the x, y, z axes of three circular coils with nested configuration, six circular coils with hexagonal configuration, three circular coils with nested configuration, three triangular coils with array configuration, and two trapezoid coils designs were compared. Trapezoid coil circular coil can produce homogeneous magnetic flux density for all 3 axes. Compared with circular coils and trapezoid coils, it is thought that the trapezoidal coil can provide ease of movement to the technician or doctors during application due to the larger area.

Different coil designs reveal different magnetic flux densities on different axes. Depending on the type of application to be carried out, different coil designs can be selected for homogeneous-inhomogeneous, weak magnetic field-strong magnetic field, magnetic field region-magnetic non-magnetic region needs.

5. ACKNOWLEDGMENTS

6. REFERENCES

Azpurua, M. A. (2012). A semi-analytical method for the design of coil-systems for homogeneous magnetostatic field generation. Progress in Electromagnetics Research, 37, 171-189.

Beiranvand, R. (2013). Analyzing the uniformity of the generated magnetic field by a practical one-dimensional Helmholtz coils system. Review of Scientific Instruments, 84(7), 075109.

Bell, G. B., & Marino, A. A. (1989). Exposure system for production of uniform magnetic fields. Journal of Bioelectricity, 8(2), 147-158.

Cvetkovic, D., & Cosic, I. (2007, August). Modelling and design of extremely low frequency uniform magnetic field exposure apparatus for in vivo bioelectromagnetic studies. In 2007 29th Annual International Conference of the IEEE Engineering in Medicine and Biology Society (pp. 1675-1678). IEEE.

Go, G., Choi, H., Jeong, S., Lee, C., Ko, S. Y., Park, J. O., & Park, S. (2014). Electromagnetic navigation system using simple coil structure (4 coils) for 3-D locomotive microrobot. IEEE Transactions on Magnetics, 51(4), 1-7.

Hoff, B. W., Mardahl, P. J., Chen, C. H., Horwath, J. C., & Haworth, M. D. (2013). U.S. Patent No. 8,358,190. Washington, DC: U.S. Patent and Trademark Office.

Jensen, J. H. (2002). Minimum-volume coil arrangements for generation of uniform magnetic fields. IEEE transactions on magnetics, 38(6), 3579-3588.

Kędzia, P., Czechowski, T., Baranowski, M., Jurga, J., & Szcześniak, E. (2013). Analysis of uniformity of magnetic field generated by the two-pair coil system. Applied magnetic resonance, 44(5), 605-618.

Khalil, I. S., Abelmann, L., & Misra, S. (2014). Magnetic-based motion control of paramagnetic microparticles with disturbance compensation. IEEE Transactions on Magnetics, 50(10), 1-10.

Koss, P. A., Crawford, C., Bison, G., Wursten, E., Kasprzak, M., & Severijns, N. (2017). Pcb coil design producing a uniform confined magnetic field. IEEE Magnetics Letters, 8, 1-5.

Li, T. T. K. (2004). Tri-axial square Helmholtz coil for neutron EDM experiment. The Chinese University of Hong Kong, Hong Kong, China.

Merritt, R., Purcell, C., & Stroink, G. (1983). Uniform magnetic field produced by three, four, and five square coils. Review of Scientific Instruments, 54(7), 879-882.

Modi, A., Singh, R., Chavan, V., Kukreja, K., Ghode, S., Manwar, K., & Kazi, F. (2016, December). Hexagonal coil systems for uniform

magnetic field generation. In 2016 IEEE Asia-Pacific Conference on Applied Electromagnetics (APACE) (pp. 47-51). IEEE.

Nouri, N., & Plaster, B. (2013). Comparison of magnetic field uniformities for discretized and finite-sized standard cosθ, solenoidal, and spherical coils. Nuclear Instruments and Methods in Physics Research Section A: Accelerators, Spectrometers, Detectors and Associated Equipment, 723, 30-35.

Petković, D. M., & Radić, M. D. (2015). Generalization of Helmholtz coil problem. Serbian Journal of Electrical Engineering, 12(3), 375-384.

Piergentili, F., Candini, G. P., & Zannoni, M. (2011). Design, manufacturing, and test of a real-time, three-axis magnetic field simulator. IEEE Transactions on Aerospace and Electronic Systems, 47(2), 1369-1379.

Restrepo Alvarez, A. F., Franco Mejia, E., Cadavid Ramirez, H., & Pinedo Jaramillo, C. R. (2016). Analysis of the magnetic field homogeneity for an equilateral triangular helmholtz coil. Progress In Electromagnetics Research, 50, 75-83.

Restrepo, A. F., Franco, E., & Pinedo, C. R. (2014). Metodología de diseño e implementación de un sistema para generación de campos magnéticos uniformes con bobinas Helmholtz Cuadrada Tri-Axial. Información tecnológica, 25(2), 03-14.

Restrepo, A. F., Franco, E., Cadavid, H., & Pinedo, C. R. (2017, December). A comparative study of the magnetic field homogeneity for circular, square and equilateral triangular helmholtz coils. In 2017 International Conference on Electrical, Electronics, Communication, Computer, and Optimization Techniques (ICEECCOT) (pp. 13-20). IEEE.

Restrepo, A. F., Martinez, L. J., Pinedo, C. R., Franco, E., & Cadavid, H. (2013). Design study for a cellular culture bioreactor coupled with a magnetic stimulation system. IEEE Latin America Transactions, 11(1), 130-136.

Restrepo-Álvarez, A. F., Franco-Mejía, E., Cadavid-Ramírez, H., & Pinedo-Jaramillo, C. R. (2017). A simple geomagnetic field compensation system for uniform magnetic field applications. Revista Facultad de Ingeniería Universidad de Antioquia, (83), 65-71.

Sakellariou, D., Hugon, C., Guiga, A., Aubert, G., Cazaux, S., & Hardy, P. (2010). Permanent magnet assembly producing a strong tilted homogeneous magnetic field: towards magic angle field spinning NMR and MRI. Magnetic Resonance in Chemistry, 48(12), 903-908.

Shirzadfar, H., Dohani, S., Ghaedi, M., & Edalati, B. (2019). Creating the new generation coils to generate a uniform magnetic field using for medical applications simulation and analysis. International Journal of Biosensors & Bioelectronics, 5(5).

Shirzadfar, H., Edalati, B., Dohani, S., & Ghaedi, M. (2019). The design and manufacture of a trapezoidal coil to produce a homogeneous

magnetic field for use in medical applications. International Journal of Biosensors & Bioelectronics, 5(5).

Shirzadfar, H., Nadi, M., Kourtiche, D., Yamada, S., & Hauet, T. (2015). Needle-type GMR sensor to estimate the magnetic properties of diluted ferrofluid for biomedicine application. IRBM, 36(3), 178-184.

Smith, A., Anderson, B. E., Chaudhury, S., & Jessen, P. S. (2011). Three-axis measurement and cancellation of background magnetic fields to less than 50 µG in a cold atom experiment. Journal of Physics B: Atomic, Molecular and Optical Physics, 44(20), 205002.

STATISTICAL ANALYSIS OF ANNUAL MAXIMUM PRECIPITATION AND DETERMINATION BEST-FIT PROBABILITY DISTRIBUTIONS: A CASE STUDY OF SUSURLUK BASIN AND VAN LAKE BASIN, TURKEY

Tuğçe HIRCA[1], Gökçen ERYILMAZ TÜRKKAN[2]

---

1 Ph.D. Candidate, Bayburt University, tugcehirca@ogr.bayburt.edu.tr
2 Asst. Prof. Dr., Bayburt University, geryilmazturkkan@bayburt.edu.tr

1. Introduction

It is necessary to have sufficient knowledge about the maximum precipitation that may occur in certain repetition years in the design of water structures and urban drainage systems, management of water resources and taking some precautions against flood disaster (Olofontiye, Sule & Salami, 2009). However, hydrological cycle elements such as precipitation show random characteristics (Demir, 2014). Therefore; by taking into account some parameters such as procedure of occurrence of previous events, average of recorded data and probability of occurrence, it is possible to estimate future events with statistical analysis (Khosravi, Majidi & Nohegar, 2012).

The primary purpose of frequency analysis is to relate the frequency of occurrence with the magnitude of extreme events using probability distributions (Chow et al., 1988). Frequency analysis consists of three basic steps (Aşıkoğlu, 2007).

✓ To define a simple and logical probability distribution model of the event studied.

✓ Estimating the parameters of the distribution model is defined, and

✓ Estimating the risk of the event being examined at an appropriate sensitivity level.

Accurate estimations of excessive precipitation through frequency analysis, it can mitigate damage caused by storms and floods and help design hydraulic structures more efficiently. The three main characteristics of precipitation; quantity, frequency and intensity vary from day to day, year to year and region to region. Many statistical models have been developed for the estimation of annual maximum precipitation. (Tao, Nguyen & Bourque, 2002). However, determining the appropriate distribution of precipitation records is still one of the most important problems of engineering applications. Because there is a general opinion on which probability distribution function is suitable. Therefore, it is necessary to evaluate many existing probability distribution functions in order to find a suitable model that can provide accurate extreme precipitation estimates.

1.1 Literatür Review

Numerious studies have been conducted in the literature on frequency analysis of hydrological events, the selection and use of different probability distribution models and different parameter estimation methods. A research by Lee (2004) the most appropriate distribution for the precipitation distribution characteristic of the Chia-Nan plain area is Log Pearson Type III. Salami (2004) reported that he established probability distribution models for estimating the annual flow regime along the Asa River. The

study results showed that LP3 and Gumbel distributions were proposed for minimum and maximum flows respectively. Husak et al. (2006) applied the Gamma and Weibull probability distribution to monthly precipitation data in Africa. Kolmogorov Smirnov test, which is goodness of fit test, was applied to determine the distribution suitable for precipitation records. As a result of the study, it was determined that 98% of the regions in Africa were in compliance with Gamma distribution. Atroosh and Moustafa (2012) have applied Gamma, Weibull, Pearson 6, Rayleigh, Beta, Kumaraswamy and exponential distributions to model the distribution of Wadi Bana flows. They used Kolmogorov-Smirnov, Anderson-Darling and Chi-Square tests to determine the optimal probability distribution. The most appropriate probability distribution in the study was determined to be Gamma. Kalita et al. (2017) frequency analysis of 24-year daily precipitation data was conducted to determine Ukiam's annual maximum precipitation and discharge. Weibull's plotting position Gumbel, Log Pearson and Log Normal probability distribution functions were used in the study. Chi-Square test was performed to determine the appropriate probability distribution. As a result of the study, it was determined that Log Pearson and Log Normal probability distributions were most appropriate. In the study conducted by Esberto (2018), the most suitable probability distribution was determined using 60 probability distribution functions. Kolmogorov Smirnov and Chi-Square tests were performed to determine the model suitable for precipitation data. Baghelet al. (2019) used 56-year daily precipitation data of Udaipur region. In the evaluation of maximum daily precipitation (Gamble's extreme value type I, Log Pearson Type III, Log Normal, Normal, Exponential, Pearson type III and Gamma distribution) were used in the study. Chi-Squared test was used to determine the appropriate distribution. Results showed that Log Normal distribution and Gumbel distribution were most appropriate. The aim of this study is to determine the variation of precipitation from region to region by using precipitation statistical analysis and using different probability distribution functions. Also purpose of the study to determine the most appropriate probability distribution for precipitation records by using fit tests. Therefore, the current and actual monthly maximum precipitation records of the 12 observation stations selected in the Susurluk Basin in western Turkey and Lake Van Basin in eastern Turkey were used in the study. The study consists of two stages. The first stage of the study; statistical analysis was performed using Normal, Log Normal, Log-Pearson Type III and Gumbel probability distribution functions. In the second stage of the study, EasyFit packet program was used to determine which probability distribution function each station fits. Kolmogorov Smirnov, Anderson Darling and Chi-Square goodness tests were used in the program.

2. Study area and precipitation observation stations

2.1 Study Area

Precipitation data of a total of 12 stations, 6 in the Susurluk Basin and 6 in the Van Lake Closed Basin, operated by the General Directorate of State Meteorological Affairs, were used in this study. tabure 1 shows the position of the study areas in the map of Turkey basins. The Susurluk Basin has a precipitation area of 22.399 km^2, covering about 2.9% of Turkey's surface area. The Susurluk Basin is located in western Turkey, between the northern latitudes of 39°-40° and the eastern longitudes of 27°-30°. The Susurluk Basin in the south of the Marmara region includes parts of Bursa, Balıkesir, Kütahya, Bilecik, Çanakkale, Manisa and Izmir provinces (Aytulun, 2019). Susurluk Basin and stations are shown in Figure 2.

Figure 1. Location of Susurluk and Van Lake Basins (Red: Susurluk Basin, Blue: Lake Van Basin)

Figure 2. Susurluk Basin and precipitation observation stations used in the study

Susurluk Basin is located to the northwest of the Anatolian. The total area of the basin covers approximately 3.11% of Turkey is approximately 24.299 km^2 in area (as shown in Table 1) (Susurluk Havzası Yönetim Planları Ekleri,2018). The two main lakes within the Susurluk Basin are Kuşgölü and Ulubat Lakes.

Table 1. Lower Basins

Lower Basin Code	Name of Lower Basin	Area (km²)
03-1	Orhaneli Lower Basin	4.745
03-2	Emet Lower Basin	4.921
03-3	Mustafakemalpaşa-Ulubat	981
03-4	Nilüfer Lower Basin	1.998
03-5	Simav-Susurluk Lower Basin	7.028
03-6	Kocaçay-Manyas Lower Basin	4.072
03-7	Göynük Lower Basin	79
03-8	Bandırma-Kapıdağ Lower Basin	474
Total		24.299

Figure 3 shows the annual maximum precipitation data of the selected stations in the Susurluk basin between 2007 and 2017. In this notation; (a) Bandırma, (b) Bursa, (c) DursunBey, (d) Keles, (e) Simav, (f) Tavsanli station.
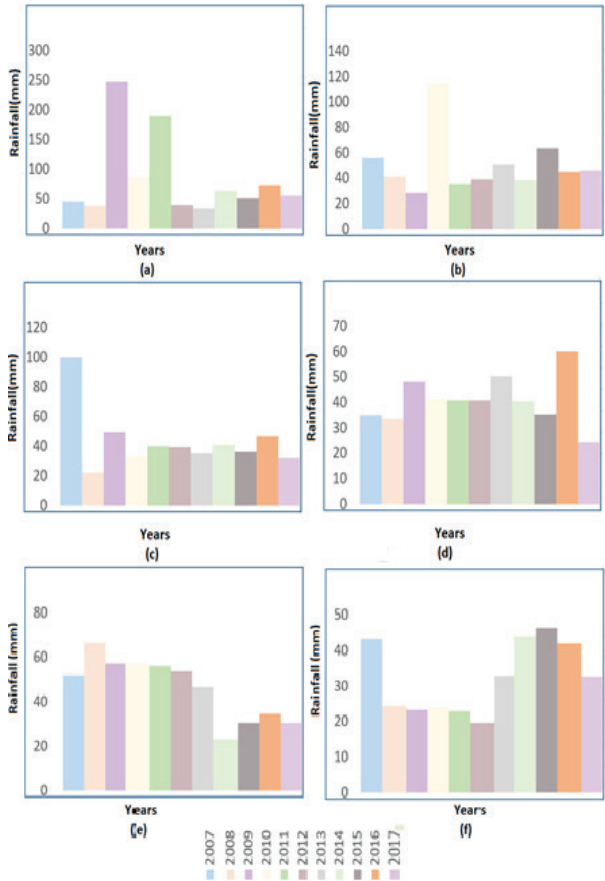
Figure 3. Annual maximum precipitation of the stations in the Susurluk Basin 2007-2017

The Van Lake Basin showing the closed basin property, 16 096 km² area after the Interior Anatolia Closed Basin is Turkey's 2nd largest inward flow basin. Van Lake, which is considered as soda due to the high content of soda in the salt content of its waters, is the largest soda lake in the world (Aytulun, 2019). Van Lake Basin and stations are shown in Figure 4.
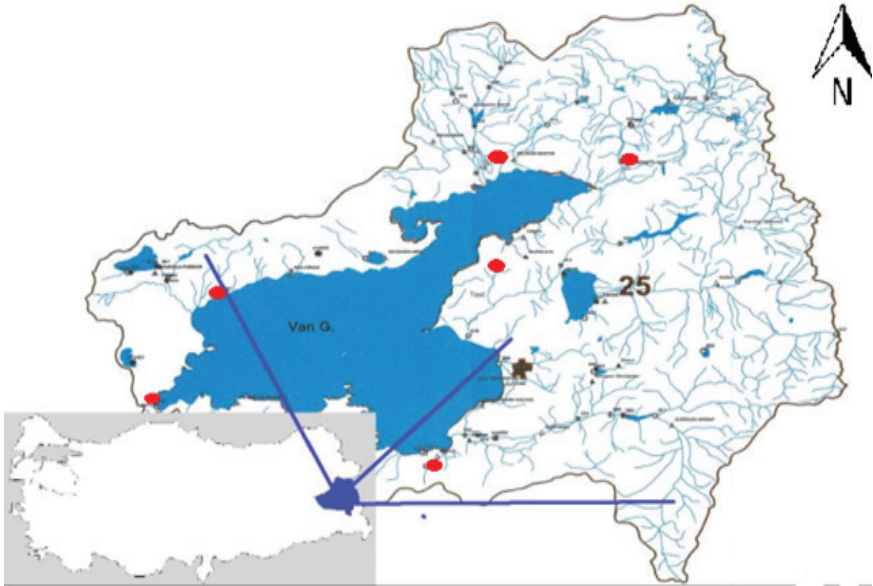
Figure 4.Van Lake Basin and precipitation observation stations used in the study

There are 15 wetland in the Lake Van Basin approved by the Ministry of Agriculture and Forestry and the General Directorate of Nature Conservation and National Parks. These wetlands are shown in Table 2. There are 9 lakes outside the wetlands. These lakes; Ak Lake, Gövelek Lake, Tuz Lake, Kazlı Lake, Çegen Lake, Hasan Timur Lake, Süphan (Sultan) Lake, Norşin Lake and Adırum Lake.

Table 2. Wetlands in the Van Closed Basin

Batmış Lake	Erçek Lake
Aygır Lake	Kaz Lake
Bendimahi Delta	Nazik Lake
Çaldıran Plain Wetlands	Nemrut Lake
Çelebibağı Reeds	Sodalı Lake
Çiçekli Lake	Turna Lake
Çimenova Lakes	Van Lake
Dönemeç Delta	

Figure 5 shows the annual maximum precipitation data of selected stations in the Lake Van basin between 2007 and 2017. In this notation; (a) Ahlat, (b) Erciş, (c) Gevaş, (d) Muradiye Van, (e) Tatvan, (f) Van Regional station.
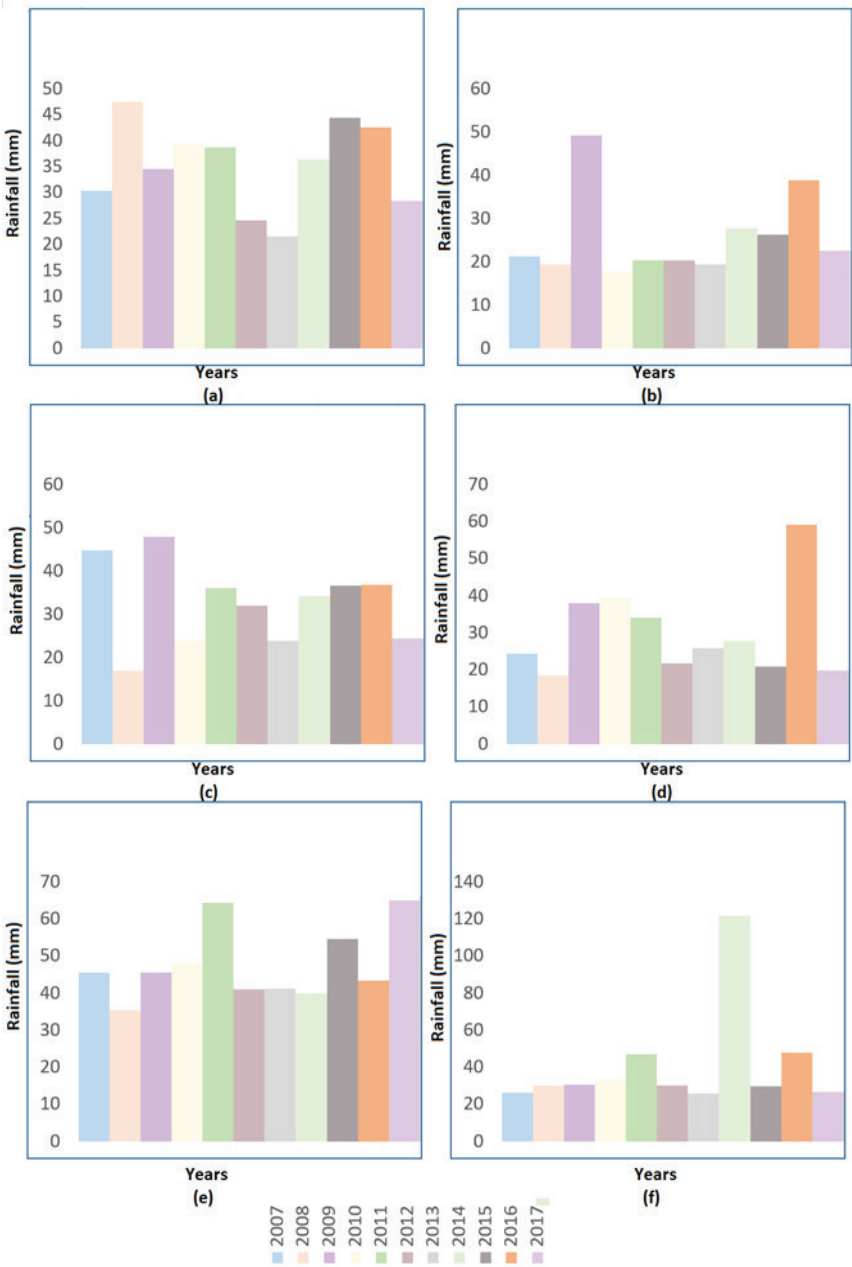
Figure 5. Annual maximum precipitation of the stations in Lake Van Basin 2007-2017

2.2 Precipitation observation stations data

Figure 1 shows the locations of susurluk Basin and Van Lake Basin which are the subjects of the study. The geographical coordinates of the 12 locations in this study are detailed in Table 3 and Table 4. Their locations are shown in Figure 2 and Figure 4.

Table 3. Information about the precipitation observation stations in the Susurluk Basin

Sta. Name	Sta. No	Observation	Latitude	Longitude	Altitude
Bandırma	17114	1970-2017	40.3315	27.9965	63
Bursa	17116	1970-2017	40.2308	29.0133	100
Keles	17695	1970-2017	39.9150	29.2313	1063
Dursunbey	17700	1970-2017	39.5778	28.6322	637
Tavşanlı	17704	1970-2017	39.5384	29.4941	833
Simav	17748	1970-2017	39.0925	28.9786	809

Table 4. Information about the precipitation observation stations in   the Van Lake Basin

Sta. Name	Sta. No	Observation	Latitude	Longitude	Altitude
Ahlat	17810	1970-2017	38.7487	42.4750	1730
Erciş	17784	1970-2017	39.0197	43.382	1678
Gevaş	17852	1982-2017	38.467	43.350	1662
Muradiye	17786	1970-2017	38.9897	43.7627	1706
Tatvan	17205	1972-2017	38.5033	42.2808	1665
Van Bölge	17172	1970-2017	38.4693	43.3460	1675

12 precipitation observation stations, 6 of which are susurluk basin and 6 of which are lake basin, were used in this study. Observation time of precipitation observation stations varies between 1970-2017.Monthly maximum precipitation data was obtained from meteorology general directorate (MGM). In this study, the maximum annual precipitation data was obtained by selecting the maximum from the monthly maximum precipitation data.

3. Research methods

3.1 Statistical Analysis

Possible precipitations are determined according to Normal, Log-Normal, Log-Pearson Type III and Gumbel method commonly used in hydrology. The maximum precipitation that can occur in T repeat year is ex-

pressed in equation (3.1) (Chow, 1951; Yuan et al., 2018).

$$X_T = \mu + (K_T \times \delta) \tag{3.1}$$

Where;

$X_T =$ The maximum value of an event corresponding to return period,

$\mu =$ Average annual maximum precipitation,

$K_T =$ Frequency factor (as shown in Table 7)

$\delta =$ Standard deviation of annual maximum precipitation.

The value of the parameter corresponding to the probability of exceedance of P and the intermediate variable used in the calculation of this value is calculated as follows.

$$P = \frac{1}{T} \tag{3.2}$$

$$w = \sqrt{\ln\left(\frac{1}{p^2}\right)} \tag{3.3}$$

$$z = w - \frac{u_1}{u_2} \tag{3.4}$$

Where, u_1 and u_2 are connected expressions w and equation (3.5 and 3.6) are calculated as specified.

$$u_1 = 2.515517 + 0.802853w + 0.010328w^2 \tag{3.5}$$

$$u_2 = 1 + 1.432788w + 0.189269w^2 + 0.001308w^3 \tag{3.6}$$

Table 5. *Formula of statistical parameters*

Parameter Name	Formula
Arithmetic mean	$\overline{x} = \dfrac{\sum\limits_{N}^{i=1} X_{\hat{Y}}}{N}$
Standard deviation	$\sqrt{\sum\limits_{i=1}^{N} \dfrac{(x_i - \overline{x})^2}{N-1}}$

Coefficient of variation	$C_V = \dfrac{S}{\overline{X}}$	

Coefficient of skewness	$C_S = \dfrac{N\sum\left(x-\overline{x}\right)^3}{\left(N-1\right)\left(N-2\right)S^3}$	

The definition of probability distribution functions is shown in Table 5. The frequency factor (K_T) is summarized and shown in the Table 6.

Table 6. *Description of five different probability distribution functions*

Distribution	Probability Distribution Function	Parameters in terms of the sample moment
Normal	$f(x) = \dfrac{1}{\delta\sqrt{2\pi}} \exp\left(-\dfrac{\left(x-\mu\right)^2}{2\delta^2}\right)$	$\mu = \overline{x}$ $\delta = S_X$
Log-Normal (LN)	$f(x) = \dfrac{1}{x\delta\sqrt{2\pi}} \exp\left(-\dfrac{\left(y-\mu_y\right)^2}{2\delta_y^{\,2}}\right)$ Where; $y = \log x$	$\mu_y = \overline{y}$ $\delta_y = S_y$
Gumbel	$f(x) = \dfrac{1}{a}\exp\left[-\dfrac{\left(x-u^2\right)}{a} - \exp\left(-\dfrac{x-u}{a}\right)\right]$	$a = \dfrac{\sqrt{6S_X}}{\pi}$ $u = \overline{x} - 0.5772\alpha$

The range of probability distributions specified in Table 6 is as follows; Normal distribution: $-\infty \le x \le +\infty$, Log Normal Distribution: $x > 0$, Gumbel distribution: $-\infty \le x \le +\infty$.

Table 7. *Frequency factor (K_T) of four different distributions*

Distribution	Frequency Factor (K_T)
Normal	$K_T = z$
Log-Normal (LN)	$K_T = z$ Where, $y_T = \overline{y} + K_T * S_y$, $y = \log x$

Log Pearson Type III	$K_T = z + (z^2-1)k + \dfrac{1}{3}(z^3-6z)k^2 - (z^2-1)k^3 + zk^4 + \dfrac{1}{3}k^5$
	Where, $k = C_S/6$
	C_S is coefficient of skewness of y
	K_T can also be read from the table depending on the coefficient of skew and the year of repetition (T) (as shown in Figure 6) (Usul,2013).
Gumbel	$K_T = -\dfrac{\sqrt{6}}{\pi}\left\{0.5772 + \ln\left[\ln\left(\dfrac{T}{T-1}\right)\right]\right\}$
	Where, T is the return period in years

	Repeat Period (T)										
	1.010	1.25	2	5	10	25	50	100	200	500	
Cs	Exceedance Probability (P)										Cs
	99	80	50	20	10	4	2	1	0.5	0.1	
3.0	-0.667	-0.636	-0.396	0.420	1.180	2.278	3.152	4.051	4.970	7.250	3.0
2.8	-0.714	-0.666	-0.384	0.460	1.210	2.275	3.114	3.973	4.847	6.915	2.8
2.6	-0.769	-0.696	-0.368	0.499	1.238	2.267	3.071	3.889	4.718	6.672	2.6
2.4	-0.832	-0.725	-0.351	0.537	1.262	2.256	3.023	3.800	4.584	6.423	2.4
2.2	-0.905	-0.752	-0.330	0.574	1.248	2.240	2.970	3.705	4.444	6.168	2.2
2.0	-0.990	-0.777	-0.307	0.609	1.302	2.219	2.912	3.605	4.298	5.908	2.0
1.8	-1.087	-0.799	-0.282	0.643	1.318	2.193	2.848	3.499	4.147	5.642	1.8
1.6	-1.197	-0.817	-0.254	0.675	1.329	2.163	2.780	3.388	3.990	5.371	1.6
1.4	-1.318	-0.832	-0.225	0.705	1.337	2.128	2.706	3.271	3.828	5.095	1.4
1.2	-1.449	-0.844	-0.195	0.732	1.340	2.087	2.626	3.149	3.661	4.815	1.2
1.0	-1.588	-0.852	-0.164	0.758	1.340	2.043	2.542	3.022	3.489	4.531	1.0
0.8	-1.733	-0.856	-0.132	0.780	1.336	1.993	2.453	2.891	3.312	4.244	0.8
0.6	-1.880	-0.857	-0.099	0.800	1.328	1.939	2.359	2.755	3.132	3.956	0.6
0.4	-2.029	-0.855	-0.066	0.816	1.317	1.880	2.261	2.615	2.949	3.666	0.4
0.2	-2.178	-0.850	-0.033	0.830	1.301	1.818	2.159	2.472	2.763	3.377	0.2
0.0	-2.326	-0.842	0	0.842	1.282	1.751	2.054	2.326	2.576	3.090	0.0
-0.2	-2.472	-0.830	0.033	0.850	1.258	1.680	1.945	2.178	2.388	2.808	-0.2
-0.4	-2.615	-0.816	0.366	0.855	1.231	1.606	1.834	2.029	2.201	2.533	-0.4
-0.6	-2.755	-0.800	0.099	0.857	1.200	1.528	1.720	1.880	2.016	2.268	-0.6
-0.8	-2.891	-0.780	0.132	0.856	1.166	1.448	1.606	1.733	1.837	2.017	-0.8
-1.0	-3.022	-0.758	0.164	0.852	1.128	1.366	1.492	1.588	1.664	1.786	-1.0
-1.2	-3.149	-0.732	0.195	0.844	1.086	1.282	1.379	1.449	1.501	1.577	-1.2
-1.4	-3.271	-0.705	0.225	0.832	1.041	1.198	1.270	1.318	1.351	1.394	-1.4
-1.6	-3.388	-0.675	0.254	0.817	0.994	1.116	1.166	1.197	1.216	1.238	-1.6
-1.8	-3.499	-0.643	0.282	0.799	0.945	1.035	1.069	1.087	1.097	1.107	-1.8
-2.0	-3.605	-0.609	0.307	0.777	0.895	0.959	0.980	0.990	0.995	1.999	-2.0
-2.2	-3.705	-0.574	0.330	0.752	0.844	0.888	0.900	0.905	0.907	0.909	-2.2
-2.4	-3.800	-0.537	0.351	0.725	0.795	0.823	0.830	0.832	0.833	0.833	-2.4
-2.6	-3.889	-0.499	0.368	0.696	0.747	0.764	0.768	0.769	0.769	0.769	-2.6
-2.8	-3.973	-0.460	0.384	0.666	0.702	0.712	0.714	0.714	0.714	0.714	-2.8
-3.0	-4.051	-0.420	0.396	0.636	0.660	0.666	0.666	0.667	0.667	0.668	-3.0

Figure 6. Frequency Factors K_T for log Pearson Type III Distributions

3.2 Goodness of fit tests for precipitation data

Stations with reliable monitoring for at least 10 years are used in maximum precipitation repetition analysis (MGM, 2019). However, longer precipitation records can provide more reliable results. EasyFit package program was used to determine which distribution fits to precipitation records of observation stations. EasyFit is a data analysis and simulation software that allows us to fit and simulate statistical distributions. Normal, Log-Normal, Log-Pearson Type III and Gumbel probability distribution functions (pdf) are frequently used in hydrological events. These four distributions were selected in the program in order to shorten the processing time. Kolmogorov-Smirnov, Anderson Darling and Chi-Square goodness of fit tests were used in the study. In the K-S test, the maximum difference between the additive probability function, P0 (x), which is assumed to be accepted by the annexed probability function, P (x), is the measured difference between the theoretical model and the observed data. This difference; Equation (3.7) can be shown as. If the Dn value is less than the critical value, the default distribution is assumed; otherwise, it is rejected at the stated level of significance (Karahan & Özkan, 2013).

$$D_{Max} = Max \left| p(x) - p_0(x) \right| \tag{3.7}$$

The Anderson-Darling test uses the critical value of the distribution unlike the K-S test. Anderson-Darling, one of the most powerful normality tests, is more sensitive to the type of distribution. A^2 test statistics were corrected for small volume samples. The corrected A^2 test statistic is given in equation (3.8) (Karahan & Özkan, 2013; Şeker, 2015).

$$A_{adj}^2 = A^2 \left(1 + \frac{0.75}{n} + \frac{2.25}{n^2} \right) \tag{3.8}$$

A^2 critical values; $A_{0.05}^2 = 0.752$, $A_{0.025}^2 = 0.873$, $A_{0.01}^2 = 1.035$

Chi-Square test statistic is calculated according to equation (3.9). To make a reliable estimate in the Chi-Square test expected frequencies should not be less than 5.

$$X_P^2 = \sum_{i=1}^{k} \frac{(G_i - T_i)^2}{T_Ý} \tag{3.9}$$

Where; G_i and T_i are observed frequencies and theoretical frequencies, respectively.

4. Results and discussion

The probability distribution analysis of annual maximum precipitation for the chosen locations is computed using various probability distribution functions. The values used in the probability distribution functions calculated from the precipitation data are shown in the Table 8. The probability distribution function (pdf) parameters are given in Table 9.

Table 8. Parameters used in statistical models for Susurluk Basin

Parameter	Stations (Name/No)					
	Bandırma 17114	**Bursa 17116**	**Dursun Bey 17700**	**Keles 17695**	**Simav 17748**	**Tavşanlı 17704**
Observation Years	48	48	48	48	48	48
Linear Average	65,16	49,31	40,05	44,86	59,76	36,99
Linear Standard Deviation	41,11	16,87	15,01	16,06	23,83	15,03
Linear Skew	2,94	1,41	2,02	3,37	1,90	2,45
Logarithmic Average	1,76	1,67	1,57	1,63	1,74	1,54
Logarithmic Standard Deviation	0,19	0,13	0,13	0,12	0,15	0,14
Logarithmic Skew	1,32	0,23	0,73	1,25	0,16	0,67

Table 9. *The pdf parameters for Susurluk Basin*

Station	Normal	Log-Normal	Log Pearson Type III	Gumbel Max.
Bandırma	σ=41,115 μ=65,165	σ=0,4411 μ=4,0584	α=2,2895 β=0,29457 γ=3,384	σ=32,058 μ=46,66
Bursa	σ=16,874 μ=49,317	σ=0,31661 μ=3,8469	α=70, 507 β=0,0381 γ=1,1602	σ=13,157 μ=41,722
DursunBey	σ=15,015 μ=40,052	σ=0,31866 μ=3,6352	α=7,3158 β=0,11906 γ=2,7642	σ=11,707 μ=33,295
Keles	σ=16,064 μ=44,869	σ=0,27641 μ=3,7602	α=2,528 β=0,17569 γ=3,3161	σ=12,525 μ=37,639
Simav	σ=23,832 μ=59,769	σ=0,36092 μ=4,0236	α=140,54 β=0,03077 γ=-0,3004	σ=18,582 μ=49,043
Tavşanlı	σ=15,031 μ=36,998	σ=0,33857 μ=3,5486	α=8,6797 β=0,11614 γ=2,5406	σ=11,72 μ=30,233

The results obtained with the application of the statistical models indicated in the 48-year precipitation records are given in Table 10.

Table 10. *Probable precipitations according to pdf for Susurluk Basin*

	Probability Distribution Function	Year of repetition							
		2	5	10	25	50	100	200	500
Bandırma	Normal	65,1	99,6	117	137	150	161	171	183
	LogNormal	57,8	84,1	102	126	145	164	183	208
	LP III	52,7	79,3	104	148	192	247	315	431
	Gumbel	58,4	94,7	118	149	171	194	216	245
Bursa	Normal	49,3	63,4	70,9	78,9	84,1	88,7	92,9	97,8
	LogNormal	46,8	61,2	70,5	82,1	90,6	98,9	107	117
	LP III	46,2	60,9	71,1	84,3	94,4	104	115	128
	Gumbel	46,5	61,4	71,3	83,8	93,1	102	111	123
Dursunbey	Normal	40,0	52,6	59,2	66,4	71,0	75,1	78,8	83,2
	LogNormal	37,9	49,6	57,2	66,7	73,6	80,4	87,1	95,6
	LP III	36,4	48,7	58,1	71,8	83,2	95,6	109	128
	Gumbel	37,5	50,8	59,6	70,7	78,9	87,1	95,2	106
Keles	Normal	44,8	58,3	65,4	73,0	78,0	82,4	86,3	91,0
	LogNormal	42,9	54,2	61,4	70,1	76,4	82,5	88,4	95,8
	LP III	40,6	52,4	62,2	77,2	90,5	105	122	148
	Gumbel	42,2	56,4	65,8	77,7	86,5	95,2	103	115
Simav	Normal	59,7	79,7	90,3	101	108	115	121	128
	LogNormal	55,9	75,9	89,2	106	118	131	143	159
	LP III	55,3	75,6	89,7	108	122	137	152	171
	Gumbel	55,8	76,9	90,8	108	121	134	147	164
Tavşanlı	Normal	36,9	49,6	56,2	63,4	68,0	72,1	75,8	80,1
	LogNormal	34,7	46,3	53,8	63,4	70,4	77,3	84,1	92,9
	LP III	33,4	45,5	54,7	68,1	79,3	91,5	104	123
	Gumbel	34,5	47,8	56,6	67,7	75,9	84,1	92,3	103

The values used in statical models calculated from the precipitation data are shown in the Table 11. The pdf parameters are given in Table 12.

Table 11. *Parameters used in statistical models for Van Lake Basin*

Parameters	Stations (Name/No)					
	Ahlat 17810	Erciş 17784	Gevaş 17852	Muradiye 17786	Tatvan 17205	Van 17172
Observation Years	48	48	36	48	46	48
Linear Average	35,53	27,81	36,96	33,98	46,42	31,27
Linear Standard Deviation	11,19	8,76	11,51	14,08	12,79	16,08
Linear Skew	0,70	1,45	0,77	1,30	0,49	4,09
Logarithmic Average	1,52	1,42	1,54	1,49	1,65	1,46
Logarithmic Standard Deviation	0,13	0,12	0,13	0,17	0,12	0,15
Logarithmic Skew	-0,23	0,66	-0,03	0,12	-0,21	1,51

Table 12. *The pdf parameters for Van Lake Basin*

Station	Normal	Log-Normal	Log Pearson Type III	Gumbel Max.
Ahlat	σ=11,199 μ=35,538	σ=0,31507 μ=3,5221	α=75,243 β=-0,03671 γ=6,284	σ=8,7316 μ=30,497
Erciş	σ=8,7634 μ=27,817	σ=0,28136 μ=3,2837	α=9,0802 β=0,09436 γ=2,4269	σ=6,8328 μ=23,873
Gevaş	σ=11,513 μ=36,967	σ=0,30411 μ=3,564	α=2899 β=-0,00573 γ=20,17	σ=8,9764 μ=31,785
Muradiye	σ=14,08 μ=33,988	σ=0,38816 μ=3,4496	α=238,88 β=0,02538 γ=-2,6132	σ=10,978 μ=27,651
Tatvan	σ=12,797 μ=46,428	σ=0,27692 μ=3,8003	α=90,691 β=-0,0294 γ=6,4666	σ=9,9782 μ=40,669
Van	σ=16,085 μ=31,277	σ=0,34911 μ=3,3684	α=1,7342 β=0,26791 γ=2,9038	σ=12,541 μ=24,038

Table 13. *Probable precipitations according to pdf for Van lake Basin*

	Probability Distribution Function	Years of repetition							
		2	5	10	25	50	100	200	500
Ahlat	Normal	35,5	44,9	49,8	55,2	58,6	61,7	64,4	67,7
	LogNormal	33,8	44,2	50,9	59,2	65,3	71,2	77,0	84,5
	LP III	34,2	44,3	50,4	57,6	62,7	67,4	71,9	77,4
	Gumbel	33,6	43,5	50,1	58,4	64,5	70,6	76,7	84,7
Erciş	Normal	27,8	35,1	39,0	43,2	45,9	48,2	50,4	53,0
	LogNormal	26,6	33,8	38,3	43,9	47,9	51,8	55,6	60,3
	LP III	25,8	33,3	38,9	46,6	52,8	59,4	66,4	76,2
	Gumbel	26,3	34,1	39,2	45,7	50,5	55,3	60,0	66,3
Gevaş	Normal	36,9	46,6	51,7	57,1	60,7	63,8	66,7	70,0
	LogNormal	35,3	45,7	52,4	60,6	66,7	72,5	78,3	85,6
	LP III	35,3	45,7	52,3	60,4	66,3	71,9	77,4	84,4
	Gumbel	35,0	45,2	51,9	60,4	66,8	73,0	79,3	87,5
Muradiye	Normal	33,9	45,7	52,0	58,7	63,0	66,8	70,3	74,5
	LogNormal	31,4	43,7	52,0	62,7	70,7	78,7	86,7	97,2
	LP III	31,2	43,6	52,3	63,8	72,7	81,7	91,0	103
	Gumbel	31,6	44,1	52,3	62,7	70,4	78,1	85,7	95,8
Tatvan	Normal	46,4	57,1	62,8	68,9	72,8	76,3	79,4	83,2
	LogNormal	44,7	56,5	64,0	73,1	79,6	86,0	92,1	99,9
	LP III	45,1	56,6	63,5	71,6	77,1	82,3	87,2	93,1
	Gumbel	44,3	55,6	63,1	72,5	79,6	86,5	93,5	102
Van	Normal	31,2	44,7	51,8	59,5	64,4	68,8	72,8	77,5
	LogNormal	29,0	39,0	45,6	53,9	60,1	66,2	72,2	80
	LP III	26,7	36,8	46,2	61,9	77,0	95,5	118	154
	Gumbel	28,6	42,8	52,2	64,1	72,9	81,7	90,4	101

Probable precipitation obtained by using probability distribution functions depending on the recurrence years is shown in Table 13.

5.   Conclusion

Statistical analysis is carried out for various purposes such as agriculture, planning of water structures and drainage. Annual maximum precipitation records of precipitation observation stations in two different basins were used in this study. Observation times of these stations range from 36 to 48 years. The probability distribution function which is suitable in the study was determined by using EasyFit package program. The Easy-Fit package program lists the probability distribution functions by giving the number 1 to the most appropriate distribution. All three fit goodness tests were used to determine which distribution station matched. For this purpose, the number sequences of the probability distribution functions in Kolmogorov-Smirnov, Anderson Darling and Chi-Square tests were collected. The distribution with the lowest score is considered to be the most appropriate distribution.

The Susurluk Basin, which is in the Western position of Turkey, is expected to receive more precipitation than the Lake Van Basin, which is in the eastern position of Turkey, during the same time period. The reason for this situation may be that the continental climate is seen in the east of Turkey and the temperate climate type appears in the West.

As a result of the study, it was determined that Log Normal probability distribution function fits all precipitation observation stations in Susurluk basin. The most suitable probability distribution function for the Dursunbey station is both Log Pearson Type III and Log Normal because the score of both probability distribution functions is equal. However, Log Pearson Type III in the first place in two of the conformity tests (K-S and AD) may cause this probability distribution to be preferred. The probability distributions fitting the precipitation records of precipitation observation stations in Lake Van Basin are as follows: Gumbel compatible for Ahlat and Erciş, Log Pearson Type III compatible for Gevaş and Muradiye. The most suitable probability distribution function for the Tatvan station is both Log Pearson Type III and Gumbel because the score of both probability distribution functions is equal . However, log pearson type III in the first place in two of the conformity tests (K-S and AD) may cause this probability distribution to be preferred. Finally, the probability distribution for the Van station was determined to be Log Normal.

al Directorate/Sakarya for providing the necessary data for the realization of the study.

References

Aşıkoğlu, L. Ö. (2017). Frekans analizinde alternatif bir parametre tahmin metodu. *S.Ü. Müh. Bilim ve Tekn. Derg.* 4(5), 445-459. DOI: 10.15317/ Scitech.2017.104

Atroosh, K. B. and Moustafa A.T. (2012). An estimation of the probability distribution of Wadi Bana Flow in the Abyan Delta of Yemen. *Journal of Agricultural Science*, 6(4), 80-89. DOI: 10.5539/jas.v4n6p80

Aytulun, U. 2019. İklim değişikliğinin Susurluk ve Van Gölü Havzalarının meteorolojik verilerine etkisinin trend analiz yöntemleri ile araştırılması. Sakarya Uygulamalı Bilimler Üniversitesi, Fen Bilimleri Enstitüsü, İnşaat Mühendisliği Bölümü, Yüksek Lisans Tezi.

Baghel,H., Mittal H.K., Singh P. K., Yadav, K.K. and Jain, S. (2019). Frequency analysis of rainfall data using probability distribution models. *International Journal of Current Microbiology and Applied Sciences,* 6(8): 1390-1396.

Chow, V. T. (1951). A general formula for hydrologic frequency analysis. *Eos, Transactions American Geophysical Union,* 2(32): 231-237.

Chow, V. T., Maidment, D. R., Mays, L. W. (1988). *Applied Hydrology*. New York: McGraw-Hill.

Demir, F. 2014. Aşağı Sakarya Nehri Adapazarı kesimi taşkın risk tayini. Sakarya Üniversitesi, Fen Bilimleri Enstitüsü, İnşaat Mühendisliği Bölümü, Yüksek Lisans Tezi.

Esberto, M.D.P. (2018). probability distribution fitting of rainfall patterns in Philippine Regions for effective risk management. *Environment and Ecology Research,* 6(3): 178-86.

Husak, G. J., Michaelsen J. and Funk C. (2006). Use of the gamma distribution to represent monthly rainfall in Africa for drought monitoring applications. *International Journal of Climatology*, 7(27), 935-944. DOI: 10.1002/joc.1441.

Kalita, A., Bormudoi, A. and Saikia M.D. (2017). Probability distribution of rainfall and discharge of Kulsi River Basin. *International Journal of Engineering and Advanced Technology (IJEAT),* 6(4):31-37.

Karahan, H. and Özkan, E. (2013). Ege bölgesi standart süreli yıllık maksımum yağışları için en uygun dağılımlar. *Pamukkale Üniversitesi Mühendislik Bilimleri Dergisi*, 3(19), 152-157.DOİ: 10.5505/ pajes.2013.29392

Khosravi, Gh, Majidi, A. and Nohegar, A. (2012). Determination of suitable probability distribution for annual mean and peak discharges estimation (Case Study: Minab River- Barantin Gage, Iran).

International Journal of Probability and Statistics, 1(5), 160-163. DOI: 10.5923/j.ijps.20120105.03.

Lee, C. (2005). Application of rainfall frequency analysis on studying rainfall distribution characteristics of Chia-Nan Plain Area in Southern Taiwan. *Crop, Environment & Bioinformatics.* (2), 31-38.

MGM, Maksimum Yağışlar Şiddet ve Tekerrür Analizleri. (16/08/2019 and https://www.mgm.gov.tr)

Olofintoye, O.O, Sule, B.F. and Salami, A.W. (2009). Best–fit Probability distribution model for peak daily rainfall of selected Cities in Nigeria. *New York Science Journal*, 2(3), 1-12.

Salami, A.W. (2004). Prediction of the annual flow regime along Asa River using probability distribution models. *AMSE periodical, Lyon, France. Modelling C.* 65 (2), 41-56.

Susurluk Havzası Yönetim Planları Ekleri (2018). (15/08/2019 and https://www.tarimorman.gov.tr)

Şeker, M. 2015. Antalya havzasının taşkın frekans analizi. Pamukkale Üniversitesi, Fen Bilimleri Enstitüsü, İnşaat Mühendisliği Bölümü, Yüksek Lisans Tezi.

Tao, D.Q, Nguyen, V.T and Bourque, A. (2002). On selection of probability distributions for representingnextreme precipitations in Southern Quebec. *Annual Conference of the Canadian Society for Civil Engineering*, 5th -8th June 2002, Canada, 1-8.

Usul, N. (2013). *Mühendislik Hidrolojisi*. Ankara: Odtü Yayıncılık.

Yuan, J., Emura, K., Farnham, C. and Alam Md. (2018). Frequencyanalysis of annual maximum hourly precipitation anddetermination of bestfit probability distribution for regions in Japan. *Urban Climate,* 24:276-286.

Chapter 18

DETECTION METHODS AND NOVEL SENSOR STUDIES FOR CORONA VIRUS

Yeliz İPEK[1], Özlem ERTEKİN[2]

1 Dr. Öğr. Üyesi , Munzur University, Vocational School of Tunceli, Rare Earth Element Research and Application Center, Munzur University, yelizipek@munzur.edu.tr, ORCID 0000-0002-9390-9875

2 Dr. Öğr. Üyesi , Department of Nutrition and Dietetics, Faculty of Health Sciences, Munzur University,

Introduction

The coronavirus appeared under the name COVID-19 in Wuhan, Hubei province of China in December 2019, causing it to spread rapidly all over the world, resulting in the death of a large number of people due to respiratory or multiple organ failure. In contrast, the COVID-19 outbreak was declared by the world health organization as a pandemic. Then, various coronavirus measures were taken all over the world and every area of life was affected by this situation [1, 2, 3, 4].

Figure 1. A picture taken from a metro in pandemi days.

The new virus causing the current pandemic has been named COVID-19 (SARS-CoV-2) [5, 6]. With the spread of the epidemic, similar cases have been detected in other cities in China and in many countries [1]. This current event in the world has been declared an epidemic by the World Health Organization (WHO) [7, 8, 9].

Figure 2. Corona virus disease (Covid-19) in a hospital.

Health systems involving sensitive measures were needed for the COVID-19 outbreak. This requires long-term planning. In this context, it was necessary to invest in health services due to the conditions of COVID-19 [10]. World Health Organization (WHO) and the US Center for Disease Control and Prevention (CDC) are working to better understand the epidemic in rapidly changing situations and help the public [11, 4]

According to research, in China Wuhan, the COVID-19 outbreak occurred in the live seafood and meat market. This situation led to important changes in food habits for the public. Food is required to be cooked and consumed properly; Warnings were given about how food can lead to disease crises such as COVID-19 when not consumed by cooking. Accordingly, the Chinese government has banned the trade and consumption of wild animals as food [12].

Coronaviruses are single-chain, positive polarity, RNA viruses [4, 10, 12, 13]. Because they have positive polarity, they do not contain RNA-dependent RNA polymerase enzymes, but in their genomes they encode this enzyme. They have rodlike extensions on their surfaces. Because of these extensions, these viruses are called coronavirus [13]. Coronaviruses are in the Coronaviridae family. They are classified into four main types. These are classified as alpha, beta, gamma and delta coronaviruses. These viruses can be found in humans, bats, pigs, cats, dogs, rodents and poultry [13]. Also, coronaviruses are zoonotic pathogens [12]. These viruses can often infect animals, including birds and mammals. Causes mild respiratory infections in humans, such as those often observed in the common cold [4]. This virus is genetically approximately 70% similar to the SARS virus and 96% similar to a bat coronavirus. This virus is suspected to be bat-borne [14].

COVID-19 is due to SARS-CoV-2, a betacoronavirus. Sequence analysis of the SARS-CoV-2, although it belongs to the Coronavirinae subfamily, which is part of the Coronaviridae family, showed a unique structure [10].

The results obtained from phylogenetic analysis for SARS-CoV and MERS-CoV, which are considered as reservoir hosts, are thought to be important starting points for the investigation of the virus source [15].

In etiological examinations, SARS-CoV-2 nucleic acids in nasopharyngeal swab samples, in the secretions of the lower respiratory tract, in the blood and feces; It can be detected using RT-PCR and new generation sequencing (NGS) technologies. Detection from secretions of the lower respiratory tract can give more accurate results [1].

In the initial stage of the COVID-19 outbreak, RT-PCR-based testing provided specific diagnosis for the detection of SARS-CoV-2 RNA in

samples. This test played a critical role in the early diagnosis of patients in Wuhan [16].

In the coronavirus Covid-19 outbreak, the importance of studies in molecular biology and genetics has increased. Coronavirus tests are used to help diagnose infections and prevent the spread of the disease. It is tried to provide fast and accurate diagnosis of the virus by using samples from nose, throat or lungs. The most commonly used tests to detect the 2019-nCoV, formerly COVID-19 corona virus, are divided into 2 categories: the Covid-19 Rapid Test Kit and the Covid-19 PCR Test Kit. First, the COVID-19 Rapid Test Kit gives quick results and no device is required. COVID-19 rapid test kits are also divided into 2 categories. These; Rapid Antibody Test (lgG/lgM Antibody) and Rapid Antigen Test (Fluorescence Ag) [17]. The human body forms antibodies in response to many infections. These antibodies are proteins called immunoglobulins. Antibody tests are lgG, lgA, lgM analysis of immunoglobulins produced in response to infections. Antibodies can be found in the blood of people tested after the infection and show people's immune response to infection. Antibody test results are also important for the detection of infections that have had little or no symptoms. lgG, lgM and lgA antibodies are examined for COVID-19 infection. Different types of antibodies can be analyzed by various analysis methods. It is a very important parameter that shows that individuals with positive lgG Antibody have had Covid-19 infection [18].

The second method is the PCR test. This test is also known as molecular diagnostic test. This method, which includes molecular technique, is real-time PCR technique. Thanks to the PCR test, the virus in the sample taken from the patient can be detected directly. In order to perform PCR test, a throat and nose swab sample or sputum sample is taken from the patient. PCR testing requires a laboratory, PCR device and trained personnel in accordance with the standards [17].

If the coronavirus tests are summarized briefly; The PCR test looks for virus RNA; The sample to be taken is a nose or throat swab. Virus proteins are examined in antigen testing; The sample to be taken is a nose or throat swab. In the antibody test, immune system molecules are examined; the sample to be taken is blood. In other words, laboratory tests for coronavirus disease (COVID-19) and associated SARS-CoV-2 virus detect the presence of the virus and antibodies produced in response to infection. That is, the presence of viruses in the samples is confirmed by RT-PCR, which detects coronavirus RNA. This test is specific. Detection of antibodies shows both diagnosis and how many people have the disease. Test using real-time reverse transcription polymerase chain reaction (rRT-PCR) can be performed on respiratory samples obtained by various methods, including nasopharyngeal swab or sputum sample [19]. Basical-

ly, Polymerase chain reaction (PCR) is the method that allows the desired regions to be replicated in any organism's DNA. PCR technique is the reproduction of nucleotides in the tube under suitable conditions. It is the enzymatic synthesis of copies of certain DNA fragments by directing them with primers.

In the use of real-time (Real-Time, RT) PCR technique kits, direct detection is made using the virus RNA in the sample. For the operation of the kit, RNA isolation is performed by taking a throat and nose swab sample first. Then, the RNA sample is mixed with the kit and analyzed with the qPCR device. Synthetic DNA sequences, called primers or probes, are designed that can specifically bind to the protected gene region of the virus. The RNA of the virus is first converted to DNA using a special enzyme. Primers recognize and bind to the desired gene in this DNA, and copies of DNA are synthesized with the enzyme Polymerase working during the PCR reaction [20].

As a result, the COVID-19 outbreak has been recognized as a global health problem. It is thought that the effect of this viral infection will continue. Therefore, a virus-specific vaccine needs to be developed. Obviously, due to the rapid spread of the COVID-2019 outbreak with pandemic potential, it is important to increase the studies in molecular biology and genetics and to share the research findings obtained.

Electrochemical Sensors and Detection Principals

The existance of microorganisms can be determined by various traditional test methods, as well as new detection techniques are being developed in parallel with developing science and technology. Electrochemical sensors or electrochemical biosensors are one of these new techniques. They allow very precise and accurate measurements. However, in order to do this, it should be designed to be selective and sensitive to the substance or microorganism to be analyzed. The sensitivity of the sensors is critical in detecting their target molecule. The detection limit of the sensors are also critical parameters as they can influence their positive and negative predictive values. Researchers also report the linear range of biosensors, which indicates the detection limit of the sensor [21]. The detection limit (lower limit of detection, or LOD: limit of detection), is the lowest quantity of a substance that can be sensed by the electrochemical sensor.

Measurement principle with a three electrode cell consisting electrochemical sensor is based on the reaction taking place at the working electrode surface between the working electrode (WE) and analyte. In such a three-electrode cell, the reaction takes place at the interface between the working electrodes (WE) and electrolyte. There are four types of electrochemical sensors according to measured signal type: Amperometric sen-

sor, potentiometric sensor, impedimetric and capacitive and conductometric sensor.

Figure 3. Three electrode cell consisting electrochemical sensor studies.

Amperometric Sensors:

An amperometric sensor a constant potential is maintained between the reference electrode (RE) and the WE. The third electrode, the counter electrode (CE), provides a current path to the WE. When there is an interaction on the working electrode surface, current of the system changes. The change is calculated depending on the reference electrode and provided as an observable data using a computer software [22]. Amperometric sensors measure the current resulting from a chemical reaction of electroactive materials on transducer/working electrode surface while a constant potential is applied. The change of current intensity is depended on the concentration of the analyte. The working electrode material may be a noble metal (gold, titanium, nickel, etc.), indium tin oxide (ITO) coated glass, or glassy carbon. The sensor material makes an electrode specific for the analyte which is coated on the working electrode. In an amperometric biosensor, a measured current change is in the range of nA to mA because of being a very sensitive process. The glucose sensor is the most widely known amperometric sensor and is also the most widely used biosensor.

Potentiometric Sensors:

Potentiometric sensors can detect potential change from a chemical

reaction of electroactive materials when constant current is applied to the system. The potentimetric signal is measured as the potential difference (voltage) between the working electrode and the reference electrode. The working electrode's potential change depends on the concentration of the analyte. Potentiometric biosensors are based on ion-sensitive field effect transistors (FETs). Potentiometry is important for the detection of redox potential and as an analytical tool for the measurement of a variety of ionic and ionizable species. In both cases, the open circuit potential of a two-electrode cell is observed where an inert metal electrode or an ion-selective electrode (also called indicator electrode) is measured against a suitable reference electrode [23].

From the viewpoint of charge transfer, there are two types of electrochemical interfaces: ideally polarized (purely capacitive) and nonpolarized. As the name implies, the ideally polarized interface is only hypothetical. Although possible in principle, there are no chemical sensors based on a polarized interface at present and we consider only the nonpolarized interface at which at least one charged species partitions between the two phases [24].

Impedimetric and Capacitive Sensors:

Electrochemical Impedance Spectroscopy (EIS) represents one of the most powerful methods, due to the ability of EIS-based sensors to be more easily integrated into multi-array or microprocessor-controlled diagnostic tools. Impedimetric or capacitive immunosensors have been successfully applied at the academic level. However, no prototypes have been released into the market, since major fundamental issues still exist. This fact has brought the reliability of impedimetric immunosensors into question [25].

Impedance changes that occurs in culture mediums due to bacterial growth as changes in conductance, due to charged ions and compounds resulting from biological metabolism, or due to bacteria cell adhesion to the electrode surface in interfacial capacitance. [26]

Impedance microbiology is one of the most successful of all the recently introduced rapid methods. Several analytical systems have been developed for bacteria detection, such as Bactometer (Bio Merieux, Nuertingen, Germany), Malthus systems (Malthus Instruments Ltd., Crawley, UK), rapid automated bacterial impedance technique (RABIT) (Don Whitley Scientific Ltd., Shipley, UK), and BacTrac (Sy-Lab, Purkersdorf, Austria) [27–30].

Conductometric Sensors:

Sensors in this group rely on changes of electric conductivity of a film or a bulk material, whose conductivity is affected by the analyte pres-

ent. There are some very practical considerations that make conductimetric methods attractive, such as low cost and simplicity, since no reference electrodes are needed. Resistance measured from a DC current is typical. Often the measurement is done with AC current (impedance), which also allows one to obtain changes in capacitive impedance [31]. The electron transfer resistance (Rct) was calculated from the diameter of the semicircle in the Nyquist diagram and provides information about the electron transfer rate at the electrode and electrolyte interface. [32]

Properties of Electrochemical Sensors

Selectivity, sensitivity, reproducibility, stability, linearity, response time, cost-effectiveness and simple usage are the main properties of an electrochemical sensor. Being selective and sensitive against the target analyte is crutial for an electrochemical sensor. Selectivity is ability to detect a specific and wanted analyte in a mixture template with other samples and contaminants. Sensitivity is limit of detection (LOD), also it is known as the smallest amount which an electrochemical sensor can detect. Stability provides incorporate constant monitoring or long incubation time. Reproducibility is the accuracy of the transducer and the electronics part of the electrochemical sensor which characterizes ability to produce similar results from each measurement of a template. The sensor gets close to the average real value of a template when the test is repeated more than once. Linearity: When the graph of the concentration value is plotted versus the signal value obtained from an electrochemical sensor, it is the range of concentration at which the signal changes linearly. the range at which a linear response is given by the sensor while measurement of an analyte is defined with linear range term. Linearity is related to its resolution and the scope of template concentration being examined [33]. When an input parameter changes, output state of the sensors do not change immediately. It will change to the new state after a period of time. This time is called as the response time (T_r).

Cost-effectiveness is an advantage of electrochemical sensors compared to conventional techniques which are more costly and time-consuming. Another advantage of an electrochemical sensor is their simple useage, which provides them to be used by patients themselves.

Electrochemical CoV sensor development studies

Coronaviruses (CoVs), which are enveloped, positive-sense, single-stranded RNA viruses of zoonotic origin and belong to the family Coronaviridae in the order Nidovirales, are divided into four genera: alpha, beta, delta and gamma coronavirus. The emerging CoVs, including severe acute respiratory syndrome coronavirus (SARS-CoV) and Middle East respiratory syndrome coronavirus (MERS-CoV), both belonging to

beta coronavirus, have caused recent pandemics of respiratory infectious diseases with high mortality [34, 35]. It has been reported that the 2019-nCoV is also genetically close to SARS-CoV [36, 37].

The coronavirus contains a spike protein as a surface protein, and the spike protein includes S1 and S2 sites. When the S1 region of the spike protein binds to the host cell, it is cleaved with S1 and S2 by a protease, and the hydrophobic region at the end of S2 is exposed and activated. When a surface protein of a virus reacts with a biomolecule, the surface protein of the virus is changed to form a fused peptide or the like. In other embodiments, the reaction of the activated virus with the probe may be a fusion reaction or an aggregation reaction. When the proteolytic enzyme and the surface protein of the coronavirus are reacted, the action of the hydrolytic enzyme occurs at the interface between the sites of S1 and S2. Therefore, the coronavirus is activated as the hydrophobic region of S2 is exposed after cleavage by the action of the hydrolase, and can be detected using the probe of the electrochemical sensor. Activation of the viral surface protein means that the fusion protein or fusion peptide present in the surface protein of the virus is in a condition capable of causing a fusion reaction with the membrane of the host cell or the surface of the probe of the sensor.

The surface protein, Sp protein (S protein), is converted into an exposed form by the biomolecule in the form of the hydrophobic part existing inside the spike protein in an inactive form. Specifically, when the S1 portion of the spike protein binds to the host cell, it is cleaved with S1 and S2 by a protease, and the hydrophobic region at the end of S2 is exposed to activate the virus. In S2, the exposed hydrophobic region is attached to the hydrophobic region in the cell membrane of the host cell and the other is bound to the viral outer membrane, and the conformational change in the middle of the S2 region occurs and membrane fusion occurs. Therefore, when the probe of the sensor reacts with the activated corona virus, the stability of the probe changes and various signals are generated. The virus infection can be detected by measuring the change [38].

Immunological detection methods such as enzyme-linked immunosorbent assay (ELISA), enzyme immunoassay (EIA) and immunofluorescence assay (IFA), and RNA detection methods by RT-PCR are known as traditional diagnostic methods for such viruses. Such a method has problems like excessive time for virus diagnosis, high cost of testing, low specificity and sensitivity due to nonspecific reaction [39, 40].

Recently an alternative technique using electrochemical sensor has been studied for detection of various types of analytes. Electrochemical sensors for determining viruses are divided into four main groups includ-

ing nucleic acid-based, antibody-based, aptamer-based and antigen-based electrochemical biosensors [41]. The electrochemical techniques can be classified into four major groups including potentiometry, amperometry, cyclic voltammetry, and impedimetry. The properties such as high sensitivity and selectivity, low cost, simple operation, portability and fast analysis makes electrochemical methods suitable for detection of a virus which spread all over the world rapidly.

GenMark Diagnostics, Inc. Developed an electrochemical SARS-CoV-2 sensor on March, 2020 in USA with a detection limit of 1×10^5 copies/mL. eSensor technology is based on the principles of competitive DNA hybridization and electrochemical detection, which is highly specific and is not based on fluorescent or optical detection. The target DNA is mixed with ferrocene-labeled signal probes that are complementary to the specific targets on the panel. Target DNA hybridizes to its complementary signal probe and capture probes, which are bound to gold-plated electrodes, as shown below in Figure 4. The presence of each target is determined by voltammetry which generates specific electrical signals from the ferrocene-labeled signal probe. Target-specific capture probes are bound to the gold electrodes in the eSensor microarray on the ePlex cartridge. The amplified target DNA hybridizes to the capture probe and to a complementary ferrocene-labeled signal probe. Electrochemical analysis determines the presence or absence of targets using voltammetry.
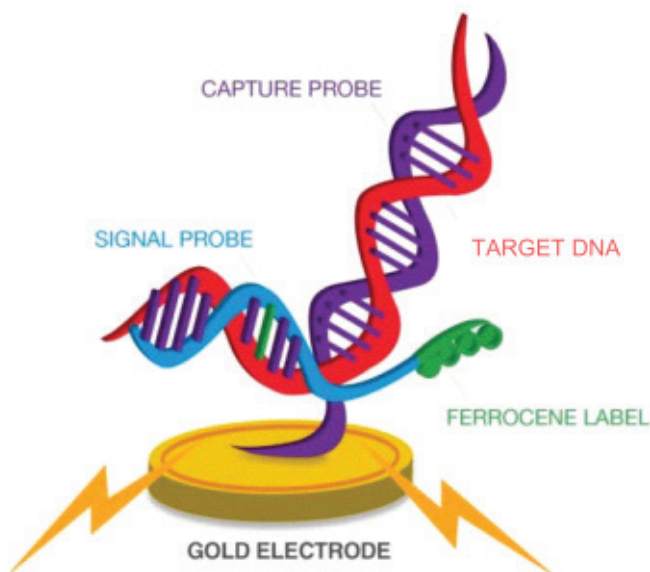

Figure 4. Design of the sensor probe of SARS-CoV-2 sensor [42].

Mahari et al. developed an in-house built biosensor device (eCovSens) and compared it with a commercial potentiostat machine for the detecti-

on of nCovid-19 spike protein antigen (nCovid-19 Ag) in spiked saliva samples. A potentiostat based sensor was fabricated using fluorine doped tin oxide electrode (FTO) drop casted with gold nanoparticle (AuNPs) and immobilized with nCovid-19 monoclonal antibody (nCovid-19 Ab) to measure change in the electrical conductivity. Similarly, eCovSens was used to measure change in electrical conductivity by immobilizing nCovid-19 Ab on screen printed carbon electrode (SPCE). The performances of both sensors were recorded upon interaction of nCovid-19 Ab with its specific nCovid-19 Ag. Under optimum conditions, the FTO based immunosensor and proposed SPCE-based biosensor device displayed high sensitivity for early detection of nCovid-19 Ag, ranging from 1fM to 1uM. Our in-house developed eCovSens device can successfully detect nCovid-19 Ag at 10 fM concentration in standard buffer that is in close agreement with FTO/AuNPs sensor where AuNPs were used for the amplification of the electrical signal. The limit of detection (LOD) was found to be 90 fM with eCovSens and 120 fM with potentiostst in case of spiked saliva samples. The proposed portable point of care (PoC) eCovSens device can be used as an alternative diagnostic tool for the rapid (within 10-30 s) detection of nCovid-19 Ag traces directly in patient saliva samples that displayed high sensitivity, stability, and specificity [43].

CoV sensor studies with other detection methods

There is also nanosensor diagnostics platforms in development to test for the virus, which would replace thermal screening guns, currently screening for high fever in people coming through airports and border controls. This technology, which will be in the form of a hand-held device, claims to give results specific for this virus and can produce a result within one minute. It does this by detecting the nucleocapsid protein specific for this virus by nanosensor and aptamer technology [44].

Zuo et al. developed a piezoelectric immunosensor for the detection of SARS-associated coronavirus (SARS-CoV). Horse polyclonal antibody against SARS-CoV was bound onto the PZ crystal surface in an ordered orientation through protein A. The antigen sample was atomized into aerosol by an ultrasonator, by which the antibody on the crystal could specifically adsorb SARS antigen and the changed mass of crystal would lead a frequency shift. A frequency counter was employed to record the admittance frequency, and the plot of changed frequency was displayed on the computer. The frequency shifts were linearly dependent on antigen concentration in the range of 0.6−4 μg/mL. The device could be reused 100 times without detectable loss of activity, was stable for more than two months when stored over silica gel blue at 4−6 °C, had short analyzing time (less than 2 min.), and specificity [45].

Jing Wang and his team from Empa, ETH Zurich and Zurich University Hospital have developed an alternative test method in the form of an optical biosensor. The sensor combines two different effects to detect the virus safely and reliably: An optical and a thermal one [46].

The sensor is based on tiny structures of gold, so-called gold nanoislands, on a glass substrate. Artificially produced DNA receptors that match specific RNA sequences of the SARS-CoV-2 are grafted onto the nanoislands. The coronavirus is a so-called RNA virus: Its genome does not consist of a DNA double strand as in living organisms, but of a single RNA strand. The receptors on the sensor are therefore the complementary sequences to the virus' unique RNA sequences, which can reliably identify the virus.

The technology the researchers use for detection is called LSPR, short for localized surface plasmon resonance. This is an optical phenomenon that occurs in metallic nanostructures: When excited, they modulate the incident light in a specific wavelength range and create a plasmonic near-field around the nanostructure. When molecules bind to the surface, the local refractive index within the excited plasmonic near-field changes. An optical sensor located on the back of the sensor can be used to measure this change and thus determine whether the sample contains the RNA strands in question.

At the moment, however, the sensor is not yet ready to measure the corona virus concentration in the air, for example in Zurich's main railway station. A number of developmental steps are still needed to do this. "This still needs development work," says Wang [46]. However, when the sensor is ready, the method used can be applied to other viruses and help to detect and stop outbreaks in the early stages.

References

1. China National Health Commission, (2020). Chinese Clinical Guidance for COVID-19 Pneumonia Diagnosis and Treatment (7th edition), China. http://kjfy.meetingchina.org/msite/news/show/cn/3337.html
2. Ding, Q., Lu, P., Fan, Y., Xia, Y., Liu, M. (2020). The clinical characteristics of pneumonia patients co-infected with 2019 novel coronavirus and influenza virus in Wuhan, China [published online ahead of print, 2020 Mar 20, J. Med. Virol. 1-7. https://doi.org/10.1002/jmv.25781
3. Wang, C., Horby, P.W., Hayden, F.G., Gao, G.F. (2020). A novel coronavirus outbreak of global health concern. Lancet 395, 470–473.
4. Ahmed, S. F., Quadeer, A. A., McKay, M.R. (2020). Preliminary Identification of Potential Vaccine Targets for the COVID-19 Coronavirus (SARS-CoV-2) Based on SARS-CoV Immunological

Studies. Viruses, 12, 254; doi:10.3390/v12030254.

5. Chen, N., Zhou, M., Dong, X.et al. (2020). Epidemiological and clinical characteristics of 99 cases of 2019 novel coronavirus pneumonia in Wuhan, China: a descriptive study. Lancet 395 (10223) 507–513.

6. Grech, V. (2020). Unknown unknowns – COVID-19 and potential global mortality. Early Human Development 144 105026.

7. Lynch, L. (2001). Not a virus, but an upgrade: The ethics of epidemic evolution in Greg Bear's Darwin's Radio. Lit Med 20020:71-93.

8. https://www.who.int/emergencies/diseases/novel-coronavirus-2019/situation-reports.

9. Chauhan, V., Galwankar, S., Arquilla, B., Garg, M., Somma, S. D., El-Menyar, A., Krishnan, V., Gerber, J., Holland, R., & Stawicki, S. P. (2020). Novel Coronavirus (COVID-19): Leveraging Telemedicine to Optimize Care While Minimizing Exposures and Viral Transmission. Journal of emergencies, trauma, and shock, 13(1), 20–24. https://doi.org/10.4103/JETS.JETS_32_2014.

10. Sohrabi, C. (2020). World Health Organization declares global emergency: A review of the 2019 novel coronavirus (COVID-19). International Journal of Surgery 76, 71–76.

11. https://www.who.int/emergencies/diseases/novel-coronavirus-2019

12. Gudi, S. K., Tiwari, K. K. (2020). Preparedness and Lessons Learned from the Novel Coronavirus Disease. Int J Occup Environ Med, 11, 108-112. doi: 10.34172/ijoem.2020.1977.

13. COVID-19 (2019-n CoV Hastalığı) Rehberi. (Bilim Kurulu Çalışması) T.C. Sağlık bakanlığı 25 şubat 2020.

14. Velavan, T. P., Meyer, C. G. (2020). The COVID-19 epidemic, Tropical Med. Int. Health, 25 (3), 278–280, https://doi.org/10.1111/tmi.13383.

15. Ralph, R., Lew, J., Zeng, T., Francis, M., Xue, B., Roux, M., Ostadgavahi, A. T., Rubino, S., Dawe, N. J., Al-Ahdal, M. N., Kelvin, D. J., Richardson,C. D., Kindrachuk, J., Falzarano, D., Kelvin, A. A. (2020). 2019-nCoV (Wuhan virus), a novel Coronavirus: human-to-human transmission, travel-related cases, and vaccine readiness.

16. Yuen, K. S., Ye, Z. W., Fung, S. Y., Chan, C. P., Jin, D. Y. (2020). SARS-CoV-2 and COVID-19: The most important research questions.

17. https://bioeasy.com.tr/koronavirus-testi-covid-19-coronavirus-rapid-test-kit/

18. https://biruni.com.tr/e-kutuphane/populer-bultenler/covid-19-sars-cov-2-antikor-testleri/

19. Real-Time RT-PCR Panel for Detection 2019-nCoV. Centers for Disease Control and Prevention. 29 Ocak 2020. 20. https://epistemturkiye.org/pcr-tabanli-covid-19-tani-kitleri-nasil-calisiyor/.

21. Peña-Bahamonde, J., Nguyen, H.N., Fanourakis, S.K. et al. (2018)

Recent advances in graphene-based biosensor technology with applications in life sciences. J Nanobiotechnol. 16, 75. https://doi.org/10.1186/s12951-018-0400-z

22. Heyu Yin, Ehsan Ashoori, Xiaoyi Mu, and Andrew J. Mason (2020). A Compact Low-Power Current-to-Digital Readout Circuit for Amperometric Electrochemical Sensors. IEEE Transactions On Instrumentation And Measurement. Vol. 69, 5.

23. Bakker E. (2014). Potentiometric Sensors. In: Moretto L., Kalcher K. (eds) Environmental Analysis by Electrochemical Sensors and Biosensors. Nanostructure Science and Technology, Springer, New York, NY.

24. Janata J. (2009). Potentiometric Sensors. In: Principles of Chemical Sensors. Springer, Boston, MA.

25. Prodromidis, M. I. (2007). Impedimetric Biosensors and Immunosensors. *Pakistan Journal Of Analytical & Environmental Chemistry,* 8(2), 3.

26. Brosel-Oliu, S., Uria, N., Abramova N., and Bratov, A. Impedimetric Sensors for Bacteria Detection. InTech. DOI: 10.5772/60741

27. Yang L., Bashir R. (2008). Electrical/electrochemical impedance for rapid detection of food borne pathogenic bacteria. Biotechnology Advances, 26, 135–150.

28. Swaminathan B., Feng P. (1994). Rapid detection of food-borne pathogenic bacteria. Annual Reviews in Microbiology, 48, 401–426.

29. Silley P., Forsythe S. (1996). Impedance microbiology—a rapid change for microbiologists. Journal of Applied Bacteriology, 80, 233–243.

30. Martins S., Selby M. (1980). Evaluation of a rapid method for the quantitative estimation of coliforms in meat by impedimetric procedures. Applied and Environmental Microbiology, 39, 518–524.

31. Stradiotto, N. R., Yamanaka, H., Zanoni, M. V. B. (2003). Electrochemical sensors: A powerful tool in analytical chemistry. J. Braz. Chem. Soc., vol.14 no.2. https://doi.org/10.1590/S0103-50532003000200003.

32. Hamid, F. M. A. (2020). Development Of Electrochemıcal Sensor Based On Modıfıed Electrode For The Determınatıon Of Carbendazım. Eskişehir Anadolu University Graduate School of Sciences, Department of Chemistry Analytical Chemistry, Master's Thesis, Eskişehir.

33. Uka, B. (2018). Development Of Electrochemical Sensor For The Detection Of Beta Lactam Antibiotics, Master Thesis, İstanbul University, Health Sciences Institute, İstanbul.

34. Yu, F., Du, L., Ojcius, D. M., Chungen P. and Jiang, S. (2020). Measures for diagnosing and treating infections by a novel coronavirus responsible for a pneumonia outbreak originating in Wuhan, China.

Microbes and Infection, 22(2), 74-79. https://doi.org/10.1016/j.micinf.2020.01.003

35. Velanki S. and Ji, H.-F. (2006). Detection of feline coronavirus using microcantilever sensors. Measurement Science and Technology, 17, 2964. https://doi.org/10.1088/0957-0233/17/11/015

36. Chan, J. F.-W., Kok, K.-H., Zheng, Z., Chu, H., To, K. K.-W., Yuan, S. & Yuen, K.-Y. (2020). Genomic characterization of the 2019 novel human-pathogenic coronavirus isolated from a patient with atypical pneumonia after visiting Wuhan. Emerging Microbes & Infections, 9:1, 221-236, DOI: 10.1080/22221751.2020.1719902.

37. Jiang, S., Du, L. & Shi, Z. (2020). An emerging coronavirus causing pneumonia outbreak in Wuhan, China: calling for developing therapeutic and prophylactic strategies. Emerging Microbes & Infections, 9(1), 275-277, DOI: 10.1080/22221751.2020.1723441.

38. Seungjoo, H., Hyun-Ouk, K., Jihye, K., Daesub, S. Kit for detecting virus. Patent No.: Cn107430129a.

39. Layqah, L. A., Eissa, S. (2019). An electrochemical immunosensor for the corona virus associated with the Middle East respiratory syndrome using an array of gold nanoparticle-modified carbon electrodes. Microchim Acta. 186, 224. https://doi.org/10.1007/s00604-019-3345-5.

40. Vidic, J., Manzano, M., Chang, C. et al. (2017). Advanced biosensors for detection of pathogens related to livestock and poultry. Vet Res 48, 11. https://doi.org/10.1186/s13567-017-0418-5.

41. Özer, T., Geiss B. J., and Henry C. S. (2020). Review—Chemical and Biological Sensors for Viral Detection. J. Electrochem. Soc., 167, 037523. https://orcid.org/0000-0002-8671-7728.

42. GenMark Diagnostics Inc. or its subsidiaries, with multiple additional foreign and domestic patents pending: U.S. Patent Nos. 6,753,143, 7,172,897, 7,312,087, 7,534,331, 7,820,391, 8,486,247, 9,222,623, 9,410,663, 9,453,613, 9,498,778, 9,500,663, 9,598,722; 9,874,542, 9,957,553, 10,001,476, International Patent Nos. 1218541, 1246699, 60125713.8, 2220102, 602008031596.7, 1246699, 2278757, 60125713.8, 3548159, 9874542, 60017809.9, 1350568, 3548159, 2965817.

43. Mahari, S., Roberts, A., Shahdeo, D., Gandhi, S. (2020). eCovSens-Ultrasensitive Novel In-House Built Printed Circuit Board Based Electrochemical Device for Rapid Detection of nCovid-19 antigen, a spike protein domain 1 of SARS-CoV-2. BioRxiv Preprint server. doi: https://doi.org/10.1101/2020.04.24.059204.

44. https://www.rapidmicrobiology.com/test-method/testing-for-the-wuhan-coronavirus-a-k-a-covid-19-sars-cov-2-and-2019-ncov

45. Zuo, B., Li, S., Guo, Z., Zhang, J., Chen, C., (2004). Piezoelectric

Immunosensor for SARS-Associated Coronavirus in Sputum. Analytical Chemistry, 76 (13), 3536-3540 DOI: 10.1021/ac035367b

46. Qiu, G., Gai, Z., Tao, Y., Schmitt, J., Kullak-Ublick, G. A., Wang, J., (2020). Dual-Functional Plasmonic Photothermal Biosensors for Highly Accurate Severe Acute Respiratory Syndrome Coronavirus 2 Detection. ACS Nano. DOI: 10.1021/acsnano.0c02439.